UNIVERSITÉ DE SHERBROOKE
Faculté de génie
Département de génie chimique et génie biotechnologique

MODÉLISATION DE LA PRODUCTION DE PÂTES ALIMENTAIRES TRADITIONNELLES ET ENRICHIES

Thèse de doctorat
Spécialité : Génie chimique

Samuel Mercier

Jury : Ryan Gosselin
Bernard Marcos (codirecteur)
Martin Mondor
Christine Moresoli (codirectrice)
Cristina Ratti

Sherbrooke (Québec) Canada Mars 2016

RÉSUMÉ

Les pâtes enrichies représentent un produit d'intérêt pour l'industrie, car elles offrent aux consommateurs la possibilité de profiter des bienfaits sur la santé de l'ingrédient d'enrichissement sans modifier leurs habitudes alimentaires. Cependant, la durée et le coût du développement de nouvelles pâtes enrichies sont significatifs et limitent leur probabilité de succès commercial. Dans cette thèse, des modèles ont été développés pour décrire la production des pâtes traditionnelles et enrichies et accélérer leur développement. Deux objectifs généraux ont été poursuivis.

Le premier objectif était l'identification et la quantification des mécanismes de transfert affectant la qualité des pâtes lors du séchage, leur étape de transformation la plus importante. L'état de l'art a révélé que les modèles développés précédemment pour décrire le séchage des pâtes combinent la description des mécanismes de transfert de masse de l'eau à partir d'un coefficient de diffusion effectif. La qualité de ces modèles a été évaluée par analyses de sensibilité, d'incertitude et d'identifiabilité. Ces analyses ont montré que l'incertitude des modèles précédents sur la prédiction du temps de séchage requis est importante (environ ± 4 h) et que cette incertitude peut être expliquée par la faible identifiabilité pratique des coefficients de transfert de masse à partir de mesures bruitées de la teneur en eau. L'analyse des modèles de séchage précédents a également montré leur imprécision à décrire les profils internes de teneur en eau générés dans les pâtes lors du séchage, alors que ces profils en eau sont critiques à la prédiction de la formation de craques. Cette thèse a donc conduit au développement d'un nouveau modèle de séchage mécanistique, couplant le transfert de masse de l'eau liquide par capillarité et convection, le transfert de masse de l'eau vapeur par diffusion et convection, le transfert d'énergie par conduction, convection et évaporation et la déformation mécanique. Ce modèle a été validé pour 3 températures de séchage (40, 60 et 80 ºC) représentatives des conditions utilisées en industrie.

Le deuxième objectif était la quantification de l'impact de l'enrichissement et des variables de procédé sur les propriétés des pâtes. Cet objectif a été atteint par la construction et la méta-analyse d'une base de données regroupant les propriétés des pâtes traditionnelles et enrichies mesurées dans la littérature. Les propriétés manquantes de la base de données ont été estimées par le développement d'une approche novatrice et originale basée sur la complétion de matrice. L'approche par complétion de matrice a permis d'expliquer en moyenne 40% de la variance des propriétés manquantes. Elle a également permis de déterminer pour près de 20% des propriétés manquantes, avec un niveau de confiance de plus de 90%, si elles sont supérieures ou inférieures à la valeur moyenne de la propriété, améliorant la caractérisation du produit sans coût expérimental additionnel.

Les travaux de cette thèse ont conduit à la réalisation de 7 articles dans des revues avec comité de lecture et ont été présentés à 4 congrès internationaux. Les travaux ont permis le développement de 2 outils, le modèle de séchage mécanistique et l'estimation des propriétés manquantes par complétion de matrice, que l'industrie pourra utiliser pour accélérer le développement de nouvelles pâtes enrichies. Plusieurs contributions majeures de cette thèse, notamment l'établissement des conditions expérimentales pour l'identifiabilité pratique des coefficients de transfert de masse et les méthodologies pour la méta-analyse d'un produit et l'estimation de ses propriétés manquantes par complétion de matrice, ont été appliquées aux pâtes enrichies, mais leur impact s'étend à de nombreux produits et procédés.

Mots-clés

Pâtes; Enrichissement; Développement de produit; Séchage; Transfert de masse; Identifiabilité; Méta-analyse; Complétion de matrice.

REMERCIEMENTS

Mes plus grands remerciements vont à mes directeurs de doctorat, Prs Bernard Marcos et Christine Moresoli, et à mes proches collaborateurs, Drs Martin Mondor et Sébastien Villeneuve. La collaboration entre chercheurs est essentielle à l'avancement de la science et je crois que nous en avons fait une belle démonstration. Merci pour votre compétence et votre ouverture. Votre implication a été d'une valeur inestimable à ma formation et j'espère que nous poursuivrons cette collaboration au cours de ma carrière.

Je remercie également les professeurs du département de génie chimique et de génie biotechnologique de l'Université de Sherbrooke pour votre expertise et votre disponibilité. Un merci particulier au Pr Ryan Gosselin, dont l'excellent cours en analyse multivariée a inspiré une importante partie de ce doctorat, pour son implication au projet en tant que membre du jury. Merci également au Pr Cristina Ratti, de l'Université Laval et membre de mon jury, pour avoir pris le temps de lire, évaluer et commenter ce travail.

Merci au Centre de Recherche et Développement de Saint-Hyacinthe, du réseau d'Agriculture et Agroalimentaire Canada, pour avoir fourni les installations nécessaires à la production et l'analyse des pâtes alimentaires. Merci aux organismes subventionnaires, le programme de bourses de doctorat Vanier et le Conseil de Recherches en Sciences Naturelles et en Génie du Canada, ayant rendu ce projet possible.

Finalement, à ma famille, mes amis et tous celles et ceux ayant contribué à forger la personne que je suis aujourd'hui, vous avez mon éternelle reconnaissance. Mes succès sont les vôtres.

TABLE DES MATIÈRES

LISTE DES FIGURES

LISTE DES TABLEAUX

CHAPITRE 1. Introduction

1.1 Mise en contexte

Les consommateurs portent de plus en plus attention aux bienfaits sur la santé que leur procure leur alimentation. C'est pourquoi, depuis la dernière décennie, le marché des aliments fonctionnels est en plein essor. Un aliment fonctionnel est défini comme étant un aliment fournissant des bienfaits sur la santé vont au-delà de ses propriétés nutritionnelles de base (Agriculture et Agroalimentaire Canada 2014). Au Canada, plus de 600 entreprises œuvrent dans ce secteur combinant un revenu total de plus de 21 milliards de dollars. À l'échelle mondiale, la croissance du marché des aliments fonctionnels se situerait entre 8 et 14% par année, un des taux de croissance les plus élevés du secteur alimentaire (Agriculture et Agroalimentaire Canada 2009; Khan et al. 2013).

Les pâtes alimentaires représentent un produit d'intérêt du secteur des aliments fonctionnels. Les pâtes sont appréciées par les consommateurs en raison de leur bon goût, polyvalence, simplicité d'utilisation et faible coût, qualités ayant stimulé une augmentation de leur production de 7 à 12 millions de tonnes par année au courant de la dernière décennie (Marti et Pagani 2013; Carini et al. 2014; Li et al. 2014). De plus, les recherches ont montré que la semoule de blé des pâtes peut être partiellement substituée par des ingrédients exogènes sans perte de l'intégrité physique du produit lors de sa production et sa cuisson (Petitot et al. 2010; Alasino et al. 2011). C'est pourquoi la tendance actuelle dans le marché des pâtes est le développement de pâtes dont la semoule de blé est partiellement remplacée par des ingrédients aux effets bénéfiques sur la santé. L'enrichissement vise généralement à augmenter leur teneur en fibres, minéraux, antioxydants ou composés bioactifs, ou à compenser une déficience nutritionnelle des pâtes, telle que leur faible concentration en lysine et thréonine (Chillo et al. 2008; Marti et Pagani 2013). Les concentrés et isolats de protéines (Alireza Sadeghi et Bhagya 2008; Mercier et al. 2011b), les farines de pois, de fèves et de graines oléagineuses (Wood 2009; Gallegos-Infante et al. 2010; Villeneuve et al. 2013), les fibres alimentaires (Brennan et Tudorica 2007; Aravind et al. 2012a; Vernaza et al. 2012), les extraits de microalgues (Zouari et al. 2011; Fradique et al. 2013) et les extraits de fruits (Pillai et al. 2012) représentent les principaux ingrédients considérés pour l'enrichissement des pâtes.

1.2 Problématique

Malgré la croissance du secteur alimentaire et l'engouement pour les aliments fonctionnels, la majorité (72-88%) des nouveaux produits alimentaires développés sont un échec commercial (Stewart-Knox et Mitchell 2003; Starling 2014). Une cause majeure de l'échec commercial d'un nouvel aliment est la durée et le coût de son développement (Stewart-Knox et Mitchell 2003; Khan et al. 2013). Il est critique de limiter la durée et le coût du développement d'un nouvel aliment afin de favoriser une entrée sur le marché plus rapide que les compétiteurs et de préserver suffisamment de ressources financières pour des activités telles que les campagnes publicitaires, facteurs augmentant significativement la probabilité de succès commercial (Cohen et al. 1996; Stewart-Knox et Mitchell 2003; Khan et al. 2013).

Pour les pâtes, une portion importante du développement de nouvelles pâtes enrichies est accordée à l'identification des conditions de production appropriées. L'identification des conditions de production appropriées lors du développement de pâtes enrichies est longue et complexe en raison de :

La nécessité de préserver la qualité des pâtes. L'introduction d'ingrédients exogènes dans la formulation des pâtes modifie leurs propriétés chimiques, physiques et sensorielles et diminue généralement leur appréciation par les consommateurs (Sabanis et al. 2006; Boroski et al. 2011; Bustos et al. 2011; Jayasena et al. 2012; Kadam et Prabhasankar 2012). Cependant, les études sur la perception des consommateurs indiquent que la majorité ne sont pas prêts à compromettre leur appréciation des produits alimentaires enrichis pour une augmentation de leurs effets bénéfiques sur la santé (Tuorila et Cardello 2002; Verbeke 2006). En conséquence, il est nécessaire d'identifier des conditions de production permettant l'obtention de pâtes enrichies avec des ingrédients bénéfiques sur la santé de qualité similaire aux pâtes traditionnelles.

La diminution potentielle de l'effet sur la santé de l'ingrédient d'enrichissement lors de la production des pâtes. Les bénéfices sur la santé associés à la consommation de pâtes enrichies peuvent être inférieurs à ceux associés à la consommation de l'ingrédient d'enrichissement seul (Fogliano et Vitaglione 2005). La réduction des bénéfices sur la santé

peut être causée par la faible biodisponibilité de l'ingrédient d'enrichissement à l'intérieur des pâtes ou sa dégradation au cours du procédé de production (Austria et al. 2008; Villeneuve et al. 2013). Il est nécessaire d'identifier des conditions de production des pâtes enrichies favorisant la biodisponibilité et le maintien de l'activité de l'ingrédient d'enrichissement.

Le grand nombre de variables de procédé à considérer. Une méta-analyse a révélé 11 variables de procédé pertinentes à ajuster lors du développement de pâtes enrichies (chapitre 7). En assumant que chacune de ces variables de procédé puisse être ajustée à un minimum de deux niveaux, nous pouvons conclure qu'au moins 2 000 combinaisons de conditions de production peuvent être envisagées pour la production de pâtes enrichies. Même avec l'application de méthodes de conception expérimentale modernes, l'analyse des propriétés des pâtes pour un tel nombre de conditions de production peut s'étendre sur plusieurs années et nécessiter l'investissement de millions de dollars (McDougall 2010).

1.3 Approche théorique

L'approche proposée dans cette thèse pour réduire la durée et le coût de développement de nouvelles pâtes enrichies est le développement de modèles favorisant une identification efficace des conditions de production appropriées. La modélisation vise le développement de relations mathématiques décrivant l'évolution des propriétés des pâtes traditionnelles et enrichies au cours de leur production. Une fois validés par comparaison avec des mesures expérimentales, les modèles favorisent une meilleure compréhension de l'impact des variables de procédé sur les propriétés des pâtes et permettent la prédiction de leurs propriétés pour de nouvelles conditions de production. Les modèles permettent de maximiser l'information obtenue de mesures expérimentales et, par extension, de minimiser le nombre d'expériences et de mesures à réaliser pour identifier des conditions de production appropriées.

Deux approches de modélisation sont proposées dans cette thèse pour la prédiction des propriétés des pâtes selon les conditions de production: une approche mécanistique, appliquée à la modélisation de l'étape de séchage des pâtes, et une approche empirique, visant à fournir

un portrait général de la qualité des pâtes et considérant l'ensemble des étapes de transformation.

Une approche mécanistique est appliquée spécifiquement à la modélisation du séchage des pâtes, considérée comme leur étape de transformation la plus importante en raison de son impact sur leurs propriétés sensorielles, esthétiques, mécaniques et de cuisson (Andrieu et Stamatopoulos 1986; Owens 2001). Le séchage des pâtes est contrôlé par des mécanismes de transfert de masse et d'énergie menant à l'atteinte d'un état d'équilibre entre la pâte et l'environnement du séchoir (Owens 2001; De Temmerman et al. 2007). Étant donné que ces mécanismes sont bien connus, le séchage se prête bien au développement d'un modèle mécanistique basé sur les premiers principes décrivant les phénomènes d'échange. Le développement d'un modèle mécanistique favorise une compréhension fondamentale de la transformation des pâtes lors de cette étape et permet la prédiction de leur teneur en eau et leur température, propriétés à partir desquelles peuvent être prédites la transition vitreuse, la formation de craques, la formation de furosine (associé au brunissement et à la digestibilité) et les propriétés mécaniques (Cuq et Icard-Verniere 2001; Cuq et al. 2003; Migliori et al. 2005).

Une approche empirique, basée sur les méthodes de régression multivariées, est utilisée pour développer un modèle général prédisant les propriétés des pâtes et considérant les conditions de production utilisées à chacune des étapes de transformation. L'utilisation d'une approche empirique est nécessaire considérant la quantité, la complexité et la dépendance des phénomènes impliqués à chacune des étapes de transformation. Le développement d'un modèle multivarié est pertinent pour la compréhension des interactions entre les étapes de transformation des pâtes, l'identification des conditions de production les plus importantes et la prédiction des conditions de production générant des pâtes traditionnelles et enrichies de qualité.

1.4 Objectifs

Le projet comporte deux objectifs généraux, chacun associé à une série d'objectifs spécifiques :

Objectif général #1 : Identifier et quantifier les mécanismes de transfert qui influencent la qualité des pâtes lors du séchage.

Objectifs spécifiques :

- Développer un modèle mécanistique décrivant le transfert de masse et d'énergie lors du séchage des pâtes;
- Valider le modèle par comparaison avec des profils internes de teneur en eau publiés dans la littérature;
- Quantifier la sensibilité du modèle pour ses paramètres d'entrée;
- Vérifier l'identifiabilité structurelle des coefficients de diffusion et de convection de l'eau à partir de la teneur en eau locale et globale;
- Identifier les conditions expérimentales favorisant l'identifiabilité pratique des coefficients de diffusion et de convection;
- Quantifier l'incertitude des coefficients de diffusion et de convection estimés à partir de la teneur en eau locale et globale;
- Comparer la contribution des mécanismes de transfert de masse et d'énergie sur le séchage des pâtes.

Objectif général #2 : Quantifier l'impact de l'enrichissement et des variables de procédé sur les propriétés des pâtes.

Objectifs spécifiques :

- Construire une base de données décrivant les propriétés des pâtes traditionnelles et enrichies selon les conditions de production;
- Développer un modèle de prédiction empirique multivarié des propriétés des pâtes traditionnelles et enrichies selon les conditons de production;
- Quantifier la précision du modèle selon les conditions de production;
- Identifier les variables de procédé ayant l'impact le plus important sur les propriétés des pâtes.

1.5 Contributions originales

Les contributions de cette thèse ont permis la réalisation de 7 articles dans des revues scientifiques avec comité de lecture. La plupart de ces contributions ont été illustrées et validées pour la production de pâtes alimentaires, mais leur impact s'étend à de nombreux autres produits et procédés. Les 4 contributions originales majeures de cette thèse sont:

L'analyse des conditions expérimentales nécessaires à l'identifiabilité des coefficients de transfert de masse. Les coefficients de diffusion et convection décrivant une opération contrôlée par le transfert de masse sont en général estimés à partir de mesures de concentrations. Les conditions expérimentales permettant l'identifiabilité de ces coefficients, considérations critiques à la validité de leur estimation, n'ont pas été déterminées. Dans cette thèse, l'identifiabilité de ces coefficients a été vérifiée selon le type, le nombre, l'instant et l'erreur des mesures de concentration (chapitres 4 et 5). Les travaux orientent la planification d'expériences maximisant la précision de l'estimation de ces coefficients critiques à la modélisation du transfert de masse et démontrent pour différents scénarios expérimentaux l'imprécision de la méthode asymptotique pour le calcul de leur incertitude. Les conclusions des travaux sont applicables à la modélisation des procédés contrôlés par des mécanismes de diffusion et de conduction.

Le développement d'un modèle de séchage mécanistique. Un modèle mécanistique décrivant le séchage des pâtes a été développé et validé pour le séchage des pâtes à température basse et élevée (chapitre 6). Le modèle décrit le transfert de masse de l'eau liquide par capillarité et convection, le transfert de masse de l'eau vapeur par diffusion et convection, le transfert d'énergie par conduction, convection et évaporation et la déformation mécanique. Les modèles de séchage des pâtes développés précédemment regroupent la description des mécanismes de transfert de masse et d'énergie à partir de coefficients de transfert effectifs. En comparaison avec ces modèles, le modèle mécanistique développé dans cette thèse favorise une compréhension fondamentale des mécanismes impliqués dans le séchage et améliore la précision des profils internes de teneur en eau générés lors du séchage, nécessaires à la prédiction du stress mécanique et la formation de craques.

La réalisation d'une méta-analyse des propriétés d'un produit. Plusieurs études ont établi la pertinence des méta-analyses, soit l'application de méthodes quantitative à l'analyse simultanée des résultats provenant de plusieurs études, pour la génération de savoir et la réalisation de revues de la littérature plus objectives et concluantes. Malgré ses avantages, les méta-analyses ont rarement été appliquées à la caractérisation d'un produit. Dans cette thèse, une méta-analyse sur les pâtes traditionnelles et enrichies a été réalisée (chapitre 7). Les travaux améliorent la compréhension des relations entre les variables de procédé et les propriétés des pâtes, illustrent la pertinence des analyses statistiques combinant les résultats de plusieurs études et fournissent une méthodologie applicable à la méta-analyse de nombreux produits.

L'estimation des propriétés inconnues d'un produit par complétion de matrice. La caractérisation détaillée d'un produit est rarement possible en raison de contraintes budgétaires, techniques et de temps. Dans cette thèse, une approche par complétion de matrice a été développée afin d'estimer les valeurs inconnues des propriétés des pâtes à partir des corrélations entre ces propriétés et les variables de procédé (chapitre 8). Les algorithmes de complétion de matrice ont à l'origine été développés, entre autres, pour utiliser les similarités entre différents films et vidéos afin de développer des systèmes de recommandation adaptés au profil des utilisateurs de sites ou applications tel que Netflix. À notre connaissance, ce travail représente la première application de ces méthodes à la caractérisation d'un produit. Le développement de cette approche pourrait avoir un impact majeur pour le développement de nouveaux produits par l'amélioration de leur caractérisation sans coût expérimental additionnel.

1.6 Contenu de la thèse

La thèse est divisée en deux parties, la première (chapitres 2-6) portant sur l'objectif général #1 de la thèse, l'identification et la quantification des mécanismes de transfert influencant la qualité des pâtes lors du séchage, et la deuxième (chapitres 7-8) sur l'objectif général #2 de la thèse, la quantification de l'impact de l'enrichissement et des variables de procédé sur les propriétés des pâtes.

Dans la première partie de la thèse, le chapitre 2 présente l'état de l'art concernant les modèles développés pour décrire le séchage des pâtes. Les chapitres 3 à 5 portent sur l'analyse de ces modèles : le chapitre 3 quantifie leur incertitude et leur sensibilité aux paramètres d'entrée et les chapitres 4 et 5 analysent l'identifiabilité des coefficients de diffusion et de convection de l'eau considérant un coefficient de diffusion constant (chapitre 4) et dépendant de la teneur en eau (chapitre 5). Le chapitre 6 présente le développement et la validation d'un modèle de séchage mécanistique prédisant avec précision les profils internes de teneur en eau générés lors du séchage. La première partie de la thèse est complétée par l'annexe A, qui fournit un complément d'information sur la contribution du transfert d'énergie à la modélisation du séchage des pâtes. Les chapitres 2, 3, 4, 5 et 6 ont été publiés dans des revues avec comité de lecture.

Dans la deuxième partie, le chapitre 7 présente la construction et la méta-analyse d'une base de données présentant les propriétés des pâtes traditionnelles et enrichies selon leurs conditions de production. Le chapitre 8 présente le développement d'une méthode de modélisation par complétion de matrice pour la prédiction des propriétés inconnues des pâtes traditionnelles et enrichies selon les conditions de production. Un complément d'information est fourni à l'Annexe B, sur la révision des méthodes de méta-analyse. Les chapitres 7 et 8 ont été publiés et soumis, respectivement, à des revues avec comité de lecture.

Finalement, le chapitre 9 rappelle les conclusions tirées des travaux et propose deux avenues de recherche pertinentes pour la poursuite des travaux de modélisation appliquée aux pâtes traditionnelles et enrichies et au développement de nouveaux produits.

CHAPITRE 2. Modélisation du séchage des pâtes: état de l'art

Titre original : Drying of durum wheat pasta and enriched pasta: a review of modeling approaches

Auteurs et affiliations :

S. Mercier, Ing. jr., étudiant au doctorat, Université de Sherbrooke, département de génie chimique et génie biotechnologique, 2500 boul. Université, Sherbrooke, Québec, Canada, J1K 2R1.

M. Mondor, Ing. stag., Ph.D., Agriculture et Agroalimentaire Canada, Centre de Recherche et Développement de Saint-Hyacinthe, 3600 Boul. Casavant Ouest, Saint-Hyacinthe, Québec, Canada, J2S 8E3.

C. Moresoli, Ing., Ph.D. University of Waterloo, Department of Chemical Engineering, 200 University Avenue West, Waterloo, Ontario, Canada, N2L 3G1.

S. Villeneuve, Ing., Ph.D., Agriculture et Agroalimentaire Canada, Centre de Recherche et Développement de Saint-Hyacinthe, 3600 Boul. Casavant Ouest, Saint-Hyacinthe, Québec, Canada, J2S 8E3.

B. Marcos, Ing., Ph.D., Université de Sherbrooke, département de génie chimique et génie biotechnologique, 2500 boul. Université, Sherbrooke, Québec, Canada, J1K 2R1.

Date d'acceptation : 8 décembre 2012

État de l'acceptation : Publié

Référence : Critical Reviews in Food Science and Food Nutrition, accepté pour publication. doi: 10.1080/10408398.2012.757691.

Résumé

Contenu : dans cet article, une revue de la littérature des modèles développés pour décrire le séchage des pâtes est réalisée. Les phénomènes fondamentaux impliqués dans des pâtes, le transfert de masse de l'eau, l'évaporation de l'eau, le transfert d'énergie, la déformation, la transition vitreuse et la formation de craques sont révisés. Les formulations mathématiques développées pour décrire ces phénomènes sont comparées et leur validation expérimentale est analysée. Les propriétés thermodynamiques nécessaires à l'utilisation des modèles sont décrites et leurs valeurs sont estimées. L'article se termine par la discussion d'avenues pour l'amélioration de la modélisation du séchage des pâtes.

Résultats : la revue de la littérature montre la prépondérance, pour la modélisation du séchage des pâtes, des modèles Fickian décrivant le transfert de masse de l'eau en phase liquide et vapeur à partir d'un coefficient de diffusion effectif. Des différences de près d'un ordre de grandeur entre les valeurs du coefficient de diffusion effectif de l'eau dans les pâtes peuvent être observées entre les études. Les modèles de séchage actuels décrivent avec précision la variation de la teneur en eau globale des pâtes au cours de leur séchage, mais sont inadéquats pour décrire les profils internes de teneur en eau, nécessaires à la prédiction de la formation de craques. L'hypothèse selon laquelle la description mécanistique du transfert de masse de l'eau liquide par capillarité et convection, l'eau vapeur par diffusion et convection et le transfert d'énergie par conduction et convection permettrait d'améliorer la précision des modèles pour décrire les profils internes de teneur en eau est établie.

Contributions à la thèse : les contributions à la thèse de cet article sont l'évaluation de la qualité et des faiblesses des modèles actuels décrivant le séchage des pâtes et d'orienter le développement de nouveaux modèles améliorant la précision des profils internes de teneur en eau générés lors du séchage.

Abstract

Models on drying of durum wheat pasta and enriched pasta were reviewed to identify avenues for improvement according to consumer needs, product formulation and processing conditions. This review first summarized the fundamental phenomena of pasta drying, mass transfer, heat transfer, momentum, chemical changes, shrinkage and crack formation. The basic equations of the current models were then presented, along with methods for the estimation of pasta transport and thermodynamic properties. The experimental validation of these models was also presented and highlighted the need for further model validation for drying at high temperatures (> 100ºC) and for more accurate estimation of the pasta diffusion and mass transfer coefficients. This review indicates the need for the development of mechanistic models to improve our understanding of the mass and heat transfer mechanisms involved in pasta drying, and to consider the local changes in pasta transport properties and relaxation time for more accurate description of the moisture transport near glass transition conditions. The ability of current models to describe dried pasta quality according to the consumers expectations or to predict the impact of incorporating ingredients high in nutritional value on the drying of these enriched pasta was also discussed.

Keywords

Pasta drying; heat transfer; mass transfer; shrinkage; stress-cracking; nutritional supplements; effective moisture diffusivity.

Nomenclature[1]

a_w	water activity coefficient, -
c	concentration, kg m^{-3}
C_P	heat capacity, J kg^{-1} K^{-1}
D	diffusion coefficient, m^2 s^{-1}
E_a	activation energy, J mol^{-1}
f	furosine concentration, mg 100 g of $protein^{-1}$
F	furosine production rate, mg 100 g of $protein^{-1}$ h^{-1}
h	overall heat transfer coefficient, W m^{-2} K^{-1}
H	enthalpy, J kg^{-1}
I	evaporation rate, kg m^{-3} s^{-1}
J	Colburn factor, -
J_n	Bessel function of the first kind and n^{th} order
k	permeability, m^2
k_h	thermal conductivity, W m^{-1} K^{-1}
$K_{m,\Delta c}$	overall mass transfer coefficient described from the gradient $c_{v,R_C,R_{ext}\ or\ X_C} - c_{v,\infty}$, m s^{-1}
$K_{m,\Delta M}$	overall mass transfer coefficient described from the gradient $M_{R_C,R_{ext}\ or\ X_C} - M_E$, kg m^{-2} s^{-1}
$K_{m,\Delta p}$	overall mass transfer coefficient described from a pressure gradient, kg Pa^{-1} m^{-2} s^{-1}
m	mass, kg
M	pasta moisture content on dry basis, kg H_2O kg dry $solid^{-1}$
MW	molecular weight, Dalton
n	mass flux, kg m^{-2} s^{-1}
N^{ext}	mass flux at the solid-gas interface, kg m^{-2} s^{-1}
p^0	vapour pressure, Pa
p	partial pressure, Pa
P	pressure, Pa
q	empirical constant in Eq. (2.72)
r	radial coordinate, m
R	ideal gas constant, J mol^{-1} K^{-1}
R_C	external radius of cylindrical pasta, m
R_{int}	internal radius of tubular pasta, m
R_{ext}	external radius of tubular pasta, m
RH	relative humidity, -
S	saturation of $V_{app} - V_s$ in water or gas, -
S_i	irreducible saturation, -
S_V	surface/volume ratio, m^2 $(m^3)^{-1}$

[1] En raison du nombre élevé de variables utilisées dans les travaux, une nomenclature séparée est fournie pour chaque chapitre de la thèse.

t	drying time, s
T	temperature, K
T_g	glass transition temperature, K
U	pasta moisture content on wet basis, kg H_2O kg wet solid^{-1}
V	volume, m^3
x	coordinate for thickness (m)
X_C	thickness of rectangular pasta, m
y	molar fraction, -
Y_n	Bessel function of the second kind and nth order
z	mass fraction, -
Greek symbol	
α	shrinkage coefficient, -
α_h	thermal diffusivity, m^2 s^{-1}
β_n	roots of the Bessel function of the first kind and zero order, -
γ	first Lame coefficient, Pa
ε	volume fraction, -
κ	mechanical compressibility coefficient, Pa
λ	latent heat of vaporization, J kg^{-1}
η	volumetric fraction of water lost replaced by air, -
ρ	density, kg m^{-3}
ς	radius in Lagrangian coordinates, m
σ	stress, Pa
τ	strain, -
τ_p	pore tortuosity, -
μ	second Lame coefficient, Pa
μ^0	viscosity, kg m^{-1} s^{-1}
χ	shrinkage, -
Dimensionless numbers	
Nu	Nusselt
Pr	Prandtl
Re	Reynolds
Sc	Schmidt
Sh	Sherwood
Superscripts	
eq	equilibrium
int	internal
ext	external

f	fluid
g	gaseous phase
Subscripts	
0	initial condition
1	first
a	air
app	apparent
eff	effective
E	equilibrium
f	at film conditions
g	gaseous phase
h	heat
i	intrinsic
lim	limit
m	mass
PPC	pea protein concentrate
r	relative
rr	radial
s	dry solid
sem	semolina
v	water vapour
vol	volume
w	water
θθ	tangential

2.1 Introduction

Drying is recognized as the step in pasta production that has the greatest impact on the quality of the final product. This operation is generally carried out under relatively severe temperature and moisture conditions which can significantly affect the physical, esthetic, textural, organoleptic and cooking properties of the pasta produced (Andrieu and Stamatopoulos, 1986; Owens, 2001). Consequently, a precise analysis of optimal drying conditions is necessary in order to improve the quality of pasta while at the same time reducing production costs.

Nowadays, optimal pasta production conditions are usually determined by trial-and-error runs and from the experience acquired by producers over the years (Andrieu and Stamatopoulos, 1986; Migliori et al., 2005a; Veladat et al., 2011). However, this method makes it difficult to completely optimize operating conditions when several interdependent variables must be considered simultaneously, such as the quality of the final products, drying time, energy used and overall production cost. In addition, when a new product is put on the market, many tests may be needed before satisfactory drying conditions are determined. That is why several mathematical models have been developed over the years describing the evolution of certain pasta properties during drying according to the operating conditions. These models make it possible to improve understanding of how the operating conditions impact the properties of dry pasta, to minimize the number of tests required to determine optimal drying conditions, and to develop efficient control strategies for the process (De Temmerman et al., 2007; Veladat et al., 2011).

The models developed to date present varying degrees of complexity depending on the mass and heat transfer mechanisms considered and the hypotheses used. Depending on this degree of complexity, the models can lead to an analytical solution or have to be solved using numerical methods. The analytical solution models are generally preferred for their simplicity. In addition, they provide more direct information in terms of the impact of operating conditions on product properties, since these variables appear directly (explicitly) or indirectly (implicitly) in the equations generated. However, obtaining analytical solutions requires greatly simplifying the phenomena involved or the operating conditions, which can reduce the

accuracy of the results. When all the phenomena that occur during drying are considered and described according to first principles equations, numerical solutions are typically generated.

Models can also be classified according to the scope of the parameters they take into consideration. At first, models generally aim to describe the evolution of moisture in pasta during drying according to the operating conditions applied. However, some models have also extended the analysis to mechanical, rheological and chemical properties of pasta, such as the dimensions, porosity, density, rigidity, formation of cracks and furosine production (Andrieu and Stamatopoulos, 1986; Ponsart et al., 2003; Migliori et al., 2005b; Mercier et al., 2011b). Incorporating these properties allows to generate a more complete database that can be used to study the relationship between product quality and drying conditions.

Finally, the models can be analyzed according to their ability to adapt to new production realities such as the addition of specific ingredients in the product's final formulation. These ingredients are generally selected for their high content in protein, omega-3, vitamins or other bioactive compounds, and aim to increase the nutritional value of the pasta. However, adding these compounds can have a significant impact on the chemical and physical properties of pasta (Nielsen et al., 1980; Zhao et al., 2005; Alireza Sadeghi and Bhagya, 2008; Gallegos-Infante et al., 2009; Wood, 2009). Consequently, it is relevant to analyze the validity of current models to represent this new reality, because these models were generally developed for pasta consisting of a standard mixture of durum wheat semolina and water.

The purpose of this review is to analyze the models on pasta drying developed up to date and to identify potential advances in the field to help optimize the production process according to product formulation and consumer needs. To achieve this, a description of the main phenomena involved in drying is first presented. The models developed to describe these phenomena are then presented, and the scope of the experimental validation of these models is analyzed. The basic equations for a mechanistic model are then developed and compared with those of current models, and modelling approaches for more accurate description of moisture transport near glass transition are presented. Finally, the ability of models to predict pasta quality as defined by consumers is discussed, along with the validity of the models for

describing new production realities such as adding ingredients with high nutritional value in the product formulation.

2.2 Main phenomena

Pasta production is a process consisting of three main steps: hydration, extrusion and drying (Veladat et al., 2011). In the first step, semolina and water are mixed until they reach a moisture content level of about 50% (d.b.). A gluten network then forms, which represents the main structure for maintaining the physical integrity of the pasta. Additional ingredients that increase the nutritional value of the product can also be added at this stage. The mixture is then extruded using Teflon or bronze matrixes to mould the fresh pasta into the desired size and shape. Drying is the last operation before the final product is packaged.

The purpose of drying is to decrease the water content of the pasta to a value below about 14% (d.b.) in order to reduce the risk of microbial growth, increase the product's shelf life and obtain pasta that is strong enough to be stored and transported easily (Owens, 2001). This operation is generally carried out by placing the pasta in a dryer at temperatures of 40–120 °C and relative humidities of 40%–95% (Owens, 2001; De Temmerman et al., 2007). Dehydration is then a result of transient mass and heat transfer phenomena occurring until a state of equilibrium between the pasta and dryer environment is reached.

According to Ogawa et al. (2012), pasta drying can be divided into a constant drying-rate period, where about 20% of water is evaporated, followed by a falling-rate period. It is generally considered that the mass transfer mechanisms involved are the diffusion of the water in liquid form to the surface of the product, followed by evaporation of the water on the surface (Migliori et al., 2005a; De Temmerman et al., 2007). Internal resistance to the transport of water is assumed to be the limiting factor. Consequently, during drying, moisture diffusion develops inside the product, which is commonly described using Fick-type laws (Andrieu and Stamatopoulos, 1986; Migliori et al., 2005a; De Temmerman et al., 2007). However, it is possible that other water transport mechanisms contribute to the dehydration of the product, such as transport of vapour or liquid water by pressure gradient (Litchfield and Okos, 1992; Waananen and Okos, 1996; Veladat et al., 2011). This is particularly true for

drying under very high temperatures (> 100 °C), which can cause the evaporation front to be displaced deeper into the pasta.

In terms of heat transfer, pasta temperature rises after the pasta is placed in dryers. This increase is caused by convection at the surface and conduction inside the pasta, although internal heat transfer through convection is also possible when there is a hydrodynamic water flow caused by a pressure gradient. When water evaporation is concentrated on the surface and water is supplied rapidly enough to this surface, the pasta acts like a wet bulb thermometer. The heat supplied by the ambient air is then equivalent to the heat absorbed by vaporization, such that the pasta temperature is uniform (wet bulb temperature). When evaporation becomes insufficient, the pasta temperature starts to rise (Bird et al., 1960). According to the relative magnitude of the pasta thermal conductivity and surface heat transfer coefficient, an internal temperature gradient will be established, or the product will be considered as spatially isotherm. The temperature increase is also dependent on the isosteric heat of desorption, defined as the difference between the heat of desorption and the heat of vaporisation. The net isosteric heat of desorption generally increases during drying, such that the energy required to break the attractive forces between the water molecules and the solid phase increases when the pasta is near the equilibrium moisture content (Escobedo-Avellaneda et al., 2011; Noshad et al., 2012). However, given the high thermal conductivity of pasta and its small thickness, the pasta and the environment generally reach thermal equilibrium rapidly compared with the duration of the mass transfer phenomena (Andrieu and Stamatopoulos, 1986; De Temmerman et al., 2007). This is why several models disregard the heat transfer phenomena and consider pasta drying as an isothermal process (Villeneuve and Gelinas, 2007; De Temmerman, 2008; Mercier et al., 2011b).

During drying, when the moisture content decreases from about 50% to fewer than 14% (d.b.), pasta usually undergoes glass transition. Glass transition represents the transition of the amorphous components from a supercooled melt to a glassy state, or the opposite (Liu et al., 2006). It is referred as a second-order state transition, which is a transition that occurs without the release or absorption of latent heat (Rahman, 2006). The point at which pasta undergoes glass transition depends both on its water content and drying temperature. Cuq et al. (2003) observed that despite of pasta heterogeneity, for a specific moisture content, it

undergoes glass transition at a single apparent glass transition temperature. The glass transition temperature is generally lower for pasta with a high moisture content, which can be explained by the plasticization effect of water on amorphous polymers.

Glass transition is usually associated with significant physical, mechanical, electrical and thermal properties changes of the product (Rahman, 1995). As observed by Cuq et al. (2003), pasta behaves as an elastic and rigid product in the glassy state and as a visco-plastic and soft product in the rubbery state, with a transition state in between. Glass transition can also affect moisture transport during drying. Xing et al. (2007) measured internal moisture profiles of pasta and observed sharper moisture profiles than those predicted from classical Fick-type models. This could be attributed to the formation of a hard, glassy surface which can induce important local changes in the transport properties within the pasta (Hills et al., 1997). The sharp internal moisture profiles could also be explained by the time-dependant viscoelastic relaxation of pasta amorphous components. In the transition state near the glass transition, the relaxation time of polymers can be of the same order as the diffusion time, thus inducing anomalous diffusion and sharper moisture profiles (Takhar, 2008). These results suggest that changes in the viscoelastic properties taking place during drying should be considered to model accurately the internal moisture profiles of pasta near the glass transition.

Pasta shrinkage also has to be considered for accurate modeling of pasta drying. Shrinkage is caused by the partial replacement of the water lost during drying by air. Mercier et al. (2011b) observed shrinkage equivalent to 21% and 30% of initial pasta volume when drying at 40 °C and 80 °C, respectively. Shrinkage seems to be greater when pasta is dried at high temperatures, which could be explained by the glass transition that occurs at lower water content in high drying temperatures, and the hypothesis that shrinkage is greater in the rubbery state than in the glassy state (Rahman, 2001). This hypothesis is supported by products where shrinkage is greater for convective drying than for freeze drying, such as apples, bananas, potatoes and carrots (Krokida and Maroulis, 1997), soybeans (Qing-guo et al., 2006) and quince (Koç et al., 2008). Pasta shrinkage is an important phenomenon to consider since its intensity has a direct influence on the apparent density and porosity of the product. Although the impact of these properties on pasta quality has not been extensively studied yet, in the case of products such as fresh apples (Vincent, 1989), potatoes (Scanlon et al., 1998) and extruded

starch (Bhatnagar and Hanna, 1997), strong dependencies have been observed between these properties and the mechanical behavior of these products. In addition, the results from Waananen and Okos (1996) indicate that pasta porosity has an impact on the effective diffusion coefficients of water, and therefore on the speed at which the product dehydrates during drying. According to these authors, this result could be explained by a more important contribution of water diffusion in vapour form for porous pasta.

The generation of mechanical stress inside the product during dehydration also has to be considered in the modelling of pasta drying. This mechanical stress can cause the formation of cracks inside the product and thereby greatly affect its quality. Generally, crack formation is explained by non-uniform shrinkage of the pasta in the direction of mass transfer (Litchfield and Okos, 1988; Ponsart et al., 2003). This phenomenon is caused by the creation of a moisture gradient inside the pasta, thereby causing non-uniform shrinkage in the direction of water diffusion. This local shrinkage generates radial and tangential stresses inside the product, which can cause cracks to form when these stresses are greater than the maximum tolerance of the gluten network (Musielak, 1996; Ponsart et al., 2003). Glass transition may also play an important role in crack formation and propagation. During drying, the rate of moisture lost at the pasta surface is higher than at the center, such that the surface can be in a glassy state while the core is still in a rubbery state. This non-uniform glass transition induces significant variations of viscoelastic properties in the product, which can contribute to the creation of internal stresses (Cnossen et al., 2001; Takhar et al., 2006; Xing et al., 2007; Hundal and Takhar, 2010).

A more common practice adopted in the industry nowadays consists of drying pasta at high (around 80 ºC) or ultra-high (above 100 ºC) temperatures. The selection of high drying temperatures reduces the time required for the operation and can increase productivity. It is also generally accepted that drying under high temperatures gives less sticky, firmer and better quality pasta (De Noni and Pagani, 2010), which can be explained by the changes in the microstructure of the product during drying. High temperature drying promotes coagulation and aggregation of the gluten proteins, as supported by their lower solubility and the formation of large polymeric proteins at the expense of monomeric proteins (Lamacchia et al., 2007; Wagner et al., 2011). Protein coagulation prior to the cooking step leads to the development

of a strong and continuous gluten network surrounding starch granules (Zweifel et al., 2003; De Noni and Pagani, 2010). This gluten network acts as a barrier limiting water penetration, starch swelling and amylose leaching during cooking, resulting in pasta with better overall properties. High drying temperature could also impact starch-proteins interactions, which has been shown to greatly impact the product rheological properties (Edwards et al., 2002).

However, high temperatures favour the development of Maillard reactions, which give the product a brown colour that is generally not appreciated by consumers (Feillet et al., 2000; De Noni and Pagani, 2010). Furthermore, using high temperatures can affect the nutritional properties of pasta because of protein denaturation and reduced digestibility (De Zorzi et al., 2007; Petitot et al., 2010; De Noni and Pagani, 2010). These phenomena have to be considered when selecting drying conditions, especially when heat-sensitive ingredients, such as those with high omega-3 and protein content, are added to the product formulation.

2.3 Modelling pasta drying

2.3.1 Mass transfer

As shown in Fig. 2.1, three different shapes are generally considered in pasta modelling: cylindrical (spaghetti, vermicelli, etc.), tubular (macaroni, penne, etc.) and rectangular (lasagna, linguini, etc.). In most models, only the mass transfer in the smallest dimension of the pasta is considered and this transfer is usually described by a Fick-type law:

$$\frac{\partial M}{\partial t} = \frac{1}{r}\frac{\partial}{\partial r}\left(rD_{eff}\frac{\partial M}{\partial r}\right) \qquad \text{(cylinder or tube)} \qquad (2.1)$$

$$\frac{\partial M}{\partial t} = \frac{\partial}{\partial x}\left(D_{eff}\frac{\partial M}{\partial x}\right) \qquad \text{(rectangle)} \qquad (2.2)$$

where M represents the total moisture content (i.e., liquid + vapour) of the pasta, D_{eff} is the moisture effective diffusion coefficient, r is the radial coordinate, x is the coordinate for the thickness and t is the time. The effective diffusion coefficient D_{eff} represents a parameter that simultaneously describes the different mass transfer mechanisms involved, including the molecular diffusion of the water that can be in liquid or vapour form, water flow in a liquid

form caused by capillarity, and flow caused by pressure gradient (Datta, 2007). The models developed from Eqs. (2.1) and (2.2) are therefore semi-empirical and provide a simplified description of product dehydration compared with the more fundamental models based on the first principles for each of the components and phases of the system.

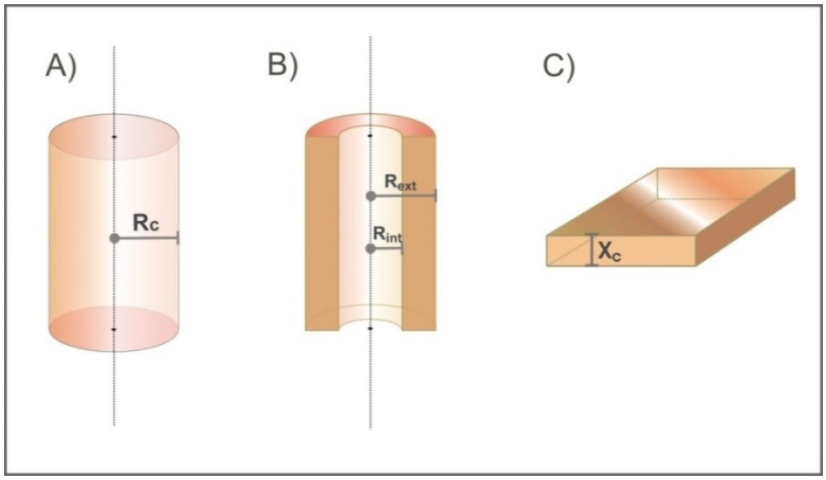

Figure 2.1. Schematic diagram of the three main shapes considered in modelling the drying of pasta (A- cylindrical; B- tubular and C- rectangular).

For one-dimensional models, the Fick-type law is usually solved using an initial condition and two boundary conditions. The initial condition refers to the uniformity of the moisture inside the pasta at the start of drying ($t = 0$):

$M = M_0$ for $0 < r < R_C$ or $R_{int} < r < R_{ext}$ (cylinder or tube) (2.3)

$M = M_0$ for $0 < x < X_C$ (rectangle) (2.4)

where M_0 represents the moisture content of the pasta at the start of drying, R_C is the radius of cylindrical pasta, R_{int} and R_{ext} are the internal and external radii of tubular pasta and X_C is the thickness of rectangular pasta. The boundary conditions vary according to the shape considered and model studied. These boundary conditions can be divided into three groups: (1) those where the water flux at a surface is specified; (2) those where the water content at a surface is specified; and (3) those where the water flux at a surface is described using a mass transfer coefficient and a surface moisture gradient. The boundary conditions of the first group are generally applied to cylindrical pasta based on their radial symmetry (Eq. 2.5), to rectangular pasta with two sides exposed symmetrically to the dryer environment (Eq. 2.6) or

to rectangular pasta where one side is placed on a plate and is considered to be isolated (Eq. 2.7):

$\frac{\partial M}{\partial r} = 0$ for $r = 0$ and $t > 0$ (cylinder) (2.5)

$\frac{\partial M}{\partial x} = 0$ for $x = \frac{X_C}{2}$ and $t > 0$ (rectangle) (2.6)

$\frac{\partial M}{\partial x} = 0$ for $x = 0$ and $t > 0$ (rectangle) (2.7)

The boundary conditions of the second group are applied when the external mass transfer resistance is neglected and, consequently, the time required for the pasta to reach an equilibrium moisture value M_E is negligible compared with the total drying time:

$M = M_E$ for $r = R_C$, R_{int} and/or R_{ext} and $t > 0$ (cylinder ou tube) (2.8)

$M = M_E$ for $x = 0$ and/or $x = X_C$ et $t > 0$ (rectangle) (2.9)

The boundary conditions for the third group are used in the models developed by Ponsart et al. (2003), Migliori et al. (2005a) and De Temmerman et al. (2007). In these models, the moisture flux at the pasta surface is described using a mass transfer coefficient K_m and one of these two driving forces: the difference between the moisture of the pasta at its surface and equilibrium moisture content M_E (Eqs. 2.10 and 2.11) or the difference between the concentration of water vapour at the surface of the pasta and inside the dryer (Eqs. 2.12 and 2.13):

$$-\rho_{app} D_{eff} \left.\frac{\partial M}{\partial r}\right]_{R_C, R_{int}\ or\ R_{ext}} = K_{m,\Delta M}\left(M_{R_C, R_{int}\ or\ R_{ext}} - M_E\right) \text{ (cylinder or tube)} \quad (2.10)$$

$$-\rho_{app} D_{eff} \left.\frac{\partial M}{\partial x}\right]_{X_C} = K_{m,\Delta M}\left(M_{X_C} - M_E\right) \text{ (rectangle)} \quad (2.11)$$

$$-\rho_{app} D_{eff} \left.\frac{\partial M}{\partial r}\right]_{R_C, R_{int}\ or\ R_{ext}} = K_{m,\Delta c}\left(c_{v,R_C, R_{int}\ or\ R_{ext}} - c_{v,\infty}\right) \text{ (cylinder or tube)} \quad (2.12)$$

$$-\rho_{app} D_{eff} \left.\frac{\partial M}{\partial x}\right]_{X_C} = K_{m,\Delta c}\left(c_{v,X_C} - c_{v,\infty}\right) \text{ (rectangle)} \quad (2.13)$$

where M_{R_c}, $M_{R_{ext}}$ and M_{X_c} represent pasta moisture (solid side) at the pasta-air interface, c_{v,R_c}, $c_{v,R_{ext}}$ and c_{v,X_c} are water vapour concentration (air side) at the pasta-air interface and ρ_{app} is the apparent density of the pasta. The water vapour concentration (air side) at the pasta-air interface $c_{v,R_C\,,R_{ext}or\;X_C}$ is calculated using an equation of state (such as the ideal gas law) and an activity coefficient a_w assuming a state of equilibrium at the interface (i.e., $y_v^{eq} = y_{v,R_C\,,R_{ext}or\;X_C}$):

$$Py_v^{eq} = p_w^0 a_w, \tag{2.14}$$

where P represents the pressure inside the dryer, y_v is the mole fraction of water vapour and p_w^0 is the water vapour pressure. The water activity coefficient is assumed to be dependent on the temperature T and the moisture content of the pasta. Many equations have been developed to relate these variables, and their accuracy for describing pasta dehydration isotherms has been studied by De Temmerman et al. (2008). The best results were obtained with an Oswin equation:

$$\overline{M} = (A_1 - A_2 T)\left[\frac{a_w}{1-a_w}\right]^{(B_1+B_2T)}, \tag{2.15}$$

where A_1= 0.138, A_2 = 10.4 x 10^{-4}, B_1 = 0.396, B_2 = 11.6 x 10^{-4}, $\overline{M}$ is the pasta average moisture content (according to r or x) and T is in ºC.

The choice of the boundary conditions is a determining factor in the ability to solve the Fick-type law and obtain an analytical solution. Table 2.1 shows the analytical solutions obtained for several pairs of boundary conditions. These solutions were developed by the separation of variables method and are valid under the following assumptions: (1) the initial moisture profile of the pasta is uniform or analytical; (2) pasta shrinkage is negligible and (3) the effective diffusion coefficient is constant for the considered moisture range.

Table 2.1. Fick-type law analytical solutions (Eqs. 2.1 and 2.2) for different shapes and boundary conditions (Crank, 1975)

Shape	First Boundary Condition	Second Boundary Condition	Analytical Solution
Cylinder	For $r = 0$ and $t > 0$: $\frac{\partial M}{\partial r} = 0$	For $r = R_C$ and $t > 0$: $M = M_E$	$\frac{\bar{M}-M_E}{M_0-M_E} = \sum_{n=1}^{\infty} \frac{4}{\beta_n^2} \exp\left(-\frac{\beta_n^2 D_{eff} t}{R_C^2}\right)$
	For $r = 0$ and $t > 0$: $\frac{\partial M}{\partial r} = 0$	For $r = R_C$ and $t > 0$: $-\rho_{app} D_{eff} \frac{\partial M}{\partial r}\Big]_{R_C} = K_{m,\Delta M}\left(M_{R_C} - M_E\right)$	$\frac{\bar{M}-M_E}{M_0-M_E} = \sum_{n=1}^{\infty} \frac{4Bi^2}{\Upsilon_n^2(\Upsilon_n^2+Bi^2)} \exp\left(-\frac{\Upsilon_n^2 D_{eff} t}{R_C^2}\right)$, where B_i is the Biot number: $Bi = \frac{R_C k_{m,\Delta M}}{D_{eff}}$ and Υ the roots of the equation: $\Upsilon J_1(\Upsilon) - Bi J_0(\Upsilon) = 0$, with J_0 et $J_1$the Bessel functions of the first kind and orders zero and one, respectively.
Tube	For $r = R_{int}$ and $t > 0$: $M = M_E$	For $r = R_{ext}$ and $t > 0$: $M = M_E$	$\frac{\bar{M}-M_E}{M_0-M_E} = \frac{4}{{R_{ext}}^2-{R_{int}}^2} \sum_{n=1}^{\infty} \frac{J_0(R_{int}\phi_n)-J_0(R_{ext}\phi_n)}{\phi_n^2[J_0(R_{int}\phi_n)+J_0(R_{ext}\phi_n)]} \exp\left(-\phi_n^2 D_{eff} t\right)$, where ϕ_n are the positive roots of the equation : $H_0(R_{int}\phi_n) = J_0(R_{int}\phi_n)Y_0(R_{ext}\phi_n) - J_0(R_{ext}\phi_n)Y_0(R_{int}\phi_n)$, with J_0 et Y_0 the Bessel functions of the first and second kind.
Rectangle	For $x = {X_c}/{2}$ and $t > 0$: $\frac{\partial M}{\partial x} = 0$	For $x = X_C$ and $t > 0$: $M = M_E$	$\frac{\bar{M}-M_E}{M_0-M_E} = \frac{8}{\pi^2} \sum_{n=0}^{\infty} \frac{1}{(2n+1)^2} \exp\left[-\frac{(2n+1)^2\pi^2 D_{eff} t}{4\left({X_c}/{2}\right)^2}\right]$
	For $x = 0$ and $t > 0$: $\frac{\partial M}{\partial x} = 0$	For $x = X_C$ and $t > 0$: $M = M_E$	$\frac{\bar{M}-M_E}{M_0-M_E} = \frac{8}{\pi^2} \sum_{n=0}^{\infty} \frac{1}{(2n+1)^2} \exp\left[-\frac{(2n+1)^2\pi^2 D_{eff} t}{4(X_c)^2}\right]$

2.3.1.1 Mass transfer coefficients

The use of boundary conditions (2.10)-(2.13) requires the value of the mass transfer coefficient K_m to be known. In the models developed by Migliori et al. (2005a) and De Temmerman et al. (2007), the value of the mass transfer coefficients $K_{m,\Delta c}$ is estimated using Colburn factors for the mass (J_m) and heat (J_h) transfer. These factors are related to the *Nu*, *Sh*, *Sc* and *Pr* numbers of the system according to the following definitions:

$$J_m = \frac{Sh}{ReSc^{1/3}} \tag{2.16}$$

$$J_h = \frac{Nu}{RePr^{1/3}} \tag{2.17}$$

The mass transfer coefficient can then be determined using the Chilton-Colburn analogy according to which, for the system being considered, $J_m = J_h$. The following equation is thus obtained:

$$\frac{h}{K_{m,\Delta c}} = \rho_a C_{p,a} \left(\frac{\alpha_{h,a}}{D_{v-a}}\right)^{2/3} \tag{2.18}$$

In Eq. (2.18), the density (ρ_a), heat capacity ($C_{p,a}$) and thermal diffusivity of the air ($\alpha_{h,a}$), as well as the diffusion coefficient of water in the air (D_{v-a}), are dependent on the temperature. As a function of the temperature inside the dryer T_∞, Eq. (2.18) becomes (De Temmerman et al., 2007):

$$\frac{h}{K_{m,\Delta c}} = -208.09 \ln(T_\infty) + 1795.4 \tag{2.19}$$

Eq. (2.19) makes it possible to determine the value of the mass transfer coefficient when the heat transfer coefficient *h* is known. In the model developed by De Temmerman et al. (2007), the value of coefficient *h* is determined experimentally. In the model by Migliori et al. (2005a), the following two-parameter equation is used:

$$J_h = aRe^b, \tag{2.20}$$

where, for the conditions and geometry (tubular) considered, a = 0.4096 and b = -0.4485. However, the model developed by Migliori et al. (2005a) initially led to lower moisture results

compared with the experimental data. It was assumed that this difference was caused by an overestimate of the mass transfer coefficient. New optimized transfer coefficients were then calculated in order to minimize the squared error between the experimental data and the data derived from the model. A ratio between the optimized coefficients and the initial coefficients of 0.0085 was obtained. However, the hypothesis that the divergence between the theoretical and experimental results was caused solely by a poor initial estimate of the mass transfer coefficient was not verified.

In the case of pasta, few data are available to estimate the value of the mass transfer coefficient when the difference between the moisture of pasta (solid side) at the surface and the equilibrium moisture content is used as the driving force (Eqs. 2.10 and 2.11). It does not seem possible to relate this coefficient to the value for the mass transfer coefficients $K_{m,\Delta c}$ because of the non-linearity between the moisture content of the pasta and the relative humidity of the dryer (Eqs. 2.14 and 2.15). However, some values for these coefficients are available for the drying of different products with a similar shape. For instance, a ratio $K_{m,\Delta M}/\rho_{app}$ of 3.798 x 10^{-7} m s^{-1} has been calculated for the drying of rice (modelled as cylinders with a diameter of 2.34 mm and an infinite length) at 60 °C and under an air velocity of 1.5 m s^{-1} (Silva et al., 2010).

2.3.1.2 Effective moisture diffusion coefficients

Solving the Fick-type law using its initial condition and its two boundary conditions also requires knowledge of the value of the effective diffusion coefficient D_{eff} of water in the pasta. In the model developed by Migliori et al. (2005a), the value of this coefficient is determined experimentally for pasta with a moisture content greater than 0.2 (w.b.) using nuclear magnetic resonance (NMR). In the absence of experimental measurements, the value of this coefficient can still be estimated using correlations listed in the literature. Table 2.2 presents the correlations that have been developed specifically for pasta, along with the extrusion and experimental drying conditions used to develop these equations. In addition, Table 2.3 presents the values of the effective diffusion coefficients obtained from these correlations for drying under typical conditions (T_∞ = 80 °C, *RH* = 65%, P_∞ = 101 kPa, *M* =

0.30 and $\varepsilon = 0.10$). This table also presents the effective diffusion coefficients obtained when more extreme values of these five parameters are applied one by one compared with the reference scenario.

Table 2.2. Empirical correlations developed to determine the value of the effective diffusion coefficient and experimental conditions validated

Equation	Parameters	Extrusion Conditions	Drying Conditions			Reference
			T **(°C)**	***RH*** **(%)**	***P*** **(kPa)**	
$D_{eff} = \left[A\exp\left(\frac{-E_a}{RT_\infty}\right)[1-\exp(-BM^C)+M^D]\right] * 10^{-12}$	$E_a = 26.0\frac{kJ}{mol}$ $A = 2.9320\ x\ 10^5$ $B = 7.9082\ x\ 10^{14}$ $C = 1.5706\ x\ 10^1$ $D = 6.8589\ x\ 10^{-1}$	Adjustable ribbon die of 2-3 mm thickness	40-85	1-94	101	Litchfield and Okos, 1992
$D_{eff} = \left(C'_{10} + \varepsilon\frac{C'_{20}}{P_\infty}\right)\exp\left[-\frac{E_a+E_b}{RT_\infty}\right]$	$E_a = 22.6\frac{kJ}{mol}$ $E_b = [6.0\exp(-20M)]\frac{kJ}{mol}$ $C'_{10} = 1.2\ x\ 10^{-7}\frac{m^2}{s}$ $C'_{20} = 8\ x\ 10^{-5}\frac{m^2}{s}$	Circular Teflon die of 3.18, 4.76 and 5.56 mm	40-122	1-94	77-202	Waananen and Okos, 1996
$D_{eff} = \left[\exp\left(\frac{-E_a}{RT_\infty} - ARH - B\right)\right] * 10^{-4}$	$E_a = 11.4\frac{kJ}{mol}$ $A = 0.0221$ $B = 8.635$	Circular die of 2.5 mm	40-80	65-85	101	Villeneuve and Gelinas, 2007
$D_{eff} = Aexp\left[-B\left(\frac{1}{T_\infty} - \frac{1}{T_{Ref}}\right)\right]\exp(CM)$	$T_{Ref} = 293\ K$ $A = 1.2\ x\ 10^{-11}$ $B = 3036.95$ $C = 6.46\ x\ 10^{-3}$	Laminated pasta of 1.3 mm thickness	40-90	3-12	101	De Temmerman et al., 2007

Table 2.3. Effective moisture diffusion coefficients (x 10^{-12}) from the correlations presented in Table 2.2 and for the following reference scenario: T_∞ = 80 °C, RH = 65%, P_∞ = 101 kPa, M = 0.30 and ε = 0.10

Parameter		**Equation**				**Average ± SD**
		Litchfield and Okos, 1992	Waananen and Okos, 1996	Villeneuve and Gelinas, 2007	De Temmerman et al., 2007	
Base Case		45	57	87	70	65 ± 18
Drying temperature (°C)	40	14	21	53	23	28 ± 17
	120	112	125	129	168	133 ± 24
	$\lvert\Delta D_{eff}\rvert$	98	104	76	145	105 ± 29
Relative humidity (%)	0	-	-	365	-	365
	100	-	-	40	-	40
	$\lvert\Delta D_{eff}\rvert$	-	-	325	-	325
Pressure (Pa)	77 000	-	58	-	-	58
	222 000	-	55	-	-	55
	$\lvert\Delta D_{eff}\rvert$	-	3	-	-	3
Pasta moisture (kg H_2O kg dry $solid^{-1}$)	0.1	11	-	-	70	41
	0.5	51	-	-	70	31
	$\lvert\Delta D_{eff}\rvert$	39	-	-	0	20
Pasta porosity (%)	0	-	54	-	-	54
	25	-	62	-	-	62
	$\lvert\Delta D_{eff}\rvert$	-	8	-	-	8

Basically, the equations in Table 2.2 have a similar structure by the description of the dependence of the effective diffusion coefficient for the temperature based on an Arrhenius equation of the form $D_{eff} = A\exp(-E_a/RT_\infty)$. An increase in the drying temperature is therefore related to an increase in the effective diffusion coefficients of a magnitude determined by the value of the activation energy E_a. According to the data presented in Table 2.3, rising the drying temperature from 40 °C to 120 °C would result in an increase in the effective diffusion coefficient in the order of 10^{-10} m^2 s^{-1}. For illustration purposes, according to the analytical solution of the Fick-type law for cylindrical pasta under boundary conditions (5) and (8) (see Table 2.1), the time required to reduce the moisture from 0.5 to 0.14 (d.b.) in pasta 2.5 mm in diameter with an equilibrium moisture content of 0.1 would be about 370 minutes at 40 °C and 80 minutes at 120 °C.

Depending on the correlation considered, terms are added to the Arrhenius equation to describe the impact of additional parameters on D_{eff}, including the relative humidity maintained inside the dryer. In general, an increase in relative humidity is associated with a decrease in the value of the effective diffusion coefficients. In the correlation developed by Villeneuve and Gelinas (2007), this effect is taken into account by introducing an additional term inside the exponential. According to their sensitivity analysis using this equation, the effect of relative humidity on the effective diffusion coefficient value would be greater than the effect of temperature. However, this result contradicts those of Andrieu and Stamatopoulos (1986) and Litchfield and Okos (1992), whose experimental data suggest that the impact of this parameter tends to be negligible. According to Villeneuve and Gelinas (2007), these differences could be attributed to their drying system that consists of an environmental chamber in which moisture is controlled using an electric steam generator and a cooling circuit. This system could allow more precise, stable and efficient control of relative humidity compared with systems where this parameter is measured using dry-bulb and wet-bulb thermometers and controlled with salt solutions or generators located in separate compartments.

In the equations developed by Litchfield and Okos (1992) and De Temmerman et al. (2007), terms are also added to the Arrhenius equation to describe the dependence of the effective diffusion coefficient for pasta moisture. In general, studies suggest that the value of

the effective diffusion coefficients decreases during drying as the amount of free water (i.e., $M - M_E$) diminishes. Nevertheless, these variations can sometimes be neglected within certain water content ranges (Datta, 2007). In the model developed by Villeneuve and Gelinas (2007), the value of the effective diffusion coefficient is considered to be constant throughout drying. This hypothesis seems to be supported by the correlation from De Temmerman et al. (2007) according to which a negligible difference in the value of the effective diffusion coefficients is obtained within the moisture range of 0.1 to 0.5 (d.b.) at the drying conditions considered. The results of Andrieu and Stamatopoulos (1986) suggest that the variation of diffusion coefficients is negligible for the following three moisture ranges (d.b.): $M > 0.27$; $0.27 > M > 0.18$ and $0.18 > M > M_E$. According to their experimental data of pasta Young's modulus as a function of its water content, these three ranges match the transition of pasta from a rubbery state to a transient state and then to a glassy state. Consequently, it is possible that the variation in effective diffusion coefficients during drying could be partially attributed to changes in the rheological properties of the pasta. As shown in Table 2.3, a difference of about 40×10^{-12} m^2 s^{-1} can be observed between the value of the effective diffusion coefficient at the start and end of drying for a temperature of 80 °C. This difference is an order of magnitude similar to the one calculated using the Litchfield and Okos (1992) correlation for moisture contents between 0.5 and 0.1 (d.b.) at this same temperature.

Waananen and Okos (1996) studied the effect of porosity and pressure on the effective diffusion coefficient. Their results indicate that the value of the effective diffusion coefficients is proportional to the porosity of the pasta and inversely proportional to the pressure maintained inside the dryer. This effect could be attributed to a larger contribution of water diffusion in the form of vapour for pasta with a high porosity and dried at low pressures. However, according to the data in Table 2.2, the sensitivity of the effective diffusion coefficients for these two parameters seems to be lower than their sensitivity for temperature, relative humidity and water content of the pasta.

Overall, according to the results presented in Table 2.3, a difference of a little more than one order of magnitude in the value of D_{eff} is observed depending on the equation used. Many reasons could contribute to explaining this degree of variability, including:

(1) The type of experimental drying system used in developing the equations. This parameter can influence the precision with which the operating conditions are controlled, and can have an impact on the parameters that are not considered in the models such as air velocity at the surface of the pasta.

(2) The experimental drying conditions used in developing the equations. These parameters can influence the precision of the value obtained for the effective diffusion coefficients, particularly when the equations are used to estimate the effective diffusion coefficient in drying conditions that are different from those considered experimentally.

(3) The method used to calculate D_{eff} from experimental data. In the studies considered, the main variable measured during drying is the evolution of the water content of the pasta. The value of the effective diffusion coefficients is then determined by minimizing the error between the experimental water content data and the water content predicted from a model. Consequently, the value of D_{eff} is directly dependant on the model used. For example, the correlations from Litchfield and Okos (1992), Waananen and Okos (1996) and Villeneuve and Gelinas (2007) were developed using D_{eff} values obtained from the analytical solutions of the Fick-type law (Table 2.1), while the experimental values of D_{eff} from the De Temmerman et al. (2007) correlation were determined using a model where the external mass transfer resistance, heat transfer and pasta shrinkage were considered.

2.3.2 Heat transfer

Heat transfer is treated differently according to the model studied. In the models developed by Migliori et al. (2005a) and De Temmerman et al. (2007), heat transfer is treated according to a unidirectional energy balance equation:

$$\rho_{app} C_{p,app} \frac{\partial T}{\partial t} = \frac{1}{r} \frac{\partial}{\partial r}\left(r k_h \frac{\partial T}{\partial r}\right) \quad \text{(cylinder or tube)} \quad (2.21)$$

$$\rho_{app} C_{p,app} \frac{\partial T}{\partial t} = \frac{\partial}{\partial x}\left(k_h \frac{\partial T}{\partial x}\right), \quad \text{(rectangle)} \quad (2.22)$$

where $C_{p,app}$ is the specific heat capacity of pasta and k_h is its thermal conductivity. This equation is valid for products that have negligible internal water evaporation, since the evaporation term is included in the boundary condition (Eq. 2.27), and not in the energy balance itself. Similarly to the mass transfer modelling, the initial condition required to solve the heat balance equation is deduced from the hypothesis of a uniform initial temperature T_0. For cylindrical or rectangular pasta, a first boundary condition generally results from the symmetry of the product (Eqs. 2.23 and 2.24) or when there is an isolated surface (Eq. 2.25):

$$\frac{\partial T}{\partial r} = 0 \text{ for } r = 0 \text{ and } t > 0 \qquad \text{(cylinder)} \qquad (2.23)$$

$$\frac{\partial T}{\partial x} = 0 \text{ for } x = \frac{X_c}{2} \text{ and } t > 0 \qquad \text{(rectangle)} \qquad (2.24)$$

$$\frac{\partial T}{\partial x} = 0 \text{ for } x = 0 \text{ and } t > 0 \qquad \text{(rectangle)} \qquad (2.25)$$

The boundary condition at the surface of the product is described based on a heat transfer coefficient:

$$-k_h \frac{\partial T}{\partial r}\Big]_{R_C, R_{int}\ or\ R_{ext}} = h\left(T_{R_C, R_{int}\ or\ R_{ext}} - T_\infty\right) - \lambda N_w^{ext} \qquad \text{(cylinder or tube)} \qquad (2.26)$$

$$-k_h \frac{\partial T}{\partial r}\Big]_{X_C} = h\left(T_{X_C} - T_\infty\right) - \lambda N_w^{ext} \qquad \text{(rectangle)} \qquad (2.27)$$

where λ represents water latent heat of vaporization and N_w^{ext} is the water flow at the solid-air interface. Depending on the type of dryer, a term for the radiation (proportional to $T_{R_C, R_{ext} or X_C}^4 - T_\infty{}^4$) can also be incorporated in the boundary condition (De Temmerman et al., 2007).

Modelling the temperature based on Eqs. (2.21)-(2.27) requires the knowledge of the specific heat capacity and thermal conductivity of pasta. For the specific heat capacity, Migliori et al. (2005a) and De Temmerman et al. (2007) assume that it is equivalent to that of the main components (water, starch and proteins) weighted according to their mass fraction (z_i):

$$C_{p,app} = \sum z_i C_{p,i}, \qquad (2.28)$$

where $C_{p,w} = 4184$, $C_{p,starch} = 5.737T + 1328$ and $C_{p,proteins} = 6.329T + 1465$.

Thermal conductivity is determined by the following equation (Saravacos and Maroulis, 2001):

$$k_h = \frac{0.273}{1+M} + \frac{0.8M}{1+M} \exp\left[\frac{-2700}{R}\left(\frac{1}{T} - \frac{1}{60}\right)\right], \quad (2.29)$$

where R is the ideal gas constant (J mol^{-1} K^{-1}) and T is the temperature in ºC.

In the model developed by Ponsart et al. (2003), the internal heat transfer resistance is neglected and the internal temperature of pasta is therefore assumed to be uniform. The temperature variation is then determined from an energy balance that quantifies the difference between the heat lost by water vaporisation and the heat absorbed by convection at the surface of the pasta:

$$\frac{dT}{dt} = \frac{S_v \lambda K_{m,\Delta p}}{\rho_s\left(C_{p,s} + C_{p,s}\overline{M}\right)}\left[65(T_\infty - T) - \left(p_w^0 - p_{v,\infty}\right)\right], \quad (2.30)$$

where S_v represents the surface/volume ratio of the product, p_w^0 is the vapour pressure of pasta at its surface, $K_{m,\Delta p}$ is the mass transfer coefficient and $p_{v,\infty}$ is the partial pressure of the water vapour inside the dryer.

Finally, in the models developed by Andrieu and Stamatopoulos (1986), Litchfield and Okos (1992), Villeneuve and Gelinas (2007) and De Temmerman (2008), heat transfer is considered to be substantially faster than mass transfer and pasta temperature is thus assumed to be equivalent to the dryer temperature.

2.3.3 Other properties considered

2.3.3.1 Shrinkage

In the models developed by Ponsart et al. (2003) and De Temmerman et al. (2007), shrinkage is considered by solving the Fick-type law in Lagrangian coordinates (ζ):

$$\frac{\partial M}{\partial t} = \frac{1}{\xi}\frac{\partial}{\partial \xi}\left[\left(\frac{D_{eff}}{(1+\alpha_{vol}M)}\xi\right)\frac{\partial M}{\partial \xi}\right] \quad \text{(cylinder or tube)} \quad (2.31)$$

$$\frac{\partial M}{\partial t} = \frac{\partial}{\partial \xi}\left[\left(\frac{D_{eff}}{(1+\alpha_{vol}M)^2}\right)\frac{\partial M}{\partial \xi}\right] \quad \text{(rectangle)} \quad (2.32)$$

where α_{vol} represents the volumetric shrinkage coefficient. This coefficient is defined by the following equation:

$$\frac{\rho_{app}}{\rho_s} = \frac{1+\bar{M}}{1+\alpha_{vol}\bar{M}} \quad (2.33)$$

The apparent density ρ_{app} and the density of the dry matter ρ_s can be linked to the apparent volume of the pasta (V_{app}), to the mass (m_s) of the dry matter and to the volume (V_s) of the dry matter using the following definitions:

$$\rho_{app} = \frac{m_s(1+\bar{M})}{V_{app}} \quad (2.34)$$

$$\rho_s = \frac{m_s}{V_s} \quad (2.35)$$

Substituting these two definitions in Eq. (2.33) makes it possible to link the apparent volume of the pasta to its moisture content:

$$V_{app} = V_s(1 + \alpha_{vol}\bar{M}) \quad (2.36)$$

Consequently, the description of the mass transfer in Lagrangian coordinates based on this definition of the volumetric shrinkage coefficient is valid only under the hypothesis of a linear relation between pasta shrinkage and water content. This hypothesis is supported by experimental results from Andrieu et al. (1989). However, these results were obtained after fresh pasta was placed in different desiccators at room temperature, which diverges significantly from the drying process used in the industry. Linear relations between shrinkage and water content were also observed in the drying of potatoes (Wang and Brennan, 1995), carrots (Krokida and Maroulis, 1997) and Japanese noodles (Inazu et al., 2005), among others.

In the model developed by De Temmerman et al. (2007), the volumetric shrinkage coefficient is considered to be equivalent to the ratio between the density of the pasta dry matter and the density of the water (ρ_w):

$$\alpha_{vol} = \frac{\rho_s}{\rho_w} \quad (2.37)$$

The density of the water can be linked to the moisture and mass of pasta dry matter using the following equation:

$$\rho_w = \frac{m_s \bar{M}}{V_w}, \tag{2.38}$$

where V_w represents the volume occupied by the water. Substituting Eqs. (2.37) and (2.38) in Eq. (2.36) gives the following:

$$V_{app} = V_s + V_w \tag{2.39}$$

Consequently, the hypothesis in which the volumetric shrinkage coefficient is equivalent to the ratio between the dry matter and water densities is valid only for non-porous pasta, since the volume occupied by air (V_{air}) is not included in Eq. (2.39). Shrinkage is also considered to be ideal, i.e., the volume of water lost is assumed to be directly equivalent to the shrinkage.

In the model developed by Mercier et al. (2011b), shrinkage is considered using a dimensionless coefficient (η) describing the fraction of water lost during drying that is replaced by air inside the gluten network:

$$\eta = 1 - \frac{V_{app,0} - V_{app}}{V_{w,0} - V_w} \quad (\text{for } t > 0) \tag{2.40}$$

Substituting Eqs. (2.34) and (2.38) in Eq. (2.40) makes it possible to develop a relation between the evolution of the apparent volume and water content of the pasta during drying:

$$V_{app} = V_{app,0}[1 - \beta(M_0 - \bar{M})], \tag{2.41}$$

where: $\beta = \frac{1-\eta}{\rho_w / \rho_{app,0}(1+M_0)}$

Thus, Mercier et al. (2011b) also assume a linear relation between the evolution of the apparent volume of pasta and its water content. However, shrinkage is not assumed as ideal since the dimensionless coefficient is calculated from experimental measurements of the apparent density of the pasta at the start and end of drying. Values of 0.28 ± 0.03 and 0.15 ± 0.01 of coefficient η for pasta dried at 40 °C and 80 °C were obtained, respectively.

In the model developed by Migliori et al. (2005a), evolution of the pasta radius during drying is described using the following equation:

$$R_C = R_{C,0}[1 + \alpha_{rr}(\bar{U} - U_0)], \quad (2.42)$$

where α_{rr} represents the radial shrinkage coefficient and U is the moisture content on a wet basis. In this model, a constant value of 0.42 is calculated for this parameter based on experimental data from Andrieu et al. (1989). However, the value of this parameter is expected to change with temperature. Furthermore, no experimental data is available to validate the assumption that the shrinkage is a linear function of the water loss for the entire range of moisture content usually encountered during pasta drying.

For cylindrical pasta ($V_{app} = \pi {R_C}^2 L$), Eq. (2.42) can be rewritten to express the evolution of pasta volume as a function of its moisture content on a dry basis:

$$V_{app} = \frac{L}{L_0} V_{app0} \left[1 + \alpha_{rr}\left(\frac{\bar{M}}{1+\bar{M}} - \frac{M_0}{1+M_0}\right)\right]^2 \quad (2.43)$$

Consequently, the evolution of pasta radius based on Eq. (2.42) is valid for a non-linear relation between pasta volume and water content. Under most conditions, using Eq. (2.42) would indicate that pasta shrinkage is less important at the end of drying than at the beginning for an equivalent loss of water. Using this equation to estimate the variation of pasta volume during drying also requires the knowledge of longitudinal shrinkage. According to experimental data from Mercier et al. (2011b) compiled for drying at 40 °C and 80 °C, longitudinal shrinkage contributes to about 30% of the volumetric shrinkage of pasta.

2.3.3.2 Porosity and density

Mercier et al. (2011b) studied the evolution of the density and gas phase porosity (ε^g) of pasta fortified with pea protein concentrate during drying. The following porosity definition was used:

$$\varepsilon^g = 1 - \frac{V_{sem} + V_{PPC} + V_w}{V_{app}}, \quad (2.44)$$

where V_{sem} and V_{PPC} represent the volumes occupied by the semolina and pea protein concentrate, respectively. Using the definitions for the shrinkage coefficient η (Eq. 2.40), water density (Eq. 2.38) and apparent density of pasta (Eq. 2.34), the following equations were developed for cylindrical pasta:

$$\rho_{app}(t) = \frac{\rho_w(1+\Delta M\delta+M_E)}{\Delta M(\eta-1)(1-\delta)+\nu(1+M_0)} \tag{2.45}$$

$$\varepsilon^g(t) = 1 - \frac{\rho_w}{\Delta M(\eta-1)(1-\delta)+\nu(1+M_0)}\left[\left(\frac{1}{(1+1/\psi)\rho_{sem}} + \frac{1}{(1+\psi)\rho_{PPC}}\right) + \frac{\Delta M\delta+M_E}{\rho_w}\right], \tag{2.46}$$

where $\delta = \frac{\bar{M}-M_E}{M_0-M_E} = \sum_{n=1}^{\infty}\frac{4}{\beta_n^2}\exp\left(-\frac{\beta_n^2 D_{eff}t}{R_C^2}\right)$, $\nu = \frac{\rho_w}{\rho_{app,0}}$, $\Delta M = M_0 - M_E$, $\psi = \frac{m_{sem}}{m_{PPC}}$, m_{sem} is the mass of the semolina, m_{PPC} is the mass of the pea protein concentrate and β_n are the roots of the Bessel function of the first kind and zero order. These equations make it possible to predict the evolution of the density and porosity of pasta during drying using the effective diffusion coefficient. They were developed for cylindrical pasta, but they can also be used for tubular or rectangular pasta by substituting the δ with the term equivalent to $\frac{\bar{M}-M_E}{M_0-M_E}$ in the analytical solutions of Table 2.1. For standard white pasta, Eq. (2.46) can be used considering the value of ψ as equivalent to $+\infty$.

2.3.3.3 Mechanical stress

Some drying conditions can promote the development of cracks inside pasta, which can greatly affect the quality of the final product. To determine the risks of crack formation based on drying conditions, Ponsart et al. (2003) developed a model to estimate the mechanical stress generated inside cylindrical pasta. In this model, it is assumed that the mechanical stress is a consequence of the pasta differential shrinkage. This shrinkage is described using the volumetric shrinkage coefficient α_{Vol} according to the following differential equation (Eq. 2.47) and initial and boundary conditions (Eqs. 2.48 and 2.49):

$$r\frac{\partial r}{\partial t} = \alpha_{Vol}D_{eff}\left(\frac{r}{\xi(1+\alpha_{vol}M)}\right)^2 \xi\frac{\partial M}{\partial \xi} \tag{2.47}$$

$r = \xi$ for $t = 0$ (2.48)

$\xi = 0$ for $r = 0$ (2.49)

Numerical resolution of this partial differential equation makes it possible to quantify the local strain of pasta from radial position. Two local strains are calculated, radial (τ_{rr}) and tangential ($\tau_{\theta\theta}$):

$$\Delta\tau_{rr} = \frac{\partial\Delta\Gamma}{\partial r} \quad (2.50)$$

$$\Delta\tau_{\theta\theta} = \frac{\Delta\Gamma}{r} \quad (2.51)$$

where : $\Gamma = r_t - r_0$ and $\Delta\Gamma = r_{t+\Delta t} - r_t$

The radial (σ_{rr}) and tangential ($\sigma_{\theta\theta}$) stresses are then calculated from the strains:

$$\Delta\sigma_{rr} = \gamma\Delta tr\tau + 2\mu\Delta\tau_{rr} - \kappa\Phi\Delta M \quad (2.52)$$

$$\Delta\sigma_{\theta\theta} = \gamma\Delta tr\tau + 2\mu\Delta\tau_{\theta\theta} - \kappa\Phi\Delta M, \quad (2.53)$$

where : $\Phi = \frac{1}{\alpha_{vol}+M}$

In Eqs. (2.52) and (2.53), γ and μ represent the Lame coefficients derived from pasta effective Young's modulus and Poisson's coefficient (measured experimentally) and κ is the mechanical compressibility coefficient. The model therefore makes it possible to estimate the compressive and tensile stresses in pasta as a function of radial position during drying. It is then assumed that cracks will form when the generated stresses exceed a tolerance limit σ_{lim}. However, the model was not validated using experimental data, and no consideration was given to the potential impact of glass transition on the formation and the propagation of cracks.

2.4 Experimental validation

2.4.1 Moisture profile

Litchfield and Okos (1992), Migliori et al. (2005), De Temmerman et al. (2007), De Temmerman et al. (2008) and Mercier et al. (2011b) experimentally validated the capacity of their model to predict the evolution of water content in pasta during drying. Table 2.4 summarizes the structure of these models with respect to the shape of the pasta, diffusion law, boundary conditions, heat transfer description, shrinkage description and method for calculating the effective diffusion coefficients. Table 2.5 reports the experimental extrusion and drying conditions used in validating the models, and the goodness of fit between the model predictions and experimental data.

Table 2.4. Structure of models describing pasta drying where experimental validation has been done

Model	Shape	Mass Transfer				Heat Transfer		Shrinkage
		Equation	Boundary Conditions	D_{eff}	K_m	Equation	h	
Litchfield and Okos, 1992	Rectangular	Eq. (2.2)	Eq. (2.6) and (2.9)	Table 2.2: correlation by Litchfield and Okos (1992)	-	Neglected	-	Neglected
Migliori et al., 2005a	Tubular	Eq. (2.1)	Eq. (2.12) for the interior and exterior surface of tubular pasta	Value determined by NMR for pasta with $U > 0.2$; Table 2.2, correlation by Waananen and Okos (1996) for $U \leq 0.2$	K_m^{ext}: Optimization by the non-linear least squares method; K_m^{int}: Eqs. (2.16)-(2.17), assuming that the air velocity inside tubular pasta is 3 times lower than the external velocity	Eq (2.21)	Eq. (2.20)	Eq. (2.42), with $\alpha_{rr} = 0.42$
De Temmerman et al., 2007	Rectangular	Eq. (2.32)	Eqs. (2.7) and (2.13)	Table 2.2: correlation by De Temmerman et al. (2007)	Eq. (2.19)	Eq (2.22) in Lagrangian coordinates	Measured using a heat flux sensor	Eqs. (2.32) and (2.33), with $\alpha_{vol} = \frac{\rho_S}{\rho_w}$
De Temmerman et al., 2008	Cylindrical	Eq. (2.31)	Eqs. (2.5) and (2.12)	Table 2.2: correlation by De Temmerman et al. (2007)	Eq. (2.19)	Neglected	Measured using a heat flux sensor	Eqs. (2.31) and (2.33), with $\alpha_{vol} = \frac{\rho_S}{\rho_w}$
Mercier et al., 2011b	Cylindrical	Eq. (2.1)	Eqs. (2.5) and (2.8)	Optimization by the non-linear least squares method	-	Neglected	-	Neglected in mass transfer description

Table 2.5. Experimental conditions validated for the models of Table 2.4 and goodness of fit between experimental and predicted data

Model	Extrusion Conditions	Drying System	Drying Conditions			Experimental Data Measured	Goodness of fit
			T (°C)	RH (%)	P (kPa)		
Litchfield and Okos, 1992	Adjustable ribbon die of 2-3 mm thickness; fresh pasta equilibrated 24h at 4 °C	Convection dryer in which pasta is hung vertically on poles	40-85	1-94	101	Evolution of pasta moisture content M at different positions according to x during drying	Overestimation of the moisture gradient inside pasta
Migliori et al., 2005a	Circular die of 5 mm	Static oven in which pasta is placed horizontally on plates	70-80	58-68	101	Evolution of pasta average moisture content $\overline{U}$ during drying	Good estimate of the evolution of average pasta moisture content
De Temmerman et al., 2007	Laminated pasta of 1.3 mm thickness; fresh pasta equilibrated 24h at 4 °C and 80% RH	Convection oven with laminar air flow in which pasta is placed horizontally on aluminum sheets	40-100	0-80	101	Evolution of pasta average moisture content $\overline{M}$ during drying	Good estimate of the evolution of average pasta moisture content
De Temmerman et al., 2008	Circular die of 4.0 mm thickness; fresh pasta equilibrated 24h at 4 °C and 80% RH	Low-temperature oven	10-90	0.1-15	101	Evolution of pasta average moisture content $\overline{M}$ during drying	Good estimate of the evolution of average pasta moisture content
Mercier et al., 2011b	Circular die of 2.5 mm	Environmental chamber in which pasta is hung vertically on poles	40-80	65	101	Evolution of pasta average moisture content $\overline{M}$ during drying	Good estimate of the evolution of average pasta moisture content

The results of most studies therefore suggest that the evolution in average water content of pasta $\overline{M}$ during drying is Fickian and can be described using the equations presented in section 2.3. Furthermore, the results from Mercier et al. (2011b) indicate that the evolution in average moisture content of pasta can be described using a simplified model where the heat transfer, shrinkage and external resistance to mass transfer can be neglected. These hypotheses make it possible to describe the evolution in average water content of pasta using the analytical solutions of Table 2.1.

Nevertheless, some observations can be made about the extent of experimental validation conducted to date. Few studies have been conducted on validating the models to describe drying at temperatures above 100 °C. At such temperatures, phenomena such as water vaporization within the pasta can occur and have an impact on the mass transfer mechanisms, on the relative contribution of the water transfer in liquid form and vapour form, and on pasta structure. It would therefore be relevant to verify the validity of current models to describe the drying of pasta under such conditions, especially since this practice is becoming increasingly common in the industry because it allows for a significant reduction in the time required to produce pasta.

Litchfield and Okos (1992) studied the evolution of the moisture profile that developed inside pasta during drying. To achieve this, the pasta was taken out of the dryer at different moisture stages, frozen in liquid nitrogen and cut into sections 0.1 mm thick. The moisture of each section was then measured. Their results show that the moisture profile generated inside the pasta can be adequately estimated using a Fickian diffusion model for drying at 40 °C. However, for temperatures of 60 °C and 80 °C, the moisture profile measured was flatter that the one predicted by the model and moisture near the surface of the pasta was higher than expected. The authors propose three hypotheses to explain these results:

(1) Water diffusion by concentration gradient is not the mechanism by which the mass transfer occurs, or other mechanisms are also present in addition to the concentration gradient diffusion.

(2) The surface of the pasta does not dry to the equilibrium moisture value M_E, or the surface of the pasta was remoistened before it was placed in the liquid nitrogen or while the frozen samples were being cut.

(3) The mass transfer resistance of the pasta at the surface could be considerable, which could be explained by the smooth texture of the pasta after extrusion.

Xing et al. (2007) also studied the moisture profile inside pasta during drying. To do this, the moisture profile was measured by NMR, a non-destructive technique that limits the risk of changing pasta moisture when the pasta is cut. Pasta with an initial moisture content level of about 0.20 (d.b.) was used and dried at two temperatures (22 °C and 40 °C) that were selected based on the operational constraints of the NMR unit. The results suggest that for drying at 40 °C, the moisture profile inside the pasta according to r is relatively flat for moisture content between 0.20 and 0.15, and more curved for lower moisture content. Similar results were also obtained by Hills et al. (1997). The change in moisture profile is consistent with the glass transition of pasta which occurs at a moisture content of 0.15 (d.b.) at this temperature (Kulkarni, 2005). The authors thus explain this result with the hypothesis that, as observed for other biopolymers, moisture transport cannot be described from previous Fick-type models near the glass transition (Singh et al., 2003). As noted previously, this could be explained by the local changes in pasta transport properties, or by the time-dependant conformational changes in food biopolymers, which adds an additional stress term to fluid flow near the glass transition (Hills et al., 1997; Takhar, 2008). At 22 °C, a relatively curved moisture profile was observed for the entire duration of drying. Given that at this temperature the glass transition of pasta occurs at a moisture content of about 0.24 (d.b.), which is higher than the initial moisture of the pasta during the experiment, this result suggests that water diffusion is Fickian for pasta in the glassy state (Liu et al., 1997).

Furthermore, it is important to note that these experiments were conducted by drying commercial pasta with a moisture content level of about 0.09 (d.b.). To achieve this, the pasta had to first be pre-moistened in an environmental chamber at a temperature of 30ºC and under controlled relative humidity. It could therefore be relevant to measure the moisture profile generated inside pasta when it is dried by a method more representative of the industrial process, i.e., using fresh pasta extruded from hydrated semolina. It would also be relevant to

study the moisture profile generated inside pasta during drying using a non-destructive method such as NMR imaging for temperatures that are more representative of those used in the industry (40-120 °C). The knowledge of the moisture profiles under these conditions could provide a better understanding of the mass transfer mechanisms involved in pasta drying, as well as promoting more accurate prediction of crack formation within the product.

2.4.2 Pasta properties

Using the models presented in section 2.3 requires the knowledge of pasta properties such as heat capacity, thermal conductivity, effective diffusion coefficients, and mass and heat transfer coefficients. The value of most of these parameters can be estimated from data found in literature, which are often available as correlations or semi-empirical models. However, many of these correlations and models were developed by extrapolating experimental measurements taken on products other than pasta, or under different operating conditions than those considered, which can cause considerable variability in the results obtained. Consequently, the value of some of these parameters must be revised in many studies using estimation methods based on experimental moisture content data. For example, the model developed by Migliori et al. (2005a) initially overestimated the average moisture content in pasta during drying when the external mass transfer coefficient value was calculated using Eqs. (2.16), (2.17) and (2.20). To correct the data from the model, a new value for this parameter was calculated using the non-linear least squares method. A value of about two orders of magnitude higher than the one initially calculated was obtained, but it was not confirmed that the lack of goodness of fit between experimental and predicted moisture content was entirely caused by a poor initial estimate of this parameter.

2.4.3 Drying systems

Few studies were conducted regarding the reproducibility of the drying curves between the different types of experimental drying systems. The drying system has an impact on important parameters such as the air velocity or the air humidity at the pasta surface.

According to the results of Inazu et al. (2003) for the drying of Japanese noodles, an increase in air velocity to about 2 m s^{-1} cause an increase in the value of the effective diffusion coefficients. Beyond this velocity, the impact of this parameter becomes negligible. However, this value could also depend on the angle at which the air comes into contact with the pasta. The drying system can also influence the accuracy with which drying conditions, like air humidity, are controlled. For instance, Villeneuve and Gelinas (2007) suggest that the value of the effective diffusion coefficients is more sensitive to variations in air relative humidity than air temperature in contrast with the results of Andrieu and Stamatopoulos (1986) and Litchfield and Okos (1992). This could be explained by the drying system used where air humidity is controlled using an electric steam generator and a cooling circuit. Such a system could permit more precise, rapid control of air humidity compared with systems where this parameter is controlled using salt solutions or an external steam generator.

Another aspect of drying systems concerns the orientation in which pasta is dried. Depending on the system used, pasta can be placed horizontally on plates or hung vertically on racks. If pasta sags in the amorphous state because of its weight, the consequences are likely to be different depending on the drying system. For pasta hung vertically, sagging could result in a larger radius or thickness at the bottom of the pasta rather than near the rack, thereby affecting the uniformity of the moisture profile in the longitudinal direction. For cylindrical pasta placed horizontally on plates, sagging could affect the radial symmetry of pasta that is generally assumed when models are developed. Pasta orientation could also affect the mechanical stresses generated inside the product and the crack formation process.

2.5 Development of mechanistic models

The models of pasta drying developed to date are semi-empirical models where the description of the mass transfer mechanisms is lumped in a single coefficient, the effective diffusion coefficient. In these models, no distinction is made between the transport of water in liquid or in vapour form, or between diffusion, flow by capillary action and flow by pressure gradient. In contrast, mechanistic models are more fundamental and are developed from the mass, heat and momentum balances for each of the phases and substances of the system.

These models are mathematically more complex, but the physical considerations behind the equations are generally better understood, the hypotheses are clearer and the parameters are better defined (Datta, 2007). Therefore, the development of mechanistic models should improve our understanding of the mass and heat transfer mechanisms involved in pasta drying.

Since no mechanistic model on pasta drying has been developed so far, this section describes an approach derived from model on the drying or baking of other porous media that could lead to such models. For the drying rectangular pasta, assuming a unidirectional mass transfer, models could be developed from Eqs. (2.54)-(2.56) (Bird et al., 1960; Whitaker, 1977; Datta, 2007). These equations describe the conservation of the three main components of the system considered, which are water in a liquid state, water in a vapour state and air.

$$\frac{\partial c_w}{\partial t} = \frac{\partial c_w}{\partial x} - I \tag{2.54}$$

$$\frac{\partial c_v}{\partial t} = \frac{\partial n_v}{\partial x} + I \tag{2.55}$$

$$\frac{\partial c_a}{\partial t} = \frac{\partial n_a}{\partial x}, \tag{2.56}$$

where c_w, c_v and c_a represent the liquid water, water vapour and air concentration, I is the evaporation rate and n_w, n_v and n_a are the mass fluxes of water in a liquid state, water in a vapour state and air. Taking the concentration and pressure gradients as the two main driving forces of the mass transfer, the mass fluxes n_w, n_v and n_a can be described using Eqs. (2.57)-(2.59):

$$n_w = \rho_w \frac{k_w}{\mu_w^0} \frac{\partial P}{\partial x} + D_w \frac{\partial c_w}{\partial x} \tag{2.57}$$

$$n_v = \rho_v \frac{k_g}{\mu_g^0} \frac{\partial P}{\partial x} + D_{g,eff} \frac{\partial c_v}{\partial x} \tag{2.58}$$

$$n_a = \rho_a \frac{k_g}{\mu_g^0} \frac{\partial P}{\partial x} + D_{g,eff} \frac{\partial c_a}{\partial x}, \tag{2.59}$$

where k_w and k_g represent the permeability of the liquid and gas phases, μ_w^0 and μ_g^0 are the viscosity of the water and the gas phase, D_w is the diffusivity of the water in the pasta and $D_{g,eff}$ is the effective diffusivity of the water vapour or the air in the gaseous phase. When the

temperature profile developed inside the pasta during drying is to be studied as well, the Eqs. above (2.54)-(2.59) can be linked with an energy balance:

$$\rho_{app} C_{p,app} \frac{\partial T}{\partial t} = \frac{\partial}{\partial x}(n_w H_w + n_v H_v + n_a H_a) + \frac{\partial}{\partial x}\left(k_h \frac{\partial T}{\partial x}\right) - \lambda I, \quad (2.60)$$

where $H_w = C_{p,w}T$, $H_v = C_{p,v}T$ and $H_a = C_{p,a}T$ represent the enthalpy of the components. In the previous equation, the first term on the right-hand side represents the convective heat transfer, the second term is the conductive transfer and the third is the latent heat of vaporization. Solving the system composed of Eqs. (2.54)-(2.60) requires an additional equation to describe the evaporation rate *I*. It is generally developed by assuming a liquid-vapour equilibrium at all points in the medium that is described using an activity coefficient. However, no experimental data obtained to date make it possible to validate this hypothesis. To avoid using this hypothesis, it would be possible to describe the evaporation rate using a kinetic law, which could be particularly suitable for the drying of pasta with a low moisture content or in high drying temperature (Ousegui et al., 2010; Rakesh and Datta, 2011).

One of the main difficulties in using mechanistic models involves estimating the value of diffusivities and permeabilities. In the following paragraphs, typical parameter values are mainly given for products that have a porosity in the range of 0-30%, in agreement with the results of Waananen and Okos (1996) and Mercier et al. (2011b). These parameter values can be used as a first approximation of the order of magnitude of the transport properties of durum wheat pasta. However, it should be expected that these properties are highly dependent on the product being dried, such that experimental measurements on pasta would be required to develop more accurate models.

Few data are available to estimate the liquid water diffusion coefficient in pasta D_w since the data are usually collected as effective diffusivities D_{eff}. For potatoes, a product with a similar porosity as pasta (Wang and Brennan, 1995), Ni (1997) describes the liquid water diffusivity with the following equation:

$$D_w = 1.0 * 10^{-8} \exp(-2.8 + 2.0M) \quad (2.61)$$

This relation was developed primarily from the following two hypotheses: (1) for high moisture content, the diffusion coefficient value should be similar to the effective diffusion

coefficient value, because the contribution from the transfer of water in vapour form is negligible and (2) for low moisture content levels, the diffusion coefficient value should be such that an internal moisture profile matching those generally observed in the falling-rate period is obtained, meaning a sigmoidal profile where the fall in moisture in the centre of the product is slow.

The effective diffusion value of water vapour and air inside a porous medium $D_{g,eff}$ could be estimated using the following equation (Geankoplis, 2003):

$$D_{g,eff} = D_{a-v}\frac{\epsilon}{\tau_p}, \tag{2.62}$$

where ϵ represents the volumetric fraction of pasta occupied by the gaseous phase, D_{a-v} is the diffusivity of the binary system of water vapour–air and τ_p is pore tortuosity. For inert solids, tortuosity generally varies from 1.5 to 6 (Aguilera and Stanley, 1999; Geankoplis, 2003). To estimate the value of the diffusion coefficient of the binary system of water vapour–air inside tubular pasta, Migliori et al. (2005a) use the Fuller-Schettler-Giddings correlation (Fuller et al., 1966):

$$D_{a-v} = \frac{10^{-3}T_f^{1.75}\left(\frac{MW_w+MW_a}{MW_wMW_a}\right)^{0.5}}{P\left[(\sum v)_v^{1/3}+(\sum v)_a^{1/3}\right]^2}, \tag{2.63}$$

where T_f represents the film temperature (which can be estimated by calculating the arithmetic average between T_∞ and $T_{R_C,R_{ext}or\ X_c}$), MW_w and MW_a are the molecular weight of water and air, $(\sum v)_v$ and $(\sum v)_a$ are the atomic diffusion volume of the components ($cm^3\ mol^{-1}$) and P is the pressure (atm). For water vapour and air, values of the atomic diffusion volume of 12.7 and 20.1 $cm^3\ mol^{-1}$ were suggested, respectively (Perry and Green, 1984).

Finally, studying the presence of flow caused by pressure gradient inside pasta also requires estimating the value of the pasta's liquid and gaseous permeability. According to Darcy's law, zero permeability would indicate that no flow caused by pressure gradient can be observed, whereas high permeability would suggest a more significant contribution from the product's dehydration mechanism caused by pressure gradient. Permeability can be broken

down into intrinsic k_i and relative k_r permeabilities using the following relations (Datta, 2006):

$$k_w = k_{i,w} k_{r,w} \tag{2.64}$$

$$k_g = k_{i,g} k_{r,g} \tag{2.65}$$

These two types of permeability are generally related to the saturation levels in liquid (S_w) and in gas (S_g) defined using the following equations:

$$S_w = \frac{V_w}{V_{app} - V_s} \tag{2.66}$$

$$S_g = \frac{V_v + V_a}{V_{app} - V_s} \tag{2.67}$$

Intrinsic permeability represents the permeability for the liquid or gas when the product is saturated, i.e., when the entire volume of apparent pores of the product is occupied by liquid water ($S_w = 1$) or gas ($S_g = 1$), respectively. Datta (2006) measured an intrinsic liquid permeability in the order of 10^{-17} to 10^{-19} m^2 for potatoes and beef slices. For gas permeability, Zhang and Datta (2006) and Chaunier et al. (2008) obtained results in the order of 10^{-10} to 10^{-12} m^2 for bread.

Eqs. (2.68) and (2.69) are commonly used to describe the relative permeability of porous media (Datta, 2006):

$$k_{r,w} = \left(\frac{S_w - S_i}{1 - S_i}\right)^3 \quad \text{for } S_w > S_i$$

$$k_{r,w} = 0 \quad \text{for } S_w \leq S_i \tag{2.68}$$

$$k_{r,g} = 1 - 1.1 S_w \quad \text{for } S_w \leq 0.9$$

$$k_{r,g} = 0 \quad \text{for } S_w > 0.9 \tag{2.69}$$

These equations were developed primarily from experimental measurements of the permeability of a system consisting of a porous medium, a non-wetting phase, oil, and a wetting phase, water (Scheidegger, 1960). S_i represents the irreducible permeability, i.e., a

critical water saturation value below which the liquid phase is not continuous and the permeability of the product for this phase is zero. In the model describing transport phenomena inside porous media by Nasrallah and Perre (1988), a value for S_i of 0.09 is assumed. However, this value is not based directly on experimental measurements and mostly represents an initial estimate used to carry out a sensitivity analysis of the model parameters. The value of S_i is sometimes assumed to be zero, such as in the model describing the dehydration of apples from Feng et al. (2004), which assumes that flow caused by pressure gradient can be observed even when the water phase is non-continuous.

2.6 Modelling pasta drying near glass transition

Current experimental data suggest that the evolution of the average moisture content during drying can be predicted adequately with the semi-empirical models described in section 2.3 for the operating conditions investigated to date (Migliori et al., 2005a; De Temmerman et al., 2007; De Temmerman et al., 2008; Mercier et al., 2011b). However, significant differences exist between the models estimates and experimental results for the internal moisture profiles (Litchfield and Okos, 1992; Xing et al., 2007).

NMR imaging showed that the lack-of-fit between model estimates and experimental moisture profiles is particularly significant near glass transition. Sharper moisture profiles were observed compared to the profiles estimated from current semi-empirical models, which suggests that the stress resulting from the time-dependant conformational changes has a significant impact on the moisture transport, or that local changes in pasta transport properties should be considered to model accurately moisture transfer (Hills et al., 1997; Xing et al., 2007).

A number of modeling approaches have been proposed to improve the description of moisture transport near glass transition for biopolymers. Hills et al. (1997) developed a model in which moisture transport is Fickian, but where the formation of a hard, glassy layer at the surface of the pasta is considered by adjusting the diffusion coefficient according to the local moisture content of the product. While the estimated moisture profiles were more

representative of experimental results compared to previous models, there was no quantitative validation of this model.

Xing et al. (2007) suggested that non-Fickian models, which consider the stress induced by polymers relaxation, can provide a good representation of experimental results. One such non-Fickian model was developed for biopolymers by Singh et al. (2003) using the hybrid mixture theory. This multi-scale model showed good agreement with the experimental drying curves for soybeans. It takes into account the relaxation time using the following equation:

$$\dot{\varepsilon^f} + (\varepsilon^f - 1)\nabla \cdot (D\nabla\varepsilon^f) - (\varepsilon^f - 1)\nabla \cdot \left[\int_0^t B_C G(t - t^*)\nabla\dot{\varepsilon^f}(t^*)dt^*\right] = 0, \quad (2.70)$$

where ε^f is the volume fraction of the fluid, $\dot{\varepsilon^f}$ is the material time derivative of ε^f with respect to the motion of the solid phase, ∇ is the gradient operator in spatial dimensions, G is the stress relaxation function (which can be described with an equation as the generalized Maxwell model) and B_C is a parameter that links the effect of polymer relaxation with the fluid movement. Overall, the first two terms of Eq. (2.70) are similar to typical Fick-type models, while the integral term accounts for the additional stress related to the time-dependant conformational changes within the product.

The resolution of such models for pasta requires the knowledge of the viscoelastic properties of pasta. Takhar et al. (2006) measured the pasta storage modulus and tanδ (i.e. the ratio of the loss modulus to the storage modulus) at different temperatures and moisture contents using a mechanical thermal analyzer. Cuq et al. (2003) measured the apparent strength of pasta (here defined as the force at 0.3 mm deformation) and apparent relaxation coefficient (defined as the relative change between the force measured at a 0.3 mm deformation and the force recorded 30 s after relaxation). The following equation showed good agreement with their experimental results (Cuq et al., 2003):

$$Z(W,T) = \frac{Z_H(T) - Z_L(T)}{\left(1 + \exp\left(\frac{M - M_i(T)}{A(T)}\right)\right)} + Z_L(T), \quad (2.71)$$

where $Z(W,T)$ is the mechanical property considered, $Z_H(T)$ is the maximum value of the property, $Z_L(T)$ is the minimum value, $M_i(T)$ is the moisture content (d.b.) at the inflection

point, $A(T)$ is the transition spread and T is in ºC. The values of these parameters are related to temperature using the exponential functions presented in Table 2.6. Eq. (2.71) can be used to show that the pasta behaves as a soft and visco-plastic product at high moisture content, but as a more rigid and elastic product at moisture contents under glass transition.

Table 2.6. Model parameters of Eq. (2.71)

Apparent strength (N)	Apparent relaxation coefficient
$Z_L = 4.3\exp(1.1 * 10^{-3}T)$	$Z_L = 2.09\exp(0.1 * 10^{-3}T)$
$Z_H = 70.4\exp(1.1 * 10^{-3}T)$	$Z_H = 56.5\exp(0.1 * 10^{-3}T)$
$M_i = 37.9\exp(-1.24 * 10^{-3}T)$	$M_i = 32.7\exp(-1.2 * 10^{-3}T)$
$A = 4.55\exp(-7.1 * 10^{-3}T)$	$A = 3.13\exp(-1.45 * 10^{-3}T)$

The range of conditions for which classical Fick-type models cannot describe accurately moisture transport without considering the glass transition remains to be identified. Cuq and Icard-Verniere (2001) measured the glass transition of pasta at different moisture contents using modulated differential scanning calorimetry. Good agreement was found between their experimental results and the Kwei model:

$$T_g = \frac{\frac{1}{1+M}T_{g,1} + q_1\frac{M}{1+M}T_{g,2}}{\frac{1}{1+M} + q_1\frac{M}{1+M}} + q_2\frac{M}{(1+M)^2}, \qquad (2.72)$$

where $T_{g,1}$ and $T_{g,2}$ are the glass transition temperature of semolina and water (ºC), and q_1 and q_2 are two empirical constants. For drying, these parameters take the following values: $T_{g,1}$ = 273 ºC, $T_{g,2}$ = -135 ºC, q_1 = 9.5 and q_2 = 346. Moreover, results of Cuq et al. (2003) show that the sharp changes in apparent strength and apparent relaxation coefficient of pasta during drying occur within a moisture range of about 2 – 5 kg water kg dry matter^{-1}. As a first approximation, this range could also be assumed to correspond to the spread near the glass transition where moisture transport cannot be describe accurately with classical Fick-type models. However, measurement of internal moisture profiles for a wider range of conditions is needed before an accurate assessment of the impact of glass transition on moisture transport can be made.

2.7 Modelling the evolution in pasta quality

The main objective of pasta drying models is generally to describe the evolution of pasta water content as a function of drying conditions. Several models have also expanded the analysis to additional properties, such as the porosity, shrinkage, density and mechanical properties of pasta. However, for consumers and pasta producers, pasta quality is determined by its cooking characteristics and its organoleptic, esthetic and nutritional properties, and not by the physical and thermodynamic properties that are described by current models. Consequently, there seems to be a need to develop models that allow predicting pasta quality as defined by consumers.

This approach was used by Migliori et al. (2005b) in order to quantify the evolution of furosine production. Since furosine is an early product in Maillard reactions, monitoring it provides information on the browning of a product and its digestibility, among other things (Feillet et al., 2000; De Zorzi et al., 2007). In this model, a zero-order kinetic production is assumed:

$$\frac{df}{dt} = F(a_w, T), \tag{2.73}$$

where f is the furosine content of pasta and F is its production rate. In addition, an Arrhenius equation is established between the kinetic coefficient F and the two dependent variables:

$$F = F_0 \exp\left(-\frac{E_a a_w}{RT}\right) \tag{2.74}$$

Since Eqs. (2.73) and (2.74) ultimately depend on the temperature and water content of pasta, inserting them into current models makes it possible to directly predict the furosine content according to the drying conditions. Other pasta properties could also be suitable for developing similar models, such as firmness, adhesiveness, rheological properties and cooking loss, because many studies have demonstrated that these properties are highly dependent on the drying conditions applied (Güler et al., 2002; Zweifel et al., 2003; Lamacchia et al., 2007).

2.8 Adding ingredients high in nutritional value

Pasta is a relatively affordable product that is consumed frequently in many regions of the world. Moreover, the matrix of pasta generally has the capacity to be partially substituted (up to about 10-15%) with other ingredients without an apparent loss of quality in the final product (Torres et al., 2007a; Petitot et al., 2010). These properties have led to a new practice in the pasta industry that involves introducing ingredients high in nutritional value into the formulation of the product. Most of the studies on this subject focus on the addition of compounds with a high protein content, such as plant protein flours, concentrates or isolates (Nielsen et al., 1980; Bahnassey et al., 1986; Yanez-Farias et al., 1999; Zhao et al., 2005; Sabanis et al., 2006; Shogren et al., 2006; Torres et al., 2007a; Gallegos-Infante et al., 2009; Wood, 2009; Petitot et al., 2010; Martinez-Villaluenga et al., 2010). Adding these proteins makes it possible to compensate for pasta deficiencies in lysine and threonine, two essential amino acids (Kies and Fox, 1970; Abdel-Aal and Hucl, 2002). Supplementation with ingredients rich in animal proteins or in fibre and with certain oils has also been considered (Fuad and Prabhasankar, 2010; Krishnan and Prabhasankar, 2012).

Studies on the enrichment of semolina with ingredients high in nutritional value show that this practice can affect pasta properties related to texture (Nielson et al., 1980), colour (Gallegos-Infante et al., 2009), cooking properties (Zhao et al., 2005) and organoleptic properties (Alireza Sadeghi and Bhagya, 2008). In general, these changes are attributed to the properties of the ingredient added, the weakening of the gluten network associated with its dilution and the chemical bonds formed between the new ingredients and the starch or gluten of the semolina (Ribotta et al., 2005; Roccia et al., 2009; Petitot et al., 2010; Mercier et al., 2012).

However, few studies have been conducted on the impact of enrichment on the drying process. Mercier et al. (2011b) observed that fortifying pasta with 5% or 10% of pea protein isolate causes an increase in the effective diffusion coefficients at 80 °C, which could be attributed to the impact of fortification on the fundamental mass and heat transfer mechanisms involved. Current pasta drying models are therefore not necessarily adapted to this new reality, since these models are semi-empirical and group all the mass transfer mechanisms within a single parameter, the effective diffusion coefficient. More fundamental models based on

continuity, heat and momentum equations could thus be better adapted to this reality and could be used to increase the understanding of how enrichment impacts the mass and heat transfer mechanisms involved in the drying of fortified pasta.

2.9 Conclusion

Drying is a step in pasta production that can greatly influence the properties of the final product. In the last few years, many models have been developed to describe the transport phenomena that occur during this step of production. Most of these models are semi-empirical and combine mass transfer mechanisms within a single parameter, the effective diffusion coefficient. The main differences between the models are the hypotheses related to the mass transfer at the interface, the treatment of shrinkage and the consideration of heat exchanges. In general, the models considered in this study allows an adequate description of the evolution in average water content of pasta during drying based on the temperature and relative humidity applied. However, major differences can be observed between experimental and modelled data regarding the moisture profile generated inside the product during drying, particularly around the glass transition. In the light of these observations, different recommendations can be made regarding future work on modelling the drying of pasta, including:

(1) Expand the experimental validation of the models. On the one hand, there seems to be a need to study the validity of the models for drying in temperatures higher than 100 °C, because phenomena such as water vaporization can be more important and affect pasta structure and mass transfer mechanisms. On the other hand, applying the models currently requires data extrapolated from experimental measurements obtained with other products than pasta or under different operating conditions than those considered. Consequently, it also seems relevant to continue collecting experimental data for the value of some physico-chemical and thermodynamic properties of pasta, including the effective diffusion coefficient and the mass and heat transfer coefficients.

(2) Develop mechanistic models. These models, which are more fundamental than the current ones, would improve our understanding of the mass and heat transfer mechanisms involved in the dehydration of pasta.

(3) Measure internal moisture profiles of pasta for industrially relevant drying conditions. As of now, internal moisture profiles were obtained with low-precision destructive techniques, or for temperature conditions rarely used in the pasta making industry. The knowledge of internal moisture profiles would be particularly relevant near the glass transition of pasta, in order determine the range of moisture content where current Fick-type models are inadequate for modeling pasta drying.

(4) Develop models describing the evolution of pasta quality during drying as defined by the consumers and the industry. These properties, such as colour, texture, taste and presence of cracks are generally not taken directly into account by current models, but represent critical factors in the choice of optimal operating conditions.

(5) Adapt the models to pasta enriched with ingredients high in nutritional value. Adding these ingredients can modify the physico-chemical properties of pasta and add additional constraints to production, such as using low temperatures for drying products containing heat sensitive ingredients. These models could promote better understanding of interactions between the new ingredients and the pasta matrix, and answer questions such as the maximum amount of exogenous ingredients that the gluten network can support without affecting the physical integrity of the product.

2.10 Acknowledgements

The authors would like to thank François Lamarche for the preparation of Fig. 2.1 and the Natural Sciences and Engineering Research Council of Canada for funding this project.

CHAPITRE 3. Analyse de sensibilité et d'incertitude des modèles décrivant le séchage des pâtes

Titre original : Sensitivity analysis of parameters affecting the drying behaviour of durum wheat pasta

Auteurs et affiliations :

S. Mercier, Ing. jr., étudiant au doctorat, Université de Sherbrooke, département de génie chimique et génie biotechnologique, 2500 boul. Université, Sherbrooke, Québec, Canada, J1K 2R1.

C. Moresoli, Ing., Ph.D. University of Waterloo, Department of Chemical Engineering, 200 University Avenue West, Waterloo, Ontario, Canada, N2L 3G1.

S. Villeneuve, Ing., Ph.D., Agriculture et Agroalimentaire Canada, Centre de Recherche et Développement de Saint-Hyacinthe, 3600 Boul. Casavant Ouest, Saint-Hyacinthe, Québec, Canada, J2S 8E3.

M. Mondor, Ing. stag., Ph.D., Agriculture et Agroalimentaire Canada, Centre de Recherche et Développement de Saint-Hyacinthe, 3600 Boul. Casavant Ouest, Saint-Hyacinthe, Québec, Canada, J2S 8E3.

B. Marcos, Ing., Ph.D., Université de Sherbrooke, département de génie chimique et génie biotechnologique, 2500 boul. Université, Sherbrooke, Québec, Canada, J1K 2R1.

Date d'acceptation : 22 mars 2013

État de l'acceptation : Publié

Référence : Journal of Food Engineering, 118, 108-116.

Résumé

Contenu : la revue de la littérature (chapitre 2) a révélé l'importante variabilité entre les valeurs du coefficient de diffusion effectif de l'eau dans les pâtes selon les études sur la modélisation du séchage. Dans cet article, l'impact de cette variabilité sur la prédiction de la teneur en eau et de la transition vitreuse des pâtes au cours du séchage est évalué. Pour ce faire, l'incertitude sur la valeur du coefficient de diffusion effectif est estimée par la comparaison des valeurs utilisées dans les études sur la modélisation du séchage des pâtes. Des analyses de sensibilité et de propagation de l'incertitude sont appliquées pour quantifier l'incertitude résultante sur la prédiction du temps requis pour sécher les pâtes selon la température de séchage utilisée.

Résultats : le coefficient de diffusion effectif de l'eau dans les pâtes est le paramètre d'entrée du modèle de séchage Fickian ayant l'impact le plus significatif sur la prédiction de la teneur en eau et de la transition vitreuse en comparaison avec le coefficient de rétrécissement, la perte d'eau lors de la période de séchage à taux constant et le coefficient de transfert de masse par convection. L'incertitude du coefficient de diffusion effectif résulte en une incertitude de l'ordre de ± 3.5 h sur la prédiction du temps requis pour sécher les pâtes, incertitude trop élevée pour l'application du modèle en industrie.

Contributions à la thèse : les contributions à la thèse de cet article sont l'identification des paramètres d'entrée des modèles Fickian ayant un impact significatif sur la modélisation du séchage des pâtes et la démonstration de la nécessité de collecter des valeurs plus précises du coefficient de diffusion effectif pour améliorer la représentation de leur teneur en eau et leur transition vitreuse.

Abstract

In this work, a comprehensive model of pasta drying combining Neumann boundary conditions, differential shrinkage and with consideration of the constant drying rate period and falling drying rate period was investigated through sensitivity and uncertainty analysis. Results confirmed that shrinkage, moisture loss and drying rate during the constant drying rate period and external resistance to mass transfer did not have a significant impact on the predicted required drying time. The predicted required drying time was influenced predominantly by the effective moisture diffusion coefficient. A correlation to estimate the effective moisture diffusion coefficient was developed from published values and was used to predict the required drying time with an uncertainty of ± 3.5 hours at a 90% confidence interval. Since this magnitude of uncertainty is unreasonable for most industrial uses, accurate data collection of effective moisture diffusivity should be viewed as a major objective in pasta drying research.

Keywords

Pasta drying; moisture transport; sensitivity analysis; uncertainty; effective moisture diffusion coefficient

Nomenclature

a_w	water activity coefficient, -
A	drying area, m^2
Bi_m	mass Biot number, -
C	concentration, kg m^{-3}
D_{eff}	effective moisture diffusion coefficient, m^2 s^{-1}
DS	mass of pasta dry solid, kg
E_a	activation energy, J mol^{-1}
h_m	surface mass transfer coefficient, m s^{-1}
M	pasta moisture content (liquid water+ water vapor) on dry basis, kg H_2O kg dry $solid^{-1}$
MW	molecular weight, Dalton
N	mass flux, kg m^{-2} s^{-1}
P	pressure, Pa
r	radial coordinate, m
R	pasta radius, m
R_C	drying rate during the constant drying rate period, kg H_2O m^{-2} s^{-1}
R_g	ideal gas constant, J mol^{-1} K^{-1}
RDT	drying time required to reduce pasta moisture content below 0.1 (d.b.), s
RH	relative humidity, %
Sr	relative sensitivity, -
t	time, s
$t_{(1-\alpha)/2,\nu}$	value of the Student's t-distribution for a confidence interval α and a number of degrees of freedom ν
T	temperature, K
T_g	glass transition temperature, K
V	volume, m^3
$\%C$	relative moisture lost during the constant drying rate period, %

Greek symbol

α	confidence interval, -
β	shrinkage coefficient, -
ε	porosity, %
η	volumetric fraction of water lost replaced by air, -
ρ	density, kg m^{-3}
σ	standard deviation
ν	number of degrees of freedom

Superscripts

0	reference scenario

ext	external
Subscripts	
0	initial condition
$0 \rightarrow r$	from the center of the pasta to r
app	apparent
c	critical
DS	dry solid
E	equilibrium
R	at $r = R$
sat	saturation
w	water
∞	in the bulk environment

3.1 Introduction

Multiple studies have shown that the selection of adequate drying conditions is critical for the production of high quality pasta (Manthey and Schorno, 2002; Zweifel et al., 2003; Mercier et al., 2011b). However, the selection of adequate drying conditions is generally not a straightforward task. Temperature and relative humidity profiles should be selected carefully such that drying is fast enough to minimize operating time, but sufficiently slow to promote adequate microstructural changes of the starch and proteins (Lamacchia et al., 2007; Petitot et al., 2009; De Noni and Pagani, 2010).

In order to streamline the selection of drying conditions, models have been developed to predict pasta properties during drying without the need to perform costly trial-and-error runs. The first pasta drying model was developed by Andrieu and Stamatopoulos (1986). In their model, the decrease in pasta moisture content is described using a semi-empirical Fick-type law. In the model, moisture transport was assumed to be by diffusion and other mass transport mechanisms were considered to be lumped into the diffusion coefficient. So, the diffusion coefficient is an effective parameter. Using Dirichlet boundary conditions and assuming the effective moisture diffusion coefficient to be independent of the product moisture content, the Fick-type law can be solved analytically. Ponsart et al. (2003), Migliori et al. (2005) and De Temmerman et al. (2007) modified this model by considering the effect of shrinkage on mass transfer, either through one or two-way coupling, and by describing the effective moisture diffusion coefficient as a function of the product moisture content. Ogawa et al. (2012) improved the accuracy of the description of moisture transport at the beginning of the drying process by introducing a constant drying rate period. Although the validity of these models to predict internal moisture profiles remains to be investigated, these models have shown good agreement between the estimated and experimental pasta average moisture content during drying.

The selection of adequate drying conditions should also consider the pasta glass transition. Glass transition represents the transition of amorphous components from a supercooled melt to a glassy state or the opposite (Liu et al., 2006). Pasta undergoes glass transition during drying, which induces important changes in its mechanical, rheological and transport properties. Pasta behaves as a visco-plastic and soft material in the rubbery state and

as an elastic and rigid material in the glassy state, with a transition state in between (Rahman, 1995; Cuq et al., 2003). Adequate drying conditions should promote uniform glass transition within the pasta such as to limit internal stresses and the risk of crack formation. The moisture content at which pasta undergoes glass transition can be predicted from the model of Cuq et al. (2003), which was developed from modulated scanning calorimetry measurements.

The selection of adequate pasta drying conditions from mass transfer and glass transition models requires the knowledge of multiple input parameters including pasta thermophysical and geometrical properties, heat and mass transfer coefficients, and initial and boundary conditions. These input parameters can generally be estimated from literature data. However, especially in the food industry, considerable variability is observed for the values reported from different studies. The lack of precision of the parameter estimates can lead to significant uncertainty in the prediction of pasta drying behaviour and glass transition conditions. The quantification of this uncertainty, a prerequisite to confirm the validity of the models, has not been investigated. The aims of this work were to determine the models parameters that influenced predominantly the prediction of pasta required drying time, quantify the uncertainty of the predicted required drying time for relevant industrial processing conditions and evaluate the impact of the uncertainty of the pasta effective moisture diffusion coefficient on the description of pasta glass transition. More specifically, a drying model combining Neumann boundary conditions, differential shrinkage and separation in a constant and a falling drying rate period was first presented and validated with published experimental moisture profiles. The contribution of the major input parameters of this model on the estimates of the drying time was evaluated for a reference scenario. The required drying time predicted according to five published correlations of the effective moisture diffusion coefficient was compared. Estimates of the rubbery, glassy and transition states of pasta according to pasta radial position and drying time were obtained and used to demonstrate the importance of the effective moisture diffusion coefficient correlation. Finally, a new effective moisture diffusion coefficient estimate was established by selecting the average conditions of the five published correlations.

3.2 Methodology

3.2.1 Model of moisture mass transfer

A comprehensive model combining Neumann boundary conditions, differential shrinkage and separation in a constant and a falling drying rate period was used in this study for pasta of cylindrical geometry. The following assumptions were made: (1) heat transfer was much faster than mass transfer, such that the difference between the pasta and the bulk air temperature was negligible (Andrieu and Stamatopoulos, 1986; De Temmerman et al., 2007); (2) the moisture transport occurred only in the radial direction because of the large ratio between the pasta length and diameter; (3) the bulk air near the pasta surface behaved as an ideal gas and (4) the longitudinal shrinkage of the pasta was considered negligible.

3.2.1.1 Constant drying rate period

As proposed by Ogawa et al. (2012), pasta drying was divided in a constant drying rate period and a falling rate period. During the constant drying rate period, the pasta moisture content was described as follows:

$$\frac{d\bar{M}}{dt} = \frac{-R_C A}{DS}, \tag{3.1}$$

where $\bar{M}$ is the pasta average (averaged according to its radius *r*) moisture (liquid + vapor) content, *t* is the time, R_C is the constant drying rate, A is the surface area of the pasta and DS is the dry solids mass content of pasta. During the constant drying rate period, the moisture transport within the pasta is sufficient to maintain saturation at the surface of the pasta. The drying process is mainly controlled by the rate of mass transfer in the gas-phase boundary layer at the surface of the pasta, and the moisture content is assumed to remain uniform within the pasta (Selih al. 1996; Hadjidavallo and Hamdullahpur, 2000; Srikiatden and Roberts, 2007).

3.2.1.2 Falling drying rate drying period

Once the pasta moisture content is below its critical moisture content (M_C), the drying rate starts to decrease. During this period, drying is described with the following Fick-type law (Andrieu and Stamatopoulos, 1986):

$$\frac{\partial M}{\partial t} = \frac{1}{r}\frac{\partial}{\partial r}\left(rD_{eff}\frac{\partial M}{\partial r}\right), \tag{3.2}$$

where M is the moisture content and D_{eff} is the effective moisture diffusion coefficient of the pasta. Eq. (3.2) is a semi-empirical Fick-type law which describes simultaneously the transport of liquid water and water vapor and is therefore not developed from first principles. One initial condition and two boundary conditions are required to solve Eq. (3.2). At the beginning of the falling rate drying period, the pasta moisture content is at its critical moisture content:

$$M = M_C, \qquad (\text{for } 0 \le r \le R \text{ and } t = t_c) \tag{3.3}$$

where $t_c$isthe time at the end of the constant drying rate period and R is the pasta external radius. The first boundary condition is derived from radial symmetry (Eq. 3.4). Neumann boundary conditions are used to describe the mass transfer at the surface of the product (Eq. 3.5):

$$\frac{\partial M}{\partial r} = 0 \qquad (\text{for } r = 0) \tag{3.4}$$

$$-D_{eff}C_{DS}\frac{\partial M}{\partial r} = N^{ext} = h_m(C_R - C_\infty), \qquad (\text{for } r = R), \tag{3.5}$$

where C_{DS} is the dry solid concentration, N^{ext} is the moisture mass flux at the surface of the pasta, h_m is the mass transfer coefficient, C_R is the water vapor concentration at the air-pasta interface (air side) and C_∞ is the water vapor concentration in the bulk environment. The water vapor concentration were obtained from the ideal gas law, Raoult's law and the water activity coefficient at the pasta surface (for C_R) or the dryer relative humidity (for C_∞):

$$C_R = \frac{p_{sat}a_w M_w}{R_g T} \tag{3.6}$$

$$C_\infty = \frac{p_{sat}RHM_w}{R_g T}, \tag{3.7}$$

where p_{sat} is the saturation vapor pressure (calculated with the Clausius-Clapeyron equation), a_w is the activity coefficient, M_w is the molecular weight of water, R_g is the ideal gas constant, *RH* is the relative humidity in the dryer and T is the drying temperature. The activity coefficient was calculated from the drying temperature with the following Oswin equation (De Temmerman et al., 2007):

$$a_w = \frac{\left[\frac{M}{A_1 - A_2(T-273)}\right]^{\left[\frac{1}{B_1 + B_2(T-273)}\right]}}{1+\left[\frac{M}{A_1 - A_2(T-273)}\right]^{\left[\frac{1}{B_1 + B_2(T-273)}\right]}}, \quad (3.8)$$

where A_1 = 0.138, A_2 = 10.4 x 10^{-4}, B_1= 0.396 and B_2 = 11.6 x 10^{-4}.

3.2.1.3 Pasta Shrinkage

During drying, the water removed from the pasta is not totally replaced by air, thus causing shrinkage. Shrinkage was described with a dimensionless parameter (η) representing the volumetric fraction of water lost in the pasta and replaced by air as proposed by Mercier et al. (2011b):

$$\eta = 1 - \frac{V_{app,0} - V_{app}}{V_{w,0} - V_w}, \quad (3.9)$$

where V_{app} is the pasta apparent volume and V_w is the volume occupied by liquid water. The apparent volume of pasta was related to its moisture content on a dry basis by introducing in Eq. (3.9) the pasta initial apparent density ($\rho_{app,0}$) and the water density (ρ_w):

$$V_{app} = V_{app,0}[1 - \beta(M_0 - \bar{M})], \quad (3.10)$$

where: $\beta = \frac{1-\eta}{\rho_w/\rho_{app,0}(1+M_0)}$. Eq. (3.10) represents shrinkage as a linear function of the pasta moisture content, which is supported by the experimental results of Andrieu et al. (1989).

3.2.1.4 Numerical implementation

The model of pasta drying was numerically solved with Matlab 7.5.0 using an explicit finite difference method to calculate mass transfer and a one-way coupling technique to calculate shrinkage. This method is schematised in Fig. 3.1. The first step was the estimation of the moisture content at the calculation node "*i*" after a time step Δt using a forward-difference approximation in time (Eq. 3.11) and central-difference approximations in space (Eqs. 3.12 and 3.13):

$$\left.\frac{\partial M}{\partial t}\right|_{i,t} \approx \frac{M_{i,t+\Delta t}-M_{i,t}}{\Delta t} \tag{3.11}$$

$$\left.\frac{\partial M}{\partial r}\right|_{i,t} \approx \frac{M_{i+1,t}-M_{i-1,t}}{\Delta r_{i-1}+\Delta r_{i+1}}, \tag{3.12}$$

$$\left.\frac{\partial^2 M}{\partial r^2}\right|_{i,t} \approx \frac{M_{i+1,t}-2M_{i,t}+M_{i-1,t}}{((\Delta r_{i-1}+\Delta r_{i+1})/2)^2}, \tag{3.13}$$

where $M_{i,t}$ is the moisture content at node "*i*", Δr_{i-1} is the distance between the node "*i*" and the node "*i*-1" and Δr_{i+1} is the distance between the node "*i*" and the node "*i*+1". The nodes became non-equidistant during the falling rate period because of the faster shrinkage at the surface than at the center of the pasta.

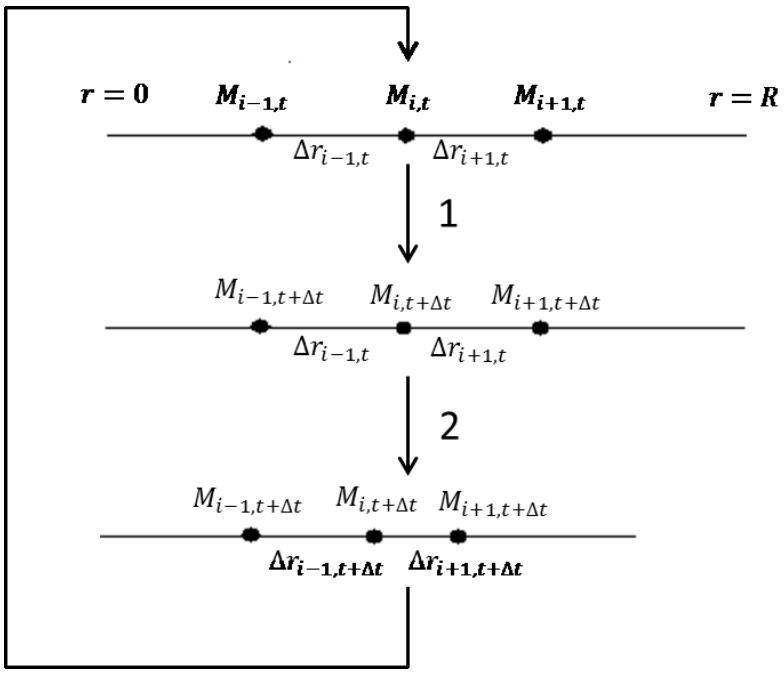

Figure 3.1. Numerical procedure implemented to solve the mass transfer model (Eqs. 3.1-3.10).

The second step was to calculate the shrinkage from the decrease in moisture content using a one-way coupling method between shrinkage and mass transfer as proposed by Migliori et al. (2005). This was achieved using a modified form of Eq. (3.10):

$$r_{0\to i,t+\Delta t}^2 = r_{0\to i,t}^2\left[1-\beta\left(M_{0\to i,t}-M_{0\to i,t+\Delta t}\right)\right], \quad (3.14)$$

where $r_{0\to i}$and $M_{0\to i}$ are the distance and the average moisture content from the center of the pasta to the node "*i*", respectively. The model was solved using 100 nodes ($\Delta r = 1.25 * 10^{-5}$for $t \leq t_c$) and with the shrinkage calculated after every five seconds ($\Delta t = 5$), which respects the Courant–Friedrichs–Lewy condition for convergence ($D_{eff}\frac{\Delta t}{\Delta r^2} < 0.5$). Simulations were also run with a higher number of nodes and with smaller time steps, but no influence on the results was observed.

3.2.1.5 Model validation

The mass transfer model (Eqs. 3.1-3.10) was validated with previously published experimental moisture profiles for semolina pasta drying at two different temperatures, 313 and 353K, and 65% relative humidity (Mercier et al. (2011b). The semolina pasta (M_0 = 0.47 d.b.) were extruded through a Teflon die (R_0 = 0.00125 m) in a temperature-humidity controllable chamber and their weight was measured online every minute with a 5-kg load cell connected to a data acquisition system. Experiments were repeated in duplicate. The model input parameters are presented in Table 3.1. The effective moisture diffusion coefficient was determined from the minimization of the mean square error between experimental and predicted data. The mean square error minimization was achieved using Newton method with central finite difference approximations to derivatives.

Table 3.1. Model parameters for experimental validation

Parameter	Value for 313 K drying	Value for 353 K drying	Reference

Effective moisture diffusion coefficient (D_{eff})	2.4 x 10^{-11} m^2 s^{-1}	4.4 x 10^{-11} m^2 s^{-1}	Least squares optimization from the experimental drying curves of Mercier et al. (2011b) (Fig. 3.2)
Surface mass transfer coefficient (h_m)	0.03 m s^{-1}	0.03 m s^{-1}	De Temmerman et al. (2007)
Shrinkage coefficient (β)	0.64	0.75	Mercier et al. (2011b)
Drying rate during the constant rate period (R_C)	6.9 x 10^{-5} kg H_2O m^{-2} s^{-1}	1.4 x 10^{-4} kg H_2O m^{-2} s^{-1}	Ogawa et al. (2012)
Relative moisture lost during the constant rate period ($\%C$)	20%	20%	Ogawa et al. (2012)

3.2.2 Description of glass transition

The Kwei model of Cuq and Icard-Verniere (2001) was used to estimate the glass transition temperature (T_g) of the pasta at different moisture content:

$$T_g = \frac{\frac{1}{1+M}T_{g,1} + k\frac{M}{1+M}T_{g,2}}{\frac{1}{1+M} + k\frac{M}{1+M}} + q\frac{M}{(1+M)^2}, \quad (3.15)$$

where $T_{g,1}$ and $T_{g,2}$ are the glass transition temperature of semolina and water and k and q are two empirical constants. For durum wheat pasta drying, these parameters take the following values: $T_{g,1}$= 273 ºC, $T_{g,2}$= -135 ºC, k = 9.5 and q = 346 (Cuq and Icard-Verniere, 2001).

Cuq et al. (2003) measured the mechanical properties of pasta at different moisture contents and temperatures. They observed that, around glass transition, sharp changes occur in the apparent strength of the pasta and the relaxation coefficients. These changes occur within a range of 2 – 5 kg water kg dry $matter^{-1}$, which should correspond to conditions where the pasta is in transition between its rubbery state and its glassy state. These observations were used for this work, where the pasta was assumed to be in the transition state when its moisture content

was at ± 1.5 kg water kg dry matter^{-1} of the moisture at glass transition (calculated with Eq. 3.15).

3.2.3 Sensitivity analysis

A sensitivity analysis was performed to evaluate the relative importance of five input parameters (the effective moisture diffusion coefficient (D_{eff}), the surface mass transfer coefficient (h_m), the shrinkage coefficient (β), the drying rate during the constant rate period (R_C) and the relative moisture lost during the constant drying rate period ($\%C$)) for the moisture transport model (Eqs. 3.1-3.10) and a reference scenario (Table 3.1, T = 353 K). The initial conditions of the pasta were a moisture content of 0.47 (d.b.), a radius of 0.00125 m and an apparent density of 1310 kg m^{-3} (Mercier et al., 2011b; Ogawa et al., 2012). Only one input model parameter was changed at a time. The required drying time (*RDT*), here defined as the time required to produce pasta with an average moisture content lower than 0.1 kg water kg dry matter^{-1}, was selected as output parameter. The relative impact of the input parameters was estimated by eliminating the effect of their units or scale using the method proposed by Chokmani et al. (2001):

$$Sr(X_i) = \frac{\partial f(X)}{\partial X_i}\Big|_{X^0} \frac{X_i^0}{f(X^0)}, \quad (3.16)$$

where $Sr(X_i)$ is the relative sensitivity of the *RDT* for the input parameter X_i, $\frac{\partial f(X)}{\partial X_i}\Big|_{X^0}$ is the partial derivative of the *RDT* with respect to X_i (evaluated for the reference scenario X^0) and X_i^0 is the value of the input parameter "*i*" at the reference scenario. The partial derivative in Eq. (3.16) was calculated numerically with a finite difference method.

3.2.4 Propagation of uncertainty

The standard deviation of the *RDT* was estimated from the knowledge of the standard deviation of the five input parameters of Table 3.1 ($X_1, X_2, \ldots X_5$) using a first-order approximation as described by Da Silva et al. (2012):

$$\sigma_f = \sqrt{\sum_{i=1}^{5}\sum_{j=1}^{5}\frac{\partial f}{\partial X_i}\frac{\partial f}{\partial X_j}\mathrm{cov}(X_i, X_j)}, \quad (3.17)$$

where σ_f is an estimator of the standard deviation of the *RDT* and $\mathrm{cov}(X_i, X_j)$ is the covariance between the input parameters X_i and X_j. When the standard deviation of one of the input parameters is significantly more important than the standard deviation of the other parameters or their covariance, Eq. (3.17) simplifies to:

$$\sigma_f = \frac{\partial f}{\partial X}\sigma_X, \quad (3.18)$$

where X is the input parameter with the dominant standard deviation. The uncertainty of the *RDT* for a predetermined confidence limit was calculated by multiplying σ_f with a factor $t_{(1-\alpha)/2,\nu}$ determined from the Student's distribution (Da Silva et al., 2012):

$$RDT = f(X_1, X_2, \ldots X_5) \pm t_{(1-\alpha)/2,\nu}\sigma_f, \quad (3.19)$$

where RDT is the actual (real) required drying time, $f(X_1, X_2, \ldots X_5)$ is the required drying time estimated from the model, α is the confidence interval and ν is the number of degrees of freedom.

3.3 Results and discussion

3.3.1 Moisture profiles estimates and experimental data

Fig. 3.2 compares the evolution of the predicted pasta average moisture content during drying according to the mass transfer model (Eqs. 3.1-3.10) to those measured by Mercier et al. (2011b) for the input parameters presented in Table 3.1. The estimated moisture profile described accurately the experimental data for two different drying temperatures. The relative difference between the measured and the predicted required drying time to reduce the pasta moisture content below 0.1 (d.b) (*RDT)* is 5% at 353 K. The *RDT* could not be calculated at 313 K drying conditions because the equilibrium moisture content of the pasta was higher than the target moisture content, 0.1 kg water kg dry matter^{-1}. Although the ability of the mass transfer model (Eqs. 3.1-3.10) to predict internal moisture profiles remains to be investigated,

the agreement between experimental and predicted average moisture content suggests that *RDT* can be predicted accurately from a model where the water mass transfer mechanisms (liquid water capillarity, water vapor diffusion, liquid water convection and water vapor convection) are described with a single parameter, the effective moisture diffusion coefficient.

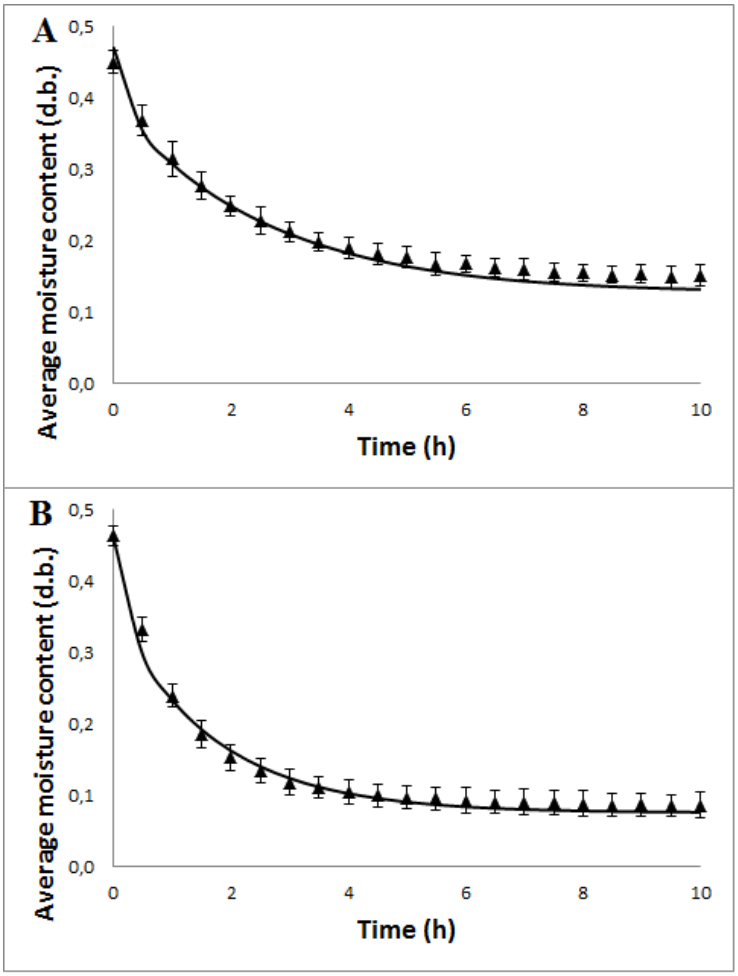

Figure 3.2. Evolution of pasta average moisture content for 313 K (A) and 353 K (B) drying: mass transfer model predictions (line) and experimental measurements (Mercier et al. (2011b) (▲ ± standard deviation).

3.3.2 Predicted required drying time sensitivity analysis

The relative sensitivity of the *RDT* predicted from the mass transfer model (Eqs. 3.1-3.10) for D_{eff}, h_m, β, $\%C$ and R_c was evaluated for the reference scenario (Table 3.1, T = 353

K). The results, presented in Fig. 3.3, show that the effective moisture coefficient was the most significant parameter. The effect of the surface mass transfer coefficient was negligible. In accordance with mass Biot number ($Bi_m = \frac{h_m R}{D_{eff}}$), which is of the order of 10^5, the internal resistance to mass transfer significantly dominates the moisture transport. Therefore, assuming that the selected empirical correlations for the estimation of the mass transfer coefficient were sufficiently accurate, the sensitivity analysis supports the validity of the Dirichlet boundary conditions to describe moisture transport during the falling drying rate period.

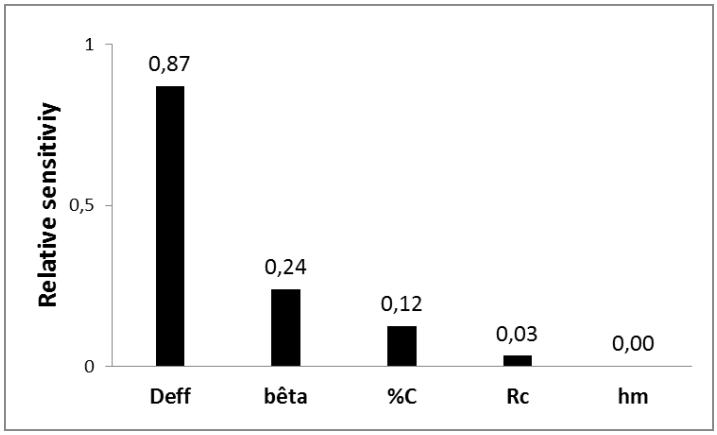

Figure 3.3. Relative sensitivity (Eq. 3.16) of the required drying time for the input parameters.

The shrinkage coefficient showed the second most significant impact on the *RDT*. Fig. 3.4 shows the drying curves obtained for the reference scenario (Table 3.1, $T = 353$ K) for the cases where pasta shrinkage was considered ($\beta = 0.75$) or neglected ($\beta = 0$). The predicted *RDT* was shorter when shrinkage was considered because of the reduced distance travelled by moisture to reach the surface of the pasta. The relative difference between the moisture content predicted with and without shrinkage never exceeded 10%, which supports the validity of the hypothesis of negligible shrinkage considered in previous models (Andrieu and Stamatopoulos, 1986; Villeneuve and Gelinas, 2007; Ogawa et al., 2012) unless high accuracy *RDT* estimate is desired. When shrinkage is neglected and D_{eff} is considered independent of the pasta moisture content, the Fick-type law can be solved analytically (Crank, 1975). Nevertheless, pasta shrinkage has to be considered when phenomena such as crack formation and propagation are modeled (Ponsart et al., 2003).

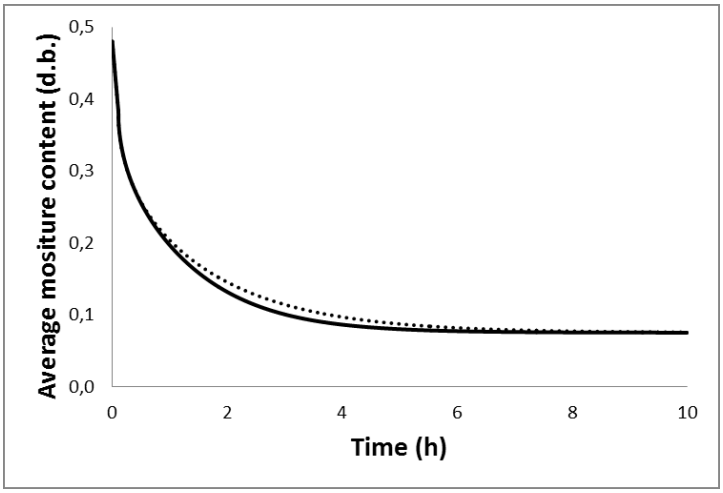

Figure 3.4. Predicted average pasta moisture profile for the reference scenario of Table 3.1 when shrinkage is considered (-) and neglected (•).

Drying rate and water lost during the constant drying rate period have minimal effect on the predicted *RDT*. For the reference scenario, the constant drying rate period was less than 10 min, which is only a small fraction of the total drying time. Therefore, the constant drying rate period can be neglected when estimating pasta *RDT*. However, the constant drying rate period should be included when modeling the quality of the pasta, because the first few minutes of drying have a critical impact on the formation and the propagation of cracks (Inazu et al., 2005; Ogawa et al., 2012).

3.3.3 Impact of the effective moisture diffusion coefficient on the predicted required drying time

The sensitivity analysis showed that the effective moisture diffusion coefficient was the parameter which affected the most the *RDT* predictions. A wide range of experimental effective moisture diffusion coefficient values are available in the form of correlations representing D_{eff} in terms of operating conditions (Table 3.2). In these correlations, the effect of the drying temperature is generally represented through an Arrhenius equation of the form $D_{eff} = A\exp(-E_a/R_gT)$. An increase in the drying temperature is therefore related to an increase in the effective diffusion coefficient with magnitude determined by the value of the activation energy (E_a). Depending of the correlation considered, additional terms are

introduced to describe their impact on $D_{eff,}$ including the dryer relative humidity (RH) and pressure (P), and the pasta average moisture content ($\overline{M}$) and porosity (ε).

Table 3.2. Empirical correlations developed to determine pasta effective moisture diffusion coefficient

Equation	Parameters	Reference
$D_{eff} = \left[A\exp\left(\frac{-E_a}{R_g T}\right)[1-\exp(-BM^C)+M^D]\right] * 10^{-12}$	$E_a = 26.0\frac{kJ}{mol}$ $A = 2.9320\ x\ 10^5$ $B = 7.9082\ x\ 10^{14}$ $C = 1.5706\ x\ 10^1$ $D = 6.8589\ x\ 10^{-1}$	Litchfield and Okos (1992)
$D_{eff} = \left(C'_{10} + \varepsilon\frac{C'_{20}}{P}\right)\exp\left[-\frac{E_a+E_b}{R_g T}\right]$	$E_a = 22.6\frac{kJ}{mol}$ $E_b = [6.0\exp(-20M)]\frac{kJ}{mol}$ $C'_{10} = 1.2\ x\ 10^{-7}\frac{m^2}{s}$ $C'_{20} = 8\ x\ 10^{-5}\frac{m^2}{s}$	Waananen and Okos (1996)
$D_{eff} = \left[\exp\left(\frac{-E_a}{R_g T} - ARH - B\right)\right] * 10^{-4}$	$E_a = 11.4\frac{kJ}{mol}$ $A = 0.0221$ $B = 8.635$	Villeneuve and Gelinas (2007)
$D_{eff} = A\exp\left[-B\left(\frac{1}{T}-\frac{1}{T_{Ref}}\right)\right]\exp(CM)$	$T_{Ref} = 293\ K$ $A = 1.2\ x\ 10^{-11}$ $B = 3036.95$ $C = 6.46\ x\ 10^{-3}$	De Temmerman et al. (2007)
$D_{eff} = [A + B(T-273) + CRH + D(T-273)^2 + E(RH)^2 + F(T-273)RH]\frac{4 * 10^{-10}}{\pi^2}$	$A = -4.27\ x\ 10^{-1}$ $B = 6.45\ x\ 10^{-2}$ $C = -1.32\ x\ 10^{-2}$ $D = -2.73\ x\ 10^{-4}$ $E = 4.05\ x\ 10^{-5}$ $F = 1.02\ x\ 10^{-4}$	Ogawa et al., (2012)

Fig. 3.5 shows the predicted average moisture profiles obtained with each of the five correlations (Table 3.2) when the other input parameters of the mass transfer model were selected according to the reference scenario (Table 3.1, T = 353 K). Results show that the

predicted drying curves are influenced significantly by the D_{eff} correlation. According to the correlation of Ogawa et al. (2012), drying time of about four hours would be sufficient to obtain pasta with $\bar{M}$< 0.1 d.b. In contrast, an additional five hours would be necessary to reach the same moisture content when the correlation of Litchfield and Okos (1992) is selected. These drying time predictions highlight the need for more accurate estimates of D_{eff} in order to improve the accuracy of pasta drying models.

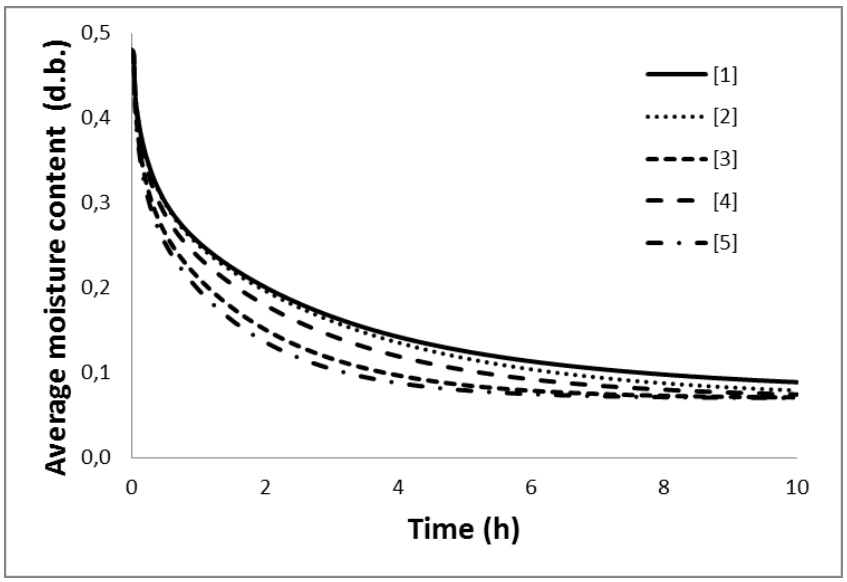

Figure 3.5. Predicted average moisture profile for D_{eff} correlations of Litchfield and Okos (1992) [1], Waananen and Okos (1996) [2], Villeneuve and Gelinas (2007) [3], De Temmerman et al. (2007) [4] and Ogawa et al. (2012) [5] for the drying conditions T = 353 K, RH = 60%, M = 0.3 (d.b.) and ε = 6%.

Fig. 3.6 presents the predicted state of the pasta (rubbery, glassy or in transition) for different drying times using the five D_{eff} correlations presented in Table 3.2 and Eq. (3.15) for the estimation of the moisture content at glass transition, i.e. when the glass transition temperature (T_g) becomes equivalent to the drying temperature. As shown in Fig. 3.6, during drying, model predictions indicate that a glassy region formed quickly at the surface of the pasta, while most of the interior remained in a rubbery state. After a given drying time, a glassy region, a rubbery region and a transition region coexisted within the pasta. Such conditions have been associated with significant local variations in the mechanical and rheological properties of pasta (Cnossen et al., 2001; Takhar et al., 2006; Xing et al., 2007; Hundal and Takhar, 2010). These local variations can induce internal stresses and promote

crack formation and propagation, such that it is generally recommended to select drying conditions that promote a uniform glass transition in the pasta.

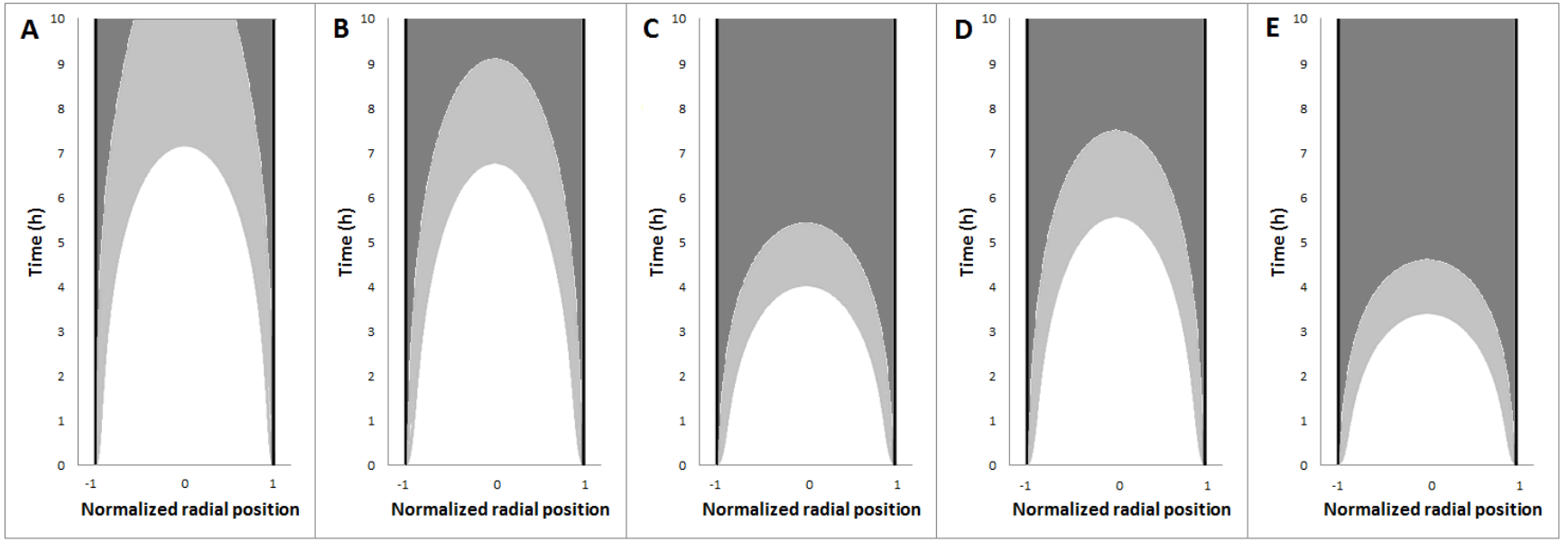

Figure 3.6. Localisation of the rubbery (white), transition (light grey) and glassy (dark grey) regions according to the pasta radial position as predicted from the correlations of Litchfield and Okos (1992) (A), Waananen and Okos (1996) (B), Villeneuve and Gelinas (2007) (C), De Temmerman et al. (2007) (D) and Ogawa et al. (2012) (E) for the drying conditions of Fig. 3.5.

The mapping of the different states presented in Fig. 3.6 also highlights the impact of the D_{eff} correlations. According to the correlation of Ogawa et al. (2012), pasta would be entirely in the glassy state after nearly four hours of drying while, according to the correlation of Litchfield and Okos (1992), the core would still be in a transition state six hours later. The selection of the D_{eff} correlation affects the uniformity of the glass transition state. For instance, the core of the pasta reached the transition state after about 6.5 hours according to the correlation of Litchfield and Okos (1992) and the correlation of Waananen and Okos (1996). However, the duration of the coexistence of a transition state and a glassy state was much longer according to the former correlation than the latter. This result could be explained by the dependence on the pasta moisture content for the correlation of Litchfield and Okos (1992) which is not included in the correlation of Waananen and Okos (1996). This dependence leads to the decrease of D_{eff} during drying for the correlation of Litchfield and Okos (1992), while D_{eff} remains constant according to the correlation of Waananen and Okos (1996). The mapping analysis illustrates the effect of the limited accuracy of D_{eff} estimates which induces significant uncertainty in the description of the glass transition and critically hinders the selection of adequate drying conditions.

3.3.4 Development of an average equation for the estimation of D_{eff}

In an attempt to improve the accuracy of D_{eff} estimates and to quantify their uncertainty, a modified correlation for D_{eff} was developed by considering the average of the five published correlations presented in Table 3.2. This correlation was developed by minimising the square errors function (J) for values of input operating parameters relevant to industrial drying processes ($313 < T < 373\ K$, $40 < RH < 80\%$, $0.1 < M < 0.5$ and $0 < \varepsilon < 0.3$):

$$J = \int_{T=313}^{373} \int_{RH=40}^{80} \int_{M=0.1}^{0.5} \int_{\varepsilon=0}^{0.3} (D_{eff} - \overline{D_{eff}})^2 d\varepsilon dM dRH dT, \qquad (3.20)$$

where D_{eff} is the effective moisture diffusion coefficient calculated from the modified correlation and $\overline{D_{eff}}$ is the average effective moisture diffusion coefficient calculated from the five published correlations (Table 3.2). The impact of the drying pressure was not considered

since most correlations were validated experimentally at atmospheric pressure. Good representations ($R^2 > 0.99$) were obtained with a linear function:

$$D_{eff} = (1.01T - 0.37RH + 17.67M + 0.06\varepsilon - 267.74) * 10^{-12} \quad (3.21)$$

Fig. 3.7 presents the effective moisture diffusion coefficient calculated with Eq. (3.21), and the average effective moisture diffusion coefficient calculated from the five published correlations (Table 3.2), when the value of one operating condition is modified one by one from the reference scenario (Table 3.1, T = 353 K). As suggested by the relative magnitude of the slope of the curves, the drying temperature has a more significant impact on D_{eff} than the dryer relative humidity, the moisture content or the porosity of the pasta.

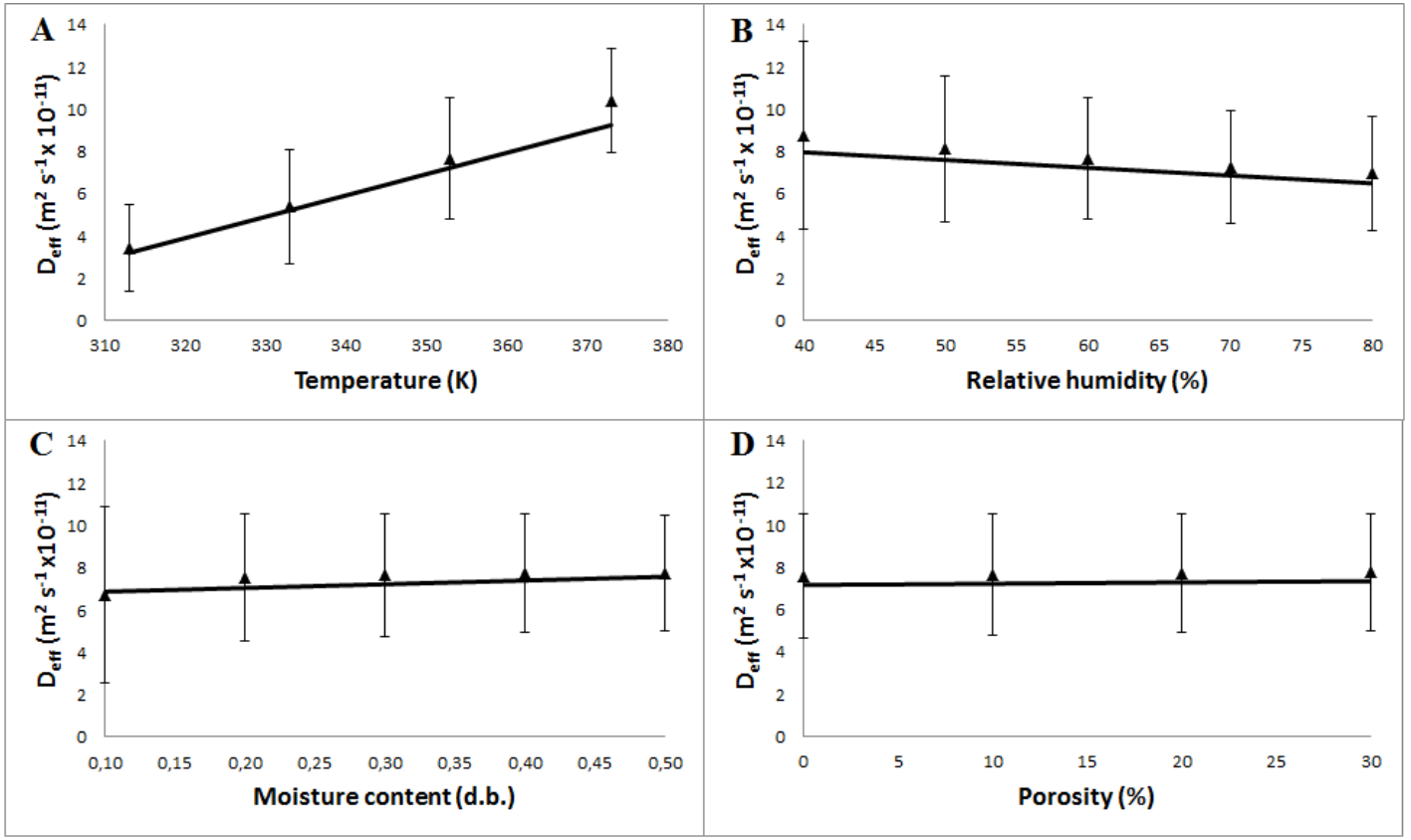

Figure 3.7. Effective moisture diffusion coefficient calculated from Eq. (3.21) (line) and from the average of the five correlations of Table 3.2 (▲ ± standard deviation) when T(A), RH(B), M (C) and ε(D) are modified one by one from the drying conditions of Fig. 3.5.

The standard deviation of D_{eff} calculated from the published correlations (Table 3.2) was between 2.1 x 10^{-11} and 3.5 x 10^{-11} m^2 s^{-1} for the range of operating conditions considered. According to Eq. (3.18), an average standard deviation of ± 2.8 x 10^{-11} m^2 s^{-1} would induce a standard deviation of ± 1.7 hours for the predicted *RDT* and the model input parameters of the reference scenario (Table 3.1, T = 353 K). It can be shown from Eq. (3.17) that a similar impact on the uncertainty of the predicted *RDT* would require standard deviation for β, $\%C$, R_C and h_m to be 0.75 ± 1.73, 20 ± 92%, 1.4 x 10^{-4} ± 2.6 x 10^{-3} kg H_2O m^{-2} s^{-1} and 0.03 ± 6.2 m s^{-1}, respectively. These parameters can be estimated much more precisely, since it is well known that, for instance, pasta does not swell during drying or does not gain water during the constant drying rate period. Therefore, the standard deviation of these parameters should be negligible in comparison to the effective moisture diffusion coefficient. The analysis of the propagation of the uncertainty indicates that the research efforts in the development of models for pasta drying should be primarily directed at the collection of more accurate D_{eff} values for a variety of drying systems and operating conditions and the investigation of the ingredients properties (hydration level, gluten content, presence of non-tradition ingredients, particles size distribution) impact on D_{eff}.

For a 90% confidence interval and four degree of freedom (i.e. five correlations -1), the Student *t*-factor in Eq. (2.19) is 2.1. Therefore, under the assumption of negligible systematic errors, Eq. (2.21) and the drying model presented in section 3.2 can be used to predict *RDT* of pasta with an uncertainty of about ± 3.5 hours. This estimate is of significant importance because it can serve as a quantitative basis for the assessment, on a case by case basis, whether the model precision is sufficient for its intended use or if additional measurements are required. Furthermore, a number of authors have commented that future challenges in pasta modelling will be associated with food quality concepts, such as microbial safety, texture properties, crack formation and flavour composition (Migliori et al., 2005; De Temmerman et al., 2007; Veladat et al., 2011). Since most of these properties are closely dependant on the internal moisture profiles during drying, most models will have pasta transport properties, such as the effective moisture diffusivity, as input parameters. In this context, the present work represents a starting point in the development of models and the assessment of their validity and the quantification of their uncertainty.

3.4 Conclusion

In this study, recent advances in pasta drying modeling were investigated by conducting sensitivity and uncertainty analysis on a drying model output parameter, the required drying time, and five major input model parameters, the effective moisture diffusion coefficient, the shrinkage coefficient, the relative water lost during the constant drying rate period, the drying rate of the constant drying rate period and the external mass transfer coefficient. Results indicated that shrinkage and external mass transfer resistance had negligible effects and that the required drying time could be estimated accurately from an analytical solution of Fick-type law. Prediction of the required drying time was influenced predominantly by the effective moisture diffusion coefficient. An analysis of the published correlations for the effective moisture diffusion coefficient indicated their important variability which results in significant uncertainty in the prediction of drying curves and the representation of the glass transition. A comprehensive linear equation relating the effective moisture diffusion coefficient to the processing conditions was developed based on the published correlations. The modified effective moisture diffusion coefficient correlation indicated that the uncertainty of the predicted required drying time was about ± 3.5 hours at 90% confidence interval.

Since a 3.5 hours uncertainty in the prediction of the required drying time would be considered inappropriate for most industrial operations, there is a need for more accurate effective moisture diffusion coefficient estimates at different drying conditions and pasta formulation. Development of mechanistic models for pasta drying should also improve the accuracy of the required drying time predictions. These mechanistic models could distinguish the liquid water flow by capillarity and convection and the water vapor flow by diffusion and convection. Therefore, the moisture transport would be predicted from individual and distinct physical properties like the liquid water diffusivity, liquid water permeability, water vapor diffusivity and water vapor permeability, instead of the current effective moisture diffusion coefficient, an aggregation of individual moisture and pasta properties.

3.5 Acknowledgements

The authors would like to thank the Natural Sciences and Engineering Research Council (NSERC) of Canada for their financial support.

CHAPITRE 4. Identifiabilité des coefficients de diffusion et de convection à partir de la mesure de la teneur en eau

Titre original : Effect of the water content measurements on the estimation and identifiability of water diffusion and convection mass transfer coefficients

Auteurs et affiliations :

S. Mercier, Ing. jr., étudiant au doctorat, Université de Sherbrooke, département de génie chimique et génie biotechnologique, 2500 boul. Université, Sherbrooke, Québec, Canada, J1K 2R1.

B. Marcos, Ing., Ph.D., Université de Sherbrooke, département de génie chimique et génie biotechnologique, 2500 boul. Université, Sherbrooke, Québec, Canada, J1K 2R1.

C. Moresoli, Ing., Ph.D. University of Waterloo, Department of Chemical Engineering, 200 University Avenue West, Waterloo, Ontario, Canada, N2L 3G1.

M. Mondor, Ing. stag., Ph.D., Agriculture et Agroalimentaire Canada, Centre de Recherche et Développement de Saint-Hyacinthe, 3600 Boul. Casavant Ouest, Saint-Hyacinthe, Québec, Canada, J2S 8E3.

S. Villeneuve, Ing., Ph.D., Agriculture et Agroalimentaire Canada, Centre de Recherche et Développement de Saint-Hyacinthe, 3600 Boul. Casavant Ouest, Saint-Hyacinthe, Québec, Canada, J2S 8E3.

Date d'acceptation : 26 juin 2015

État de l'acceptation : Publié

Référence : International Journal of Heat and Mass Transfer, 90, 480-490.

Résumé

Contenu : la revue de la littérature (chapitre 2) a révélé l'importante variabilité entre les valeurs du coefficient de diffusion effectif de l'eau dans les pâtes selon les études sur la modélisation du séchage et l'analyse de sensibilité (chapitre 3) a montré que cette variabilité engendre une incertitude significative sur la prédiction du temps de séchage requis. Le coefficient de diffusion effectif de l'eau est généralement estimé à partir de mesures de la teneur en eau. Dans cet article, il est déterminé si la variabilité du coefficient de diffusion effectif pourrait être causée par des problèmes d'identifiabilité structurelle (l'unicité de la solution par moindres carrés) ou pratique (la précision de l'estimation par moindres carrés). Pour ce faire, des mesures de la teneur en eau globale et locale ont été générées par l'ajout de bruit gaussien aux simulations d'un modèle de transfert de masse Fickian. Les coefficients de diffusion et de convection ont été estimés à partir de la teneur en eau selon le type (globale ou locale), le nombre et le bruit de mesure. L'identifiabilité des coefficients a été déterminée à partir de leur intervalle de confiance calculée par la méthode asymptotique et la méthode par profil de vraisemblance.

Résultats : les coefficients de diffusion et de convection sont (au moins localement) structurellement identifiables à partir de la mesure de la teneur en eau. Les coefficients de diffusion et de convection sont estimés plus précisément à partir de la mesure de la teneur en eau locale que de la teneur en eau globale. Les coefficients sont pratiquement identifiables à partir de la mesure de la teneur en eau globale pour un bruit de mesure inférieure à 2% et à partir de la teneur en eau locale pour un bruit inférieur à 5%. Pour un bruit supérieur à ces valeurs, le nombre de mesures de la teneur en eau doit être adapté au bruit de mesure. Les intervalles de confiances des coefficients décrivant le transfert de masse sont asymétriques et peuvent être sous-estimés par plus de 50% par la méthode asymptotique.

Contributions à la thèse : les contributions à la thèse de cet article sont la démonstration de la pertinence de mesurer la teneur en eau locale pour l'estimation des coefficients décrivant le transfert de masse, la quantification du nombre de mesures de la teneur en eau globale ou locale pour l'identifiabilité pratique des coefficients et la démonstration que la méthode asymptotique sous-estime l'intervalle de confiance des coefficients pour certains scénarios d'expérience. Cet article suggère également que l'importante variabilité entre les valeurs du

coefficient de diffusion effectif de l'eau dans les pâtes selon les études sur la modélisation du séchage pourrait être causée par leur faible identifiabilité pratique en présence de bruit sur les mesures de la teneur en eau globale.

Abstract

The aim of this work was to determine the impact of water content measurements on the structural and practical identifiability of the diffusion and the convection mass transfer coefficients. Global or internal water content were generated from the diffusion model with the addition of Gaussian noise. The diffusion and convection mass transfer coefficients were estimated from the water content by least-squares minimization and their confidence interval was calculated using the profile likelihood and the asymptotic methods. A unique combination of mass transfer coefficients reproduced exactly water content values without noise, indicating their structural identifiability. The coefficients were practically identifiable from the internal water content or the global water content if the noise intensity was less than 2% and 5%, respectively. The confidence intervals of the coefficients were asymmetric and were not accurately described by the asymptotic method.

Keywords

Identifiability; Uncertainty; Mass transfer; Diffusion coefficient; Least-squares minimization

Nomenclature

CI	95% confidence interval
cor	correlation coefficient
cov	covariance matrix
D	water diffusion mass transfer coefficient ($m^2\ s^{-1}$)
df	number of degrees of freedom
FIM	Fisher information matrix
h	water convection mass transfer coefficient ($m\ s^{-1}$)
H	measurement operator
J	least-squares objective function
l	product width (m)
L	product length (m)
M	water content (kg H_2O kg dry $matter^{-1}$)
$\overline{M}_i$	global water content without noise (kg H_2O kg dry $matter^{-1}$)
$\overline{M}_i^*$	global water content with noise (kg H_2O kg dry $matter^{-1}$)
$M_{i,j}$	internal water content without noise (kg H_2O kg dry $matter^{-1}$)
$M_{i,j}^*$	internal water content with noise (kg H_2O kg dry $matter^{-1}$)
n	number of times with a water content value
N	total number of water content values ($N = n \times p$)
N_{min}	minimum number of water content values for the practical identifiability of the mass transfer coefficients
p	number of internal water content values for a given time
S	state variable sensitivity
$\bar{S}$	global (according to x) state variable sensitivity
SSE	error sum of squares
t	time (s)
u	state variable
w	product thickness (m)
x	thickness coordinate (m)
y	vector of output variables
Greek symbols	
$\mathcal{B}$	uncertainty region for practical identifiability
ε	noise
σ	standard deviation of the noise
λ	sensitivity matrix
θ	vector of model coefficients
$\hat{\theta}$	vector of model coefficients estimated from water content
θ^*	value of the model coefficients used to generate water content

Θ_{ad}	set of admissible values for θ
σ^2	variance of the noise
Subscripts	
0	initial
1	first
2	second
E	equilibrium
i	time i
j	internal position j
f	final
w	at $x = w$

4.1 Introduction

Multiple unit operations such as drying, soaking, baking, frying and lyophilisation involve the addition or the removal of water from a product. These unit operations can be described by developing mathematical models relating the state variables of the product (water content, temperature, velocity) to the model coefficients (diffusion and convection mass transfer coefficients, thermal conductivity, initial water content, density) using conservation equations. The conservation equations are ordinary or partial differential equations for given time interval $[t_0,t_f]$ and are formulated as mathematical model $M = \{\Phi(\theta, u) = 0, y = H(u)\}$ where Φ is the differential operator, θ the vector of coefficients, u the vector of state variables, y the vector of output variables and H the measurement operator. For most products, one or multiple elements of the vector of coefficients are unknown and need to be estimated to apply the model. A typical method to estimate these coefficients is based on the measurement of the state variable and the application of an inverse method, such as least-squares minimization. However, this approach is only applicable if the coefficients of the model are identifiable.

The identifiability of the coefficients of a model can be divided in structural and practical identifiability. Structural identifiability refers to the unicity of the inverse method for measurements of the state variable without noise (Tayakout-Fayolle et al. 2000; Navarro-Laboulais et al. 2006; Davidescu et al. 2008). Assuming that θ_1 belongs to a set of admissible values Θ_{ad}, θ_1 will be structurally identifiable if no other admissible vector of coefficients θ_2 can give the same output variable y:

$$y(\theta_1) = y(\theta_2) \Longrightarrow \theta_1 = \theta_2 \tag{4.1}$$

If all vectors θ of Θ_{ad} are identifiable, the model is globally structurally identifiable.

Practical identifiability refers to the identifiability of the coefficients from noisy measurements of the observed variable and reflects the quality of the experimental measurements. In this context, the identifiability of model coefficients can be formulated using a least-squares objective function J:

$$J(\theta) = \left\| y(\theta) - y_{exp} \right\|_H, \tag{4.2}$$

where y_{exp} is the vector of measured variables and $\|\cdot\|_H$ is the norm (generally the Euclidian norm) over the measurement operator H. An estimate ($\hat{\theta}$) of the value of the coefficients (θ*) is calculated by minimizing the least-squares function. Since the estimate is obtained from noisy measurements, $\hat{\theta}$ is a random vector and the coefficients θ* can only be estimated within a confidence interval. Although no formal definition of the practical identifiability is accepted, a common definition is that the coefficient is practically identifiable if the estimate is considered sufficiently accurate, e.g. if the confidence interval of the estimate is a subset of a predetermined uncertainty region $\mathcal{B}$ in the coefficient space (Jang et al. 2011; Berthoumieux et al. 2013):

$$CI(\theta) \subseteq \mathcal{B} \tag{4.3}$$

The uncertainty region for practical identifiability $\mathcal{B}$ is selected such that the confidence interval is sufficiently narrow for the estimate to provide useful information. Therefore, the selection of the uncertainty region for practical identifiability depends on the model and application.

Structural identifiability of coefficients can be assessed by several techniques according to the linearity and complexity characteristics of the model and the measurement operator (time and/or position of the measurements). For models represented by ordinary differential equations, transfer matrix (by Laplace transformation) and generative series techniques can be used to determine the structural identifiability of linear models (Bellman et al. 1970; Walter et al. 1982; Godfrey et al. 1987) while differential algebra techniques are used for complex and nonlinear models (Ljung and Glad 1994; Jayasankar et al. 2009). For models with partial differential equations, structural identifiability can be determined from spectral analysis of the differential operator (Kravaris 1988; Boumenir and Tuan 2009; Gutman and Ha 2009) and systematic exploration of the likelihood in the coefficient space (Raue et al. 2009).

For linear models such as the 1-D heat equation (with source term) with Robin boundary conditions, several important results on the structural identifiability have been established from the spectral analysis of the differential operator. Kravaris (1988) showed that the thermal conductivity is structurally identifiable from the product surface temperature when there is no heat source and the heat flux at the boundary is known. Boumenir and Tuan (2009)

demonstrated the structural identifiability of the source term from the temperature at the boundary. Gutman and Ha (2009) demonstrated the structural identifiability of the thermal conductivity and transient boundary heat flux from several spatial and time distributed values of the temperature.

Structural and the practical identifiability of the diffusion and convection mass transfer coefficients for the diffusion model describing the addition or the removal of water from a product have not been investigated. The identifiability of the coefficients for mass transfer models differs from heat transfer models by the type of measurements available where only global water content measurements are generally available, the evolution of the mass of the product during processing, because internal water content measurements are difficult to obtain or inaccurate (De Temmerman et al. 2007; Xing et al. 2007). The measurement of the mass of the product allows for the calculation of the global water content but does not provide information about the internal water content of the product and it remains unclear how this affects the reliability of the estimation of the mass transfer coefficients from experimental measurements.

The aim of this work was to assess the structural and practical identifiability of water mass transfer coefficients from global or internal water content. The identifiability of the coefficients was verified for conditions consistent with a drying application (removal of water content), but the results can be easily extended to other mass transfer operations involving the addition or removal of water content described using the same mass transfer conservation equations. To accomplish this work, discrete values of the global or internal water content were generated by adding Gaussian noise to global and internal water content estimated by a mass transfer diffusion model with specified input mass transfer coefficients. These water content values were subsequently used to estimate diffusion mass transfer coefficient and convection mass transfer coefficient using least-squares minimization. The practical identifiability of these two mass transfer coefficients was assessed from the confidence intervals calculated with the profile likelihood method and the asymptotic method. The type (global or internal), number and position of the water content and the noise intensity were investigated using Monte Carlo simulations to determine the experimental conditions for the identification of the two mass transfer coefficients.

4.2 Methods

4.2.1 Mass transfer model

One dimension (1-D) Fick-type diffusion model with Robin boundary conditions was considered in this work. This model assumes that the product is a continuum material at the macroscopic scale and describes the combined mass transfer of liquid and water vapor using an effective diffusion mass transfer coefficient (D). This model was considered in this work because it may represent the most widely used mass transfer model to describe the addition or removal of water content and has been validated for many chemical, pharmaceutical or bioproducts (Fey and Boles 1987; Daud et al. 1997; Park et al. 2007; Cernak and Trcala 2012; Garcia et al. 2012; Ho et al. 2013; Perussello et al. 2013; Zhu and Shen 2014). A rectangular product of dimensions L x l x w, where $L >> w$, $l >> w$ and w is the product thickness was considered:

$$\frac{\partial M}{\partial t} = D\frac{\partial^2 M}{\partial x^2}, \tag{4.4}$$

where M is the water content of the product on a dry basis, t is the time, D is the diffusion mass transfer coefficient and x is the coordinate in the w dimension. The product has uniform initial water content (M_0):

$$M = M_0 \qquad (\text{for } 0 \leq x \leq w \text{ and } t = 0) \tag{4.5}$$

The product surface at $x = 0$ is considered insulated:

$$\frac{\partial M}{\partial x} = 0 \qquad (\text{at } x = 0) \tag{4.6}$$

Eq. (4.6) could also describe the mass transfer of water at the center of a product with the two external surfaces exposed. The mass transfer of water at the surface $x = w$ is described using a Robin boundary condition:

$$-D\frac{\partial M}{\partial x} = h(M - M_E), \qquad (\text{at } x = w) \tag{4.7}$$

where h is the convection mass transfer coefficient in the air and M_E is the equilibrium water content.

4.2.2 Generation of water content values

Water content (M) as a function of the spatial coordinate (x) and time (t) were generated from the diffusion model (Eqs. 4.4-4.7) and the input parameters shown in Table 4.1 describing drying of a generic product. A finite difference method using Matlab 7.12 was adopted with a 6.25 x 10^{-5} m discretization in space and 15 s in time. A finer space (3.12 x 10^{-5} m) and time (7.5 s) discretization gave similar results indicating grid independency. The model was solved for 3 x 10^4 s, the time required for the product to reach ~99% of the difference between its initial water content (M_0) and its equilibrium water content (M_E).

Two types of water content values were considered for the estimation of the mass transfer coefficients, global and internal water content. Global water content ($\overline{M}_i = \frac{1}{w}\int_0^w M(x,t_i)dx$) were estimated for discrete times t_i. Internal water content ($M_{i,j}$) were estimated at discrete positions x_j and times t_i. Zero mean Gaussian noise (ε) was added to represent experimental error:

$$\overline{M}_i^* = \overline{M}_i(\theta^*) + \varepsilon \qquad \text{(global water content with noise)} \qquad (4.8)$$

$$M_{i,j}^* = M_{i,j}(\theta^*) + \varepsilon \qquad \text{(internal water content with noise)} \qquad (4.9)$$

where $\overline{M}_i$ and $M_{i,j}$ are the water content simulated with the mass transfer model (Eqs. 4.4-4.7) with $\theta^* = [D^*, h^*] = [10^{-10}\ \text{m}^2\ \text{s}^{-1},\ 4 \times 10^{-7}\ \text{m s}^{-1}]$ (Table 4.1), and $\overline{M}_i^*$ and $M_{i,j}^*$ are the water content values generated from the addition of noise ε. The noise was assumed to be Gaussian, $\varepsilon \sim N(0, \sigma^2)$, a common hypothesis to represent experimental error (Candes et al. 2006; Liu et al. 2005; Zhou et al. 2007; Chakrabortty 2011; Luo et al. 2013). The standard deviation (σ) of the noise was expressed as the percentage of the average between the initial and the equilibrium water content (0.3).

Table 4.1. Properties of the generic product used to generate water content values (Eqs. 4.8 and 4.9)

Parameters	Value
Diffusion mass transfer coefficient (D*)	10^{-10} m^2 s^{-1}
Convection mass transfer coefficient (h*)	4 x 10^{-7} m s^{-1}
Product thickness (w)	1.25 mm
Initial water content (M_0)	0.5 kg water kg dry solid^{-1}
Equilibrium water content (M_E)	0.1 kg water kg dry solid^{-1}

4.2.3 Least-squares minimization

The diffusion mass transfer coefficient (D) and convection mass transfer coefficient (h) were estimated from the water content generated from the model by minimizing a least-squares objective function J. For the global water content ($\bar{M}$), the least-squares objective function was calculated from the error sum of squares (SSE), defined as:

$$J(\theta) = SSE = \sum_{i=1}^{n}(\bar{M}_i(\theta) - \bar{M}_i^*)^2, \quad (4.10)$$

where $\theta = [D, h]$ and n is the number of time values. For internal water content, the objective function was:

$$J(\theta) = SSE = \sum_{i=1}^{n}\sum_{j=1}^{p}\left(M_{i,j}(\theta) - M_{i,j}^*\right)^2, \quad (4.11)$$

where p is the number of internal positions for a given time. The objective function was minimized with Nelder-Mead simplex search algorithm using Matlab 7.12. Minimization with Nelder-Mead simplex search algorithm was performed using $0.5\theta^*$, θ^* and $2\theta^*$ as the vector of initial values to verify that least-square estimates of the mass transfer coefficients were independent of the initial values. The vector of mass transfer coefficients estimated by least-squares minimization was denoted as $\hat{\theta} = [\hat{D}, \hat{h}]$.

4.2.4 Estimation of the confidence intervals for the diffusion mass transfer coefficient and the convection mass transfer coefficient

4.2.4.1 Profile likelihood method

The profile likelihood method was applied to obtain the confidence intervals of the estimated mass transfer coefficients ($\hat{\theta}$) as detailed by Raue et al. (2009). The method consists of modifying the estimated coefficient by an incremental step of $\Delta\theta_i$, find the coefficient $\theta_{j\neq i}$ that minimize *SSE* and plot $\frac{SSE}{\sigma^2}$ as a function of θ_i, where σ^2 is the noise variance. For instance, the profile likelihood of the diffusion mass transfer coefficient (*D*) was calculated from the following steps:

(1) Starting from its optimized value ($\widehat{D}$), modify the coefficient *D* by incremental step ΔD in the increasing and decreasing directions of *D;*
(2) Find the value of *h* that minimize *SSE* (Eqs. 4.10 or 4.11);
(3) Plot the profile likelihood of *D*, that is value of $\frac{SSE}{\sigma^2}$ as a function of *D*;

The same procedure was applied to calculate the profile likelihood of *h*. The incremental steps ΔD and Δh were taken as 5% of θ*. Smaller steps (1%) were also considered, but similar results were obtained. The confidence intervals (*CI*) of *D* and *h* were taken as the set of coefficients giving $\frac{SSE}{\sigma^2}$ values in agreement with the threshold defined by the χ^2 distribution (Raue et al. 2009):

$$CI(\theta_i) = \left\{\theta_i \middle| \frac{SSE}{\sigma^2}(\theta_i) - \frac{SSE}{\sigma^2}\left(\widehat{\theta_\iota}\right) < \Delta_{\alpha,df}\right\}, \quad (4.12)$$

where θ_i is the specific coefficient (*D* or *h*), $\widehat{\theta_\iota}$ is the coefficient obtained after least-squares minimization, $\Delta_{\alpha,df}$ is the α quantile of the χ^2 distribution and *df* is the number of degrees of freedom, which was equal to the number of coefficients (two in the present case) for simultaneous confidence intervals. A confidence level of 95% was selected.

The diffusion and convection mass transfer coefficients were considered practically identifiable if their confidence interval calculated using the profile likelihood method was a subset of the uncertainty region $0.01 \times 10^{-10} < D < 100 \times 10^{-10}$ m^2 s^{-1} and $0.01 \times 10^{-7} < h < 100 \times 10^{-7}$ m s^{-1}. Confidence intervals too wide to be a subset of this uncertainty region for

practical identifiability indicated that the order of magnitude of the coefficients could not be estimated from the water content values.

4.2.4.2 Asymptotic confidence intervals

The asymptotic confidence intervals, which represent the confidence intervals calculated in most studies to quantify the uncertainty of parameters estimated by least-squares minimization, were calculated from the model sensitivity (λ), Fisher Information (*FIM*) and covariance (*cov*) matrices. The sensitivity matrix was calculated from the sensitivity functions of the mass transfer model, obtained by differentiating the model equations (Eqs. 4.4-4.7) with respect to D and h. The sensitivity function for the diffusion mass transfer coefficient and the initial and boundary conditions required to solve the partial differential equation was as follows:

$$\frac{\partial S_D}{\partial t} = D\frac{\partial^2 S_D}{\partial x^2} + \frac{\partial^2 M}{\partial x^2} \tag{4.13}$$

$$S_D = 0 \qquad (\text{for } 0 \le x \le w \text{ and } t = 0) \tag{4.14}$$

$$\frac{\partial S_D}{\partial x} = 0, \qquad (\text{at } x = 0) \tag{4.15}$$

$$-D\frac{\partial S_D}{\partial x} - \frac{\partial M}{\partial x} = h\,S_D, \qquad (\text{at } x = w) \tag{4.16}$$

where S_D is the state variable (M) sensitivity for the diffusion mass transfer coefficient ($S_D(x,t) = \frac{\partial M}{\partial D}$). The sensitivity function for the convection mass transfer coefficient and the initial and boundary conditions were:

$$\frac{\partial S_h}{\partial t} = D\frac{\partial^2 S_h}{\partial x^2}, \tag{4.17}$$

$$S_h = 0 \qquad (\text{for } 0 \le x \le w \text{ and } t = 0) \tag{4.18}$$

$$\frac{\partial S_h}{\partial x} = 0 \qquad (\text{at } x = 0) \tag{4.19}$$

$$-D\frac{\partial S_h}{\partial x} = (M - M_e) + h\,S_h, \qquad (\text{at } x = w) \tag{4.20}$$

where S_h is the sensitivity for the convection mass transfer coefficient ($S_h(x,t) = \frac{\partial M}{\partial h}$). The sensitivity functions were solved using the finite difference method, as described in section 4.2.2, and the input parameters of Table 4.1.

For the global water content, the sensitivity matrix (λ) was defined as:

$$\lambda = \begin{bmatrix} \bar{S}_{D,1} & \bar{S}_{h,1} \\ \cdots & \cdots \\ \bar{S}_{D,i} & \bar{S}_{h,i} \\ \cdots & \cdots \\ \bar{S}_{D,n} & \bar{S}_{h,n} \end{bmatrix}, \tag{4.21}$$

where $\bar{S}_D(t) = \frac{\partial \bar{M}}{\partial D} = \frac{1}{w}\int_0^w S_D(x,t)dx$ and $\bar{S}_h(t) = \frac{\partial \bar{M}}{\partial h} = \frac{1}{w}\int_0^w S_h(x,t)dx$. For the internal water content, the sensitivity matrix was defined as:

$$\lambda = \begin{bmatrix} S_{D,1,1} & S_{h,1,1} \\ \cdots & \cdots \\ S_{D,n,1} & S_{h,n,j} \\ \cdots & \cdots \\ S_{D,i,j} & S_{h,i,j} \\ \cdots & \cdots \\ S_{D,1,p} & S_{h,1,p} \\ \cdots & \cdots \\ S_{D,n,p} & S_{h,n,p} \end{bmatrix}, \tag{4.22}$$

where $S_{i,j}$ is the sensitivity at time *i* and position *j* inside the product.

The Fisher Information Matrix is the negative Hessian of the log-likelihood function. For a model with Gaussian noise of constant variance (homoscedasticity) as considered in this work, the FIM is well approximated by the inner product sensitivity matrix and the noise variance (Dobre 2010; Ramachandran and Barton 2010):

$$FIM = \frac{\lambda^T \lambda}{\sigma^2} \tag{4.23}$$

The covariance matrix of the model is the inverse of the *FIM* ($cov = FIM^{-1}$). The asymptotic confidence intervals were calculated from the normal distribution at 95% significance level:

$$CI(\theta_i) = \left\{ \theta_i \middle| \left|\theta_i - \widehat{\theta_i}\right| < Z_{\alpha/2}\sqrt{cov_{i,i}\big|_{\widehat{\theta}_i}} \right\}, \tag{4.24}$$

where $Z_{\alpha/2}$ is the standard normal distribution with $\alpha/2$ significance level and $cov_{i,i}\big|_{\widehat{\theta}_i}$ is the *ii* element of the covariance matrix evaluated at $\theta_i = \widehat{\theta}_i$.

4.2.5 Correlation between the diffusion and convection mass transfer coefficients

Correlation between the diffusion mass transfer coefficient and the convection mass transfer coefficient ($cor_{D,h}$) was calculated from the covariance matrix (Ashyraliyev et al. 2009):

$$cor_{D,h} = \frac{cov_{D,h}}{\sqrt{cov_{D,D}cov_{h,h}}}, \tag{4.25}$$

where $cov_{D,h}$ is the covariance between *D* and *h* (corresponding to the off-diagonal element of the symmetric covariance matrix) and $cov_{D,D}$and $cov_{h,h}$ are the variance of *D* and *h*, respectively (corresponding to the first and second elements of the main diagonal of the covariance matrix).

4.2.6 Monte Carlo simulation

Monte Carlo simulations with 500 input conditions were conducted to assess the practical identifiability of the mass transfer coefficients (*D* and *h*) according to the intensity of the noise (σ) and the number of water content values (*N*). The input conditions of σ and *N* were generated randomly from uniform distributions $\sigma \sim U(0\%, 20\%)$ and $N \sim U(3, 200)$. For each input condition, a set of *N* values of the water content were generated for constant time and space intervals as described in section 4.2.2. Monte Carlo simulations were performed for global water content and internal water content values. Internal water content values were generated at ten equally spaced positions within the product in accordance with Litchfield and Okos (1992). The mass transfer coefficients $\widehat{D}$ and $\hat{h}$ were estimated from these water content values by least-squares minimization as described in section 4.2.3 and their 95% confidence interval was calculated using the profile likelihoods (Eq. 4.12). As indicated previously (section 4.2.4.1), the mass transfer coefficients were assumed to be practically

identifiable if the lower and upper limits of their confidence interval were within the uncertainty region $0.01 \times 10^{-10} < D < 100 \times 10^{-10}$ m^2 s^{-1} and $0.01 \times 10^{-7} < h < 100 \times 10^{-7}$ m s^{-1}.

4.3 Results and discussion

4.3.1 Contour plots of the error sum of squares for the diffusion and convection mass transfer coefficients

Fig. 4.1 shows the *SSE* contour plot (Eqs. 4.8 or 4.9) as a function of the diffusion mass transfer coefficient (D) and the convection mass transfer coefficient (h) for the global water content at ten equally spaced times (Fig. 4.1A) and the internal water content at five equally spaced positions for $t = 0.5 \times 10^4$ s and $t = 1.5 \times 10^4$ s (Fig. 4.1B) without noise ($\varepsilon = 0$). For both types of water content, the unique minimum of the least-squares function J was the value of the coefficients used to generate water content values ($D^* = 10^{-10}$ m^2 s^{-1} and $h^* = 4 \times 10^{-7}$ m s^{-1}), indicating that the coefficients D and h are structurally identifiable (Raue et al. 2009; Graciano et al. 2014).

For the internal water content (Fig. 4.1B), the contour lines had an elliptical shape at the vicinity of the value of the coefficients used to generate water content values ($D^* = 10^{-10}$ m^2 s^{-1} and $h^* = 4 \times 10^{-7}$ m s^{-1}), but asymptotic profiles for increasing *SSE*. Asymptotic profiles indicate the presence of a functional relationship between the diffusion mass transfer coefficient and the convection mass transfer coefficient along which the increase of *SSE* is minimal (Raue et al. 2009; Hines et al. 2014). For the global water content (Fig. 4.1A), the elliptical shape of the error was not observed even for very small *SSE* (5×10^{-6}), indicating that wider range of D and h can reproduce with equal accuracy global water content than internal water content.

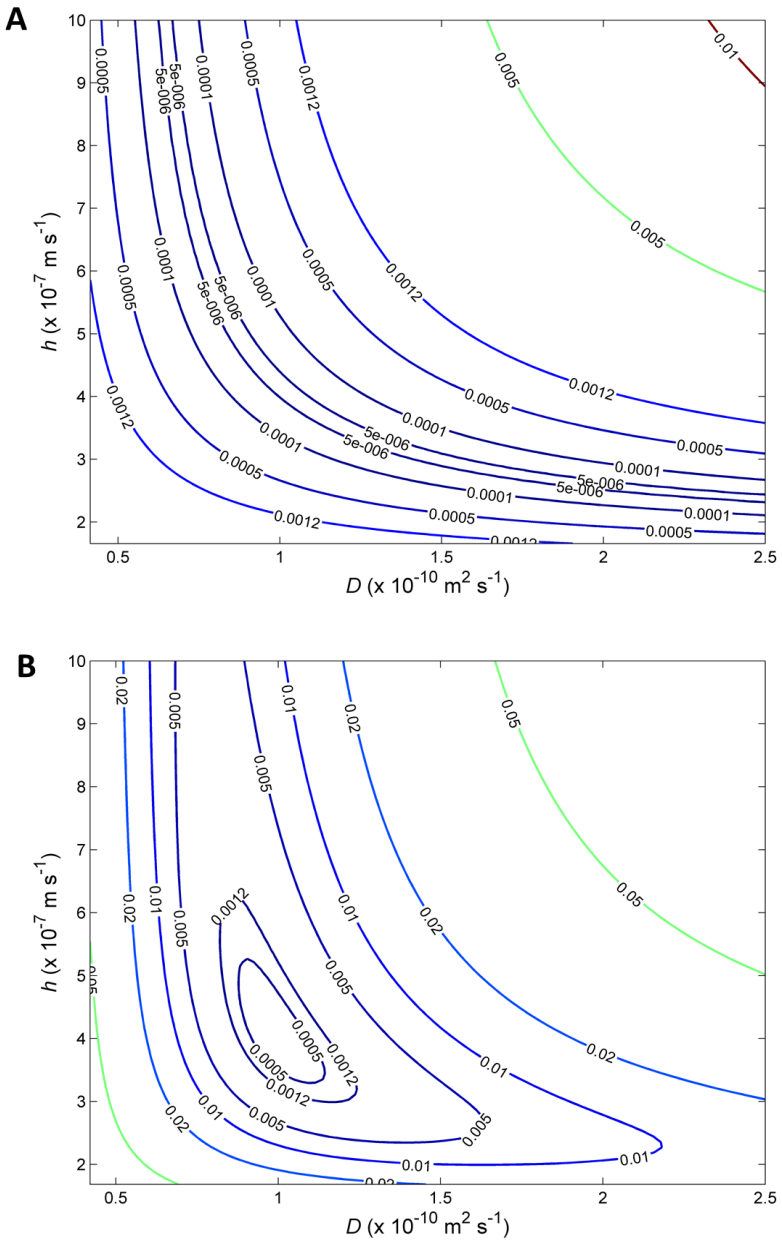

Figure 4.1. Contour plots of the error sum of square (*SSE*) for the diffusion mass transfer coefficient (D) and convection mass transfer coefficient (h) with 10 water content values (σ = 0): (A) global water content and (B) internal water content.

Regardless of the type of water content or the intensity of the noise, *SSE* increased sharply with decreasing magnitude of the two mass transfer coefficients while *SSE* remained relatively constant for increasing magnitude of the coefficients (Fig. 4.1). This was confirmed by the sensitivity functions (Eqs. 4.13-4.20) illustrated in Fig. 4.2 for t = 1 x 10^4 s and $x = w/2$. The

sensitivity of the state variables S_D and S_h increased significantly as the diffusion or the convection mass transfer coefficients approached zero, indicating that the sensitivity of *SSE* is higher for underestimation than for overestimation of the mass transfer coefficients.

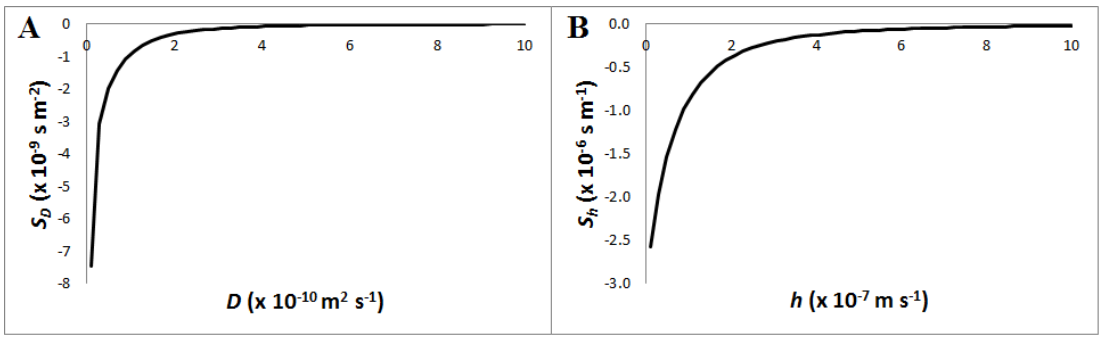

Figure 4.2. Sensitivity of the state variable S_D (A) and S_h (B) according to the diffusion mass transfer coefficient (D) and convection mass transfer coefficient (h) for t = 1 x 10^4 s and x = w/2.

4.3.2 Influence of the noise intensity on the confidence intervals of the mass transfer coefficients

The profile likelihoods of the mass transfer coefficients are presented in Fig. 4.3 for 10 values of the global or internal water content obtained as described in section 4.3.1 with noise σ = 2% and σ = 10%. The corresponding 95% confidence intervals are presented in Table 4.2.

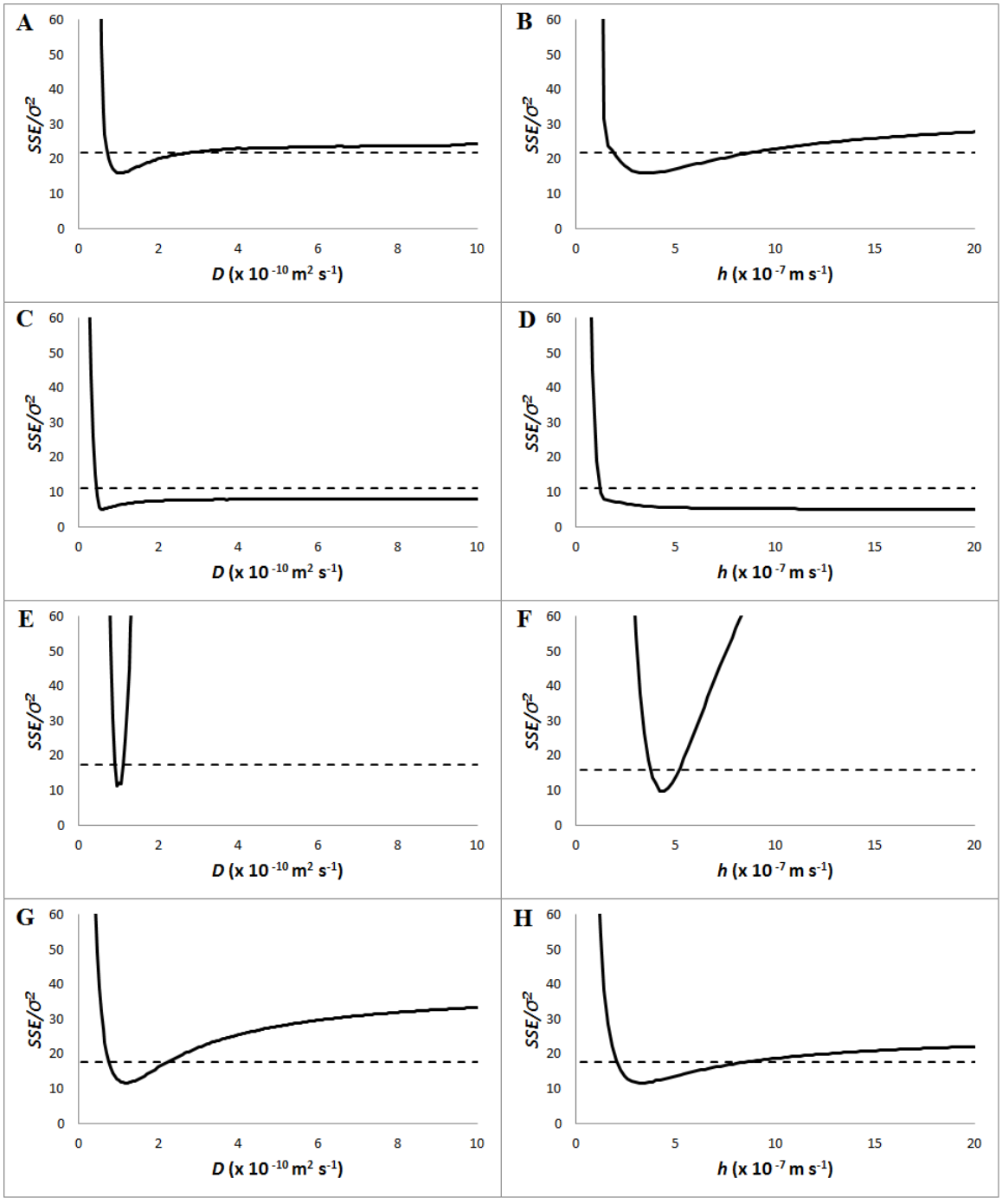

Figure 4.3. Profile likelihoods (continuous line) and 95% confidence intervals (dotted line) of the diffusion mass transfer coefficient (D) (left panel) and convection mass transfer coefficient (h) (right panel): global water content and $\sigma = 2\%$; (A-B); $\sigma = 10\%$ (C-D); internal water content and $\sigma = 2\%$ (E-F); $\sigma = 10\%$ (G-H).

Table 4.2. 95% confidence intervals (*CI*) of the diffusion and convection mass transfer coefficients calculated using the profile likelihood and asymptotic methods for ten water content values

Water content	Diffusion mass transfer coefficient (x 10^{-10} m^2 s^{-1})			Convection mass transfer coefficient (x 10^{-7} m s^{-1})			$cor_{D,h}$
	$\widehat{D}$	Profile likelihood *CI*	Asymptotic *CI*	$\widehat{h}$	Profile likelihood *CI*	Asymptotic *CI*	
Global, σ = 2%	1.02	0.72, 2.86	0.63, 1.40	3.60	1.87, 8.82	1.66, 5.53	-0.98
Global, σ = 10%	0.55	0.43, > 100	< -10, > 100	364.5	1.17, > 100	< -10, > 100	-0.97
Internal, σ = 2%	0.99	0.90, 1.10	0.92, 1.06	4.40	3.72, 5.14	3.82, 4.98	-0.76
Internal, σ = 10%	1.18	0.76, 2.22	0.72, 1.64	3.20	2.04, 8.50	1.71, 4.69	-0.74

As observed with the *SSE* contour plots (Fig. 4.1), $\frac{SSE}{\sigma^2}$ increased sharply for decreasing values of the diffusion or the convection mass transfer coefficient. Consequently, when one of the coefficients is underestimated, the other coefficient can not be adjusted to obtain an accurate estimation of the water content and a lower limit of the confidence interval is obtained in the uncertainty region for practical identifiability regardless of the noise intensity or the type of water content (global or internal). The profile likelihoods were relatively constant for increasing values of the mass transfer coefficients and the practical identifiability of an upper limit for the confidence intervals was affected by the type of water content.

Narrow 95% confidence intervals were obtained for ten internal water content values with a low noise intensity (σ = 2%) and the mass transfer coefficients were practically identifiable (Fig. 4.3E-F). The mass transfer coefficients were also practically identifiable for internal water content values with higher noise intensity (σ = 10%). However, the confidence intervals of the coefficients were approximately 10 times wider than for σ = 2%, illustrating the significant impact of the noise on the accuracy of the mass transfer coefficient estimates.

An upper limit of the confidence interval in the uncertainty region for practical identifiability was obtained for global water content with σ = 2% (Fig. 4.3A-B), confirming the practical identifiability of the mass transfer coefficients for global water content values at 10 different times with low noise intensity. The confidence intervals were approximately 10 (for *D*) and 5 (for *h*) times wider when compared to those for internal water content with the same noise intensity (σ = 2%), indicating that relevant information was lost for global water content. For global water content values with significant noise intensity (σ = 10%), the profile likelihoods were relatively constant for increasing values of *D* and *h* (Fig. 4.3C-D) and the mass transfer coefficients estimated from water content ($\widehat{D}$ = 0.55 x 10^{-10} m^2 s^{-1} and $\hat{h}$ = 364.5 x 10^{-7} m s^{-1}) were significantly different from the mass transfer coefficients used to generate water content values (D^* = 10^{-10} m^2 s^{-1} and h^* = 4 x 10^{-7} m s^{-1}). Accordingly, the upper limit of the confidence intervals was outside of the uncertainty region for practical identifiability and the coefficients were not practically identifiable. An application where such a situation may occur is in the case of pasta drying. Migliori et al. (2005) measured the water content of pasta during drying at 14 drying times using a weighting method. The average standard deviation of the measurements was near 10%. The identifiability analysis presented in Fig.

4.3C-D indicates that the water diffusion and convection mass transfer coefficients during pasta drying would not be practically identifiable from the measurements because of their high noise intensity. Simulation of pasta drying with the mass transfer model (Eqs. 4.4-4.7) would require prior estimate of one of the two mass transfer coefficients from literature sources or additional data, such as the internal water content of the pasta during drying, would need to be obtained to identify both mass transfer coefficients from the measurements.

A strong correlation between the diffusion and convection mass transfer coefficients ($cor_{D,h} \approx$ -0.98) was observed for global water content (Table 4.2). The strong correlation indicates that fluctuation of one of the mass transfer coefficient can be compensated by fluctuation of the other mass transfer coefficient. For instance, an overestimation of the diffusion mass transfer coefficient increases the rate of water migration inside the product, but similar global water content values could be obtained with a smaller convection mass transfer coefficient which increases the external resistance to mass transfer. Consequently, as illustrated in Fig. 4.4 (black and grey continuous lines), significantly different combinations of D and h can provide similar representation of the global water content, explaining the practical non-identifiability of the mass transfer coefficients for situations where global water content values contain significant noise.

The correlation between the diffusion and the convection mass transfer coefficients was not as strong for internal water content ($cor_{D,h} \approx$ -0.75) compared to global water content ($cor_{D,h} \approx$ -0.98) (Table 4.2). The weaker correlation explains the practical identifiability of the coefficients for internal water content with significant noise intensity (σ = 10%) and suggests that the estimation of the mass transfer coefficients should be based on internal water content values.

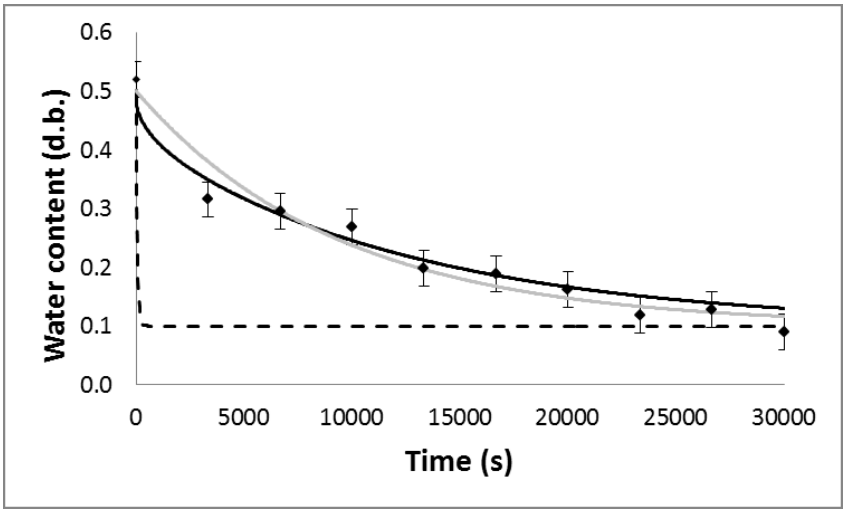

Figure 4.4. Water content values (♦ ± standard deviation) generated with N = 10 and 10% noise intensity for D = 0.5 x 10^{-10} m^2 s^{-1} and h = 9400 x 10^{-7} m s^{-1} (black continuous line), D = 100 x 10^{-10} m^2 s^{-1} and h = 1.34 x 10^{-7} m s^{-1} (grey continuous line) and D = 100 x 10^{-10} m^2 s^{-1} and h = 9400 x 10^{-7} m s^{-1} (dotted line).

4.3.3 Asymptotic confidence intervals

The asymptotic confidence intervals of the mass transfer coefficients for 10 water content values are presented in Table 4.2. Asymptotic confidence intervals were obtained from a quadratic approximation of the log-likelihood and thus restrict the confidence interval to an ellipsoid around $\hat{\theta}$ (Raue et al. 2009; Liu et al. 2005). Asymptotic confidence intervals are exact for linear models and represent a good approximation for nonlinear models if the number of measurements is sufficient and the experimental noise intensity is low (Raue et al. 2009; Schaber and Klipp 2011). The asymptotic confidence intervals were similar to the confidence intervals calculated using the profile likelihoods for internal water content with low noise intensity (σ = 2%) (Table 4.2). For internal water content with high noise intensity (σ = 10%) or global water content with low noise intensity (σ = 2%), the upper limit of the asymptotic confidence intervals was closer to the estimated coefficients $\hat{\theta}$ than the upper limit obtained using the profile likelihoods. The asymptotic confidence intervals thus underestimated the uncertainty caused by the relatively constant likelihood for increasing values of the coefficients around $\hat{\theta}$ and overestimated the accuracy of the coefficients. The

lower limit of the asymptotic confidence intervals extended in the negative range for 10 global water content values with high noise intensity (σ = 10%), which is not physically realistic, while more realistic lower limits of $D > 0.43 \times 10^{-10}$ m^2 s^{-1} and $h > 1.17 \times 10^{-7}$ m s^{-1} were obtained using the profile likelihoods. The lack of accuracy of the asymptotic confidence intervals is caused by the curvature of *SSE* according to the diffusion and convection mass transfer coefficients (Fig. 4.1) and indicates that a systematic analysis of the coefficient space, such as based on the profile likelihoods, should be considered for a more robust estimation of the confidence intervals.

4.3.4 Effect of the number of water content values

Increasing the number of water content values generally narrows the confidence interval of the coefficients estimated by least-squares minimization. Table 4.3 presents the confidence intervals calculated using the profile likelihoods and the asymptotic confidence intervals for global water content at 100 equally spaced times and the internal water content at ten equally spaced internal positions for ten equally spaced times. The confidence intervals for 100 water content values were narrower for all noise intensities and for the two types of water content values compared to the confidence intervals for 10 water content values (Table 4.2). The confidence intervals calculated using the profile likelihoods were within ± 25% of the coefficients used to generate water content values ($D^* = 10^{-10}$ m^2 s^{-1} and $h^* = 4 \times 10^{-7}$ m s^{-1}) for global water content and σ = 2%, a significant increase in accuracy compared to the confidence intervals calculated with ten water content values (Table 4.2). Therefore, the mass transfer coefficients can be estimated accurately from global water content provided that the noise intensity is low and sufficient water content values are available.

Increasing the number of water content values reduced the confidence interval of the convection mass transfer coefficient for global water content with σ = 10% and enabled its practical identifiability. However, the confidence interval of the diffusion mass transfer coefficient was located outside the uncertainty region for practical identifiability ($0.01 \times 10^{-10} < D < 100 \times 10^{-10}$ m^2 s^{-1} and $0.01 \times 10^{-7} < h < 100 \times 10^{-7}$ m s^{-1}). Consequently, having 100

global water content values was not sufficient to guaranty practical identifiability of the mass transfer coefficients when noise intensity was significant.

The asymptotic confidence intervals were closer to the confidence intervals calculated using the profile likelihoods when 100 water content values were considered (Table 4.3) compared to 10 values (Table 4.2). Nevertheless, the confidence intervals calculated using the profile likelihoods with 100 water content values remained skewed to the right, an asymmetry that was not captured by the asymptotic confidence intervals (Table 4.3). The difference between the asymptotic confidence intervals and the confidence intervals obtained with the profile likelihoods was most significant for global water content with σ = 10%. For these conditions, a relatively narrow asymptotic confidence interval was obtained for the convection mass transfer coefficient (0.37×10^{-7} m s^{-1} < h < 3.45×10^{-7} m s^{-1}), but this interval did not contain the value of the coefficient used to generate water content values ($h^* = 4 \times 10^{-7}$ m s). In contrast, the asymptotic confidence interval of the diffusion mass transfer coefficient (-6.54×10^{-10} m^2 s^{-1} < D < 12.64×10^{-10} m^2 s^{-1}) included the value used to generate water content values ($D^* = 10^{-10}$ m^2 s^{-1}). However, as shown in Fig. 4.5, nearly identical water content values were obtained with significantly higher diffusion mass transfer coefficients (such as $D = 50 \times 10^{-10}$ m^2 s^{-1}) by decreasing the convection mass transfer coefficient. It is unrealistic to conclude that the diffusion mass transfer coefficient is lower than 12.64×10^{-10} m^2 s^{-1} considering that diffusion mass transfer coefficients well above this threshold value provide similar water content values. Consequently, 100 values of the global water content was not sufficient to describe the confidence intervals as an ellipsoid surrounding the estimated coefficients and the confidence intervals calculated using the profile likelihoods provided more robust estimates of the uncertainty of the coefficients than the asymptotic method.

Table 4.3. 95% confidence intervals (*CI*) of the diffusion and convection mass transfer coefficients calculated using the profile likelihood and asymptotic methods for 100 global or internal water content values

Water content	Diffusion mass transfer coefficient (x 10^{-10} m^2 s^{-1})			Convection mass transfer coefficient (x 10^{-7} m s^{-1})		
	$\widehat{\boldsymbol{D}}$	Profile likelihood *CI*	Asymptotic *CI*	$\widehat{\boldsymbol{h}}$	Profile likelihood *CI*	Asymptotic *CI*
Global, σ = 2%	0.97	0.88, 1.10	0.88, 1.05	4.20	3.50, 5.03	3.58, 4.81
Global, σ = 10%	3.05	0.72, > 100	-6.54, 12.64	1.91	1.55, 10.39	0.37, 3.45
Internal, σ = 2%	0.99	0.97, 1.06	0.96, 1.02	4.20	3.74, 4.40	3.94, 4.46
Internal, σ = 10%	0.93	0.77, 1.13	0.78, 1.08	4.60	3.27, 8.59	3.03, 6.17

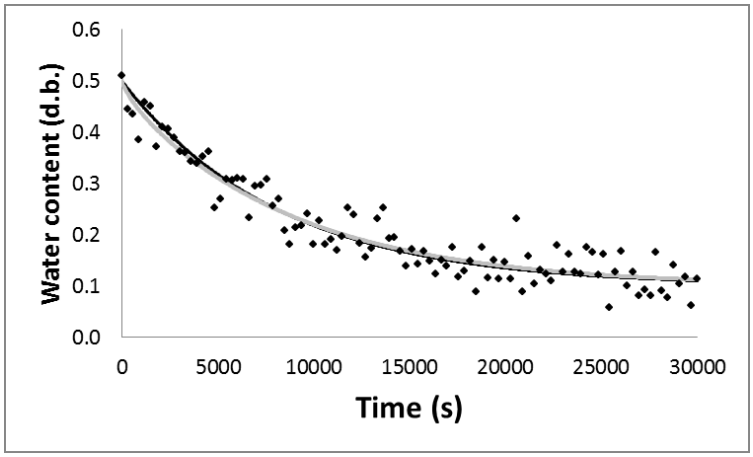

Figure 4.5. Water content values (♦) generated with N = 100 and 10% noise intensity for D = 50 x 10^{-10} m^2 s^{-1} and h = 1.54 x 10^{-7} m s^{-1} (black line) and D = 3.05 x 10^{-10} m^2 s^{-1} and h = 1.91 x 10^{-7} m s^{-1} (grey line).

4.3.5 Impact of the position of the internal water content

Fig. 4.6 presents the profile likelihoods for internal water content near the insulated surface of the product (x = 0) (black continuous line), the exposed surface ($x = w$) (dotted line) or at the centre of the product (grey continuous line) for water content at five positions and 10 different times corresponding to N = 50. The curvature of the profile likelihood for the diffusion and convection mass transfer coefficients was more pronounced for water content near the exposed surface of the product and narrow 95% confidence intervals were obtained (0.81 x 10^{-10} m^2 s^{-1} < D < 1.78 x 10^{-10} m^2 s^{-1} and 2.55 x 10^{-7} m s^{-1} < h < 5.12 x 10^{-7} m s^{-1}). The confidence intervals for water content at the centre of the product were wider (0.81 x 10^{-10} m^2 s^{-1} < D < 4.94 x 10^{-10} and 1.67 x 10^{-7} m s^{-1} < h < 7.24 x 10^{-7} m s^{-1}) than for water content near the exposed surface. For water content near the insulated surface, the profile likelihoods were relatively constant for increasing values of D and h and these coefficients were not practically identifiable. Accordingly, mass transfer coefficients were strongly correlated (-0.99) for water content near the insulated surface, but the correlation was weaker for water content at the centre of the product (-0.95) or near the exposed surface (-0.72). The weaker correlation could be explained by the steep water gradient near the exposed surface of the product with magnitude given by the ratio between the external (h) and the internal (D) resistance to mass transfer. The confidence intervals based on the position of the internal water content indicate

that water content near the exposed surface of the product provides more accurate estimates of the mass transfer coefficients than water content near the insulated surface.

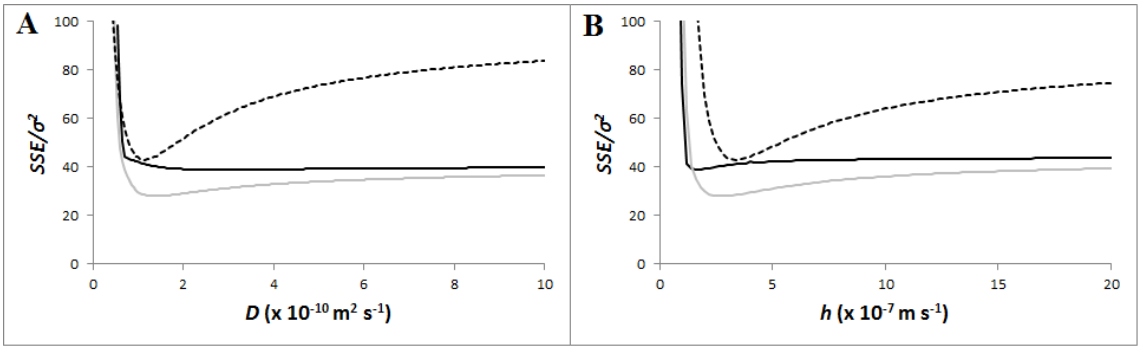

Figure 4.6. Profile likelihoods of the diffusion mass transfer coefficient (D) (A) and convection mass transfer coefficient (h) (B) for five equally spaced internal water content between $x = 0$ and $x = w/2$ (black continuous line); $x = w/4$ and $x = 3w/4$ (grey continuous line) and $x = w/2$ and $x = w$ (dotted line).

4.3.6 Number of water content values for the practical identifiability of the mass transfer coefficients

Monte Carlo simulations were performed to develop guidelines on the selection of the number of water content values (N) and noise intensity (σ) for practical identifiability of the mass transfer coefficients. The practical identifiability of the mass transfer coefficients for 500 N and σ conditions selected randomly is presented in Fig. 4.7. For global water content with $\sigma < 2\%$ or internal water content with $\sigma < 5\%$, three water content values were sufficient to identify the mass transfer coefficients. For higher noise intensity, the number of water content values for the practical identifiability of the mass transfer coefficients increased with the noise intensity. The minimum number of water content values required for the practical identifiability of the mass transfer coefficients (N_{min}) was modeled as a linear function of the noise intensity:

$$N_{min} = 25.8 * \sigma - 48.1 \quad \text{(global water content with } \sigma > 2\%) \tag{4.26}$$

$$N_{min} = 10.2 * \sigma - 48.9 \quad \text{(internal water content with } \sigma > 5\%) \tag{4.27}$$

where σ is the noise intensity expressed as the standard deviation (%) of the average water content (0.3). Eqs. (4.26) and (4.27) were obtained using linear classifiers by minimizing their area under the curve ($\int_0^{20} N_{min}\, d\sigma$) with the constraint that all N and σ conditions where at least one mass transfer parameter was not practically identifiable (red crosses of Fig. 4.7) fell below the curve (Brereton et al. 2010). Experiments should be designed such that the number of water content values is above the threshold calculated from Eqs. (4.26) or (4.27) given the level of noise intensity. If the number of water content values is insufficient, the estimation of the mass transfer coefficients using least-squares minimization will be appropriate for the purpose of water content estimation. However, the physical meaning of the mass transfer coefficients will be limited as multiple combinations of the mass transfer coefficients could reproduce equally well the water content values. Furthermore, one should not mix the combinations of D and h reproducing equally well the water content values, which can produce inaccurate model simulations, as illustrated in Fig. 4.4 (dotted line).

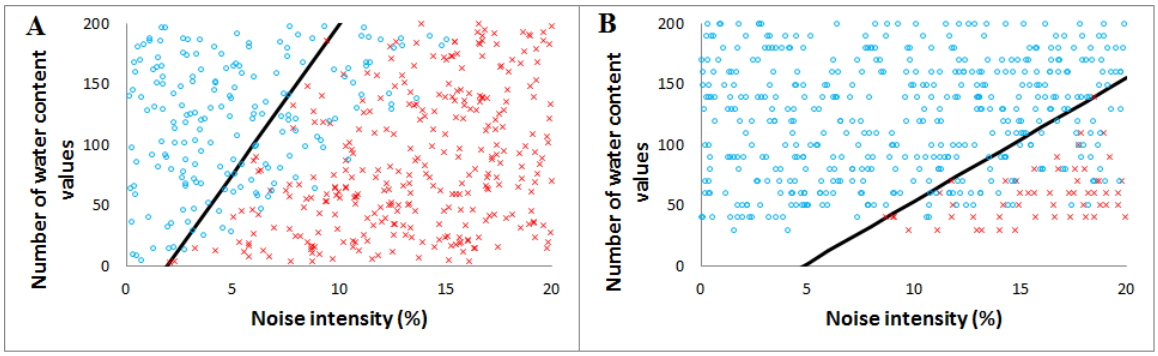

Figure 4.7. Identifiability of the mass transfer coefficient for global water content (A) and internal water content (B) according to number of water content values (N) and noise intensity (σ) with Monte Carlo simulation. The blue circles represent the input conditions where the diffusion mass transfer coefficient and the convection mass transfer coefficient were identifiable; red crosses inputs conditions for which at least one of the coefficients was not practically identifiable and the continuous lines Eqs. (4.26) (A) and (4.27) (B).

4.4 Conclusion

In this work, the structural and practical identifiability of the two mass transfer coefficients associated with the diffusion model was assessed using the profile likelihood and the asymptotic method. The main conclusions of this work were:

(1) The unique minimum observed on the error sum of squares contour plots suggests that the diffusion and convection mass transfer coefficients are structurally identifiable for global and internal water content values;

(2) The diffusion and convection mass transfer coefficients are not practically identifiable for noise over 2% when estimated from an insufficient number of global water content values;

(3) The accuracy of the diffusion and convection mass transfer coefficient estimates can be increased by using internal water content instead of global water content for similar number of water content values and noise intensity;

(4) Water content near the exposed surface of the product provides more accurate estimates of the mass transfer coefficients than water content near the insulated surface of the product;

(5) The confidence intervals of the mass transfer coefficients were asymmetric and were not accurately estimated by the asymptotic method. The profile likelihood method should be selected for the estimation of the confidence intervals of the mass transfer coefficients;

(6) Guidelines were developed for the number of water content values required for the practical identifiability of the diffusion and the convection mass transfer coefficients according to noise intensity (Eqs. 4.26 and 4.27). When using an insufficient number of water content values, the estimated mass transfer coefficients can not be considered robust estimates of these coefficients even if the water content estimates may still provide a realistic representation of the water content.

This work focused on the structural and practical identifiability of the mass transfer coefficients for the water mass transfer diffusion model. The diffusion model describes the material as a continuum at the macroscopic scale and provides an accurate representation of water mass transfer for multiple products and processing conditions. As increasingly accurate knowledge of product microstructure is obtained from the development of imaging techniques at the micro and mesoscopic scales, more complex and multiscale mass transfer models are being developed to provide a detailed representation of mass transfer during processing. Future work will expand on the application of the methodology developed in this work to the new generation of mass transfer models to assess the impact of their increased complexity on

the structural and practical identifability of the model parameters and evaluate the experimental measurements required for accurate parameter estimation.

4.5 Acknowledgement

The authors thank the Natural Sciences and Engineering Research Council (NSERC) of Canada for their financial support.

CHAPITRE 5. Identifiabilité des coefficients décrivant une diffusivité dépendante de la teneur en eau

Titre original : Impact of the number and sampling time of water content measurements on the identifiability of a concentration-dependent water diffusivity

Auteurs et affiliations :

S. Mercier, Ing. jr., étudiant au doctorat, Université de Sherbrooke, département de génie chimique et génie biotechnologique, 2500 boul. Université, Sherbrooke, Québec, Canada, J1K 2R1.

B. Marcos, Ing., Ph.D., Université de Sherbrooke, département de génie chimique et génie biotechnologique, 2500 boul. Université, Sherbrooke, Québec, Canada, J1K 2R1.

C. Moresoli, Ing., Ph.D. University of Waterloo, Department of Chemical Engineering, 200 University Avenue West, Waterloo, Ontario, Canada, N2L 3G1.

M. Mondor, Ing. stag., Ph.D., Agriculture et Agroalimentaire Canada, Centre de Recherche et Développement de Saint-Hyacinthe, 3600 Boul. Casavant Ouest, Saint-Hyacinthe, Québec, Canada, J2S 8E3.

S. Villeneuve, Ing., Ph.D., Agriculture et Agroalimentaire Canada, Centre de Recherche et Développement de Saint-Hyacinthe, 3600 Boul. Casavant Ouest, Saint-Hyacinthe, Québec, Canada, J2S 8E3.

État de l'acceptation : accepté pour publication dans la revue *International Journal of Heat and Mass Transfert*. doi:10.1016/j.ijheatmasstransfer.2016.03.119

Résumé

Contenu : le coefficient de diffusion de l'eau (D) dans plusieurs produits hygroscopiques est fonction de la teneur en eau. Cette dépendance est souvent exprimée à partir d'une relation exponentielle $D = D_0 \exp(AM)$, où D_0 et A sont des coefficients estimés par moindres carrés. L'identifiabilité structurelle des coefficients D_0 et A n'a pas été vérifiée et les conditions expérimentales favorisant l'identifiabilité pratique des coefficients n'ont pas été déterminées. Dans cet article, l'impact du nombre, du moment et du bruit des mesures de la teneur en eau sur l'identifiabilité des coefficients D_0 et A a été vérifié par l'analyse de la fonction objective et le calcul de leur incertitude par la méthode asymptotique et par profil de vraisemblance.

Résultats : les coefficients D_0 et A sont (au moins localement) structurellement identifiables à partir de la mesure de la teneur en eau. L'estimation du coefficient D_0 à partir de la teneur en eau est plus précise que l'estimation du coefficient A en raison de la sensibilité plus importante du modèle pour ce coefficient. Les mesures de la teneur en eau au début du séchage, près de l'atteinte de l'équilibre ou concentrées dans une courte période ne permettent pas une estimation précise des coefficients en raison de la faible sensibilité du modèle à ces instants et de la corrélation entre les coefficients. Pour un bruit de mesure supérieur à environ 0.5%, le nombre de mesures de la teneur en eau nécessaires à l'identifiabilité pratique des coefficients doit être ajusté selon le bruit de mesure.

Contributions à la thèse : les contributions à la thèse de cet article sont l'établissement des conditions expérimentales requises à l'identifiabilité pratique des coefficients décrivant une diffusivité dépendante de la teneur en eau et la compréhension de l'impact du moment des mesures dans le temps sur la précision des coefficients. En accord avec l'analyse de l'identifiabilité d'un coefficient de diffusion indépendant de la teneur en eau (chapitre 4), cet article suggère également que l'importante variabilité entre les valeurs du coefficient de diffusion effectif de l'eau dans les pâtes selon les études sur la modélisation du séchage pourrait être causée par leur faible identifiabilité pratique en présence de bruit sur les mesures de la teneur en eau.

Abstract

The aim of this work was to determine the impact of the experimental conditions (number and sampling time) of measurements of the water content on the identifiability of a concentration-dependent water diffusivity. Water contents simulating a drying process were generated from a diffusion model with the addition of Gaussian noise. An infinite slab with Dirichlet boundary conditions was considered. The coefficients describing a concentration-dependent water diffusivity were estimated from the water content by least-squares minimization. The identifiability of the coefficients was investigated from the model sensitivity functions and using the asymptotic method, the profile likelihood method, and Monte Carlo simulation. The inner product sensitivity matrix was full rank, indicating that the coefficients were locally structurally identifiable. The coefficients were estimated more accurately from water content obtained over the whole drying process, because sampling times concentrated in a short period increased the correlation between the coefficients and increased their uncertainty. The coefficients were practically identifiable from the water content for noise intensity below 0.4%. Above that threshold, the number of measurements of the water content required for the practical identifiability of the coefficients increased linearly with the noise intensity of the water content.

Keywords

Identifiability; Sensitivity; Mass transfer; Drying; Diffusion coefficient

Nomenclature

A	coefficient of the concentration-dependent water diffusivity
$\hat{A}$	least-squares estimate of A
CI	95% confidence interval
$cor_{D_0,A}$	correlation between D_0 and A
cov	covariance matrix
D	water diffusivity ($m^2\ s^{-1}$)
D_0	coefficient of the concentration-dependent water diffusivity ($m^2\ s^{-1}$)
$D_{0.3}$	water diffusivity for a water content $M = 0.3$ ($m^2\ s^{-1}$)
$\widehat{D}_0$	least-squares estimate of D_0 ($m^2\ s^{-1}$)
FIM	Fisher information matrix
Fo	Fourier number ($\mathrm{Fo} = \frac{D_{0.3}t}{w^2}$)
M	water content (kg H_2O kg dry $matter^{-1}$)
$\overline{M}_i$	global water content without noise (kg H_2O kg dry $matter^{-1}$)
$\overline{M}_i^*$	global water content with noise (kg H_2O kg dry $matter^{-1}$)
n	number of water content values
n_{min}	minimum number of water content values for the practical identifiability of the coefficients D_0 and A
S	state variable sensitivity
$\bar{S}$	global (according to x) state variable sensitivity
SSE	error sum of squares
t	time (s)
w	product half-thickness (m)
x	thickness coordinate (m)

Greek symbols

ε	noise
λ	sensitivity matrix
ρ	square root of the determinant for the inner product sensitivity matrix
σ	standard deviation of the noise
σ^2	variance of the noise

Subscripts

0	initial
E	equilibrium
i	time i

5.1 Introduction

Efficient drying operations and accurate estimation of the drying rate can be achieved by modeling the movement of water inside a product. For drying operations controlled by a diffusion mass transfer mechanism, estimation of the water diffusivity is required for model application. Because it cannot be measured directly, the water diffusivity of a product (the input variable of the drying model) is generally estimated from measurements of the product's global water content (the output variable of the drying model) by least-squares minimization. A proper experimental design, in terms of the number of global water content measurements and their sampling time, is critical for an accurate estimation of the water diffusivity. Experiments should be designed considering the structural and practical identifiability of the water diffusivity. Structural identifiability refers to the unicity of the least-squares objective function for the theoretical situation of perfect (noise-free) measurements of the output variable (Nguyen and Wood 1982; Navarro-Laboulais et al. 2006; Raue et al. 2009; Graciano et al. 2014). The input variables are structurally identifiable if the model mapping from the input variable space to the output variable space is injective (Deistler 1998; van den Hof 1998; Lagrange et al. 2008). Practical identifiability refers to the accuracy of the input variable estimate from experimental (noisy) measurements of the output variable (Berthoumieux et al. 2013). Practical identifiability reflects the sensitivity of the input variable to measurement noise and can be assessed from the confidence interval of the estimate (Berthoumieux et al. 2013).

The identifiability of a constant diffusivity (independent of the position, time, or concentration) and a convection mass transfer coefficient has been investigated. Analysis of the least-squares objective function by Mercier et al. (2015) showed the structural identifiability of the water diffusivity and the convection mass transfer coefficient from local or global measurements of the water content. However, a high number of measurements is required for the practical identifiability of the coefficients if the measurement noise is above 2% for global water content and above 5% for local water content. Mercier et al. (2015) also showed that the confidence intervals of the water diffusivity and the convection mass transfer coefficient need to be calculated using a systematic method, such as the profile likelihood method, because the local asymptotic method assumes symmetric confidence intervals and

underestimates the uncertainty of the coefficients. In accordance with Mercier et al. (2015), Martinez-Lopez et al. (2015) showed that local measurements of the output variable provide more accurate estimates of the coefficients than global measurements do and that local measurements hence promote the coefficients' practical identifiability. Wan et al. (2015) studied the impact of the number of measurements of the output variable on the practical identifiability of the coefficients for different geometries and showed that the coefficients are practically identifiable if the ratio of noise to the number of measurements is low and if the Biot number (dimensionless ratio between the internal and external resistances) is close to unity. Wan et al. (2015) also showed the importance of higher-order nonlinearities in the asymptotic estimation of the coefficient confidence intervals.

The identifiability of a position-dependent coefficient has been investigated by DuChateau (2013) and Teergele and Danai (2015). DuChateau (2013)demonstrated the identifiability of a position-dependent diffusivity in a parabolic partial differential equation from the controllability of the adjoint problem. Teergele and Danai (2015) used the sensitivity of the output variable for the coefficients to determine the impact of the sensor location on the identifiability and applied their method to the 2D dispersion of pollutants in air described by an advection–diffusion equation.

To our knowledge, the identifiability of a concentration-dependent diffusivity for a transient process has not been investigated. For hygroscopic products, including many polymers and food products, the water diffusivity decreases during drying as the ratio of bound to free water increases (Coumans 2000; Migliori et al. 2005; Loulou et al. 2006; De Temmerman et al. 2007). The dependence of the water diffusivity for the water content is generally expressed using an exponential function:

$$D = D_0 \exp(AM) \tag{5.1}$$

where D is the water diffusivity, M is the local water content, D_0 is a coefficient determining the water diffusivity at the limit $M \rightarrow 0$, and A is a coefficient describing the sensitivity of the water diffusivity for the water content. The dependence for the water content modifies the identifiability, given that the diffusivity becomes both position- and time-dependent and that two coefficients, D_0 and A, need to be estimated from the water content.

The aim of this work was to assess the structural identifiability of a concentration-dependent water diffusivity from global water content and to determine the experimental conditions (number and sampling time of measurements of the global water content) required for its practical identifiability. To that end, global water content values were generated by adding Gaussian noise to drying model predictions. The coefficients describing a concentration-dependent water diffusivity, D_0 and A, were estimated from these global water content values by least-squares minimization. The structural identifiability of the coefficients was investigated from the least-squares objective function and the drying model sensitivity functions. The practical identifiability was assessed from the confidence intervals calculated using the asymptotic method and the profile likelihood method. The impact of the number and sampling time of measurements of the global water content on the accuracy of least-squares estimates was investigated according to the noise intensity using Monte Carlo simulation.

5.2 Methods

5.2.1 Drying model

Drying of an infinite slab was described using a diffusion model with a concentration-dependent water diffusivity:

$$\frac{\partial M}{\partial t} = \frac{\partial}{\partial x}\left[D_0 \exp(AM)\frac{\partial M}{\partial x}\right] \tag{5.2}$$

where t is the drying time, and x is the coordinate in the mass transfer direction. Eq. (5.2) was solved considering uniform initial water content M_0 (Eq. 5.3) and Dirichlet boundary conditions (Eq. 5.4):

$$M(x, t = 0) = M_0 \tag{5.3}$$

$$M(x = -w, t) = M(x = w, t) = M_E \tag{5.4}$$

where M_E is the equilibrium water content, and w is the product half-thickness, where the origin of the drying model was established.

5.2.2 Generation of global water content values

Global water content values simulating experimental measurements were generated at different sampling times by the addition of Gaussian noise to the drying model predictions:

$$\bar{M}_i^* = \frac{1}{w}\int_0^w M(x,t_i)dx + \varepsilon \quad (5.5)$$

where $\bar{M}_i^*$ is the global water content generated at sampling time $t = t_i$, and ε is the noise. The drying model was solved using the input parameters in Table 5.1. These input parameters describe a product with water diffusivity values of 6×10^{-11} m^2 s^{-1} for $M = M_0 = 0.5$ (db) and 4×10^{-11} m^2 s^{-1} for $M = M_E = 0.1$ (db), which are typical values for hygroscopic products (Mercier et al. 2013b). The noise was assumed to be Gaussian, $\varepsilon \sim N(0, \sigma^2)$, with the standard deviation (σ) expressed as the percentage of the average between the initial water content and the equilibrium water content (0.3). The drying model was solved for 3×10^4 s, the time required to reach approximately 90% of the difference between the initial water content (M_0) and the equilibrium water content (M_E). The drying model was implemented using the finite difference method using an implicit difference scheme with a 6.25×10^{-5} m discretization in space (corresponding to 40 points on the grid) and a 15 s discretization in time. Simulations were performed using the software Matlab 7.12.

Table 5.1. Input parameters used to generate the global water content values (Eq. 5.5)

Parameter	Value
Coefficient D_0	3.6×10^{-11} m^2 s^{-1}
Coefficient A	1.0
Half-thickness (w)	1.25 mm
Initial water content (M_0)	0.5 kg water kg dry matter^{-1}
Equilibrium water content (M_E)	0.1 kg water kg dry matter^{-1}

5.2.3 Estimation of the coefficients by least-squares minimization

The coefficients D_0 and A were estimated from the global water content values $\bar{M}_i^*$ by minimizing the error sum of squares (*SSE*):

$$SSE = \sum_{i=1}^{n}(\bar{M}_i(D_0, A) - \bar{M}_i^*)^2 \quad (5.6)$$

where $\bar{M}_i(D_0, A)$ is the global water content estimate at sampling time $t = t_i$ according to the coefficients D_0 and A and n is the number of global water content values. Minimization of *SSE* was performed using the Nelder–Mead simplex search algorithm following Mercier et al. (2015). The coefficients minimizing *SSE* were denoted by $\widehat{D}_0$ and $\hat{A}$.

5.2.4 Confidence intervals of the least-squares estimates

5.2.4.1 Profile likelihood method

The confidence intervals of the least-squares estimates were calculated using the asymptotic method and the profile likelihood method. For the profile likelihood method, confidence intervals were calculated following Mercier et al. (2015). Briefly, the method consisted of modifying the value of one coefficient, starting from its least-squares value, by increments of 5% in the increasing and decreasing directions and minimizing *SSE* (Eq. 5.6) with respect to the second coefficient. The confidence interval represented the displacement from the least-squares value that caused a statistically significant increase in *SSE*:

$$CI(\theta) = \left\{\theta \middle| \frac{SSE}{\sigma^2}(\theta) - \frac{SSE}{\sigma^2}\left(\hat{\theta}\right) < \Delta_{\alpha,2}\right\} \tag{5.7}$$

where θ is the coefficient (D_0 or A) for which the confidence interval *CI* is calculated, and $\Delta_{\alpha,2}$ is the α quantile of the χ^2 distribution with two degrees of freedom.

5.2.4.2 Asymptotic method

The asymptotic confidence intervals were calculated analytically by developing the sensitivity functions of the drying model and calculating the coefficient covariance from the sensitivity and Fisher information matrices. The sensitivity functions were developed by differentiating the drying model (Eqs. 2–4) with respect to D_0 and A. The sensitivity function for D_0 and the initial and boundary conditions required to solve the partial differential equation were as follows:

$$\frac{\partial S_{D_0}}{\partial t} = \frac{\partial}{\partial x}\left[\left(1 + AD_0S_{D_0}\right)\exp(AM)\frac{\partial M}{\partial x} + D_0\exp(AM)\frac{\partial S_{D_0}}{\partial x}\right] \quad (5.8)$$

$$S_{D_0}(x, t = 0) = 0 \quad (5.9)$$

$$S_{D_0}(x = -w, t) = S_{D_0}(x = w, t) = 0, \quad (5.10)$$

where $S_{D_0} = \frac{\partial M}{\partial D_0}$ is the sensitivity of the water content for D_0. For A, the sensitivity function and the initial and boundary conditions were as follows:

$$\frac{\partial S_A}{\partial t} = \frac{\partial}{\partial x}\left[(M + AS_A)D_0\exp(AM)\frac{\partial M}{\partial x} + D_0\exp(AM)\frac{\partial S_A}{\partial x}\right] \quad (5.11)$$

$$S_A(x, t = 0) = 0 \quad (5.12)$$

$$S_A(x = -w, t) = S_A(x = w, t) = 0 \quad (5.13)$$

where $S_A = \frac{\partial M}{\partial A}$ is the sensitivity of the water content for A. The sensitivity functions were solved using the finite difference method as described in section 5.2.2. The sensitivity matrix (λ) was calculated from the solution of the sensitivity functions:

$$\lambda = \begin{bmatrix} \bar{S}_{D_0,1} & \bar{S}_{A,1} \\ \cdots & \cdots \\ \bar{S}_{D_0,i} & \bar{S}_{A,i} \\ \cdots & \cdots \\ \bar{S}_{D_0,n} & \bar{S}_{A,n} \end{bmatrix} \quad (5.14)$$

where $\bar{S}_{D_0}$ is the sensitivity of the global water content for D_0 [$\bar{S}_{D_0}(t) = \frac{\partial \bar{M}}{\partial D_0} = \frac{1}{w}\int_0^w S_{D_0}(x,t)dx$], and $\bar{S}_A$ is the sensitivity of the global water content for A [$\bar{S}_A(t) = \frac{\partial \bar{M}}{\partial A} = \frac{1}{w}\int_0^w S_A(x,t)dx$]. The Fisher information matrix (*FIM*) was calculated from the sensitivity matrix (Dobre 2010; Ramachandran and Barton 2010):

$$FIM = \frac{\lambda^T\lambda}{\sigma^2} \quad (5.15)$$

The covariance matrix (*cov*) of the model is the inverse of *FIM* [21]:

$$cov = FIM^{-1} \quad (5.16)$$

The confidence intervals were calculated from the covariance matrix using the normal distribution at 95% significance level:

$$CI(\theta) = \left\{\theta \middle| |\theta - \hat{\theta}| < Z_{\alpha/2}\sqrt{cov_{j,j}\big|_{\hat{\theta}}}\right\} \quad (5.17)$$

where $Z_{\alpha/2}$ is the standard normal distribution with the significance level $\alpha/2$, and $cov_{j,j}\big|_{\hat{\theta}}$ is the j,j element (1,1 for D_0 and 2,2 for A) of the covariance matrix evaluated at $\theta = \hat{\theta}$.

5.2.5 Correlation between the coefficients

The correlation between D_0 and A ($cor_{D_0,A}$) was calculated from the covariance matrix as follows (Ashyraliyev et al. 2009):

$$cor_{D_0,A} = \frac{cov_{D_0,A}}{\sqrt{cov_{D_0,D_0}\, cov_{A,A}}} \quad (5.18)$$

where $cov_{D_0,A}$ is the covariance between D_0 and A (element 1,2 or 2,1 of the symmetric covariance matrix), cov_{D_0,D_0} is the variance of D_0 (element 1,1 of *cov*), and $cov_{A,A}$ is the variance of A (element 2,2 of *cov*).

5.2.6 Effect of the value of the coefficients D_0 and A

The effect of the value of the coefficients D_0 and A on their practical identifiability was investigated from the square root of the determinant for the inner product sensitivity matrix (ρ):

$$\rho = \sqrt{\det(\lambda^T \lambda)} \quad (5.19)$$

The determinant of the inner product sensitivity matrix increases with the squared sensitivity of the model for the coefficients D_0 and A and decreases with their correlation $cor_{D_0,A}$. A high ρ value suggests a better practical identifiability of the coefficients [10].

5.2.7 Monte Carlo simulation

Monte Carlo simulation was conducted to determine the number of global water content values n required for the practical identifiability of D_0 and A according to the noise intensity σ. A total of 500 input conditions of n and σ were generated randomly from uniform distributions $n \sim U(3, 200)$ and $\sigma \sim U(0\%, 10\%)$. For each input condition, n global water content values of noise intensity σ were generated at equally spaced sampling times as described in section 5.2.2. The coefficients $\widehat{D}_0$ and $\hat{A}$ were estimated from the global water content values by least-squares minimization as described in section 5.2.3, and the 95% confidence intervals of the coefficients were calculated using the profile likelihood method as described in section 5.2.4.1.

5.2.8 Definition of practical identifiability

The coefficient D_0 was considered practically identifiable if its 95% confidence interval calculated using the profile likelihood method (Eq. 5.7) was a subset of the interval 0 to 10×10^{-11} m^2 s^{-1}. The lower bound of 0×10^{-11} m^2 s^{-1} was selected because a confidence interval of D_0 extending into the negative region is not physically realistic. The upper bound of 10×10^{-11} m^2 s^{-1} was selected to ensure that the least-squares estimates provided the correct order of magnitude ($\times 10^{-11}$ m^2 s^{-1}) of the coefficient. The coefficient A was considered practically identifiable if its 95% confidence interval calculated using the profile likelihood method (Eq. 5.7) was a subset of the interval 0 to 10. The lower bound of 0 was selected because it cannot be concluded if the water diffusivity has a significant dependence for the water content if the confidence interval of A includes the null value. In accordance with D_0, the upper bound of 10 was selected for the correct identification of the order of magnitude of the coefficient.

5.3 Results and discussion

5.3.1 Structural identifiability of the coefficients

Fig. 5.1 shows a contour plot of the error sum of squares (Eq. 5.6) as a function of D_0 and A for global water content values without noise ($\sigma = 0$) at 10 equally spaced sampling times. The unique minimum of the error sum of squares observed on the contour plot was the value of the coefficients used to generate the global water content values ($D_0 = 3.6 \times 10^{-11}$ m^2 s^{-1} and $A = 1.0$). Accordingly, the inner product sensitivity matrix $\lambda^T\lambda$ calculated at $D_0 = 3.6 \times 10^{-11}$ m^2 s^{-1} and $A = 1.0$ was the following:

$$\lambda^T\lambda = \begin{bmatrix} 6.59 \times 10^{19} & 5.31 \times 10^{8} \\ 5.31 \times 10^{8} & 4.30 \times 10^{-3} \end{bmatrix} \tag{5.20}$$

The inner product sensitivity matrix was positive definite, supporting that *SSE* has (at least locally) a unique minimum at $D_0 = 3.6 \times 10^{-11}$ m^2 s^{-1} and $A = 1.0$. The unique minimum of the error sum of squares function observed on the contour plot and supported by the inner product sensitivity matrix indicates that the coefficients D_0 and A of a concentration-dependent water diffusivity are (at least locally) structurally identifiable from measurements of the global water content (Nguyen and Wood 1982; Raue et al. 2009; Graciano et al. 2014).

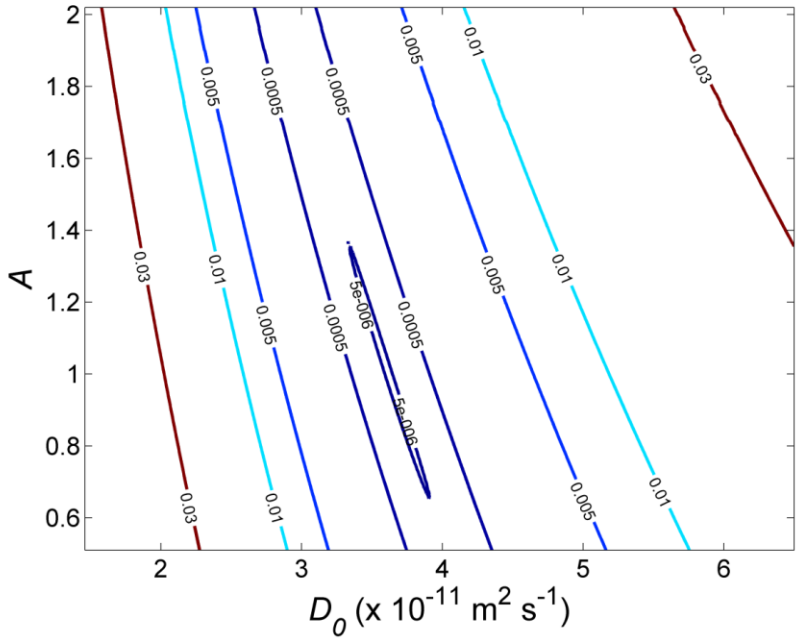

Figure 5.1. Contour plot of the error sum of squares (*SSE*) according to coefficients D_0 and A for 10 global water content values ($\sigma = 0$).

5.3.2 Effect of the noise intensity of the global water content

Table 5.2 presents the confidence intervals of D_0 and A estimated from global water content values at 10 equally spaced sampling times according to the noise intensity (σ). For low noise intensity (σ = 1%), narrow confidence intervals were obtained, and the coefficients were practically identifiable from the global water content values. Increasing the noise intensity decreased the accuracy of the coefficients and affected their practical identifiability (Table 5.2). For noise intensity σ = 2%, the confidence intervals of D_0 and A calculated using the profile likelihood method were approximately twice wider than for σ = 1%. The coefficient D_0 remained practically identifiable from the global water content values, but A was not practically identifiable, because its confidence interval extended into the negative region. The preservation of the practical identifiability of D_0 for noise intensity σ = 2% is explained by the sensitivity of the drying model for these coefficients. The average relative sensitivity of the global water content for D_0 ($\frac{3.6 \times 10^{-11}}{3 \times 10^4} \int_0^{3 \times 10^4} \bar{S}_{D_0} dt$) calculated at $D_0 = 3.6 \times 10^{-11}$ m^2 s^{-1} and A = 1.0 was −0.087, approximately five times higher than the average relative sensitivity for A ($\frac{1}{3 \times 10^4} \int_0^{3 \times 10^4} \bar{S}_A dt$), which was −0.019. The higher relative sensitivity of the global water content for D_0 can also be observed on the contour plot, given that the contour lines are stretched in the A direction (Fig. 5.1). Because of the higher relative sensitivity for D_0, small variations of this coefficient have a higher impact on the drying model prediction of the global water content, and this coefficient is estimated more accurately from global water content values than A is.

Table 5.2. 95% confidence intervals (*CI*) of coefficients D_0 and A according to the noise intensity (σ)

Noise (σ)	Coefficient D_0 ($\times 10^{-11}$ m^2 s^{-1})			Coefficient A		
	$\widehat{D}_0$	Profile likelihood *CI*	Asymptotic *CI*	$\hat{A}$	Profile likelihood *CI*	Asymptotic *CI*
1%	3.2	2.5, 4.2	2.5, 3.9	1.6	0.5, 2.8	0.7, 2.5
2%	3.3	2.0, 5.8	1.9, 4.7	1.5	−1.1, 3.7	−0.3, 3.3
5%	6.7	1.3, >10	−2.2, >10	−2.1	<−10, 5.2	−8.3, 4.1
10%	3.3	0.2, >10	−3.9, >10	1.2	<−10, >10	−8.5, >10

Increasing the noise intensity to $\sigma = 5\%$ and $\sigma = 10\%$ further widened the confidence intervals, and both coefficients were not practically identifiable, indicating that information for an accurate least-squares estimation of the coefficients is lost because of the noise (Table 5.2). The practical non-identifiability of the coefficients reflects their significant correlation (Eq. 5.18). The correlation between the coefficients calculated at $D_0 = 3.6 \times 10^{-11}$ m^2 s^{-1} and $A = 1.0$ was −0.995. The correlation is different from −1, reflecting the structural identifiability of the coefficients. However, the correlation is significantly lower than the null value, indicating that when one of the coefficients is increased, similar predictions of the global water content can be obtained with the drying model by decreasing the second coefficient. Consequently, as illustrated in Fig. 5.2, significantly different combinations of D_0 and A can provide similar representations of global water content values and cannot be distinguished from global water content values with significant noise.

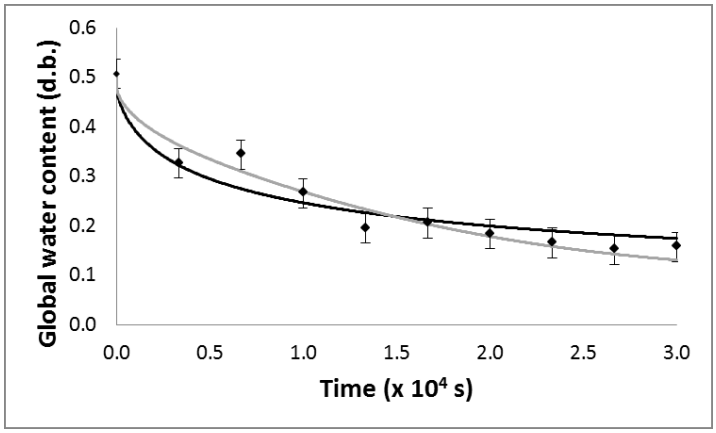

Figure 5.2. Global water content values (♦ ± standard deviation) generated with $n = 10$ and $\sigma = 10\%$ and simulated with the drying model for $D_0 = 0.3 \times 10^{-11}$ m^2 s^{-1} and $A = 11.2$ (black line) and $D_0 = 10 \times 10^{-11}$ m^2 s^{-1} and $A = -3.9$ (gray line).

5.3.3 Effect of the sampling time of the global water content

The sampling time affects the uncertainty and the practical identifiability of the coefficients. Consider the estimation of D_0 and A from the global water content at two sampling times, t_1 and t_2. The asymptotic confidence interval of D_0 (Eq. 5.17) will be

proportional to the squared root of $cov_{D_0,D_0}/\sigma^2$, which can be expressed from the sensitivities as follows:

$$\frac{cov_{D_0,D_0}}{\sigma^2} = \frac{\bar{S}_{A,1}^2+\bar{S}_{A,2}^2}{\left(\bar{S}_{D_0,1}^2+\bar{S}_{D_0,2}^2\right)\left(\bar{S}_{A,1}^2+\bar{S}_{A,2}^2\right)-\left(\bar{S}_{D_0,1}\bar{S}_{A,1}+\bar{S}_{D_0,2}\bar{S}_{A,2}\right)^2} \quad (5.21)$$

Eq. (5.21) indicates that high squared sensitivities $\bar{S}_{D_0}^2$ and a low ratio between the second and first terms of the denominator, which is equal to the squared correlation $cor_{D_0,A}{}^2$, are desired when selecting the sampling time of the measurements. For instance, assume that the sampling time of the first global water content is $t_1 = 1.3 \times 10^4$ s, selected to maximize the squared sensitivity $\bar{S}_{D_0}^2$ (Fig. 5.3A). Fig. 5.4 shows $cov_{D_0,D_0}/\sigma^2$ as a function of the second sampling time t_2. For the limiting case $t_2 = t_1$, $cov_{D_0,D_0}/\sigma^2$ rises toward ∞, illustrating that the coefficients D_0 and A cannot be estimated simultaneously from the global water content at a single sampling time. For two nearby sampling times, $t_2 \approx t_1$, high values of $cov_{D_0,D_0}/\sigma^2$ are obtained, and inaccurate estimates of D_0 from the global water content are expected. Nearby sampling times are inappropriate for the estimation of the coefficients, because when one of the coefficients is under or overestimated, the second coefficient can be adjusted to accurately reproduce both global water content values such that the correlation $cor_{D_0,A}$ is significant. Inaccurate estimates of D_0 are also expected if the second sampling time is at the beginning or end of drying, given that the squared sensitivity $\bar{S}_{D_0}^2$ is small at these moments (Fig. 5.3A) because the global water content is dependent mostly on the initial (M_0) and equilibrium (M_E) values. The optimal sampling time t_2* for the estimation of D_0, i.e. the sampling time minimizing $cov_{D_0,D_0}/\sigma^2$ and thus maximizing its expected accuracy, is obtained at 3.6×10^4 s.

The optimal sampling time t_2* as a function of the first sampling time t_1 is shown in Fig. 5.5. For small values, increasing t_1 leads to lower t_2*, which increases the squared sensitivity $\bar{S}_{D_0}^2$ (Fig. 5.3A). After 0.7×10^4 s, the proximity between t_1 and t_2* causes a significant correlation $cor_{D_0,A}$, and a further increase in t_1 also increases t_2*. When t_1 is increased above 1.8×10^4 s, the optimal sampling time t_2* becomes lower than t_1. Also of interest in Fig. 5.5 is the irreversibility of the optimal sampling times, i.e. an optimal sampling time $t_2^* = \alpha$ for a given sampling time $t_1 = \beta$ does not imply that β is the optimal sampling time t_1* for a given sampling time $t_2 = \alpha$.

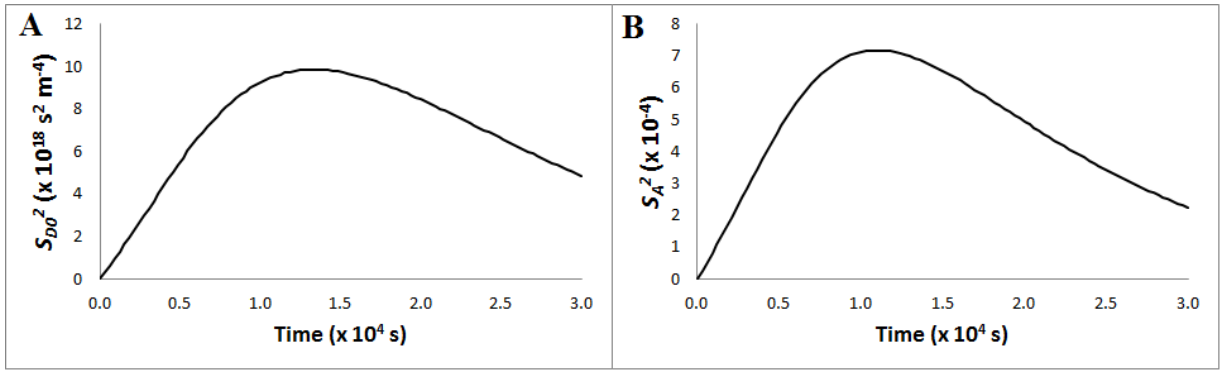

Figure 5.3. Squared sensitivity of the global water content for coefficients D_0 (**A**) and A (**B**) during drying calculated at $D_0 = 3.6 \times 10^{-11}$ m^2 s^{-1} and $A = 1.0$.

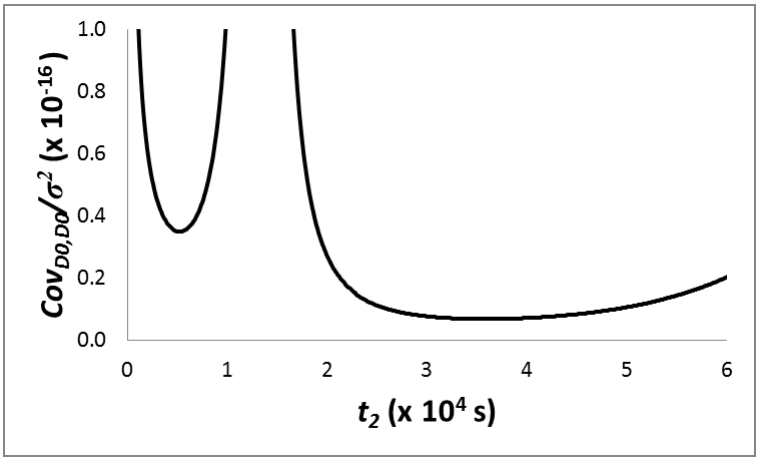

Figure 5.4. Impact of the second sampling time t_2 on $cov_{D_0,D_0}/\sigma^2$ (Eq. 5.21) for a fixed sampling time $t_1 = 1.3 \times 10^4$ s.

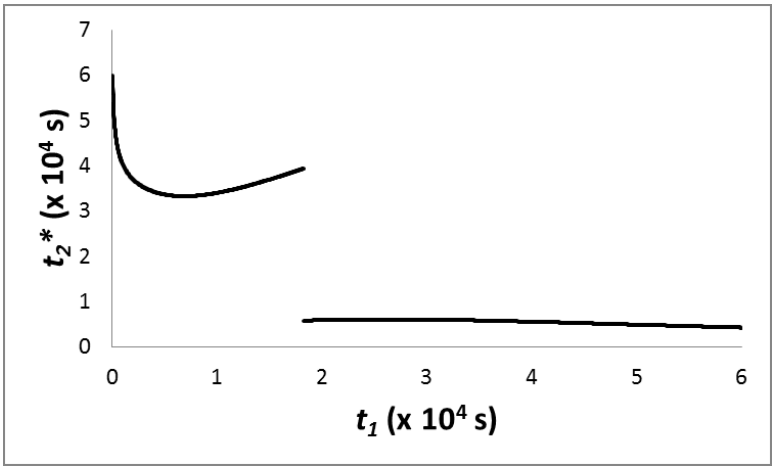

Figure 5.5. Sampling time t_2 minimizing $cov_{D_0,D_0}/\sigma^2$ (Eq. 5.21) as a function of the sampling time t_1.

Table 5.3 presents the confidence intervals of D_0 and A estimated from 10 global water content values ($\sigma = 1\%$) at equally spaced sampling times obtained at the beginning (between 0 and 1×10^4 s), middle (between 1×10^4 and 2×10^4 s), and end (between 2×10^4 and 3×10^4 s) of drying. The confidence intervals of the coefficients for global water content at the middle of drying were more than 40% narrower than for global water content at the end of drying and more than three times narrower than for global water content at the beginning of drying. The narrower confidence intervals for global water content at the middle of drying reflect the higher sensitivity of the global water content for the coefficients during this period (Fig. 5.3). However, confidence intervals were approximately twice narrower for 10 global water content values over the whole drying process (Table 5.2) than for 10 global water content values at the middle of drying (Table 5.3). When the global water content only at the middle of drying is considered, the global water content values are concentrated in a short period. As illustrated in Fig. 5.4, the proximity of the sampling times increases the correlation $cor_{D_0,A}$ and decreases the expected accuracy of the estimates. Comparison of the confidence intervals thus indicates that, although global water contents at the middle of drying are the most important, measuring global water content over the whole drying process is a better experimental strategy for an accurate estimation and the practical identifiability of D_0 and A.

Table 5.3. 95% confidence intervals (*CI*) calculated using the profile likelihood method for 10 global water content values ($\sigma = 1\%$) at the beginning (between 0 and 1×10^4 s), middle (between 1×10^4 and 2×10^4 s), and end (between 2×10^4 and 3×10^4 s) of drying.

Drying period	Coefficient D_0 ($\times 10^{-11}$ m^2 s^{-1})		Coefficient A	
	$\widehat{D}_0$	*CI*	$\hat{A}$	*CI*
Beginning	3.1	0.9, >10	1.7	<−10, 5.9
Middle	2.8	1.6, 4.7	2.3	−0.1, 4.5
End	2.3	0.7, 5.1	3.1	−0.7, 8.0

5.3.4 Asymptotic confidence intervals

Asymptotic confidence intervals are obtained from a local quadratic approximation of the log-likelihood and restrict the confidence interval to an ellipsoid surrounding the least-squares estimates (Ashyraliyev et al. 2009; Raue et al. 2009). Asymptotic confidence intervals are exact for linear models and accurate for nonlinear models if the number of measurements

is sufficient and the noise intensity is low (Raue et al. 2009; Schaber and Klipp 2011). Confidence intervals are more complex to obtain using the profile likelihood method because of the least-squares minimization performed at each iteration, but they are not limited to a local approximation of the likelihood and provide a more accurate representation of the uncertainty of least-squares estimates than the asymptotic method provides (Ashyraliyev et al. 2009; Raue et al. 2009). For 10 global water content values with noise intensity $\sigma = 1\%$, the asymptotic confidence intervals were similar to those calculated using the profile likelihood method (Table 5.2). The similarity of the confidence intervals indicates that the local quadratic approximation in the log-likelihood of the asymptotic method is accurate for low noise intensity. The asymptotic method underestimated the confidence intervals by about 25% compared to the profile likelihood method for noise intensity $\sigma = 2\%$ (Table 5.2). A 25% underestimation of the confidence intervals is significant, but the asymptotic method was more accurate for estimation of the confidence intervals of D_0 and A than for estimation of the confidence intervals of a constant water diffusivity and a convection mass transfer coefficient. For estimation of the confidence intervals of a constant water diffusivity and a convection mass transfer coefficient, the asymptotic method underestimated the confidence intervals by more than 50% for 10 global water content values with noise intensity $\sigma = 2\%$ (Mercier et al. 2015). The higher accuracy of the asymptotic method for D_0 and A is explained by the elliptical shape of their confidence region in the vicinity of the least-squares estimates (Fig. 5.1) and illustrates that the accuracy of the asymptotic method is dependent on the identifiability problem considered. For noise intensities $\sigma = 5\%$ and $\sigma = 10\%$, the asymptotic method underestimated the confidence intervals by more than 50%, indicating the necessity to calculate the confidence intervals of D_0 and A using a systematic method, such as the profile likelihood method, for an accurate representation of the uncertainty of least-squares estimates if the noise intensity is significant.

5.3.5 Effect of the number of measurements

Fig. 5.6 shows the practical identifiability of the coefficients according to the 500 input conditions of n and σ selected randomly by Monte Carlo simulation (section 5.2.7). The coefficient D_0 was practically identifiable for the majority (413) of the input conditions

(Fig. 5.6A), whereas A was practically identifiable for only 149 input conditions (Fig. 5.6B), providing additional evidence that D_0 is estimated more accurately from global water content than A is (Table 5.2). For all the input conditions providing the practical identifiability of A, D_0 was also practically identifiable, indicating that the practical identifiability of D_0 can be assumed from the practical identifiability of A (Fig. 5.6C). For noise intensity $\sigma < 0.4\%$, all input conditions provided the practical identifiability of the coefficients. For higher noise intensity, the minimum number of global water content values required for the practical identifiability of the coefficients (n_{min}) increased linearly and was modeled as follows (Fig. 5.6C):

$$n_{min} = 80\sigma - 32 \qquad (\sigma > 0.4\%) \qquad (5.22)$$

where σ is the noise intensity expressed as the standard deviation (%) of the average water content (0.3). When designing experiments for the estimation of D_0 and A by least-squares minimization, the number of global water content values measured should be selected according to the noise intensity in accordance with Eq. (5.22) in order to provide sufficiently accurate estimations for the practical identifiability of the coefficients.

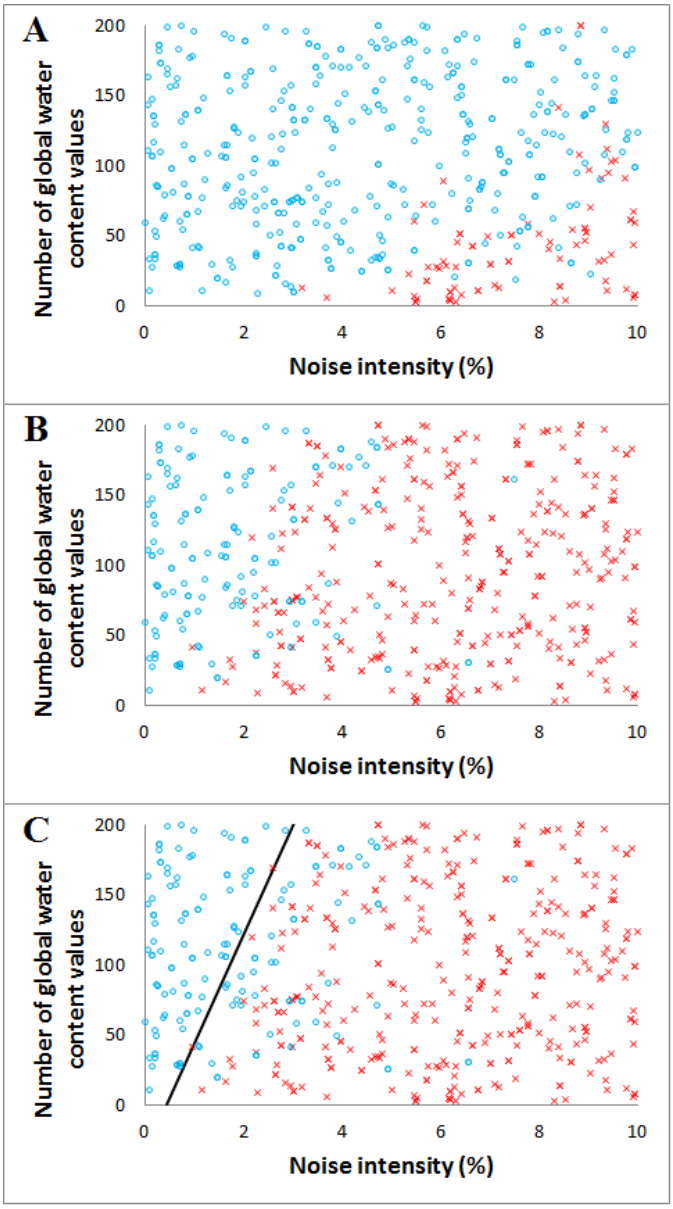

Figure 5.6. Practical identifiability of coefficients D_0 and A according to the number of global water content values and noise intensity. The blue circles represent input conditions where D_0 (**A**), A (**B**), or both coefficients (**C**) were practically identifiable; the red crosses represent input conditions where D_0 (**A**), A (**B**), or at least one of the coefficients (**C**) was not practically identifiable; and the continuous line represents Eq. (5.22).

5.3.6. Effect of the value of the coefficients D_0 and A

The value of the coefficients D_0 and A can vary among hygroscopic products according to the sensitivity of the water diffusivity for the water content. Fig. 5.7 shows the square root of the determinant for the inner product sensitivity matrix ρ (Eq. 5.19) according to the ratio D_0/A and the Fourier number (dimensionless time) of the final global water content value. The coefficients D_0 and A were estimated for each ratio D_0/A such that the water diffusivity for a water content $M = 0.3$ (db) was of 5×10^{-11} m^2 s^{-1}. The square root of the determinant for the inner product sensitivity matrix ρ was calculated for 10 global water content values without noise ($\sigma = 0$) at equally spaced sampling times. A decrease of the ratio D_0/A increased the value of ρ, indicating that a low ratio D_0/A should improve the accuracy of the coefficients estimated from global water content (Fig. 5.7). The highest ρ values were obtained for a ratio D_0/A of 1×10^{-12} m^2 s^{-1}, which corresponds to a product with a water diffusivity of 1.9×10^{-10} m^2 s^{-1} for $M = M_0 = 0.5$ (db) and 1.3×10^{-11} m^2 s^{-1} for $M = M_E = 0.1$ (db), representing a 150% difference. The highest ρ values were obtained for a Fourier number of the final global water content between 1 and 1.5, regardless of the D_0/A ratio, which corresponds to the time required to reach approximately 90% of the difference between the initial water content (M_0) and the equilibrium water content (M_E). Consequently, the determinant of the inner product sensitivity matrix indicates that global water content values when the product has reached 90% of the difference between the initial and equilibrium water contents are not relevant for the estimation of the coefficients, because of the low squared sensitivity of the drying model for the coefficients after long drying times (Fig. 5.3). However, in agreement with Table 5.3, the determinant of the inner product sensitivity matrix indicates that global water content values should not be concentrated near the start of drying, as valuable information for the estimation of the coefficients is lost.

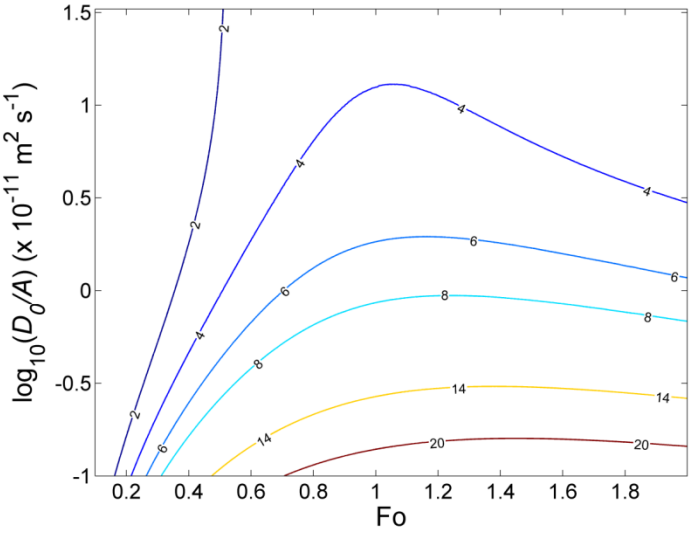

Fig. 5.7. Square root of the determinant for the inner product sensitivity matrix (ρ) ($\times 10^7$ s m^{-2}) according to the ratio between the coefficients D_0 and A on a logarithmic scale and the Fourier number (dimensionless time) of the last global water content value (Fo).

5.4 Conclusion

In this work, the structural and practical identifiability of a concentration-dependent water diffusivity was assessed according to the number, sampling time and noise intensity of measurements of global water content using the asymptotic method, the profile likelihood method, and Monte Carlo simulation. The main conclusions drawn from this work were as follows:

(1) The unique minimum of the least-squares objective function and the positive definiteness of the inner product sensitivity matrix suggest that the coefficients describing a concentration-dependent water diffusivity, D_0 and A, are (at least locally) structurally identifiable from global water content;

(2) The coefficient D_0 is estimated more accurately from global water content than A is because of the higher sensitivity of the drying model for the former coefficient than for the latter;

(3) A low ratio D_0/A, representing products with a water diffusivity sensitive to the water content, improves the practical identifiability of the coefficients;

(4) The confidence intervals of the coefficients D_0 and A should be calculated using the profile likelihood method, because the asymptotic method underestimates the uncertainty for high noise intensity;

(5) Sampling times at the very beginning or end of drying and concentrated in a short period are not appropriate for the estimation of the coefficients because of low model sensitivity and high correlation between the coefficients, respectively; and

(6) Drying experiments should be designed to measure the global water content over the whole drying process and with the number of measurements selected according to the noise intensity (Eq. 5.22) in order to provide the practical identifiability of the coefficients D_0 and A.

5.5 Acknowledgements

The authors thank the Vanier Canada Graduate Scholarships program (held by Samuel Mercier) and the Natural Sciences and Engineering Research Council of Canada (NSERC) for their financial support.

CHAPITRE 6. Modélisation mécanistique du transport d'eau à l'intérieur des pâtes lors du séchage

Titre original : Modeling of internal moisture transport during durum wheat pasta drying

Auteurs et affiliations :

S. Mercier, Ing. jr., étudiant au doctorat, Université de Sherbrooke, département de génie chimique et génie biotechnologique, 2500 boul. Université, Sherbrooke, Québec, Canada, J1K 2R1.

B. Marcos, Ing., Ph.D., Université de Sherbrooke, département de génie chimique et génie biotechnologique, 2500 boul. Université, Sherbrooke, Québec, Canada, J1K 2R1.

C. Moresoli, Ing., Ph.D. University of Waterloo, Department of Chemical Engineering, 200 University Avenue West, Waterloo, Ontario, Canada, N2L 3G1.

M. Mondor, Ing. stag., Ph.D., Agriculture et Agroalimentaire Canada, Centre de Recherche et Développement de Saint-Hyacinthe, 3600 Boul. Casavant Ouest, Saint-Hyacinthe, Québec, Canada, J2S 8E3.

S. Villeneuve, Ing., Ph.D., Agriculture et Agroalimentaire Canada, Centre de Recherche et Développement de Saint-Hyacinthe, 3600 Boul. Casavant Ouest, Saint-Hyacinthe, Québec, Canada, J2S 8E3.

Date d'acceptation : 11 septembre 2013

État de l'acceptation : Publié

Référence : Journal of Food Engineering, 124, 19-27.

Résumé

Contenu : la revue de la littérature a montré l'imprécision des modèles de séchage basés sur un coefficient de diffusion effectif pour la prédiction des profils internes de teneur en eau (chapitre 2). L'hypothèse a été établie que l'imprécision était causée par l'évaporation interne de l'eau lors du séchage et le transfert de masse de l'eau sous forme vapeur. Dans cet article, un modèle de séchage mécanistique couplant la description du transfert de masse de l'eau liquide par capillarité et convection, le transfert de masse de l'eau vapeur par diffusion et convection, le transfert d'énergie par conduction, convection et évaporation et la déformation mécanique a été développé. La précision du modèle pour la description du profil interne de teneur en eau a été validée à partir de mesures à basse (40 ºC), moyenne (60 ºC) et haute (80 ºC) températures de séchage et comparée avec la précision des modèles basés sur un coefficient de diffusion effectif.

Résultats : le modèle mécanistique (R^2 = 0.90) prédit les profils internes de teneur en eau lors du séchage plus précisément que le modèle basé sur un coefficient de diffusion effectif (R^2 = 0.69) pour les trois températures de séchage considérées (40, 60 et 80 ºC). La quantification de la contribution des mécanismes de transfert de masse et d'énergie pour un séchage à 60 ºC indique qu'environ 90% de l'eau est transporté sous forme liquide lors du séchage, le transfert de masse de l'eau liquide par convection est négligeable, la diffusion et la convection contribuent significativement au transfert de masse de l'eau vapeur et le transfert d'énergie par convection est négligeable.

Contributions à la thèse : les contributions à la thèse de cet article sont l'amélioration de la précision des profils internes de teneur en eau et la quantification de la contribution des mécanismes de transfert de masse et d'énergie lors du séchage des pâtes, améliorant la compréhension du séchage et la sélection de conditions de séchage appropriées.

Abstract

A mechanistic model considering water evaporation and distinguishing liquid water and water vapor transport during pasta drying was developed and validated with published experimental moisture profiles. Model predictions of the internal moisture profiles were more accurate and able to capture the evolution with time of the moisture profiles for drying at low and high air temperatures. Model simulations indicated that approximately 88% of the water is transported in the liquid state, the convective flow of liquid water is negligible and the diffusion and convection of water vapor are important. A sensitivity analysis showed that the diffusivities and the mass transfer coefficients were the parameters affecting the most significantly the model drying time and internal moisture profile estimates.

Keywords

Pasta drying; moisture transport; mechanistic model; mass transfer; heat transfer; sensitivity analysis

Nomenclature

a_w	water activity, -
c	concentration, kg m^{-3}
C_P	heat capacity, J kg^{-1} K^{-1}
D	diffusion coefficient, m^2 s^{-1}
E_a	activation energy, J mol^{-1}
f	output parameter for the sensitivity analysis (Eq. 6.31)
h	surface mass (m s^{-1}) or heat (W m^{-2} K^{-1}) transfer coefficient
H	specific enthalpy, J kg^{-1}
k	permeability, m^2
k_h	thermal conductivity, W m^{-1} K^{-1}
K_{ev}	evaporation rate constant, s^{-1}
I	evaporation rate, kg m^{-3} s^{-1}
l	coordinate for thickness, m
L	pasta half-thickness, m
MW	molecular weight, Dalton
n	mass flux, kg m^{-2} s^{-1}
P	pressure, Pa
R_g	ideal gas constant, J mol^{-1} K^{-1}
RH	relative humidity, %
Sr	relative sensitivity, -
t	drying time, s
T	temperature, K
V	volume, m^3
x	mass fraction in the gas phase, -
X	pasta water content on dry basis, kg H_2O (kg dry solid)$^{-1}$
z	mass fraction in the pasta, -

Greek symbol

ϵ	porosity, water vapor m^3 (gas phase m^3)$^{-1}$
λ	latent heat of vaporization, J kg^{-1}
η	volumetric fraction of water lost replaced by air, -
ξ	local shrinkage, -
ρ	density, kg m^{-3}
τ	pore tortuosity, -
μ	viscosity, kg m^{-1} s^{-1}

Subscripts

0	initial condition
a	air

app	apparent
eff	effective
e	energy
ev	evaporation
E	equilibrium
f	at film conditions
g	gaseous phase
h	heat
liq	liquid phase
m	mass
M	moisture (i.e. liquid water + water vapor)
s	dry solid
v	water vapor
w	liquid water

6.1 Introduction

Over the years, numerous studies have demonstrated the importance of the air temperature and relative humidity conditions for the drying of pasta and the production of pasta with desired moisture and quality attributes (Manthey and Schorno, 2002; Zweifel et al., 2003; Mercier et al., 2011b). Yet, the temperature and relative humidity profiles of the drying chamber for industrial pasta operations are determined mainly by trial-and-error. This method is expensive and time consuming because of the numerous potential operating conditions of pasta processing.

Models represent an attractive approach to reduce the time for the identification of appropriate drying conditions and achieve the required water removal for the production of dried pasta. To date, the modeling of the water transport during pasta drying is based on a Fick-type law relationship with a lumped parameter, the effective diffusion coefficient (D_{eff}), to represent the water mass transfer (Andrieu and Stamatopoulos (1986). Published experimental results (Andrieu and Stamatopoulos, 1986; Migliori et al., 2005; De Temmerman et al., 2007 and Mercier et al., 2013a) indicate that models based on the lumped effective diffusion coefficient provide accurate estimation for the evolution of the total water content of pasta during drying but are unable to capture the internal moisture profiles (Litchfield and Okos, 1992; Hills et al., 1997; Xing et al., 2007). The estimation of internal water profiles during pasta drying is critical for tailoring the pasta properties, the minimization of crack formation and propagation and achieving uniform glass transition conditions (Ponsart et al., 2003; Mercier et al., 2013b). Improved representation of the internal water profiles and understanding of the water mass transfer mechanisms can be obtained with the development of mechanistic models from mass, heat and momentum balances for each component and phase of the system. When considering pasta as a porous and hygroscopic material with water evaporation taking place during drying, the water mass transfer will consist of liquid water and water vapor flow. Liquid water flow will be mainly composed of capillary diffusion, resulting from the relative attraction of the liquid water molecules for each other and for those of the solid, and convection. Water vapor flow will be mainly composed of molecular diffusion and convection (Datta, 2007). The distinction of the flow of liquid water and water vapor may improve the internal moisture profile estimates as suggested by Litchfield and Okos (1992)

while the distinction of the diffusive water flow and the convective water flow would provide a detailed representation of the mass transfer mechanisms taking place during drying. Similar water transport mechanistic models have been developed for bread baking revealing the importance of moisture convection and evaporation in the baking process (Zhang and Datta, 2006; Ousegui et al., 2010).

The aim of this work was to investigate water evaporation and distinguish the internal liquid water and water vapor transport by diffusion, capillarity and convection during pasta drying. A mechanistic model was developed, validated with published experimental internal moisture profiles, and compared to estimates obtained from existing models. The potential of the model to serve as tool for the analysis of the mass and heat transfer mechanisms taking place during pasta drying will also be discussed.

6.2 Methodology

6.2.1 Mathematical modeling

6.2.1.1 Hypothesis

The model was developed for a slab of pasta having a high surface/thickness ratio. The following assumptions were made: (1) mass and heat transfer only occurs in the direction of thickness; (2) the surface of the pasta is exposed symmetrically to the air in the drying chamber; (3) the gas phase in the pasta consists of air and water vapor and behaves as an ideal gas; (4) the gas, liquid and solid phases of the pasta have the same local temperature; (5) the water vapor diffuses only in the gas phase; (6) the surface of the pasta is at atmospheric pressure; (7) water in the vapor phase is exchanged between the pasta and the drying chamber and (8) the temperature and relative humidity of the air in the drying chamber are constant.

6.2.1.2 Mass transfer

Mass balances were developed for the liquid water, the water vapor and the total gas phase (water vapor + air) as follows:

$$\frac{\partial C_w}{\partial t} = \frac{\partial n_w}{\partial l} - I \tag{6.1}$$

$$\frac{\partial C_v}{\partial t} = \frac{\partial n_v}{\partial l} + I \tag{6.2}$$

$$\frac{\partial C_g}{\partial t} = \frac{\partial n_g}{\partial l} + I, \tag{6.3}$$

where C_w, C_v and C_g are the mass concentration of liquid water, water vapor and total gas phase, l the coordinate for the pasta thickness and I the water evaporation rate. The mass flux of the individual components (n_w, n_v and n_g) includes liquid water capillary diffusion, water vapor molecular diffusion and convective moisture transport, the latter being described with Darcy's law (Bird et al., 1960):

$$n_w = D_w \frac{\partial c_w}{\partial l} + \rho_w \frac{k_w}{\mu_w} \frac{\partial P}{\partial l} \tag{6.4}$$

$$n_v = C_g D_{v,eff} \frac{\partial x_v}{\partial l} + \rho_v \frac{k_g}{\mu_g} \frac{\partial P}{\partial l} \tag{6.5}$$

$$n_g = \rho_g \frac{k_g}{\mu_g} \frac{\partial P}{\partial l}, \tag{6.6}$$

where D_w and $D_{v,eff}$ are the liquid water and water vapor diffusivity, ρ_w and ρ_v their density, x_v the water vapor mass fraction in the gas phase, k_w and k_g the liquid water and gas permeability, and μ_w and $\mu_g$the liquid water and gas viscosity. The pressure (P) was calculated from the mass concentration of the gas phase (C_g) using the ideal gas law. In addition, the density of water vapor (ρ_v) was related to its mass concentration (C_v) as follows:

$$\rho_v = \frac{C_v}{1 - \frac{C_s}{\rho_s} - \frac{C_w}{\rho_w}}, \tag{6.7}$$

where C_s and ρ_s are the mass concentration and the density of pasta dry matter. The denominator of the right-hand side of Eq. (6.7) represents the pasta porosity (ϵ), here defined as the ratio between the volume of gas and the pasta apparent volume.

Water evaporation was considered as a non-equilibrium process as proposed previously for the modeling of bread baking (Ousegui et al., 2010) and microwave puffing (Rakesh and Datta, 2011), where water evaporation was considered as a non-equilibrium process proportional to the difference between the actual vapor density and the equilibrium vapor density :

$$I = K_{ev}(\rho_v - \rho_{v,E}), \tag{6.8}$$

where K_{ev} is an empirical constant and $\rho_{v,E}$ is the equilibrium water vapor density. The latter was described with the activity coefficient (a_w) and saturation vapor pressure ($p_{v,s}$) as follows:

$$\rho_{v,E} = \frac{a_w p_{v,s} M_w}{R_g T}, \tag{6.9}$$

where M_w is the water molecular weight, $R_g$the ideal gas constant and $p_{v,s}$ is calculated at the pasta temperature T with the Clausius-Clapeyron equation.

The initial conditions required to solve the system of equations (6.1)-(6.9) were developed from the hypothesis of uniform concentration of the pasta constituents at the beginning of drying:

$$C_w = C_{w,0},\ C_v = C_{v,0} \text{ and } C_g = C_{g,0} \qquad (\text{for } t = 0) \tag{6.10}$$

A no-flux boundary condition was used at the center of the pasta ($l = 0$) with the assumption that the pasta was exposed symmetrically to the drying environment:

$$\frac{\partial C_w}{\partial l} = 0.\ \frac{\partial C_v}{\partial l} = 0 \text{ and } \frac{\partial C_g}{\partial l} = 0 \qquad (\text{for } l = 0) \tag{6.11}$$

For liquid water and water vapor, Neumann boundary conditions were used to describe their mass flux at the surface:

$$n_w = h_w(C_M - C_E) \text{ and } n_v = h_v(C_M - C_E), \qquad (\text{for } l = L) \tag{6.12}$$

where h_w and h_v are the liquid water and water vapor mass transfer coefficients, C_M the mass concentration of water (liquid + vapor) at the surface of the pasta, C_E the pasta equilibrium (at $t \to \infty$) water concentration and L the pasta half-thickness. For the total gas phase, a Neumann

boundary condition was used assuming that the surface of the pasta was at atmospheric pressure (P_{atm}):

$$P = P_{atm} \qquad \text{(for } l = L\text{)} \qquad (6.13)$$

6.2.1.3 Heat transfer

Heat transfer was represented with the energy balance:

$$\rho_{app} C_{p,app} \frac{\partial T}{\partial l} = \frac{\partial n_e}{\partial l} - \lambda I, \qquad (6.14)$$

where ρ_{app} and $C_{p,app}$ are the pasta apparent density and heat capacity, λ is the latent heat of water vaporisation and n_E is the energy flux, which consists of the conductive and the convective heat transfer mechanisms:

$$n_e = k_h \frac{\partial T}{\partial l} + n_w H_{h,w} + n_g H_{h,g}, \qquad (6.15)$$

where $H_{h,w} = C_{p,w} T$ and $H_{h,g} = C_{p,g} T$ are the specific enthalpy of the liquid water and gas phase and k_h is the pasta thermal conductivity. The initial condition required to solve Eq. (6.15) was developed from the hypothesis of a uniform initial temperature profile within the pasta, a no-flux boundary condition was used at the center of the pasta and a Neumann boundary condition was used at the surface:

$$T = T_0 \qquad \text{(for } t = 0\text{)} \qquad (6.16)$$

$$\frac{\partial T}{\partial l} = 0 \qquad \text{(for } l = 0\text{)} \qquad (6.17)$$

$$n_E = h_h (T - T_\infty), \qquad \text{(for } l = L\text{)} \qquad (6.18)$$

where h_h is the convective heat transfer coefficient at the surface of the pasta and T_∞ the temperature of the air in the drying chamber.

6.2.1.4 Shrinkage

Shrinkage of the pasta caused by the partial replacement of water with air was considered and described with a dimensionless parameter (η) representing the volumetric fraction of liquid water replaced by air within the pasta matrix (Mercier et al. 2011b):

$$\eta = 1 - \frac{V_{app,0} - V_{app}}{V_{w,0} - V_w}, \tag{6.19}$$

where V_{app} is the pasta apparent volume and V_w is the volume occupied by liquid water. The concentration and the density of liquid water were introduced in Eq. (6.19) to obtain a relationship between the pasta apparent volume and the liquid water concentration:

$$V_{app} = V_{app,0} \frac{1+(\eta-1)\frac{C_{w,0}}{\rho_w}}{1+(\eta-1)\frac{\overline{C_w}}{\rho_w}}, \tag{6.20}$$

where $\overline{C_w}$ is the average (according to l) liquid water concentration (calculated as the arithmetic average of the liquid water concentration at each discretization node of the finite difference method).

6.2.2 Physical and thermal properties

6.2.2.1 Diffusivity

The liquid water diffusivity (D_w) was calculated from the minimization of the mean square error between the model estimates and the experimental moisture profiles. The diffusion of water vapor in the liquid phase or in the solid phase was assumed to be negligible. Under this assumption, the water vapor diffusivity ($D_{v,eff}$) was expressed from the water vapor – air binary diffusivity (D_{v-a}) as follows (Geankopolis, 2003):

$$D_{v,eff} = D_{v-a} \frac{\epsilon}{\tau}, \tag{6.21}$$

where τ is the tortuosity of the pores. For inert solids, the tortuosity generally varies from 1.5 to 6 (Aguilera and Stanley, 1999; Geankoplis, 2003). For the current system, the Fuller-Schettler-Giddings correlation was used to estimate the water vapor – air binary diffusivity (Fuller et al., 1966):

$$D_{v-a} = \frac{10^{-3} T_f^{1.75} \left(\frac{M_w + M_a}{M_w M_a}\right)^{0.5}}{P\left[(\sum v)_v^{1/3} + (\sum v)_a^{1/3}\right]^2}, \quad (6.22)$$

where T_f is the arithmetic average temperature between T_∞ and the temperature at the surface of the pasta, M_a is the molecular weight of air, $(\sum v)_v$ and $(\sum v)_a$ are the atomic diffusion volume of the component ($cm^3\ mol^{-1}$), P is the external pressure (atm) and D_{v-a} is the binary diffusivity ($cm^2\ s^{-1}$). For water vapor and air, values of the atomic diffusion volume of 12.7 and 20.1 $cm^3\ mol^{-1}$ were selected, respectively (Perry and Green, 1984).

6.2.2.2 Mass and heat transfer coefficients

It was assumed that only water vapor was exchanged between the pasta and the air in the drying chamber such that the liquid water mass transfer coefficient h_w was negligible. The water vapor mass transfer coefficient was calculated from experimental moisture profiles with a least-squares method since no other estimates were available. For the surface boundary condition of the energy balance, a heat transfer coefficient h_h of 29.6W $m^{-2}\ K^{-1}$ was selected as measured by De Temmerman et al. (2007).

6.2.2.3 Permeability

The gas permeability, 2 x 10^{-14} m^2, selected in this study was based on the gas permeability of pre-gelatinized flour dough with 10% porosity (Goedeken and Tong, 1993), which was shown to be representative of the porosity of pasta dried at 40 or 80 °C (Mercier et al. 2011b). The absolute liquid water permeability was selected to be 10^{-18} m^2 based on published results for saturated potato and beef tissues (Datta, 2006), two food products with similar porosity (0-30%) as pasta (Wang and Brennan, 1995; Rahman et al., 1996; McDonald and Sun, 2001).

6.2.2.4 Evaporation rate constant

The evaporation rate constant was selected to be 100 s^{-1} based on the study conducted by Halder et al. (2007) for the development of a mechanistic model for water evaporation during the frying of porous media.

6.2.2.5 Equilibrium moisture content

The equilibrium moisture content was calculated from the temperature and the relative humidity (*RH*) in the drying chamber using the Oswin equation developed by Villeneuve and Gelinas (2007) for pasta drying:

$$X_E = \left(k_0 + k_1(T-273)\right)\left(\frac{0.01*RH}{1-0.01*RH}\right)^{\left(n_0+n_1(T-273)\right)}, \quad (6.23)$$

where X_E is the equilibrium moisture content in kg water kg dry matter^{-1}. The empirical constants of Eq. (6.23) take the following values: $k_0 = 1.522 * 10^{-1}$, $k_1 = -1.247 * 10^{-3}$ K^{-1}, $n_0 = 8.883 * 10^{-2}$ and $n_1 = 7.892 * 10^{-3}$ K^{-1}. The pasta equilibrium water concentration (C_E) was calculated by multiplying X_E by the dry solid concentration (C_S).

6.2.2.6 Water activity

The water activity was estimated from the empirical correlation developed by De Temmerman et al. (2008) for desorption isotherms of pasta:

$$a_w = \frac{\left[\frac{X}{A_1-A_2(T-273)}\right]^{\left[\frac{1}{B_1+B_2(T-273)}\right]}}{1+\left[\frac{X}{A_1-A_2(T-273)}\right]^{\left[\frac{1}{B_1+B_2(T-273)}\right]}}, \quad (6.24)$$

where A_1 = 0.138, A_2 = 10.4 x 10^{-4} °C^{-1}, B_1= 0.396 and B_2 = 11.6 x 10^{-4} °C^{-1}.

6.2.2.7 Pasta thermal conductivity

The pasta thermal conductivity was determined from the following empirical correlation (Saravacos and Maroulis, 2001):

$$k_h = \frac{0.273}{1+X} + \frac{0.8X}{1+X} exp\left[\frac{-2700}{R_g}\left(\frac{1}{(T-273)} - \frac{1}{60}\right)\right], \quad (6.25)$$

where X is the pasta water content in kg water kg dry matter^{-1}.

6.2.2.8 Heat capacity

The heat capacity of pasta was calculated from the weighted average heat capacity of its four major constituents (liquid water, starch, protein and gas phase):

$$C_{p,app} = \sum z_i C_{p,i}, \quad (6.26)$$

where z_i is the mass fraction of component "i", $C_{p,w} = 4184$, $C_{p,starch} = 5.737T + 1328$, $C_{p,protein} = 6.329T + 1465$ and T is in K (Migliori et al., 2005). The protein mass fraction was taken as 16% of pasta dry solid (Mercier et al., 2011b). The heat capacity of the gas phase was taken as the heat capacity of air at the given temperature.

6.2.2.9 Shrinkage coefficient

The shrinkage coefficient (η) was considered constant for the drying process in accordance with Andrieu et al. (1989) and Mercier et al. (2011b). Measured shrinkage coefficients of 0.28 and 0.15 for durum wheat semolina pasta dried at 40 and 80 °C, respectively were used (Mercier et al., 2011b).

6.2.2.10 Density

The pasta dry matter density (ρ_S) was assumed to be 1510 kg m^{-3} and the pasta initial apparent density ($\rho_{app,0}$) to be 1310 kg m^{-3} based on the experimental measurements reported by Mercier et al. (2011b). The density of water (ρ_w) was taken as 998 kg m^{-3}.

6.2.3 Model numerical implementation

The mass balance (Eqs. 6.1-6.13) and the energy balance (Eqs. 6.14-6.18) were solved numerically with Matlab 7.5 using a one-way coupling method between shrinkage and mass or heat transfer (Fig. 6.1). The first step of the numerical method was to compute, on a fixed meshing, the concentration of liquid water, water vapor and gas phase and the temperature at the calculation node "*i*" after a time step Δt. This was achieved using the method of lines, which required the discretization of the partial differential equations (6.1)-(6.3) and (6.14) in space to obtain a system of ordinary differential equations (ODE). Central-difference approximations were used for the discretization:

$$\left.\frac{\partial Z}{\partial l}\right|_{i,t} \approx \frac{Z_{i+1,t}-Z_{i-1,t}}{\Delta l_{i-1}+\Delta l_{i+1}} \tag{6.27}$$

$$\left.\frac{\partial^2 Z}{\partial l^2}\right|_{i,t} \approx \frac{Z_{i+1,t}-2Z_{i,t}+Z_{i-1,t}}{((\Delta l_{i-1}+\Delta l_{i+1})/2)^2}, \tag{6.28}$$

where $Z_{i,t}$ is the concentration or temperature at node "*i*", Δl_{i-1} is the distance between the node *"i"* and the node "*i*-1*"* and Δl_{i+1} is the distance between the node *"i"* and the node "*i*+1*"*. The nodes become non-equidistant during drying because of the faster shrinkage at the surface of the product than at the center. The system of non-linear ODE was solved with Matlab function *ode15s,* whose resolution algorithm is based on the Numerical Differentiation Formula method (improved version of the implicit Backward Differentiation Formula method).

The second step of the numerical method was to compute the shrinkage from the decrease of the liquid water concentration. As proposed by Migliori et al. (2005), the liquid water concentration was assumed to be constant within a small pasta volume ΔV_i.The local

shrinkage ($\xi_{i,t}$) was calculated at each node from the decrease of the liquid water content using a modified form of Eq. (6.20):

$$\xi_{i,t} = \frac{\Delta V_{i,t+\Delta t}}{\Delta V_{i,t}} = \frac{1+(\eta-1)\frac{C_{w,i,t}}{\rho_w}}{1+(\eta-1)\frac{C_{w,i,t+\Delta t}}{\rho_w}} \tag{6.29}$$

The concentration of liquid water, water vapor, gas phase and dry solid at each node was then adjusted (step 3) from the shrinkage as follows:

$$C_{i,t+\Delta t} \leftarrow \frac{1}{\xi_{i,t}} C_{i,t+\Delta t} \tag{6.30}$$

The model (Eqs. 6.1-6.18) was solved using 21 nodes and the shrinkage calculated after every five seconds of drying. Simulations were also run with a higher number of nodes (41) and with smaller time steps (1 second), but no influence on the results was observed.

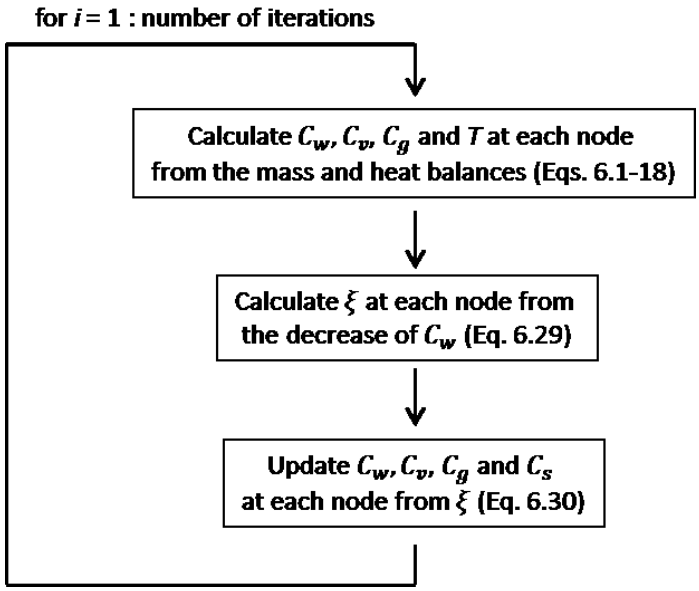

Figure 6.1. Numerical procedure for solving the mechanistic model (Eqs. 6.1-6.30).

6.2.4 Experimental validation

6.2.4.1 Published experimental internal moisture profiles

The internal moisture profile measurements obtained at different drying times by Litchfield and Okos (1992) for slabs of pasta 2.5 mm thick and drying at 40, 60 and 80 °C were used for the validation of the model estimates.

6.2.4.2 Model input parameters

The model input parameters are summarized in Table 6.1. The liquid water diffusivity and the water vapor mass transfer coefficient were determined from the minimization of the mean square error between experimental and predicted internal moisture profile estimates. The minimization of the mean square error was achieved through a genetic algorithm. Genetic algorithms are evolutionary-based global optimization methods which are easy to implement and avoid the calculation of suboptimal solutions in non-convex models (Mitra, 2008; Niazi and Leardi, 2012). In a genetic algorithm, a population of candidate solutions (input parameters) is selected and the objective function is calculated for each of them. The candidate solutions that provided the greatest minimization of the objective function are combined and this process is repeated until the population evolves toward a unique solution. The genetic algorithm was implemented with the following parameters: population size: 30; parents selection: rank-based, with the rank calculated from the mean square difference between experimental and predicted internal moisture profiles; one crossover points; position of the crossover point chosen randomly; 70% probability of crossover and 1% probability of mutation. The algorithm was repeated several times to verify that similar results were obtained.

Table 6.1. Input parameters of the drying model

Parameter	Value	Justification/Reference
Liquid water diffusivity (D_w)	-	Estimated from experimental measurements with least squares method
Water vapor diffusivity ($D_{v,eff}$)	Eqs. (6.21) and (6.22) with $\epsilon = 0.09$ and $\tau = 2$	Mercier et al. (2011b)
Liquid water mass transfer coefficient (h_w)	0 m s^{-1}	Hypothesis of negligible surface liquid water transfer

Water vapor mass transfer coefficient (h_v)	-	Determined from experimental measurements with least squares method
Liquid water permeability (k_w)	10^{-18} m^2	Datta (2006)
Gas phase permeability (k_g)	2 x 10^{-14} m^2	Goedeken and Tong (1993)
Evaporation rate constant (K_{ev})	100 s^{-1}	Halder et al. (2007)
Thermal conductivity (k_h)	Eqs. (6.25)	Saravacos andMaroulis(2001)
Heat transfer coefficient (h_h)	29.62 W m^{-2}K^{-1}	De Temmerman et al. (2007)
Apparent pasta heat capacity ($C_{p,app}$)	Eq. (6.26) with z_w = 0.23 (which corresponds to X = 0.3), z_{starch}= 0.64 and $z_{protein}$= 0.12	Mercier et al. (2011b)
Liquid water heat capacity ($C_{p,l}$)	4184 J kg^{-1}K^{-1}	Perry and Green (1984)
Gas phase heat capacity ($C_{p,g}$)	1010 J kg^{-1}K^{-1}	Perry and Green (1984)
Shrinkage coefficient (η)	0.28 (at 40 °C), 0.22 (60 °C) and 0.15 (80 °C)	Mercier et al. (2011b)
Liquid water density (ρ_l)	998 kg m^3	Perry and Green (1984)
Dry solid density (ρ_s)	1510 kg m^3	Mercier et al. (2011b)
Activity coefficient (a_w)	Eq. (6.24)	De Temmerman et al. (2008)
Liquid water viscosity (μ_l)	6.5 x 10^{-4} Pas (at 40 ºC), 4.7 x 10^{-4} Pas (60 ºC) and 3.6 x 10^{-4} Pas (80 ºC)	Perry and Green (1984)
Gas phase viscosity (μ_g)	1.5 x 10^{-5} Pas (at 40 ºC), 2.0 x 10^{-5} Pas (60 ºC) and 2.1 x 10^{-5} Pas (80 ºC)	Perry and Green (1984)

Water latent heat of vaporization (λ)	2.26 x 10^6 J kg^{-1}	De Temmerman et al. (2008)
Equilibrium moisture content (C_E)	Eq. (6.23) with RH = 68% (at 40 °C), 79% (60 °C) and 72% (80 °C)	Litchfield and Okos (1992)
Initial liquid water concentration ($C_{w,o}$)	361 kg m^{-3}	Corresponds to an initial moisture content on a dry basis of 0.38 and an initial porosity of 1% (Litchfield and Okos, 1992; Mercier et al., 2011b)
Initial water vapor concentration ($C_{v,o}$)	4.8 x 10^{-4} kg m^{-3}	From the hypothesis that liquid water and water vapor are at equilibrium at $T = T_o$
Initial gas phase concentration ($C_{g,o}$)	0.01 kg m^{-3}	From the hypothesis of an initial porosity of 1% (Mercier et al., 2011b)
Initial dry solid concentration ($C_{s,o}$)	949 kg m^{-3}	Corresponds to an initial moisture content on a dry basis of 0.38 and an initial porosity of 1% (Litchfield and Okos, 1992; Mercier et al., 2011b)
Initial pasta temperature (T_o)	40 °C	Arithmetic average between extrusion temperature (55 °C) and room temperature (25 °C)

6.2.5 Sensitivity analysis

A sensitivity analysis was performed to evaluate the effect of six input parameters on the model estimates. Each input parameter was varied by 10% one at a time for the drying reference scenario at 60 °C: water vapor mass transfer coefficient (h_v^0 = 5.5 x 10^{-7} ms^{-1}), liquid water diffusivity (D_w^0 = 8.2 x 10^{-11} m^2 s^{-1}), water vapor diffusivity ($D_{v,eff}^0$ = 1.4 x 10^{-6} m^2 s^{-1}), liquid water permeability (k_w^0 = 10^{-18} m^2), gas phase permeability (k_g^0 = 2 x 10^{-14} m^2) and evaporation rate constant (K_{ev}^0 = 100 s^{-1}). The analysis was based on two output parameters f_1

and f_2. The output parameter f_1 represents the time when the average moisture content of the pasta was less than 0.2 kg water kg dry matter^{-1} (i.e. $f_1 = t$ for $\bar{X} = 0.2$) giving a measure of the impact of the model parameters on the overall drying rate of the pasta. The output parameter f_2 represents the difference between the moisture content at the center and at the surface of the pasta when the average moisture of 0.2 kg water kg dry matter^{-1} was reached (i.e. $f_2 = X|_{l=0} - X|_{l=L}$ for $\bar{X} = 0.2$) representing the impact of the model parameters on the internal water profiles of pasta.

In order to compare the relative impact of the input parameters independently of their magnitude, the method proposed by Chokmani et al. (2001) was adopted:

$$Sr(Y_i) = \frac{\partial f(Y)}{\partial Y_i}\Big|_{Y^0} * \frac{Y_i^0}{f(Y^0)}, \quad (6.31)$$

where $Sr(Y_i)$ is the relative sensitivity of the output parameter *f* for a given input parameter, Y_i, $\frac{\partial f(Y)}{\partial Y_i}\Big|_{Y^0}$ is the partial derivative of *f* with respect to Y_i (evaluated for the reference scenario Y^0) and Y_i^0 is the value of the input parameter "*i*" for the reference scenario. The partial derivative in Eq. (6.31) was calculated numerically using a finite difference method.

6.3 Results and discussion

6.3.1 Pasta internal moisture profiles

The internal moisture profiles predicted with the mechanistic model developed in this study (Fig. 6.2) are in good agreement with the experimental moisture profiles for all drying temperatures. The accurate model predictions of the internal moisture profiles at 60 ºC and 80 ºC is a major improvement when compared to previous predictions obtained with the model developed by Litchfield and Okos (1992) where liquid water and water vapor transport are combined and represented by an effective moisture diffusion coefficient. Such differences in model predictions, particularly in the vicinity of the pasta surface, illustrate the importance of distinguishing the types of water transport, namely liquid water capillarity, liquid water convection, water vapor diffusion and water vapor convection. Internal water evaporation

appears to be an important factor in pasta drying and should be considered for accurate estimation of the internal moisture profile in pasta, a porous food material. The evaporation of liquid water increases the contribution of water vapor to the total water transport and the development of a pressure gradient, leading to less pronounced internal moisture profiles when compared to those predicted with an effective moisture diffusion coefficient.

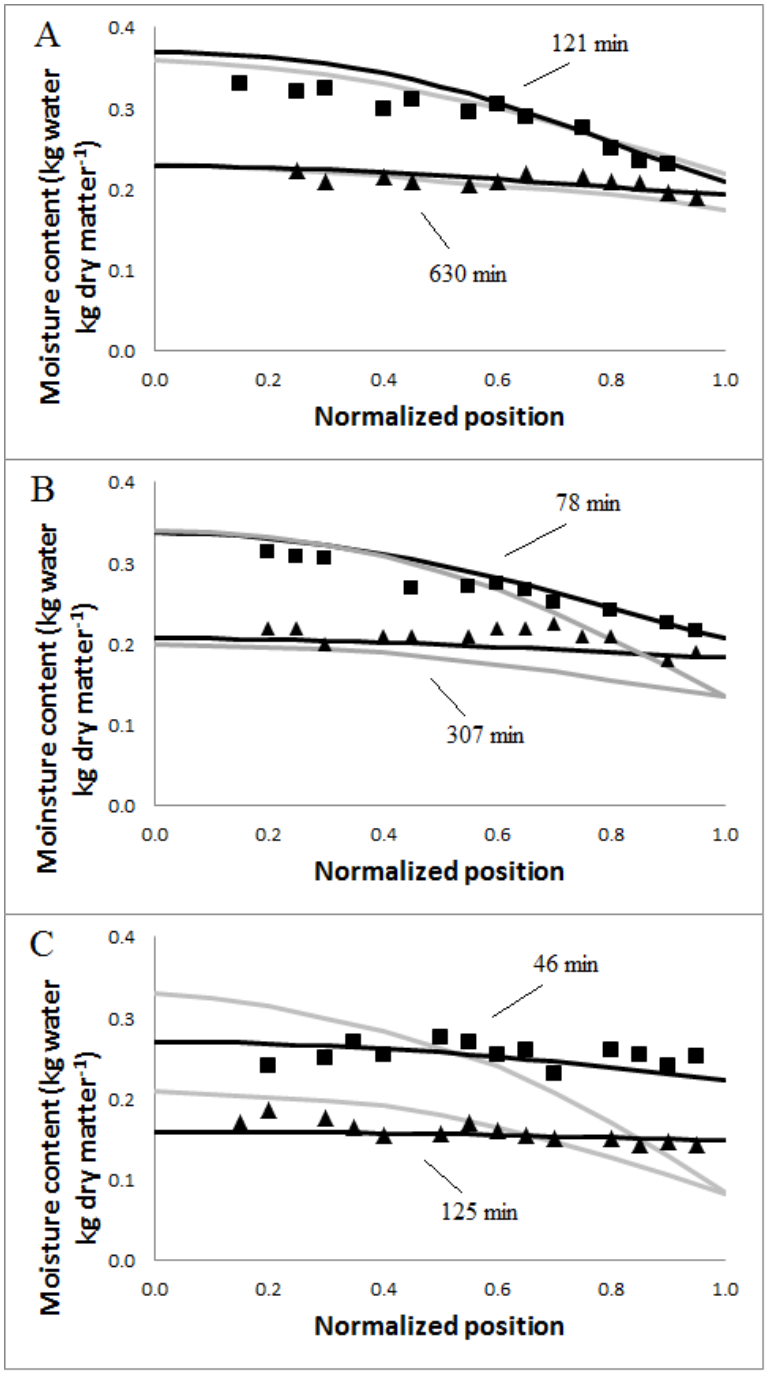

Figure 6.2. Pasta internal moisture profiles according to normalized position for drying at 40 °C (A), 60 °C (B) and 80 °C (C). Estimates according to the mechanistic model (Eqs. 6.1-6.18) (black line); estimates according to the model of Litchfield and Okos (1992) (grey lines); experimental data of Litchfield and Okos (1992) (■ and▲).

Accurate prediction of the pasta internal moisture profiles constitutes a major step forward for the prediction of crack formation and the analysis of the mass and heat transfer mechanisms taking place during pasta drying (Mercier et al., 2013b). However, pasta should be expected to have significantly different structural and mechanical properties in the glassy state and at the vicinity of glass transition region, which can impact the mass and heat transfer mechanisms involved (Cuq and Icard-Verniere, 2001; Takhar, 2008; Mercier et al., 2013b). Consequently, measurement of accurate internal moisture profiles at lower moisture contents would be required to validate the model for pasta in the glassy state or in transition from the rubbery to the glassy state.

6.3.2 Mass transfer mechanisms

The estimates of the liquid water diffusivity coefficient and water vapor mass transfer coefficient according to drying temperature (Fig. 6.2) were the following: at 40 ºC: D_w= 2.6 x 10^{-11} m^2 s^{-1} and h_v = 3.9 x $10^{-7}$$ms^{-1}$; at 60 ºC: D_w= 8.2 x 10^{-11} m^2 s^{-1} and h_v = 5.5 x $10^{-7}$$ms^{-1}$ and at 80 ºC: D_w= 5.2 x 10^{-10} m^2 s^{-1} and h_v = 5.2 x 10^{-7} m s^{-1}. The magnitude of the estimated liquid water diffusivity coefficients is in agreement with the effective moisture diffusion coefficient calculated from previous models and, as expected, increases with the drying temperature (Mercier et al., 2013b).

The evolution with time of the internal liquid water and water vapor content, temperature and porosity of the pasta estimated with the proposed model for air chamber temperature (T_∞ = 60 ºC), the input parameters (Table 6.1), a liquid water diffusivity of 8.2 x 10^{-11} m^2 s^{-1} and a water vapor mass transfer coefficient of 5.5 x 10^{-7} m s^{-1} are presented in Fig. 6.3. The liquid water content at the surface of the pasta decreased significantly as a result of the significant internal resistance to mass transfer (Fig. 6.3A). After about 10 min of drying,

the temperature of the pasta (Fig. 6.3C) was within 5 °C of its equilibrium temperature confirming that mass transfer was significantly slower than heat transfer as reported previously (Andrieu and Stamatopoulos, 1986; Villeneuve and Gelinas, 2007; De Temmerman et al., 2008). The predicted water vapor concentration was higher at the surface of the pasta than at its center, especially at the beginning of drying (Fig. 6.3B). The higher water vapor concentration at the surface can be explained by the rapid increase in the surface porosity of the pasta (Fig. 6.3D) inducing a significant increase of the water vapor equilibrium concentration. After five hours of drying, the estimated gas phase content of the pasta represented about 13% indicating that porosity should not be neglected when modeling pasta drying.

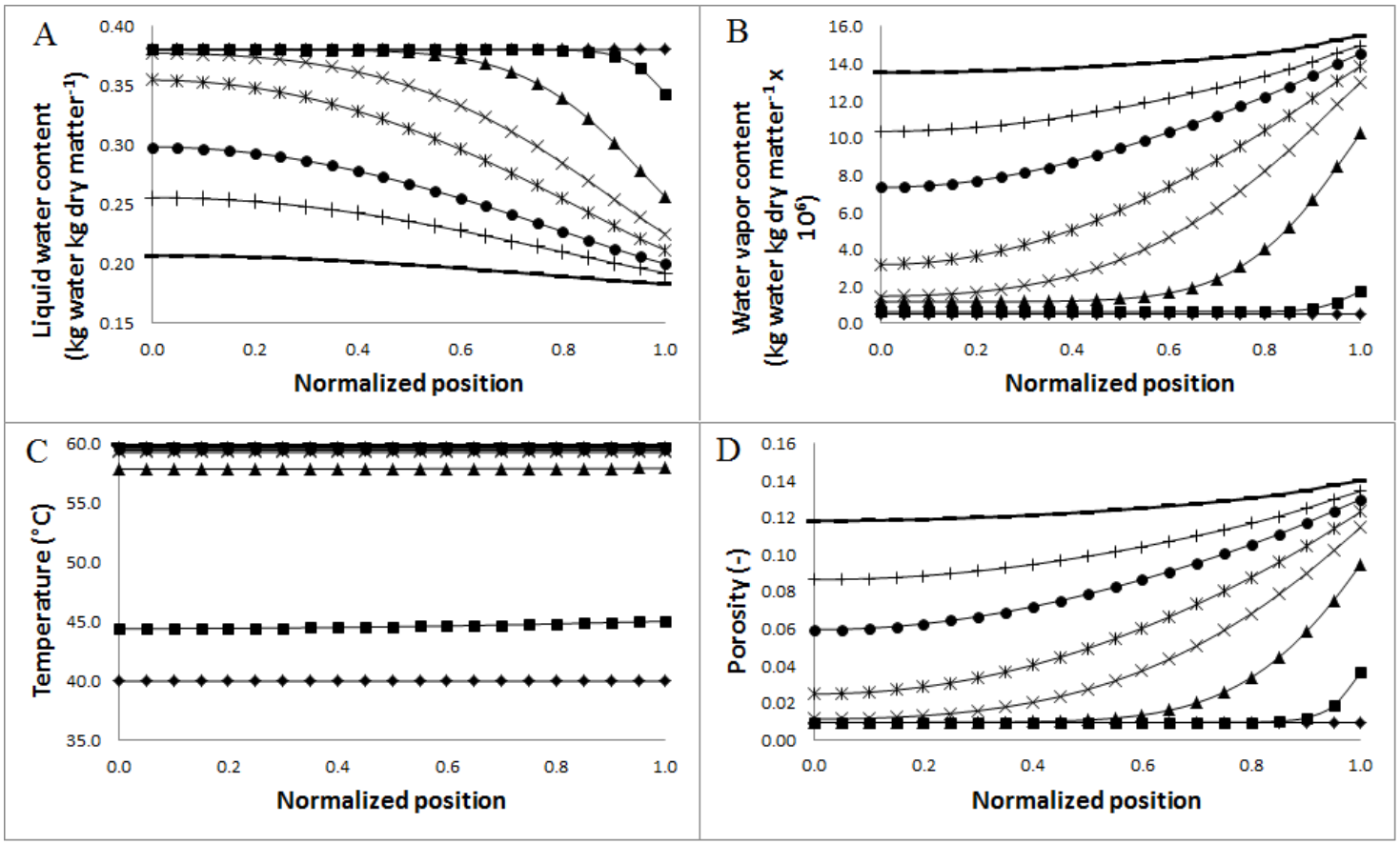

Figure 6.3. Simulation according to normalized position for pasta drying at 60 °C and 79% *RH*: liquid water content (A), water vapor content (B), temperature (C) and porosity (D) after 0 min (♦), 1 min (■), 10 min (▲), 30 min (×), 60 min (∗), 120 min (•), 180 min (+) and 300 min (-).

While the liquid water n_w and water vapor n_v mass fluxes decreased sharply during the first hour of drying, their ratio remained relatively constant for the entire process. The average liquid water mass flux accounted for 88% of the total water mass flux and the water evaporation rate was 0.0022 kg water m^{-3} s^{-1}.These results suggest that water was predominantly, but not exclusively, transported in the liquid state during pasta drying. A similar liquid water contribution to pasta drying was obtained by Waananen and Okos (1996) from their estimates of the effective moisture diffusivity (D_{eff}) of pasta with a 26% porosity and dried at 71 °C under different ambient pressures. From the hypothesis that liquid water capillarity is independent of external pressure but that water vapor diffusivity is inversely proportional to pressure, they estimated that the liquid water contribute to 78% of the total water mass flux for drying at 77 kPa and 90% for drying at 202 kPa.

The liquid water flux n_w included capillarity and convection. The average liquid water mass flux by capillarity estimated with the current model ranged from 9.0 x 10^{-6} kg m^{-2} s^{-1} to 3.1 x 10^{-7} kg m^{-2} $s^{-1}$for the first five hours of drying, while the average liquid water convective flux ranged from 9.2 x 10^{-9} kg m^{-2} s^{-1} to 1.2 x 10^{-9} kg m^{-2} s^{-1}. Since the estimated liquid water convective flux accounted for less than 1% of the total liquid water mass flow, the convective flow of liquid water can be neglected when analyzing pasta drying. The negligible liquid water convective flux can be attributed to the significant amount of bound water in hygroscopic food materials, which reduces the liquid water permeability and promotes a prevailing effect of capillary pressure over external pressure (Datta, 2007).

The average water vapor convective flux was 1.5 x 10^{-7} kg $m^{-2}s^{-1}$ at the beginning of drying and 6.2 x 10^{-8} kg m^{-2} s^{-1} after five hours, while the estimated average water vapor diffusive flux was 4.6 x 10^{-7} kg m^{-2} s^{-1} initially and 4.4 x 10^{-7} kg m^{-2} s^{-1} at the end of the five hours drying period. The convective water vapor flux occurred predominantly at the surface of the pasta, where the pressure gradient was the steepest. The estimated convective water vapor flux represented 24% (at the beginning of drying) and 12% (after five hours) of the total mass water vapor flux indicating that diffusion and convection contributed significantly to the water vapor transport during pasta drying.

6.3.3 Heat transfer mechanisms

The average energy flux, estimated from the energy balance, ranged from 4.9 x 10^4 to 5.6x 10^4 J $m^{-2}s^{-1}$ for conduction and from 2 to 17 J $m^{-2}s^{-1}$ for convection suggesting that conduction is the dominant heat transfer mechanism in pasta drying. The Biot number ($Bi = \frac{h_h L}{k_h}$) estimated with the input parameters for the drying reference scenario was close to 0.1, which supports the hypothesis that the internal resistance to energy flow can be neglected when describing pasta drying (Ponsart et al., 2003).

6.3.4 Sensitivity analysis of the model parameters

The relative sensitivity of the overall drying rate (f_1) and the internal moisture gradient (f_2) for the six input parameters is presented in Table 6.2. The liquid water diffusivity (D_w) had a more significant influence on the drying time and internal moisture profile estimates than the water vapor diffusivity parameter (D_v) in agreement with the more significant contribution of water transport in the liquid state than in the vapor state. The water vapor mass transfer coefficient (h_v) had the most significant impact on the internal moisture profile estimates. The sensitivity analysis also highlighted the different contributions of the input parameters on the overall drying rate (f_1) and the internal moisture profiles (f_2). For instance, the liquid water diffusivity parameter (D_w) had a significant effect on the drying time required to reach the predetermined moisture content ($\bar{X}$ = 0.2 d.b.), but an impact about twice lower on the pasta internal moisture profiles (f_2).

The sensitivity analysis suggests that the magnitude of the evaporation rate constant (K_{ev}) and the liquid water and water vapor permeability (k_w and k_g) have negligible impact on the model estimates for the drying reference scenario considered in this study. However, an increase in the gas phase permeability was associated with an increase of the water vapor flow and a decrease of the liquid water flow by decreasing the internal pressure build-up. Therefore, the effect of the gas phase permeability may be masked by these opposing effects.

Table 6.2. Relative sensitivity (*Sr*, Eq. 6.31) of the model estimates: time at $\bar{X} = 0.2$ (f_1) and moisture difference between the surface and the centre of the pasta (f_2) for the reference scenario

Parameter	*Sr* (f_1)	*Sr* (f_2)
Water vapor mass transfer coefficient (h_v)	0.25	0.30
Liquid water diffusivity (D_w)	0.54	0.24
Water vapor diffusivity ($D_{v,eff}$)	0.08	0.06
Evaporation rate constant (K_{ev})	0.01	0.01
Liquid water permeability (k_w)	0.00	0.00
Gas phase permeability (k_g)	0.00	0.00

6.4 Conclusion

In this study, a mechanistic model was developed by representing pasta as a porous material, considering water evaporation and distinguishing liquid water transport and water vapor transport during its drying. The estimated internal moisture profiles were in good agreement with published experimental data and provided more accurate estimates of moisture profiles at high drying temperature when compared to previous estimates for models based on a single effective moisture diffusion coefficient. Model estimates for a drying reference scenario at 60 ^{o}C indicated that approximately 88% of the total water transport occurred in the liquid state. According to the model simulations, capillarity is the predominant mass transfer mechanism for liquid water while convection and diffusion contribute significantly to water vapor transport.

A sensitivity analysis of model input parameters indicated that the water vapor mass transfer coefficient and the liquid water diffusivity coefficient required the highest accuracy for drying time and internal moisture estimates. As the values for these two model parameter were those of other types of cereal products, it would be beneficial to measure experimentally these parameters for pasta products. The evaporation rate constant, liquid water permeability and gas phase permeability had negligible effects on the drying time and internal moisture profile estimates.

The model presented in this study serves as platform that could be expanded to examine the moisture mass transfer taking place near glass transition conditions where the

coexistence of a glassy and a rubbery layer is believed to significantly impact the moisture transport.

6.5 Acknowledgements

Authors would like to thank the Natural Sciences and Engineering Research Council of Canada for their financial support.

CHAPITRE 7. Méta-analyse de l'impact des variables de procédé sur les propriétés des pâtes traditionnelles et enrichies

Titre original : A meta-analysis of enriched pasta: what are the effects of enrichment and process specifications on the quality attributes of pasta?

Auteurs et affiliations :

S. Mercier, Ing. jr., étudiant au doctorat, Université de Sherbrooke, département de génie chimique et génie biotechnologique, 2500 boul. Université, Sherbrooke, Québec, Canada, J1K 2R1.

C. Moresoli, Ing., Ph.D. University of Waterloo, Department of Chemical Engineering, 200 University Avenue West, Waterloo, Ontario, Canada, N2L 3G1.

M. Mondor, Ing. stag., Ph.D., Agriculture et Agroalimentaire Canada, Centre de Recherche et Développement de Saint-Hyacinthe, 3600 Boul. Casavant Ouest, Saint-Hyacinthe, Québec, Canada, J2S 8E3.

S. Villeneuve, Ing., Ph.D., Agriculture et Agroalimentaire Canada, Centre de Recherche et Développement de Saint-Hyacinthe, 3600 Boul. Casavant Ouest, Saint-Hyacinthe, Québec, Canada, J2S 8E3.

B. Marcos, Ing., Ph.D., Université de Sherbrooke, département de génie chimique et génie biotechnologique, 2500 boul. Université, Sherbrooke, Québec, Canada, J1K 2R1.

État de l'acceptation : accepté pour publication dans la revue *Comprehensive Reviews in Food Science and Food Safety*. doi: 10.1111/1541-4337.12207

Résumé

Contenu : une méta-analyse a été réalisée dans le but de quantifier l'impact de l'enrichissement et ses interactions avec les variables de procédé sur les propriétés des pâtes. Les mesures des propriétés des pâtes traditionnelles et enrichies ont été extraites de 66 études et compilées dans une base de données. La relation entre l'enrichissement, les variables de procédé et les propriétés des pâtes a été quantifiée par la combinaison des résultats compilés dans la base de données à partir de modèles non pondérés, à effets fixes et à effets aléatoires et de coefficients de corrélations.

Résultats : la méta-analyse révèle des différences significatives entre l'impact d'enrichir des pâtes avec des farines de légumineuses et des ingrédients riches en fibres. Les ingrédients riches en fibres semblent participer plus activement à la préservation de la microstructure et de la qualité des pâtes. La comparaison selon la température de séchage indique que l'utilisation de températures de séchage élevées favorise la qualité des pâtes enrichies possiblement grâce à la fortification du réseau de gluten. La combinaison des résultats d'analyses sensorielles indique la préservation de l'acceptation par les consommateurs des pâtes pour une concentration d'enrichissement inférieure à 10% pour la plupart des ingrédients d'enrichissement, mais une diminution de l'acceptation pour des concentrations d'enrichissement supérieures. L'analyse des coefficients de corrélation révèle que la température de gélatinisation est un bon prédicteur des propriétés de cuisson des pâtes, les propriétés de mélange (Farinographe) de bons prédicteurs des propriétés mécaniques et les propriétés de cuisson de bons prédicteurs des propriétés sensorielles.

Contributions à la thèse : les contributions à la thèse de cet article sont le développement d'une base de données décrivant les propriétés des pâtes traditionnelles et enrichies selon les conditions de production, une compréhension détaillée, grâce à une analyse quantitative, de l'impact de l'enrichissement sur les propriétés des pâtes et l'identification des variables de procédé des pâtes étant de bons prédicteurs de leur qualité.

Abstract

Pasta products enriched with ingredients to improve their nutritional value or functionality have become increasingly popular, and substantial research efforts have been directed towards the development of new enriched pasta products. In this work, a meta-analysis was conducted to quantify the impact of enrichment and process specifications on the quality attributes of pasta. A literature search revealed 66 studies on enriched pasta. Process specifications and quality attributes, namely proximate composition, dough, drying, cooking, and mechanical properties, color, and sensory attributes, were extracted from the studies and compiled in a dataset. Analysis of the dataset revealed significant differences between pasta enriched with high-fiber ingredients and pasta enriched with pulse flour. High-fiber ingredients generally preserved the quality attributes of pasta more effectively than pulse flour. Comparisons based on the drying temperature showed that high drying temperatures generally improve the cooking properties of enriched pasta. Sensory evaluations indicated that enrichment levels below 10% generally do not affect consumer acceptance, but higher enrichment levels significantly decrease it. Pearson correlation coefficients showed that the gelatinization temperature and Farinograph properties are useful indicators of the mechanical properties and sensory attributes of pasta. The meta-analysis revealed the need to better understand the impact of the processing history of the enrichment ingredient on the quality attributes and the health benefits of enriched pasta.

Keywords

Pasta; Enrichment; Meta-analysis; Sensory attributes; Functional food

Nomenclature

CI	confidence interval (Equation 7.4)
df	number of degrees of freedom (Equation 7.12)
M_{ij}	difference with the control pasta for observation j in study i (Equation 7.1)
$\overline{M}$	pooled difference with the control pasta (Equation 7.2)
n	number of replicate measurements
p	number of studies in the dataset
q	number of observations in a study
Q	weighted sum of the between-study variance (Equation 7.12)
SD	standard deviation of a quality attribute at the observation level
SE	standard error of M or r
$\overline{SE}$	standard error of $\overline{M}$ or $\bar{r}$
r	Pearson correlation coefficient (Equation 7.5)
$\bar{r}$	pooled Pearson correlation coefficient (Equation 7.15)
X_i	arithmetic average of the quality attribute or process specification X over the q observations in study i (Equation 7.5)
X_{ic}	average measurement of the quality attribute or process specification X for the control pasta (c) in study i
X_{ij}	average measurement (over n replicates) of the quality attribute or process specification X for observation j in study i (Figure 7.2)
X_{ijk}	replicate measurement k of the quality attribute or process specification X for observation j in study i (Figure 7.2)
Y_i	arithmetic average of the quality attribute or process specification Y over the q observations in study i (Equation 7.5)
Y_{ij}	average measurement (over n replicates) of the quality attribute or process specification Y for observation j in study i (Figure 7.3)
Y_{ijk}	replicate measurement k of the quality attribute or process specification Y for observation j in study i (Figure 7.3)
Z	Fisher transform of the Pearson correlation coefficient (Equation 7.8)
$\bar{Z}$	pooled Fisher transform of the Pearson correlation coefficient (Equation 7.13)

Greek symbols

σ	standard deviation of a quality attribute or process specification at the study level (Equations 7.6 and 7.7)
τ^2	between-study variance (Equation 7.12)

Subscript

FEM	fixed effects model

7.1 Introduction

Pasta is one of the most popular food products in many regions of the world. Pasta products are appreciated by consumers because of their simplicity, ease of handling, palatability, long shelf life, and accessible cost, qualities that have caused their worldwide production to increase from 7 to 12 million tons per year during the last decade (Marti and Pagani 2013; Carini and others 2014; Li and others 2014). Pasta products are good vehicles for nutrient addition, because nontraditional ingredients can be added to their formulation without apparent loss of pasta quality (Petitot and others 2010; Alasino and others 2011). Accordingly, substantial efforts have been made towards the development of enriched pasta products. Ingredients considered for pasta enrichment include: protein concentrates and isolates (Alireza Sadeghi and Bhagya 2008; Mercier and others 2011b); pea, bean, and oilseed flours (Wood 2009; Gallegos-Infante and others 2010; Villeneuve and others 2013); dietary fibers (Brennan and Tudorica 2007; Aravind and others 2012b; Vernaza and others 2012); microalgae (Zouari and others 2011; Fradique and others 2013); and fruit extracts (Pillai and others 2012). Enrichment aims to compensate for nutritional deficiencies, such as low lysine and threonine contents, or to provide additional sources of fiber, minerals, antioxidants, or bioactive components (Chillo and others 2008; Marti and Pagani 2013).

The production of enriched pasta requires the selection of appropriate enrichment ingredients, enrichment levels, and process specifications. When developing new enriched pasta products, one should first review previous work in this field, in order to benefit from existing knowledge about pasta enrichment and identify the most promising technologies and process specifications for high-quality and health-promoting pasta. An efficient method of reviewing the existing knowledge is to use a meta-analysis. A meta-analysis is defined as the application of quantitative methods for the analysis of observations from multiple studies (Nam and others 2003; Green and others 2006; Valentine and others 2010). In a meta-analysis, the observations from different studies are compiled in a dataset and analyzed with statistical methods to identify associations among the observations. Meta-analyses combine the results of multiple studies and thus increase the sample size and in most cases the power of the statistical analysis, promoting the identification of associations between properties not observed in the primary studies (Cohn and Becker 2003; Valentine and others 2010). A recent example of the

statistical power of meta-analyses is the assessment by Health Canada of a health claim about ground whole flaxseed and blood cholesterol lowering (Health Canada 2014). The reduction of total and low-density lipoprotein (LDL) cholesterol levels with consumption of whole ground flaxseed was not statistically significant in most of the studies considered by Health Canada. After the results of the studies were pooled using a meta-analysis, however, average reductions of -0.21 mmol L^{-1} ($P = 0.0001$) for total cholesterol level and -0.22 mmol L^{-1} ($P < 0.0001$) for LDL cholesterol level were obtained. Health Canada concluded that "a low proportion of studies reached statistical significance, but this was addressed by a meta-analysis which showed a statistically significant reduction in total and LDL cholesterol levels with ground flaxseed consumption," and a claim about ground whole flaxseed and blood cholesterol lowering was approved.

The statistical methods used in a meta-analysis are similar to those used in a single study, except that the statistical methods are generally applied to average measurements in a meta-analysis and to individual measurements in a single study. In a single study, a quality attribute of a product is estimated by performing replicate measurements. The average value of the replicate measurements is the estimator of the value of the quality attribute, and the confidence interval of this estimator is calculated from the variability between the replicate measurements. In a meta-analysis, the value of each replicate measurement is unknown, because only the average value of the replicate measurements and its standard deviation are published in most studies (Tonelli and others 2009). The average measurements are generally pooled across studies using a random effects model, which is a weighted model in which the confidence interval of the pooled average measurement is calculated from the sum of the standard deviation of the average measurements and the variability between the average measurements (Hunter and Schmidt 2000; Schulze 2007). If the standard deviation of the average measurements is negligible compared with the variability between the average measurements, an unweighted model can be used to simplify the calculation of the pooled average measurement (Mengersen and others 2013).

The objective of this work was to use a meta-analysis to determine the impact of enrichment and process specifications on the quality attributes of pasta. The interactions between enrichment and process specifications were also examined. To accomplish this work,

a dataset was constructed by conducting a literature search to identify studies on the development of traditional (unenriched) pasta or enriched pasta. The impact of enrichment and process specifications on quality attributes of pasta was evaluated using differences with the control pasta and Pearson correlation coefficients. Proximate composition and dough, drying, cooking, color, mechanical, and sensory properties were considered. In light of the meta-analysis, research perspectives for the development of enriched pasta were formulated.

7.2 Dataset construction and implementation

7.2.1 Data collection strategy

An extensive search of the literature on food processing was conducted to identify studies on the development of traditional wheat pasta or wheat pasta enriched with health-promoting ingredients. The studies were found by searching for the keywords "pasta," "lasagna," and "spaghetti" on the search engines Scopus and Compendex and then proceeding through the references in the studies identified from the keyword search. Studies written in English and available digitally were considered for the meta-analysis. Studies were included in the meta-analysis if the results obtained were for traditional pasta made from wheat flour or semolina or for wheat pasta enriched with ingredients aiming to improve the nutritional value or functionality of the pasta. Measurements taken by our research team of the drying properties of pasta enriched with flaxseed were also included in the meta-analysis (Annexe C).

7.2.2 Construction of the dataset

A dataset containing key results from the studies was constructed in a Microsoft Excel spreadsheet. The results extracted from the studies were the average values of n replicate measurements and, when available, their standard deviation. Results presented in tables or in the text of the studies were considered, but results presented in figures were not, because of the error inherent in their extraction.

The columns of the Excel spreadsheet contained the relevant process specifications, namely, the operating conditions used for each observation, and the quality attributes, namely, the properties of pasta during or after processing. For each process specification or quality attribute, the results extracted from the studies were standardized by applying appropriate unit conversion when required, except for the mechanical and sensory properties of the pasta, because their measurement methods or scales were too inconsistent between the studies for standardization. These factors were included "as is" in the dataset and analyzed using Pearson correlation coefficients but not using differences with the control pasta (see sections 7.4.6 and 7.4.7). The rows of the Excel spreadsheet contained the observations, with 1 observation being a pasta produced at given process specifications and for which some quality attributes were known.

7.2.3 Description of the dataset

7.2.3.1 Studies and observations

The literature search revealed 66 relevant studies on traditional or enriched wheat pasta that were considered for the meta-analysis (Table 7.1). Nearly 60% of the studies were published since 2010, an indicator of the increasing interest in the development of new pasta products. From these studies, 663 observations were extracted and compiled in the dataset. Most studies focused on the addition of 1 enrichment ingredient at different levels and its impact on the quality attributes of the pasta. In general, each study contained fewer than 10 observations. Two large-scale studies compared the impact of multiple enrichment ingredients or wheat cultivars and contained more than 40 observations (Zhao and others 2005; AbuHammad and others 2012).

Table 7.1. Description of the studies included in the meta-analysis

Content of the study	Number of observations	Reference
Wheat protein content and dough, cooking, and mechanical properties	48	AbuHammad and others (2012)
Banana flour enrichment and cooking, drying, color, and sensory properties	4	Agama-Acevedo and others (2009)
Mustard protein isolate enrichment and proximate composition, dough, cooking, color, and mechanical properties	4	Alireza Sadeghi and Bhagya (2008)
Durum bran or germ enrichment and dough, cooking, color, and mechanical properties	10	Aravind and others (2012a)
Beta-glucan enrichment and dough, cooking, color, and mechanical properties	4	Aravind and others (2012b)
Guar gum and carboxymethyl cellulose enrichment and dough, cooking, color, and mechanical properties	12	Aravind and others (2012c)
Inulin enrichment and dough, cooking, and mechanical properties	11	Aravind and others (2012d)
Resistant starch enrichment and dough, cooking, color, and mechanical properties	7	Aravind and others (2013)
Toasting and proximate composition, dough, drying, cooking, and mechanical properties	6	Baiano and others (2008)
Toasted and defatted soy flour enrichment and proximate composition, dough, cooking, and color properties	11	Baiano and others (2011a)
Toasted durum wheat kernel enrichment and dough, cooking, and color properties	8	Baiano and others (2011b)
Spinach and amaranth leaf flour enrichment and proximate composition, cooking, and sensory properties	2	Borneo and Aguirre (2008)
Carrot and oregano leaf meal enrichment and cooking and sensory properties	5	Boroski and others (2011)
Inulin enrichment and cooking properties	5	Brennan and others (2004)
Proximate composition and cooking properties of traditional pasta	1	Brennan and Tudorica (2007)
Resistant starch and oat bran enrichment and sensory properties	13	Bustos and others (2011)
Shaping method and cooking and color properties	3	Carini and others (2009)
Shaping method and color	6	Carini and others (2010)
Soy flour, carrot flour, and wheat gluten enrichment and color	3	Carini and others (2012)
Buckwheat flour and durum wheat bran enrichment and proximate composition, drying, cooking, color, and sensory properties	10	Chillo and others (2008)

Corn, flaxseed, lentil, oat, pinto bean, and soybean flour enrichment and proximate composition, cooking, and mechanical properties	21	de la Peña and Manthey (2014)
Shaping method and pejibaye flour enrichment and proximate composition, dough, cooking, and mechanical properties	4	De Oliveira and others (2006)
Microalgae biomass enrichment and cooking, mechanical, and sensory properties	10	Fradique and others (2010)
Microalgae biomass enrichment and proximate composition, cooking, and sensory properties	7	Fradique and others (2013)
Mexican common bean flour enrichment and proximate composition, drying, cooking, and mechanical properties	9	Gallegos-Infante and others (2010)
Cooking properties and proximate composition of traditional and bran-rich wheat pasta	5	Gauthier and others (2006)
Resistant starch enrichment and cooking properties	14	Gelencsér and others (2008)
Broad bean flour enrichment and proximate composition, dough, drying, and cooking properties	4	Giménez and others (2012)
Peanut flour enrichment and proximate composition, cooking, color, and sensory properties	27	Howard and others (2011)
Amaranth flour enrichment and proximate composition, drying, cooking, color, and mechanical properties	3	Islas-Rubio and others (2014)
Lupin flour enrichment and drying, cooking, color, mechanical, and sensory properties	6	Jayasena and Nasar-Abbas (2012)
Green gram semolina enrichment and proximate composition, drying, cooking, color, and mechanical properties	3	Jyotsna and others (2014)
Shrimp meat enrichment and cooking, color, mechanical, and sensory properties	4	Kadam and Prabhasankar (2012)
Wheat, rice, barley, and oat bran enrichment and proximate composition, cooking, color, and sensory properties	24	Kaur and others (2012)
Mushroom powder, Bengal gram flour, and defatted soy flour enrichment and proximate composition, cooking, and sensory properties	30	Kaur and others (2013)
Flaxseed enrichment and cooking, color, and mechanical properties	6	Lee and others (2003)
Drying temperature and drying properties	8	Lucisano and others (2008)
Black gram flour enrichment and proximate composition, drying, cooking, and mechanical properties	8	Madhumitha and Prabhasankar (2011)

Inulin enrichment and proximate composition	4	Manno and others (2009)
Oat flour, oat fiber, flaxseed, and soy flour enrichment and cooking and mechanical properties	40	Manthey and Dash (2010)
Buckwheat bran flour enrichment and proximate composition, cooking, and color properties	6	Manthey and Hall (2007)
Wheat protein content and proximate composition, dough, and color properties	16	Marconi and others (2002)
Shaping method and drying properties	4	Mercier and others (2011a)
Pea protein concentrate enrichment and proximate composition and drying properties	8	Mercier and others (2011b)
Pea protein isolate enrichment and proximate composition and dough properties	7	Mercier and others (2012)
Banana flour enrichment and proximate composition, drying, and cooking properties	4	Ovando-Martinez and others (2009)
Split pea and faba bean flour enrichment and proximate composition, cooking, color, and mechanical properties	7	Petitot and others (2010)
Onion powder enrichment and dough, cooking, and sensory properties	8	Rajeswari and others (2013)
Chickpea flour enrichment and proximate composition, dough, drying, cooking, and sensory properties	6	Sabanis and others (2006)
Grape marc powder enrichment and cooking and color properties	4	Sant'Anna and others (2014)
Yellow pea flour enrichment and proximate composition, dough, cooking, color, and sensory properties	8	Shreenithee and Prabhasankar (2013)
Ground barley enrichment and proximate composition and sensory properties	6	Sinesio and others (2008)
Flaxseed enrichment and proximate composition, color, and mechanical properties	11	Sinha and Manthey (2008)
Resistant starch enrichment and proximate composition and dough properties	2	Sozer and others (2007)
Drying temperature and dough properties	2	Stuknyte and others (2014)
Fermented pigeon pea flour enrichment and proximate composition, cooking, and sensory properties	4	Torres and others (2006)
Lupin flour enrichment and proximate composition, cooking, and sensory properties	7	Torres and others (2007a)
Germinated pigeon pea flour enrichment and proximate composition, cooking, and sensory properties	4	Torres and others (2007b)
Inulin, guar gum, and pea fiber enrichment and dough, cooking, and mechanical properties	13	Tudorică and others (2002)
Soy and maize flour enrichment and proximate composition, cooking, and color properties	21	Ugarcic-Hardi and others (2003)

Resistant starch enrichment and proximate composition, cooking, and mechanical properties	22	Vernaza and others (2012)
Flaxseed enrichment and proximate composition, drying, cooking, and color properties	8	Villeneuve and others (2013)
Chickpea flour enrichment and proximate composition, dough, cooking, color, and mechanical properties	6	Wood (2009)
Corn gluten meal addition and proximate composition, cooking, color, and mechanical properties	11	Wu and others (2001)
Green pea, yellow pea, chickpea, and lentil flour enrichment and proximate composition, cooking, mechanical, and sensory properties	42	Zhao and others (2005)
Blue-green algae enrichment and proximate composition, cooking, color, mechanical, and sensory properties	4	Zouari and others (2011)

7.2.3.2 Process specifications

Process specifications were included in the dataset when they were reported in at least 4 studies and known for at least 20 observations. A total of 11 process specifications were considered for the meta-analysis (Figure 7.1). The enrichment ingredient and level, the type of wheat, the presence of additives (eggs or emulsifiers), the shaping method, and the drying temperature were reported in nearly all the studies considered for the meta-analysis. In contrast, the pasta thickness, the dough hydration, the relative humidity during drying, and the drying time were reported in only about half of the studies (Table 7.2).

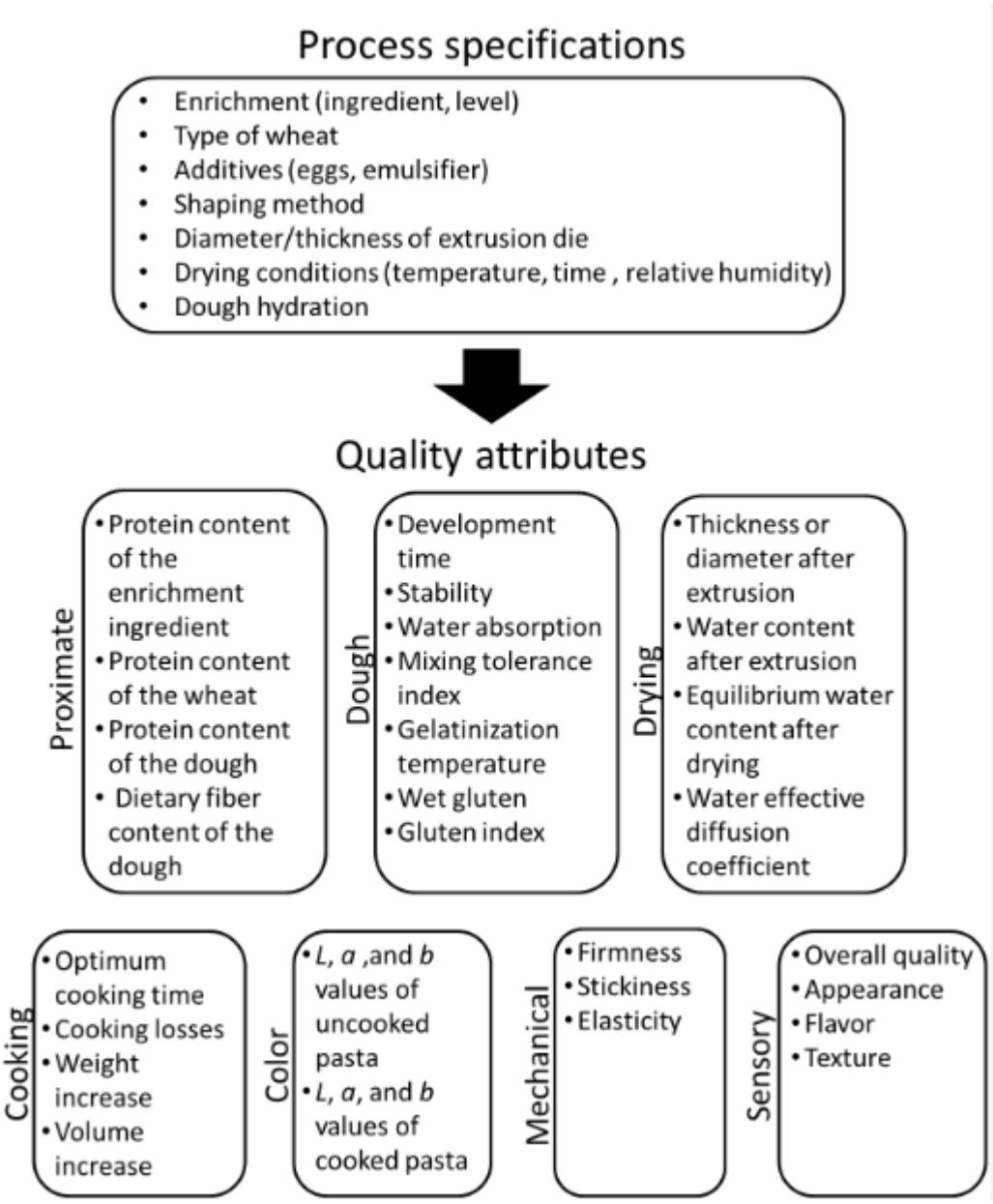

Figure 7.1. Overview of the process specifications and quality attributes considered in the meta-analysis.

Table 7.2. Process specifications considered for the meta-analysis.

Process specification	Number of observations	Traditional		Enriched	
		Average	Range	Average	Range
Enrichment ingredient	663	N/A	N/A	N/A	N/A
Enrichment level	663	0	0 to 0	17.0	0.25 to 50
Type of wheat (wheat	663	N/A	N/A	N/A	N/A

semolina or flour)					
Presence of eggs	663	N/A	N/A	N/A	N/A
Presence of an emulsifier	663	N/A	N/A	N/A	N/A
Shaping method (extruded with a Teflon or bronze die or laminated)	661	N/A	N/A	N/A	N/A
Diameter or thickness of the extrusion die (mm)	322	1.8	0.7 to 4.0	1.7	0.7 to 4.0
Drying temperature (maximum temperature applied during drying was considered) (°C)	650	59.2	37.5 to 95.0	63.5	37.5 to 95.0
Drying duration (considered if drying was isothermal) (h)	298	10.9	0.75 to 36.0	10.5	0.8 to 36.0
Average relative humidity during drying (%)	285	71.6	40.0 to 91.0	68.6	40.0 to 91.0
Dough hydration [g (100 g dry matter)$^{-1}$]	352	47.4	40.8 to 58.5	46.5	40.8 to 69.5

Note: The average values of the continuous process specifications were calculated for traditional pasta and enriched pasta using an unweighted model. N/A: not applicable

7.2.3.3 Quality attributes

A total of 32 quality attributes were considered for the meta-analysis (Figure 7.1). Like the process specifications (section 7.2.3.2), the quality attributes were selected if they were reported in at least 4 studies and known for at least 20 observations. The quality attributes were classified into 7 categories: proximate composition, dough properties, drying properties, cooking properties, color, mechanical properties, and sensory properties. The proximate composition, cooking properties, and color were the quality attributes most frequently considered in the studies and were known for roughly half of the observations compiled in the dataset. In contrast, drying, mechanical, and sensory properties were considered in about 10% to 20% of the studies and generally were known for fewer than 100 observations in the dataset (Table 7.3).

Table 7.3. Quality attributes considered for the meta-analysis.

Quality attribute	Number of observations	Relative error (%)	Traditional pasta		Enriched pasta	
			Average	Range	Average	Range
Proximate composition						
Protein content of the enrichment ingredient [g (100 g dry matter)$^{-1}$]	240	0.3	N/A	N/A	28.1	4.2 to 96.1
Protein content of the wheat flour or semolina [g (100 g dry matter)$^{-1}$]	314	0.2	13.2	9.8 to 17.8	11.9	9.8 to 16.6
Protein content of the dough or uncooked pasta [g (100 g dry matter)$^{-1}$]	328	0.4	13.2	4.9 to 17.8	17.3	9.1 to 33.3
Total dietary fiber content of the dough or uncooked pasta [g (100 g dry matter)$^{-1}$]	27	2.4	6.8	2.5 to 11.5	7.0	4.1 to 14.2
Dough properties						
Farinograph dough development time (min)	115	1.2	3.4	1.0 to 6.0	5.0	1.4 to 13.8
Farinograph stability (min)	103	2.7	7.6	1.0 to 18.0	4.5	0.9 to 18.0
Farinograph water absorption [g (100 g dough)$^{-1}$]	129	0.2	58.0	40.9 to 71.0	62.2	50.9 to 104.4
Farinograph mixing tolerance index (FU)	82	2.1	38.4	4.5 to 108	46.0	2 to 130
Gelatinization temperature (°C)	61	0.2	64.5	59.8 to 80.9	64.1	60.2 to 76.2
Wet gluten [g (100 g dough)$^{-1}$]	58	0.6	40.7	31.0 to 50.2	41.5	32 to 49.1
Gluten index (%)	101	0.6	63.0	1 to 98	84.7	47 to 99
Drying properties						
Thickness or diameter of the pasta after extrusion (mm)	41	0.7	2.2	1.6 to 2.6	2.1	1.6 to 2.6
Water content after extrusion [g (100 g dry matter)$^{-1}$]	43	0.5	42.2	35.5 to 47.9	40.6	30.1 to 59.0

Equilibrium water content after drying [g (100 g dry matter)$^{-1}$]	84	1.1	9.5	3.2 to 14.8	9.2	2.6 to 13.8
Water effective diffusion coefficient ($\times 10^{-11}$ m^2 s^{-1})	32	1.5	6.03	3.3 to 9.8	6.5	3.3 to 12.1
Cooking properties						
Optimum cooking time (min)	370	1.3	9.6	3.2 to 15	9.0	3 to 17.7
Cooking losses [g (100 g uncooked pasta)$^{-1}$]	456	1.4	5.8	1.6 to 11.8	6.5	2.2 to 21.6
Weight increase [g (100 g uncooked pasta)$^{-1}$]	324	0.9	177.5	69.2 to 242.4	152.2	70.1 to 240.8
Volume increase (%)	81	2.6	152.6	89.0 to 196.0	156.3	90.0 to 240.8
Color						
L value of uncooked pasta	264	1.2	60.4	33.6 to 87.6	55.7	16.8 to 83.9
a value of uncooked pasta	232	0.3	2.3	−2.2 to 9.6	4.4	−11.1 to 21.5
b value of uncooked pasta	237	0.8	27.6	5.3 to 52.9	25.2	2.0 to 51.4
L value of cooked pasta	94	0.6	66.8	40.0 to 84.6	59.8	30 to 76.8
a value of cooked pasta	67	0.2	−0.5	−3.3 to 2.6	1.2	−10.9 to 10.5
b value of cooked pasta	67	0.6	21.1	8.5 to 32.5	20.4	2.2 to 32.6
Mechanical properties of cooked pasta						
Firmness	321	N/A	N/A	N/A	N/A	N/A
Stickiness	66	N/A	N/A	N/A	N/A	N/A
Elasticity	49	N/A	N/A	N/A	N/A	N/A
Sensory properties						
Overall acceptability	120	N/A	N/A	N/A	N/A	N/A
Appearance	36	N/A	N/A	N/A	N/A	N/A
Flavor	42	N/A	N/A	N/A	N/A	N/A
Texture	22	N/A	N/A	N/A	N/A	N/A

Note: The average values of the continuous quality attributes were calculated for traditional pasta and enriched pasta using an unweighted model. The relative error is the ratio of the average standard deviation of the measurements to the average value of the quality attribute. N/A: not applicable

7.3. Analysis methods

7.3.1 Differences with control pasta

The impact of enrichment on a quality attribute X of pasta was quantified by calculating differences with the control pasta (Figure 7.2). In a study i, the quality attribute X for observation j is estimated by performing n replicate measurements of this quality attribute. In a meta-analysis, statistical methods are applied on the average value of the n replicate measurements, X_{ij}, because the value of each individual measurement is unknown (Figure 7.2). Differences with the control pasta indicated the change in the quality attribute with enrichment and were calculated as follows:

$$M_{ij} = X_{ij} - X_{ic}, \tag{7.1}$$

where X_{ic} is the average measurement for the control pasta in study i, and M_{ij} is the difference with the control pasta for observation j in study i. The control pasta was taken as the pasta with the lowest enrichment level made at the same process specifications and in the same study.

The differences with the control pasta were pooled across studies using an unweighted model, because results similar to those of a random effects model were obtained (Annexe D). Pooling of the differences with the control pasta was accomplished as follows:

$$\overline{M} = \frac{\sum_{i=1}^{p}\sum_{j=1}^{q} M_{ij}}{|pq|}, \tag{7.2}$$

where $\overline{M}$ is the pooled difference with the control pasta, p is the number of studies in the dataset, q is the number of observations in a given study, and $|pq|$ is the number of differences with the control pasta (M_{ij}) calculated from the dataset (Figure 7.2). The standard error of the pooled difference with the control pasta ($\overline{SE}_M$) is as follows:

$$\overline{SE}_M = \sqrt{\frac{\sum_{i=1}^{p}\sum_{j=1}^{q}\left(M_{ij}-\overline{M}\right)^2}{|pq|(|pq|-1)}} \tag{7.3}$$

The 95% confidence interval (CI) of the pooled difference with the control pasta ($\bar{M}$) was calculated considering a normal distribution, as follows:

$$CI = \{\bar{M} \pm 1.96\overline{SE}_M\} \quad (7.4)$$

The pooled difference with the control pasta ($\bar{M}$) was considered significant if its 95% confidence interval excluded the null value.

Pooled differences with the control pasta ($\bar{M}$) were first calculated considering all the observations in the dataset. Pooled differences with the control pasta different from the null value according to their 95% confidence interval (Equation 7.4) indicated that enrichment had a significant impact on the quality attribute considered. In that case, pooled differences with the control pasta were calculated separately for the set of observations enriched with pulse flour or enriched with high-fiber ingredients. These 2 groups of ingredients were the most frequent enrichment types used in the studies. Comparison of the pooled differences with the control pasta for these 2 types of enrichment provided their general impact on the quality attributes of pasta. The ingredients classified as high in fiber are barley β-glucan, carboxymethyl cellulose, guar gum, inulin, pea fiber, and resistant starch. The ingredients classified as pulse flours are Bengal gram, black gram, broad bean, chickpea, faba bean, green gram, lentil, lupin, Mexican common bean, soybean, split pea, and yellow pea flours. Pooled differences with the control pasta were also calculated separately for the set of observations with low (<15%) and high (≥15%) enrichment levels and drying at low (≤60 °C) and high (>60 °C) temperatures, in order to determine if the significant impact of enrichment on the given quality attribute could be attributed to specific enrichment levels or drying temperatures.

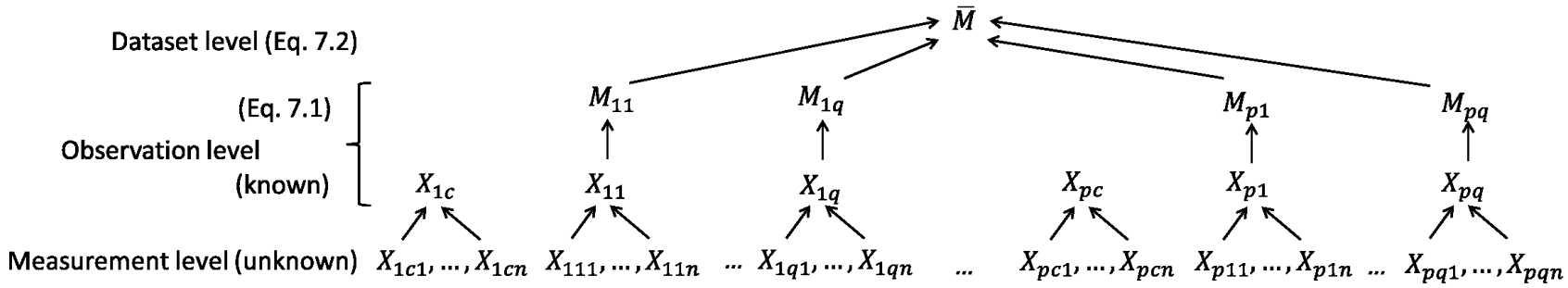

Figure 7.2. Algorithm for the calculation of the pooled difference with the control pasta ($\bar{\boldsymbol{M}}$) for a quality attribute *X*.

7.3.2 Pearson correlation coefficients

The level of association between 2 quality attributes or a process specification and a quality attribute were quantified using Pearson correlation coefficients (r) (Figure 7.3). Pearson correlation coefficients are restricted to the range $-1 < r < 1$. Positive Pearson correlation coefficients between quality attributes or process specifications X and Y indicate that an observation with a higher than average value for X will tend to have a higher than average value for Y. Negative Pearson correlation coefficients indicate that an observation with a higher than average value for X will tend to have a lower than average value for Y.

Pearson correlation coefficients were calculated for each study (Figure 7.3). Calculation at the study level provided an internal standardization which enabled consideration of the mechanical properties and sensory properties, quality attributes that were included "as is" in the dataset, because methodologies for these quality attributes were consistent within each study. Pearson correlation coefficients were calculated as follows:

$$r_i = \frac{1}{q-1}\frac{\sum_{j=1}^{q}[(X_{ij}-X_i)(Y_{ij}-Y_i)]}{\sigma_{X_i}\sigma_{Y_i}}, \tag{7.5}$$

where X_i and Y_i are the arithmetic averages of X and Y over the q observations in study i, and σ_{X_i} and σ_{Y_i} are the standard deviations, which were calculated as follows:

$$\sigma_{X_i} = \sqrt{\frac{1}{q-1}\sum_{j=1}^{q}\left(X_{ij} - X_i\right)^2} \tag{7.6}$$

$$\sigma_{Y_i} = \sqrt{\frac{1}{q-1}\sum_{j=1}^{q}\left(Y_{ij} - Y_i\right)^2} \tag{7.7}$$

Given that the Pearson correlation coefficient is restricted to the interval $-1 < r < 1$, it needs to be normalized before its confidence interval can be estimated from the normal distribution. Standardization of the Pearson correlation coefficient was accomplished using a Fisher transformation (Card 2012), as follows:

$$Z_i = 0.5\ln\left(\frac{1+r_i}{1-r_i}\right), \tag{7.8}$$

where Z_i is the Fisher transform of the Pearson correlation coefficient. The standard error of the Fisher transform of the Pearson correlation coefficient (SE_{Z_i}) is calculated as follows (Card 2012):

$$SE_{Z_i} = \frac{1}{\sqrt{q-3}} \tag{7.9}$$

To avoid division by 0 in Equation 7.9, Pearson correlation coefficients were calculated for studies with a minimum of 4 observations.

The Fisher transform of the Pearson correlation coefficients were pooled across studies using a random effects model. The Fisher transform of the Pearson correlation coefficients were weighted according to the within-study and between-study variance. The within-study variance, describing the sum of the sampling and measurement error, is equal to $1/SE_{Z_i}^2$ (Higgins and Thompson 2002). The between-study variance, describing the variance caused by differences in process specifications, was calculated with the DerSimonian and Laird estimator. This estimator is based on the *Q*-statistic calculated with a weighted error sum of squares (DerSimonian and Laird 1986), as follows:

$$Q = \sum_{i=1}^{p} \frac{(Z_i - \bar{Z}_{FEM})^2}{SE_{Z_i}^2}, \tag{7.10}$$

where $\bar{Z}_{FEM}$ is a pooled Fisher transform of the Pearson correlation coefficient calculated with a fixed effects model, that is, without considering the between-study variance (DerSimonian and Laird 1986), as follows:

$$\bar{Z}_{FEM} = \sum_{i=1}^{p} \frac{\frac{1}{SE_{Z_i}^2} Z_i}{\frac{1}{SE_{Z_i}^2}} \tag{7.11}$$

The between-study variance (τ^2) was calculated from the number of degrees of freedom (*df*) of the random effects model (DerSimonian and Laird, 1986), as follows:

$$\tau^2 = \begin{cases} \frac{Q-df}{c}, \text{if } Q > df \\ 0, \quad \text{if } Q < df \end{cases}, \tag{7.12}$$

where $c = \sum_{i=1}^{p} \frac{1}{SE_{Z_i}^2} - \frac{\sum_{i=1}^{p}\left(\frac{1}{SE_{Z_i}^2}\right)^2}{\sum_{i=1}^{p}\frac{1}{SE_{Z_i}^2}}$. The number of degrees of freedom *df* is equal to the number Z_i minus 1. The pooled Fisher transform of the Pearson correlation coefficient and its standard error were calculated from a weighted average considering both the within-study and between-study variance (Sánchez-Meca and Marín-Martínez 2010), as follows:

$$\bar{Z} = \frac{\sum_{i=1}^{p}\left[\frac{1}{SE_{Z_i}^2+\tau^2}Z_i\right]}{\sum_{i=1}^{p}\frac{1}{SE_{Z_i}^2+\tau^2}} \tag{7.13}$$

$$\overline{SE}_Z = \sqrt{\frac{1}{\sum_{i=1}^{p}\frac{1}{SE_{Z_i}^2+\tau^2}}} \tag{7.14}$$

The 95% confidence interval (*CI*) of $\bar{Z}$ was calculated using Equation 7.4 with $\bar{M}$ replaced by $\bar{Z}$ and $\overline{SE}_M$ replaced by $\overline{SE}_Z$. The pooled Fisher transform of the Pearson correlation coefficient was transformed back to a Pearson correlation coefficient using an inverse Fisher transformation, as follows:

$$\bar{r} = \frac{\exp(2\bar{Z})-1}{\exp(2\bar{Z})+1} \tag{7.15}$$

The pooled Pearson correlation coefficient ($\bar{r}$) was considered significant if its 95% confidence interval excluded the null value.

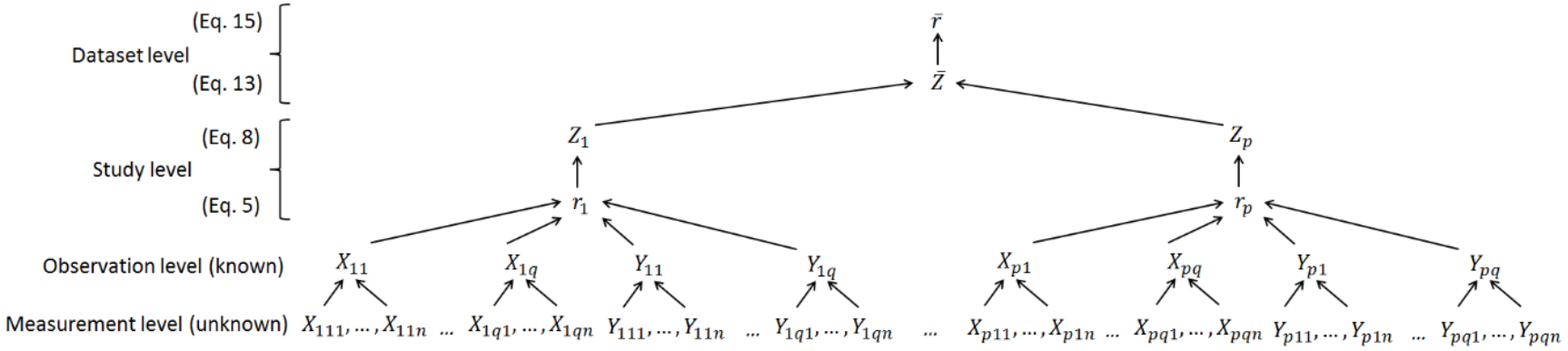

Figure 7.3. Algorithm for the calculation of the pooled Pearson correlation coefficient ($\bar{\boldsymbol{r}}$) between 2 quality attributes *X* and *Y* or a process specification *X* and a quality attribute *Y*

7.4. Impact of enrichment and process specifications on the quality attributes of pasta

The quantification of pooled differences with the control pasta (Equation 7.2) and Pearson correlation coefficients (Equation 7.15) were used to extract and summarize the impact of enrichment and process specifications on pasta quality attributes. These features are discussed in the following sections for the 7 categories of quality attributes considered for the meta-analysis (Figure 7.1).

7.4.1 Proximate composition

The enrichment level for the studies included in the dataset ranged from 0.25% to 50% (Table 7.2). The enrichment level was below 30% for 90% of the studies. The lowest enrichment level (below 2%) was used with microalgae biomass (Fradique and others 2010, 2013), and the highest enrichment levels were used with resistant starch (Aravind and others 2013), chickpea flour (Sabanis and others 2006), buckwheat flour (Chillo and others 2008), banana flour (Agama-Acevedo and others 2009), and soy flour (Baiano and others 2011a).

Enrichment affects the protein and fiber content of pasta. Pasta with a protein content as high as 33.3 g (100 g dry matter)$^{-1}$ was obtained with 50% enrichment with peanut flour (Howard and others 2011), and a total dietary fiber content of 14.2 g (100 g dry matter)$^{-1}$ was obtained with 30% enrichment with wheat bran (Aravind and others 2012a). It is worth noting that the protein content [4.9 to 17.8 g (100 g dry matter)$^{-1}$] and total dietary fiber content [2.5 to 11.5 g (100 g dry matter)$^{-1}$] varied significantly among traditional pasta products in the studies (Table 7.3). This variability may be attributed to differences between durum wheat cultivars and agricultural conditions (AbuHammad and others 2012).

Enrichment of pasta with pulse flour increased the protein content by an average of 1.8 ± 0.5 g (100 g dry matter)$^{-1}$ [where 1.8 g (100 g dry pasta)$^{-1}$ denotes the pooled difference with the control pasta $\bar{M}$ (Equation 7.2), and 0.5 g (100 g dry pasta)$^{-1}$ represents its 95% confidence interval (Equation 7.4)] for enrichment levels below 15% and by an average of 4.0 ± 1.0 g (100 g dry matter)$^{-1}$ for higher enrichment levels. Enrichment with high-fiber

ingredients reduced the protein content of pasta by an average of 1.8 ± 0.8 g (100 g dry pasta)$^{-1}$, which can be attributed to gluten dilution.

7.4.2 Dough properties

Dough development time, which is the time required for the formation of the gluten network after water addition, increased by an average of 1.28 ± 0.81 min for enriched pasta compared to traditional pasta. The longer development time could be attributed to physical disruptions of the gluten network that occurred because enrichment slowed down the reorganization of the glutenin subunits as well as to competition for water between the enrichment ingredient and the gluten (Alireza Sadeghi and Bhagya 2008; Wood 2009). An exception was the addition of broad bean flour at 20% and 30% (Giménez and others 2012), which decreased the dough development time. The authors suggested that, at such high enrichment levels, the lower gluten content reduced the time required for the formation of the gluten network (Giménez and others 2012).

The Farinograph stability, which represents the time during which the dough preserves its consistency under shear stress, was on average not affected by enrichment ($\overline{M} = -0.26 \pm 0.87$ min). The Farinograph stability was correlated to the protein content of the wheat flour or semolina ($\bar{r} = 0.57$) and the protein content of the pasta ($\bar{r} = 0.99$). The positive Pearson correlation coefficients indicate that the gluten network in pasta with a higher protein content is stronger and has higher resistance to shear stress.

Enrichment increased the Farinograph water absorption, which is the amount of water required to develop dough with a consistency of 500 Fagrinograph units (FU), by an average of 4.7 ± 2.5 g (100 g dough)$^{-1}$. Enrichment generally increases the nongluten protein content of the pasta. The nongluten protein content may compete with gluten for water during mixing, which would increase the water required for the development of the gluten network.

The mixing tolerance index, which represents the decrease in dough consistency under shear stress 4 min after dough development time, was on average 16 ± 14 FU higher for

enriched pasta. The higher mixing tolerance index of enriched pasta indicates its sensitivity to shear stress and reflects the weaker gluten network with enrichment.

Enrichment of pasta with pulse flour increased the gluten index (ratio of strong gluten to total gluten) by an average of 7.4 ± 1.6%, whereas the impact of fiber enrichment was not significant. The higher gluten index caused by pulse flour enrichment suggests that components of pulse flour were physically trapped in the gluten network, increasing the mass of dough retained by the screen during the Glutomatic test. The gluten index was positively correlated ($\bar{r}$ = 0.56) with the Farinograph water absorption. The positive correlation may be explained by the plasticizing effect of water during mixing, which increases the amount of water required for dough with a high gluten index to reach the desired consistency (AbuHammad and others 2012). The gluten index was also significantly correlated to the dough development time ($\bar{r}$ = 0.85) and the Farinograph stability ($\bar{r}$ = 0.62), suggesting that the gluten index could be a good indicator of the Farinograph characteristics of the dough.

Enrichment of the pasta with high-fiber ingredients increased the gelatinization temperature by an average of 0.7 ± 0.3 °C. Enrichment with other ingredients did not have a significant impact on the gelatinization temperature. The higher gelatinization temperature for pasta with high-fiber ingredients could reflect modifications of the polysaccharide characteristics (Aggarwal and Dollimore 1998; Shreenithee and Prabhasankar 2013). The soluble nonstarch polysaccharides could also compete with the starch for water and limit starch swelling and gelatinization events, increasing the gelatinization temperature (Tudorica and others 2002).

7.4.3 Drying properties

The water content of pasta after extrusion was on average not affected by enrichment [$\bar{M}$ = −0.32 ± 2.04 g (100 g dry matter)$^{-1}$]. A closer look at the studies revealed a balanced number of studies where hydration of the dough was higher in the enriched pasta than in the control pasta, in order to compensate for the high water-absorption capacity of the enrichment ingredient, as well as studies where the hydration of the dough was lower, in order to reduce

dough stickiness and facilitate extrusion (Yalla and Manthey 2006; Wood 2009; Jayasena and Nasar-Abbas 2012).

The equilibrium water contents of enriched pasta and control pasta were on average not significantly different [$\overline{M} = -0.24 \pm 0.36$ g (100 g dry matter)$^{-1}$]. However, the equilibrium water content was negatively correlated to the drying temperature ($\bar{r} = -0.91$), because high temperature shifts the equilibrium conditions of water towards water vapor.

Enrichment increased the diameter or thickness of pasta after drying by an average of 0.02 ± 0.01 mm for drying temperatures above 60 °C. The effect of enrichment on the diameter or thickness of the pasta was not significant for drying temperatures below 60 °C. The increase in the diameter or thickness could be caused by disruptions of the gluten matrix by the enrichment ingredient. These disruptions could be more significant for drying at high temperatures because of the denser microstructure of that pasta compared to pasta dried at lower temperatures (Zweifel and others 2003).

Enrichment increased the water effective diffusion coefficient during the drying of pasta by an average of $0.68 \pm 0.34 \times 10^{-11}$ m^2 s^{-1}. The higher water effective diffusion coefficient may reflect physical disruptions of the gluten network by the enrichment ingredient, increasing the porosity (Villeneuve and others 2013). The higher porosity increases the space available for water evaporation in the pasta and the transport of water vapor by diffusion, which is a faster mass transfer mechanism than liquid water transport by capillarity is (Mercier and others 2014a). The pooled difference with the control pasta for the water effective diffusion coefficient was higher for drying at temperatures above 60 °C ($1.08 \pm 0.51 \times 10^{-11}$ m^2 s^{-1}) than for drying at lower temperatures ($0.28 \pm 0.29 \times 10^{-11}$ m^2 s^{-1}). The more significant impact of enrichment at high temperatures could be due to the higher rates of water evaporation. The higher water effective diffusion coefficient of enriched pasta indicates that enrichment decreases the drying time required to obtain pasta with the desired water content. The water effective diffusion coefficient was significantly correlated to the drying temperature ($\bar{r} = 0.91$) because, as for the impact of porosity, high temperatures promote the evaporation of liquid water and also the transport of water vapor by diffusion (Mercier and others 2014a).

7.4.4 Cooking properties

Cooking properties were reported in at least half of the studies considered in the meta-analysis (Table 7.3). The pooled differences with the control pasta for the cooking properties (Equation 7.2) according to enrichment level (below or above 15%), type of enrichment (pulse flour or high-fiber ingredients), and drying temperature (below or above 60 °C) are presented in Table 7.4. Enrichment decreased the optimum cooking time by an average of 0.42 min compared to the control pasta. A lower optimum cooking time could be caused by modifications to the chemical composition and microstructure of the pasta when enrichment is present. Enrichment dilutes the starch content of the pasta, which could reduce the amount of water needed for starch gelatinization. Enrichment could also reduce the glutenin content and increase the content of lower-molecular-weight compounds that take less time to hydrate (Vernaza and others 2012). Alternatively, enrichment could induce physical disruptions of the gluten network, facilitating water penetration (Chillo and others 2008; Petitot and others 2010), and could modify the pasta's heat capacity, thereby affecting the rate of temperature increase during cooking (de la Peña and Manthey 2014). An exception was enrichment with shrimp meat or microalgae, for which the cooking time increased by an average of 1.02 min (Fradique and others 2010, 2013; Kadam and Prabhasankar 2012). The highest increase in the optimum cooking time, 3 min, was for pasta enriched with 2% *Chlorella vulgaris* microalgae (Fradique and others 2010). The authors suggested that, because starch is the major storage product in *Chlorella vulgaris*, its incorporation in pasta could have increased the amount of water and the time required for starch gelatinization during cooking (Fradique and others 2010). The impact of enrichment on the optimum cooking time was not affected by the enrichment level (below or above 15%) or the drying temperature (below or above 60 °C). The optimum cooking time was similar for pasta enriched with pulse flour and pasta enriched with high-fiber ingredients.

Table 7.4. Pooled differences with the control pasta (Equation 7.2) for the cooking properties according to enrichment type and level and drying temperature.

Process specification	Optimum cooking	Cooking losses [g (100 g	Weight increase [g (100 g	Volume increase

	time (min)	uncooked pasta)$^{-1}$]	uncooked pasta)$^{-1}$]	(%)
Complete dataset				
All enrichment levels	−0.42abcd*	0.81bcd*	−1.2bc	−0.8acde
Enrichment < 15%	−0.36abc*	0.51bd*	3.9ab*	1.4abcd
Enrichment ≥ 15%	−0.47bcd*	1.09ac*	−10.1def*	−3.8abcde
Enrichment with pulse flour				
All enrichment levels	−0.41abcd*	1.40abc*	2.8abc	8.4ab*
Enrichment < 15%	−0.89abcd*	1.12abc*	13.6a*	7abc*
Enrichment ≥ 15%	−0.06a	1.60a*	−9.8cdef	10.2a*
Enrichment with high-fiber ingredients				
All enrichment levels	−0.73cd*	0.71bcd*	−4.2cde*	−10.2de*
Enrichment < 15%	−0.46abcd*	0.59bcd*	−2.9cd*	−4.6abcde
Enrichment ≥ 15%	−1.46d*	0.98abcd*	−7.0cdef*	−23f*
Dried at T ≤ 60 °C				
All enrichment levels	−0.62abcd*	0.97abcd*	7.5ab*	9.5a*
Enrichment < 15%	−0.91abcd*	0.97abcd*	14.1a*	8.5a*
Enrichment ≥ 15%	−0.15abc	0.97abcd*	−5.2abcdef	11.5a*
Dried at T > 60 °C				
All enrichment levels	−0.38abc*	0.86abcd*	−9.2ef*	−8.1de*
Enrichment < 15%	−0.14ad	0.41d*	−5.1cde*	−5.9ade
Enrichment ≥ 15%	−0.53bcd*	1.10ac*	−13.4f*	−11.4ef*

Note: Pooled differences with the control pasta that share a common letter in the same column are not significantly different. Pooled differences with the control pasta that are marked with an asterisk (*) are significantly different from the null value

Cooking losses are recognized as an important property for consumer acceptance, presumably because cooking losses are associated with the leakage of amylose from the starch granules, which results in an unpleasant sticky texture (Sissons and others 2005; Islas-Rubio and others 2014). Enrichment increased cooking losses by an average of 0.8 g (100 g uncooked pasta)$^{-1}$, corresponding to an increase of 14% compared to the average cooking losses for traditional pasta (Table 7.3). Higher cooking losses are generally related to the dilution and the weakening of the gluten network caused by enrichment (Gallegos-Infante and others 2010; Petitot and others 2010; Villeneuve and others 2013). Cooking losses were on average similar for pasta enriched with pulse flour and pasta enriched with high-fiber ingredients (Table 7.4). The impact of fiber enrichment was ingredient specific. Enrichment with inulin resulted in a significant increase in cooking losses [by an average of 1.8 ± 0.3 g (100 g uncooked pasta)$^{-1}$], but enrichment with other high-fiber ingredients, including β-glucan, guar gum, and resistant starch, either had no effect or reduced the cooking losses of pasta (Tudorică and others 2002; Brennan and others 2004; Manno and others 2009; Aravind and others 2012b, 2012d, 2013). These conflicting effects on cooking losses for pasta enriched with high-fiber ingredients may reflect the dual effect that fibers exert on cooking losses. On one hand, fibers are believed to have a corrective effect on the microstructure, presumably through active participation in the development of the matrix or through physical entanglement (Koca and Anil 2007; Sabanis and Tzia 2010; Mert and others 2014). On the other hand, fibers dilute the gluten content and possess a high water-absorption capacity, which could inhibit the proper development of the gluten network if the amount of water is insufficient (Sivam and others 2010). The average increase in cooking losses for enrichment below 15% was doubled with drying at low temperatures (≤60 °C) compared to drying at high temperatures (>60 °C) (Table 7.4). The impact of the drying temperature could be explained by the strengthening of the gluten network as a result of protein coagulation, which would reduce water penetration and prevent the rupture of starch granules (Zweifel and others 2003). The lower cooking losses indicate that high drying temperatures may be more appropriate for the production of enriched pasta, assuming that the enrichment ingredient is not sensitive to thermal degradation and remains bioavailable after processing. The average increase in cooking losses was higher for dried pasta [0.90 ± 0.09 g (100 g uncooked pasta)$^{-1}$ than for fresh pasta [0.28 ± 0.20 g (100 g uncooked pasta)$^{-1}$]. The higher average increase in cooking

losses for dried pasta may be attributed to their longer cooking time and suggests that fresh pasta may be an appropriate product format for enriched pasta. Furthermore, pasta cooking losses showed a significant negative correlation to the water content after extrusion ($\bar{r} = -0.73$). Stronger dough with low cooking losses generally requires more water to obtain the proper consistency for extrusion, explaining the negative correlation (AbuHammad and others 2012). The optimum cooking time ($\bar{r} = -0.67$) and cooking losses ($\bar{r} = 0.52$) were significantly correlated to the gelatinization temperature. These significant correlations indicate that the gelatinization temperature could be a good predictor of pasta cooking properties, an expected result considering that modification of the starch structure is a critical change that occurs during pasta cooking.

Enrichment reduced the weight increase during cooking for pasta with a high enrichment level (≥15%) regardless of the drying temperature and for pasta with a low enrichment level (<15%) dried at high temperature (>60 °C). The lower weight increase during cooking could reflect the dilution of the starch content in the pasta. In contrast, a higher weight increase during cooking was observed for pasta with a low enrichment level (<15%) and dried at low temperature (≤60 °C) (Table 7.4). The higher weight increase during cooking for enriched pasta with these process specifications could reflect the weakening effect of enrichment and a low drying temperature on the pasta gluten network, which could facilitate water penetration and starch swelling and increase the amount of water absorbed during cooking despite the dilution of the starch content (Zweifel and others 2003). The weight increase during cooking was higher for pasta enriched with pulse flour at a low enrichment level (<15%) than for pasta enriched with high-fiber ingredients (Table 7.4). The lower weight increase for pasta enriched with high-fiber ingredients could be explained by the entrapment of semolina starch granules by the fiber particles, reducing the swelling of the starch granules during cooking (Steglich and others 2014). The weight increase during cooking showed a significant negative correlation to the Farinograph water absorption ($\bar{r} = -0.72$), indicating that pasta generally absorbs less water during cooking if more water is required to increase the consistency of the dough in the Farinograph method. The negative correlation may reflect the effect of enrichment, which generally increases the nongluten protein content while decreasing the starch content. The nongluten protein may compete with gluten for water during mixing, which would increase the water required for the development of the gluten network. However,

starch dilution can decrease the amount of water required for gelatinization and thus reduce the amount of water absorbed during cooking. The weight increase during cooking was significantly correlated to the Farinograph mixing tolerance index ($\bar{r} = 0.68$), which could reflect the weaker gluten network of pasta with a high mixing tolerance index and its lower resistance to water penetration during cooking. The weight increase during cooking was significantly correlated to the pasta equilibrium water content ($\bar{r} = 0.97$), indicating that the capacity of the pasta to absorb water during cooking is proportional to the amount of water retained by the pasta at the end of drying.

The impact of enrichment on the volume increase of pasta during cooking was similar to the impact on the weight increase (Table 7.4). Enrichment decreased the volume of pasta after cooking for pasta enriched with high-fiber ingredients or dried at a high temperature (>60 °C), whereas the volume after cooking increased for pasta enriched with pulse flour or dried at a low temperature (≤60 °C). The correlation between the weight increase and the volume increase during cooking was significant ($\bar{r} = 0.84$), such that one may consider measuring only 1 of these 2 properties for characterization purposes.

7.4.5 Color

The color of pasta, given as *a* value (greenness to redness), *b* value (blueness to yellowness), and *L* value (brightness), was measured in nearly half of the studies. Color is an important quality characteristic of pasta, because this property can be evaluated directly by consumers at the time of purchase (Carini and others 2009). The majority (75%) of the color measurements were performed on uncooked pasta, but it remains unclear whether the color of the pasta before or after cooking has the most significant impact on consumer perception of the pasta.

Enrichment decreased the brightness (*L* value) of uncooked pasta by an average of 7.8 (Table 7.5). The lower brightness of uncooked pasta with enrichment can be viewed as a negative quality attribute, because consumers generally expect pasta with a bright and yellow color (Debbouz and others 1995). The lower brightness with enrichment can be attributed to the dark color of most enrichment ingredients, the nonenzymatic browning of the reducing

sugars in the enrichment ingredient, and the oxidation of carotenoid pigments resulting from the high oxygen permeability of enriched pasta (Marconi and others 2002; Alireza Sadeghi and Bhagya 2008; Carini and others 2009). The lower brightness of uncooked pasta was significant for all enrichment ingredients except those high in fiber (Table 7.5), which reflects the bright color of high-fiber ingredients such as resistant starch (Aravind and others 2013). The brightness of uncooked pasta with enrichment was affected less when the pasta had been dried at a high temperature (>60 °C), presumably because the darker color, caused by Maillard reactions, partially masked the impact of enrichment on pasta appearance.

Table 7.5. Pooled differences with the control pasta (Equation 7.2) for the color of uncooked pasta according to enrichment type and level and drying temperature.

Process specification	***L* value**	***a* value**	***b* value**
Complete dataset			
All enrichment levels	−7.8c*	2.3abc*	−3.7cd*
Enrichment < 15%	−7.6c*	1.0cde*	−2.0abc*
Enrichment ≥ 15%	−7.9c*	3.0a*	−4.8cd*
Enrichment with pulse flour			
All enrichment levels	−2.4a*	2.4ab*	0.5abc
Enrichment < 15%	−2.7a*	1.6bcd*	−0.9abc
Enrichment ≥ 15%	−2.3a*	2.7ab*	1.0ab
Enrichment with high-fiber ingredients			
All enrichment levels	−1.4a	0.4de	−3.6bcd*
Enrichment < 15%	−0.6a	0.3e	0.0ab
Enrichment ≥ 15%	−2.7abc	0.5bcde	−9.2d*
Dried at T ≤ 60 °C			
All enrichment levels	−9.0c*	2.0abc*	−5.6cd*
Enrichment < 15%	−9.3c*	2.0abc*	−4.2bcd*
Enrichment ≥ 15%	−8.8c*	2.0abc*	−6.5cd*
Dried at T > 60 °C			
All enrichment levels	−6.1bc*	2.6ab*	−2.2abc
Enrichment < 15%	−3.2ab*	1.0cde*	1.4a
Enrichment ≥ 15%	−7.3c*	3.5a*	−4.0bcd*

Note: Pooled differences with the control pasta that share a common letter in the same column are not significantly different. Pooled differences with the control pasta that are marked with an asterisk (*) are significantly different from the null value

Enrichment increased the redness (*a* value) of uncooked pasta by an average of 2.3 (Table 7.5). The impact of enrichment on the redness of uncooked pasta was about 3 times greater for enrichment at a high level (≥15%) than for enrichment at a low level (<15%). Like the brightness attribute (*L* value), the redness (*a* value) of uncooked pasta was higher for all enrichment ingredients except those high in fiber.

Enrichment decreased the yellowness (*b* value) of uncooked pasta by an average of 3.7 (Table 7.5). Contrary to the brightness (*L* value) and redness (*a* value) attributes, the impact of enrichment with high-fiber ingredients on the yellowness of uncooked pasta was greater than the impact of enrichment with pulse flour, especially at high enrichment levels (≥15%). For low enrichment levels (<15%), the difference in yellowness between enriched pasta and control pasta was more significant for fresh pasta (−6.7 ± 2.8) than for dried pasta (−1.2 ± 1.9), presumably because of the darker color of dried pasta compared to fresh pasta. Accordingly, the reduction in pasta yellowness was greater for pasta dried at a low temperature (≤60 °C) than for pasta dried at a temperature above 60 °C (Table 7.5).

The brightness, redness, and yellowness of uncooked pasta were significantly correlated ($\bar{r}$ >0.75) to the brightness, redness, and yellowness of cooked pasta, indicating that the color of cooked pasta can be predicted accurately from the color of pasta before cooking. Nevertheless, the color of pasta was affected significantly by the cooking operation. Cooking increased the *L* value of pasta by an average of 3.0 ± 2.2, decreased the *a* value by an average of 3.4 ± 0.6, and decreased the *b* value by an average of 8.7 ± 2.0. The impact of cooking on pasta color could be attributed to the higher water content of cooked pasta and the degradation or leaching of color pigments in the cooking water (Zouari and others 2011; Jayasena and Nasar-Abbas 2012).

7.4.6 Mechanical properties

Mechanical properties reported in the studies were based on a wide range of measurement methods and settings, when that information was provided. Such a lack of consistency made it difficult to standardize these properties using a single unit or scale. Consequently, the reported values could not be compared directly between studies, and no

average or range was calculated (Table 7.3). The impact of enrichment on the mechanical properties could not be analyzed using pooled differences with the control pasta (section 7.3.1). Nevertheless, pooling of the Fisher transforms of the Pearson correlation coefficients (section 7.3.2) was performed, because Pearson correlation coefficients were calculated at the study level (Equations 7.5–7.7), and the measurement methodology was consistent within each study.

The mechanical properties were significantly correlated to the dough Farinograph properties. Indeed, the firmness of cooked pasta was correlated to the Farinograph stability ($\bar{r} = 0.42$) and the mixing tolerance index ($\bar{r} = -0.77$), whereas the stickiness was correlated to the dough development time ($\bar{r} = -0.91$), indicating that dough Farinograph properties are good indicators of pasta mechanical properties. The stickiness of the dough showed a significant negative correlation to the protein content of the dough ($\bar{r} = -0.86$). Considering that dried pasta consists of starch granules embedded in a protein network (Zweifel and others 2003), a low protein content could increase water penetration and starch swelling during cooking, causing leakage of amylose molecules and increasing pasta stickiness (Petitot and others 2010). The elasticity showed a significant correlation to the optimum cooking time ($\bar{r} = 0.52$). Enrichment decreased the optimum cooking time (Table 7.4) and elasticity of pasta by disrupting the gluten network and limiting the pasta's stretching ability, reflecting the positive correlation between elasticity and optimum cooking time (Tudorică and others 2002).

7.4.7 Sensory properties

The sensory properties of the pasta, namely, overall quality, appearance, flavor, and texture, that were compiled in the dataset are presented in Table 7.6. A wide range of methodologies were used with respect to hedonic scale and number as well as panelist training, age, origin, and recruitment. Consequently, the sensory properties across the studies could not be directly compared, and no average or range was calculated for these quality attributes (Table 7.3). Nevertheless, as for the mechanical properties (section 7.4.6), sensory evaluation methodologies were consistent within a given study, such that the impact of

enrichment on the sensory properties could be evaluated using Pearson correlation coefficients (section 7.3.2).

Table 7.6. Sensory properties of pasta according to the enrichment ingredient and level compiled in the dataset

Enrichment ingredient (level)	Sensory properties				Reference
	Overall	Appearance	Flavor	Texture	
None	4.37/9	-	-	-	Agama-Acevedo and others (2009)
Unripe banana flour (15%)	4.8/9	-	-	-	
Unripe banana flour (30%)	4.42/9	-	-	-	
Unripe banana flour (45%)	4.56/9	-	-	-	
Spinach green leaf flour (20%)	3.85/5	3.62/5	3.74/5	3.52/9	Borneo and Aguirre (2008)
Dried amaranth leaf flour (20%)	3.45/5	3.31/5	3.66/5	3.05/9	
Oregano leaf meal (5%) and carrot leaf meal (5%)	-	6.0/9	6.0/9	6.2/9	Boroski and others (2011)
Carrot leaf meal (10%)	-	6.0/9	6.0/9	5.9/9	
Oregano leaf meal (10%)	-	5.5/9	5.1/9	6.7/9	
Oregano leaf meal (10%) and carrot leaf meal (10%)	-	4.4/9	4.5/9	5.9/9	
None	7.9/9	-	-	-	Bustos and others (2011)
Resistant starch (10%)	7.0/9	-	-	-	
Resistant starch (10%)	6.7/9	-	-	-	
Oat bran (10%)	4.8/9	-	-	-	
None	7.3/9	8.0/9	7.5/9	-	Chillo and others (2008)
Buckwheat flour (10%) and wheat bran (10%)	7.0/9	7.0/9	7.0/9	-	
Buckwheat flour (10%) and wheat bran (15%)	7.1/9	7.0/9	6.5/9	-	
Buckwheat flour (10%) and wheat bran (20%)	7.0/9	7.0/9	6.5/9	-	
Buckwheat flour (20%) and wheat bran (10%)	7.0/9	7.0/9	7.0/9	-	

Buckwheat flour (20%) and wheat bran (15%)	6.7/9	6.5/9	6.0/9	-	
Buckwheat flour (20%) and wheat bran (20%)	6.9/9	6.5/9	6.0/9	-	
Buckwheat flour (30%) and wheat bran (10%)	7.3/9	7.0/9	7.0/9	-	
Buckwheat flour (30%) and wheat bran (15%)	7.3/9	7.0/9	7.0/9	-	
Buckwheat flour (30%) and wheat bran (20%)	7.4/9	8.0/9	7.0/9	-	
Peanut flour (30%)	5.7/9	-	-	-	Howard and others (2011)
Peanut flour (30%)	6.6/9	-	-	-	
Peanut flour (30%)	7.2/9	-	-	-	
Peanut flour (40%)	6.1/9	-	-	-	
Peanut flour (40%)	5.7/9	-	-	-	
Peanut flour (40%)	5.9/9	-	-	-	
Peanut flour (50%)	4.9/9	-	-	-	
Peanut flour (50%)	4.6/9	-	-	-	
Peanut flour (50%)	6.0/9	-	-	-	
None	7.5/9	7.0/9	7.4/9	7.2/9	Jayasena and Nasar-Abbas (2012)
Lupin flour (10%)	7.2/9	6.7/9	7.0/9	7.0/9	
Lupin flour (20%)	6.7/9	6.5/9	6.2/9	6.0/9	
Lupin flour (30%)	5.7/9	5.6/9	5.5/9	5.3/9	
Lupin flour (40%)	5.0/9	5.6/9	4.7/9	4.8/9	
Lupin flour (50%)	4.8/9	5.1/9	4.5/9	4.3/9	
None	8.6/9	8.7/9	-	-	Kadam and Prabhasankar (2012)
Shrimp meat (10%)	8.2/9	8.2/9	-	-	
Shrimp meat (20%)	8.3/9	8.3/9	-	-	
Shrimp meat (30%)	7.3/9	7.9/9	-	-	

None	7.6/9	-	-	-	Kaur and others (2012)
Wheat bran (5%)	7.4/9	-	-	-	
Wheat bran (10%)	7.3/9	-	-	-	
Wheat bran (15%)	7.1/9	-	-	-	
Wheat bran (20%)	6.4/9	-	-	-	
Wheat bran (25%)	4.6/9	-	-	-	
None	8.1/9	-	-	-	
Rice bran (5%)	7.5/9	-	-	-	
Rice bran (10%)	7.6/9	-	-	-	
Rice bran (15%)	7.7/9	-	-	-	
Rice bran (20%)	6.3/9	-	-	-	
Rice bran (25%)	6.0/9	-	-	-	
None	8.1/9	-	-	-	
Barley bran (5%)	7.6/9	-	-	-	
Barley bran (10%)	7.0/9	-	-	-	
Barley bran (15%)	5.4/9	-	-	-	
Barley bran (20%)	4.1/9	-	-	-	
Barley bran (25%)	3.9/9	-	-	-	
None	8.0/9	-	-	-	
Oat bran (5%)	7.7/9	-	-	-	
Oat bran (10%)	7.6/9	-	-	-	
Oat bran (15%)	7.6/9	-	-	-	
Oat bran (20%)	7.4/9	-	-	-	
Oat bran (25%)	7.1/9	-	-	-	
None	8.2/9	-	-	-	Kaur and others (2013)
None	8.1/9	-	-	-	
Mushroom powder (6 %)	8.4/9	-	-	-	
Mushroom powder (8%)	8.2/9	-	-	-	
Mushroom powder (10%)	7.9/9	-	-	-	
Mushroom powder (12%)	8.2/9	-	-	-	

Mushroom powder (6%)	8.3/9	-	-	-	
Mushroom powder (8%)	8.1/9	-	-	-	
Mushroom powder (10%)	7.9/9	-	-	-	
Mushroom powder (12%)	7.8/9	-	-	-	
Bengal gram flour (6%)	8.0/9	-	-	-	
Bengal gram flour (9%)	7.9/9	-	-	-	
Bengal gram flour (12%)	7.9/9	-	-	-	
Bengal gram flour (15%)	8.4/9	-	-	-	
Bengal gram flour (18%)	7.9/9	-	-	-	
Bengal gram flour (21%)	7.9/9	-	-	-	
Bengal gram flour (6%)	7.7/9	-	-	-	
Bengal gram flour (9%)	7.9/9	-	-	-	
Bengal gram flour (12%)	7.9/9	-	-	-	
Bengal gram flour (15%)	8.1/9	-	-	-	
Bengal gram flour (18%)	7.7/9	-	-	-	
Bengal gram flour (21%)	7.6/9	-	-	-	
Defatted soy flour (6%)	7.9/9	-	-	-	
Defatted soy flour (9%)	8.5/9	-	-	-	
Defatted soy flour (12%)	8.3/9	-	-	-	
Defatted soy flour (15%)	8.0/9	-	-	-	
Defatted soy flour (6%)	7.5/9	-	-	-	
Defatted soy flour (9%)	8.1/9	-	-	-	
Defatted soy flour (12%)	7.8/9	-	-	-	
Defatted soy flour (15%)	7.7/9	-	-	-	
None	8.1/10	9.0/10	8.0/10	-	Sabanis and others (2006)
Chickpea flour (5%)	8.5/10	8.8/10	8.9/10	-	
Chickpea flour (10%)	6.9/10	8.6/10	8.2/10	-	
Chickpea flour (20%)	4.9/10	5.0/10	6.5/10	-	
Chickpea flour (30%)	2.6/10	2.0/10	3.0/10	-	
Chickpea flour (50%)	1.0/10	1.0/10	2.0/10	-	

Ground barley (10%)	6.1/9	-	6.1/9	5.8/9	Sinesio and others (2008)
Ground barley (20%)	5.9/9	-	5.9/9	5.4/9	
Ground barley (30%)	5.5/9	-	5.7/9	5.6/9	
Ground barley (10%)	6.8/9	-	6.7/9	6.6/9	
Ground barley (20%)	6.9/9	-	6.6/9	6.9/9	
Ground barley (30%)	6.5/9	-	6.3/9	6.9/9	
None	9.65/15	-	-	-	Torres and others (2006)
Fermented pigeon pea flour (5%)	8.68/15	-	-	-	
Fermented pigeon pea flour (10%)	7.15/15	-	-	-	
Fermented pigeon pea flour (12%)	5.48/15	-	-	-	
None	9.65/15	-	-	-	Torres and others (2007a)
Lupin flour (5%)	8.89/15	-	-	-	
Lupin flour (8%)	8.32/15	-	-	-	
Lupin flour (10%)	4.19/15	-	-	-	
Lupin flour (5%)	9.06/15	-	-	-	
Lupin flour (8%)	8.86/15	-	-	-	
Lupin flour (10%)	8.52/15	-	-	-	
None	9.65/15	-	-	-	Torres and others (2007b)
Germinated pigeon pea flour (5%)	10.6/15	-	-	-	
Germinated pigeon pea flour (8%)	8.90/15	-	-	-	
Germinated pigeon pea flour (10%)	9.87/15	-	-	-	
None	7.46/9	7.53/9	7.39/9	7.37/9	Zhao and others (2005)
Green pea flour (15%)	6.34/9	6.84/9	6.17/9	6.44/9	
Yellow pea flour (20%)	6.19/9	6.63/9	5.94/9	6.18/9	
Chickpea flour (20%)	6.01/9	6.86/9	5.93/9	6.24/9	
Lentil flour (15%)	6.41/9	5.28/9	6.44/9	6.42/9	
None	2.4/5	-	2.6/5	-	Zouari and others (2011)

Dried blue-green algae (1%)	3.1/5	-	2.9/5	-
Dried blue-green algae (2%)	3.6/5	-	3.6/5	-
Dried blue-green algae (3%)	3.1/5	-	3.0/5	-

The enrichment level of pasta showed a significant negative correlation to its overall quality ($\bar{r} = -0.70$), appearance ($\bar{r} = -0.84$), and flavor ($\bar{r} = -0.83$), reflecting the lower acceptance of enriched pasta. Exceptions were pasta enriched with 15% unripe banana flour (Agama-Acevedo and others 2009), 6% mushroom powder, 15% Bengal gram flour, or 12% defatted soy flour (Kaur and others 2013), or 1% to 3% dried green-blue microalgae (Zouari and others 2011). For these enrichment ingredients, the overall quality of the pasta increased slightly when compared to pasta with no enrichment (Table 7.6).

The reduction in pasta sensory properties was small or not significant for most pasta products with a low enrichment level. For instance, the overall quality was reduced by less than 1 on a 9-point hedonic scale for 25 of the 27 pasta products with an enrichment level less than or equal to 10% (Table 7.6), suggesting that such levels could be used for most enrichment ingredients to produce enriched pasta with sensory properties similar to those of traditional pasta. For higher enrichment levels, the sensory properties were ingredient specific. Enrichment with more than 20% Bengal gram flour (Kaur and others 2013) or a mixture of buckwheat flour and wheat bran (Chillo and others 2008) did not significantly affect the overall quality of pasta. In contrast, the overall quality of enriched pasta was reduced from 7.5 to 4.8 on a 9-point hedonic scale by enrichment with 50% lupin flour (Jayasena and Nasar-Abbas 2012), from 8.6 to 7.3 by enrichment with 30% shrimp meat (Kadam and Prabhasankar 2012), and from 8.1 to 3.9 by enrichment with 25% barley bran (Kaur and others 2012). Significantly lower sensory properties for enriched pasta products would decrease their commercial viability, given that studies on the consumer perception of functional foods indicate that consumers are generally unwilling to compromise on the taste of food for health benefits (Verbeke 2006).

The Pearson correlation coefficients of the sensory properties with the cooking and mechanical properties and color are presented in Table 7.7. The sensory properties of pasta were significantly correlated to the cooking properties. The Pearson correlation coefficients indicate that pasta with a high optimum cooking time and weight increase during cooking and low cooking losses generally have better sensory properties. The redness color (*a* value) was negatively correlated to the overall quality, appearance, and flavor of pasta, indicating that lower redness of pasta is associated with desirable sensory properties. There was no significant

correlation between the firmness of pasta and its sensory properties, suggesting that cooking properties and color are more important for consumer acceptance. The correlations between the overall quality of pasta and its appearance, flavor, and texture were significant, reflecting the importance of these 3 sensory properties for the overall quality of pasta.

Table 7.7. Pooled Pearson correlation coefficients (Equation 7.15) of the sensory properties with the cooking, color, and mechanical properties.

Properties	Overall quality	Appearance	Flavor	Texture
Optimum cooking time	0.33	0.22	0.79*	0.88*
Cooking losses	−0.57*	−0.77*	−0.62*	−0.83*
Weight increase during cooking	0.51	0.84*	0.89*	0.82
Volume increase during cooking	N/A	N/A	N/A	N/A
L value of uncooked pasta	0.15	−0.03	−0.56	N/A
a value of uncooked pasta	−0.75*	−0.82*	−8.88*	N/A
b value of uncooked pasta	−0.58	−0.80	−0.66	N/A
L value of cooked pasta	0.45	N/A	0.42	N/A
a value of cooked pasta	−0.92*	N/A	−0.92*	N/A
b value of cooked pasta	−0.94*	N/A	−0.91*	N/A
Firmness	−0.04	0.11	−0.04	−0.15
Stickiness	N/A	N/A	N/A	N/A
Elasticity	N/A	N/A	N/A	N/A
Overall quality	1	0.93*	0.97*	0.97*
Appearance	0.93*	1	0.89*	0.89*
Flavor	0.97*	0.89*	1	0.93*
Texture	0.97*	0.89*	0.93*	1

Note: “N/A” designates quality attributes that were not measured simultaneously for a sufficient number of observations in the dataset for the calculation of a Pearson correlation coefficient. Pearson correlation coefficients that are marked with an asterisk (*) are significantly different from the null value

7.5. Research needs

7.5.1 Impact of the processing history of the enrichment ingredient

Only a few studies have investigated the impact of the processing history of the enrichment ingredient on the properties of enriched pasta. Ribotta and others (2005) studied the interactions of wheat and soy proteins in dough by electrophoresis and reported that heat

treatment of soy proteins caused their denaturation and reduced their ability to interact with wheat proteins via disulfide bonds. Similarly, Mercier and others (2012) reported that the state of pea proteins (native or denatured), induced by ultrafiltration/diafiltration, impacted their interaction with wheat gluten and starch and modified the gluten index and Farinograph development time, stability, and mixing tolerance index. Villeneuve and others (2013) compared the properties of pasta enriched with whole flaxseed and pasta enriched with whole flaxseed reconstituted after oil extraction, and they showed that oil extraction impacted the drying and the cooking properties of the pasta and the fatty acid profile after *in vitro* digestion. Torres and others (2006, 2007b) reported that the fermentation and germination of pigeon peas prior to their use as an enrichment ingredient in pasta modified the proximate composition of the peas and increased the nutritional value of the pasta. Work is required to characterize the impact of protein denaturation and starch modification in the enrichment ingredient on the properties of pasta and to determine if these elements could assist in interpreting conflicting results for the quality of pasta enriched with such ingredients.

7.5.2 Impact of the process specifications on the health benefits of enriched pasta

In many cases, the consumption of a food product enriched with a functional ingredient can have a lower biological effect than anticipated (Fogliano and Vitaglione 2005). The lower biological effect could be caused by the lower bioavailability of the enrichment ingredient as a result of interactions with the food matrix and degradation of the enrichment ingredient during processing (Fogliano and Vitaglione 2005; Power and others 2012). Consequently, assessments of the bioavailability and the health benefits of enriched pasta should be conducted to better understand the impact of enrichment on these attributes. Recently, Capraro and others (2014) studied the impact of enrichment of pasta with lupin protein fractions on the body weight and plasma glucose concentration of rats. Their results indicated that the consumption of pasta enriched with lupin protein fractions reduced the rats' body weight gain and food intake and decreased glycemia upon glucose overload trials. In a study involving 22 healthy human subjects, Khan and others (2015) observed that the consumption of pasta enriched with 30% whole-grain red sorghum flour enhanced antioxidant status and improved markers of oxidative stress. In contrast, the consumption of pasta enriched with whole-grain

white sorghum flour had no effect. There is a need for *in vivo* studies using pasta produced with different enrichment ingredients and process specifications. Such studies would contribute to our understanding of the relationship between process specifications and health benefits and would assist with the selection of suitable process specifications for enriched pasta.

7.6. Conclusion

In this work, a meta-analysis was conducted to evaluate the impact of enrichment and process specifications on the quality of pasta. The major conclusions drawn from the meta-analysis are the following:

(1) The impact of pasta enrichment with pulse flour is significantly different than that of enrichment with high-fiber ingredients. Fiber enrichment generally contributes positively to the preservation of the microstructure of pasta and entraps starch granules, thereby modifying the dough and cooking properties compared to pasta with pulse flour enrichment.

(2) Drying pasta at temperatures higher than 60 °C can partially compensate for the weakening of the pasta structure attributed to enrichment and gluten dilution, thanks to the strengthening effect provided by protein coagulation. The thermal stability of the enrichment ingredient and the preservation of its bioavailability still need to be evaluated for high drying temperatures.

(3) The sensory properties of enriched pasta are generally similar to those of traditional pasta for enrichment levels less than or equal to 10%, a critical factor for the commercial success of enriched pasta. For higher enrichment levels, the sensory properties can be significantly lower, indicating that work is required to improve processes for high enrichment levels.

(4) The application of quantitative methods to reviewing the literature provided variables that are good predictors of pasta quality. Pooled Pearson correlation coefficients indicate that:

a. the gelatinization temperature is a promising predictor of pasta cooking properties;
b. the Farinograph properties are promising predictors of pasta mechanical properties; and
c. the cooking properties are promising predictors of pasta sensory properties.

(5) Future work should focus on the use of the dataset and pooled Pearson correlation coefficients for the development of models to predict the quality of traditional and enriched pasta based on inexpensive and easy-to-measure properties.

7.7 Acknowledgements

The authors thank the Vanier Canada Graduate Scholarships program (held by Samuel Mercier) and the Natural Sciences and Engineering Research Council of Canada (NSERC) of Canada for their financial support.

CHAPITRE 8. Estimation des propriétés manquantes des aliments par complétion de matrice

Titre original : Estimation of missing values in a food property database by matrix completion using iterative and variational Bayesian principal component analyses

Auteurs et affiliations :

S. Mercier, Ing. jr., étudiant au doctorat, Université de Sherbrooke, département de génie chimique et génie biotechnologique, 2500 boul. Université, Sherbrooke, Québec, Canada, J1K 2R1.

C. Moresoli, Ing., Ph.D. University of Waterloo, Department of Chemical Engineering, 200 University Avenue West, Waterloo, Ontario, Canada, N2L 3G1.

M. Mondor, Ing. stag., Ph.D., Agriculture et Agroalimentaire Canada, Centre de Recherche et Développement de Saint-Hyacinthe, 3600 Boul. Casavant Ouest, Saint-Hyacinthe, Québec, Canada, J2S 8E3.

S. Villeneuve, Ing., Ph.D., Agriculture et Agroalimentaire Canada, Centre de Recherche et Développement de Saint-Hyacinthe, 3600 Boul. Casavant Ouest, Saint-Hyacinthe, Québec, Canada, J2S 8E3.

B. Marcos, Ing., Ph.D., Université de Sherbrooke, département de génie chimique et génie biotechnologique, 2500 boul. Université, Sherbrooke, Québec, Canada, J1K 2R1.

État de l'acceptation : soumis à la revue *Journal of Chemometrics*

Résumé

Contenu : dans le cadre de la méta-analyse sur les pâtes traditionnelles et enrichies (chapitre 7), une base de données regroupant les propriétés des pâtes selon les conditions de production mesurées dans 66 études a été construite. Le nombre de propriétés mesurées dans une étude étant limité en raison de contraintes monétaires, techniques et de temps, près de 70% des valeurs de la base de données sont manquantes. Dans cet article, des approches de complétion de matrice par analyses par composantes principales itérative (IPCA) et bayésienne variationnelle (VBPCA) ont été appliquées pour utiliser les relations entre les propriétés afin d'estimer les valeurs manquantes de la base de données.

Résultats : la comparaison des deux méthodes révèle la précision plus élevée de la méthode VBPCA que la méthode IPCA pour l'estimation des valeurs manquantes de la base de données. La complétion de matrice par VBPCA permet de décrire une portion significative (R^2 moyen = 0.42) de la variance des valeurs manquantes de la base de données. Les travaux montrent que la méthode VBPCA permet de prédire avec un niveau de confiance d'environ 90% si la valeur manquante est supérieure ou inférieure à la moyenne de la propriété considérée pour 17% de la base de données. L'analyse des coefficients de détermination indique la pertinence d'inclure dans la base de données des propriétés mesurées dans peu d'études, car bien qu'elles augmentent le pourcentage de valeurs manquantes dans la base de données, les algorithmes sont en mesure d'utiliser l'information supplémentaire qu'elles fournissent pour améliorer la précision de la prédiction pour la majorité des autres propriétés de la base de données. L'article se termine par une discussion de deux approches pour améliorer la précision des algorithmes de complétion de matrice. Ces deux approches sont les analyses par composantes principales à noyau, permettant la considération des relations non-linéaires entre les propriétés, et les analyses par composantes principales à niveaux multiples, permettant la considération de la structure hiérarchique de la base de données.

Contribution à la thèse : la contribution à la thèse de cet article est le développement d'une méthode novatrice et originale, à notre connaissance jamais appliquée à ce jour à la caractérisation d'un produit, permettant l'estimation des propriétés manquantes du produit considéré à partir des propriétés mesurées et améliorant la caractérisation du produit sans coût expérimental additionnel.

Abstract

Given that the complete experimental characterization of a food product is generally not possible because of cost, time or technical limitations, food property databases generally contain a significant proportion of missing values. The aim of this study was to estimate the missing values in a food property database by matrix completion. To this end, a database (31 properties × 663 observations) describing pasta products and containing 68.7% missing values was used. Two matrix completion algorithms were compared: iterative principal component analysis (IPCA) and variational Bayesian principal component analysis (VBPCA). VBPCA performed better than IPCA and explained on average 42% of the variance of the missing values. The accuracy of the missing value estimates varied significantly among the properties, and the coefficient of determination for each property with VBPCA ranged from 0.02 to 0.84. The accuracy of the missing value estimates was higher when properties known for only a few observations were included in the database, indicating that the matrix completion algorithms successfully used the additional information that those properties provided to improve the estimation of the other properties in the database. For 17% of the database, the matrix completion algorithms determined whether the missing value was above or below the average value of the property with a 90% confidence level, providing additional information for product characterization at no experimental cost.

Keywords

Matrix completion; Principal component analysis; Food; Database

Nomenclature

B	$p \times n$ bias matrix (Eq. 8.2)
B_{i1}	element $i1$ of B (Eq. 8.10)
$\bar{B}_{i1}$	posterior mean of B_{i1} (Eq. 8.14)
c	number of principal components retained for matrix completion (Eq. 8.2)
C	$p \times p$ covariance matrix (Eq. 8.3)
D	$p \times p$ matrix of the eigenvalues of C (Eq. 8.3)
IPCA	iterative principal component analysis
M	$p \times n$ sparse matrix to be completed (Fig. 8.1)
M_{ij}	element ij of M
M^*	centred and scaled matrix M
n	number of observations (Fig. 8.1)
p	number of properties (Fig. 8.1)
PCA	principal component analysis
pdf	probability density function
r	rank of M
$RMSE$	root mean square error
U	$p \times p$ matrix of the eigenvectors of C (Eq. 8.3)
X	$c \times n$ matrix of the principal component scores (Eq. 8.2)
$X_{:j}$	$c \times 1$ vector representing the j column of X (Eq. 8.14)
$\bar{X}_{:j}$	$c \times 1$ vector of posterior means of $X_{:j}$ (Eq. 8.14)
VBPCA	variational Bayesian principal component analysis
W	$p \times c$ matrix of the principal component loadings (Eq. 8.2)
W_{ij}	element ij of W (Eq. 8.9)
$W_{i:}$	$1 \times c$ vector representing the i row of W (Eq. 8.14)
$W_{:j}$	$p \times 1$ vector representing the j column of W (Eq. 8.9)
$\bar{W}_{i:}$	$1 \times c$ vector of posterior means of $W_{i:}$ (Eq. 8.14)
Greek symbols	
$\Sigma_{X_{:j}}$	$c \times c$ posterior covariance matrix of $X_{:j}$ (Eq. 8.14)
$\Sigma_{W_{i:}}$	$c \times c$ posterior covariance matrix of $W_{i:}$ (Eq. 8.14)
λ	eigenvalue of the kernel matrix (Eq. 8.18)
θ	VBPCA random matrices ($\theta = [X, W, B]$) (Eq. 8.12)
Ω	set of measured (known) values ij in the matrix
$\sigma_{B_{i1}}$	posterior variance of B_{i1} (Eq. 8.14)
ν_B	prior variance of the elements of B (Eq. 8.10)
ν_M	noise variance of the elements of M (Eq. 8.11)
$\nu_{W_{:j}}$	prior variance of the elements of $W_{:j}$ (Eq. 8.9)

ξ	VBPCA hyperparameters ($\xi = \left[\nu_{W_{:1}}, \ldots, \nu_{W_{:p}}, \nu_B, \nu_M\right]$) (Eq. 8.12)
Subscripts	
cal	calibration
test	test
val	validation

8.1 Introduction

In a study aiming to characterize a food product, only a subset of its relevant properties are generally measured because of cost, time or technical limitations. However, the remaining missing properties can potentially be estimated from the measured properties if they are correlated. Correlations between properties are common for food products, given that many properties are controlled by a limited number of underlying phenomena. The estimation of the unknown properties is highly beneficial, because it provides additional information on the food product at no experimental cost. The estimation of unknown properties is also useful for efficient experimental design, as experiments can be designed such that the fewest number of properties are measured and the remaining properties are estimated.

The completion of sparse matrices is an approach that has not been investigated for the estimation of the unknown properties of food products from measured properties. Matrix completion is possible if the matrix is of lower rank. A typical example of a lower-rank sparse matrix is a matrix describing user ratings of movies available on a website. The matrix is sparse, because the users have probably rated only a fraction of the hundreds or thousands of movies available. The matrix is of lower rank, because the appreciation of movies by the users is correlated. For instance, users who have rated highly a movie of a certain genre also tend to rate highly other movies of the same genre. Matrix completion algorithms use these correlations to estimate missing values in the sparse matrix. More specifically, a matrix $M \in \mathbb{R}^{p \times n}$ of rank $r < \min(p, n)$ can be completed by solving a nuclear norm minimization problem (Candes and Recht 2009):

$$\min \|Y\|_* \quad (8.1)$$

subject to $Y_{ij} = M_{ij}$ for all $ij \in \Omega$,

where Ω is the set of known elements ij of M, and $\|\cdot\|_*$ is the nuclear norm (sum of the singular values). The matrix M can be completed under certain conditions regarding the number of known values (fewer known values are required for lower-rank matrices), their position in the matrix, and the coherence of the matrix column and row spaces (Candes and Plan 2010; Chen et al. 2014). Matrix completion is a powerful approach for the estimation of missing values and has been used successfully for entertainment recommender systems (Ilin

and Raiko 2010; Gogna and Majumdar 2015), gene expression profiles (Oba et al. 2003; Ying and Guang 2009), seismic data (Kumar et al. 2015), traffic flow (Tan et al. 2014), image recovery (Wang et al. 2014) and video editing (Kim et al. 2015).

For food products that have been considered in a sufficient number of studies published in the literature, a meta-analysis can be performed to extract relevant properties measured in the studies for their compilation in a database. The database obtained is a $p \times n$ matrix M, where p is the number of properties characterizing the food product and n is the number of observations, with one observation being a sample of the food product for which the values of some of the properties have been compiled in the database. Given that only a subset of the properties is measured in most studies because of cost, time or technical limitations, matrix M is sparse (Fig. 8.1, top part). A matrix completion algorithm can be performed on matrix M to estimate its missing values and generate additional knowledge on the food product from the measured (known) values in the database (Fig. 8.1, bottom part).

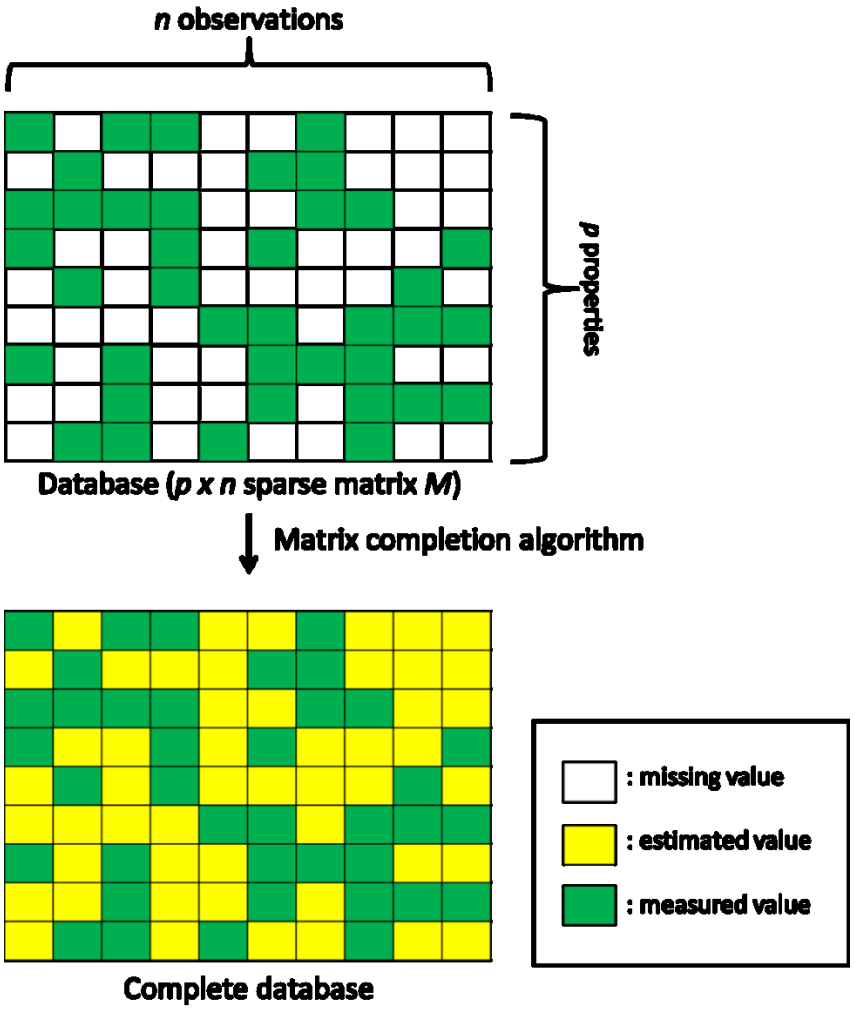

Figure 8.1. Estimation of the missing values in a food property database ($p \times n$ sparse matrix M) by a matrix completion algorithm to generate additional knowledge for food product characterization at no experimental cost.

Measurements compiled in the database are noisy because of measurement errors, and modifications therefore have to be made to the nuclear norm minimization problem (Eq. 1) for its completion to avoid overfitting, that is, an accurate representation of the measured values in the matrix but an inaccurate estimation of the missing values. A common approach for matrix completion with noisy matrices is based on principal component analysis (PCA). PCA performs an orthogonal projection from the data space to a subspace of lower dimension (Nounou et al. 2002; Smidl and Quinn 2007):

$$M \approx WX + B, \tag{8.2}$$

where $M \in \mathbb{R}^{p \times n}$ is the noisy matrix, $W \in \mathbb{R}^{p \times c}$ is the matrix of principal component loadings, $X \in \mathbb{R}^{c \times n}$ is the matrix of principal component scores, $B \in \mathbb{R}^{p \times n}$ is the bias matrix (obtained by stacking the $p \times 1$ vectors of row-wise means of M), and $c \in \mathbb{R}$ is the number of principal components retained. Matrix W indicates the weight given to each property for the c principal components, and matrix X indicates the coordinates of the observations in the subspace of lower dimension. When M is sparse, the PCA can be performed iteratively. In iterative PCA (IPCA), an initial estimate of the missing values in the matrix is established, such as the row- or column-wise mean of the measured values, to perform the PCA. The missing values are then replaced with the values obtained from Eq. (2), and the PCA is repeated again until convergence. If overfitting is significant, the measured values in the matrix can be separated into a calibration matrix and a validation matrix, and the iterations are stopped prior to convergence according the accuracy for the estimation of the validation matrix (Ilin and Raiko 2010). More recent approaches based on probabilistic PCA, Bayesian PCA and variational Bayesian PCA (VBPCA) have been developed for matrix completion that limit overfitting (Ilin and Raiko 2010; Luttinen and Ilin 2010). In probabilistic PCA, a noise term is included explicitly in the PCA model (Eq. 8.2) and the elements of X are estimated using a maximum likelihood approach (Ilin and Raiko 2010). In VBPCA, both the elements of X and W are treated as random variables and their posterior density functions are estimated from the likelihood function and assigned prior distributions (Ilin and Raiko 2010; Kim and Choi 2013; Liu et al. 2013). The prior distributions have a regularizing effect on the PCA as they penalize solutions of X and W far from the expectation of the prior distribution (Raiko et al. 2007). VBPCA also limits overfitting because model learning is based on the posterior probability mass of X and W, rather than on point estimates (Ilin and Raiko 2010; Luttinen and Ilin 2010; Liu et al. 2014).

The aim of this work was to assess the accuracy of estimating missing values in a food property database by matrix completion. To accomplish this work, the database of Mercier et al. (2016) on the properties of traditional and enriched pasta products was considered. The missing values in the database were estimated by matrix completion using IPCA and VBPCA. The accuracy of the two matrix completion algorithms was compared. The impact of the selection of the properties included in the database was investigated and improvements to the two matrix completion algorithms were discussed.

8.2 Methods

8.2.1 Description of the database

The database of Mercier et al. (2016) containing the properties of pasta products was used in this study. The database was constructed by extracting relevant measurements from 66 studies, published from 2001 to 2014, on traditional pasta or pasta enriched with health-promoting ingredients. The database compiles measurements of 43 properties describing the process specifications or quality attributes of 663 samples of pasta (Table 8.1). Five properties (wheat ingredient, enrichment ingredient, presence of eggs, presence of an emulsifier, and shaping method) in the database were categorical, and seven (firmness, stickiness, elasticity, overall acceptability, appearance, flavour and texture of the pasta) were not uniform across the observations in terms of their unit or scale. These properties were removed from the database to obtain a $p \times n$ sparse matrix M of 31×663. The proportion of missing values of M was 68.7%.

Table 8.1. Properties compiled in the database of Mercier et al. [18], with the number of observations in the database for which the property is known, the average and range of the property, and the coefficient of determination for the estimation of the missing values using IPCA and VBPCA

Property		Number of observations	Average	Range	$R^2_{test,IPCA}$	$R^2_{test,VBPCA}$
ID	**Name**					
1	Enrichment level	663	12.2	0 - 50	0.34	0.41
2	Diameter/thickness of extrusion (mm)	322	1.7	0.7 – 4.0	0.27	0.37
3	Drying temperature (°C)	571	62.3	37.5 - 95.0	0.25	0.27
4	Drying duration (h)	298	10.6	0.75 - 36.0	0.28	0.31
5	Average relative humidity during drying (%)	285	69.7	40.0 - 91.0	0.48	0.50
6	Dough hydration (g (100 g dry matter)$^{-1}$)	352	46.8	40.8 – 69.5	0.17	0.18
7	Protein content of the enrichment ingredient (g (100 g dry matter)$^{-1}$)	240	28.1	4.2 - 96.1	0.31	0.33

8	Protein content of the wheat flour or semolina (g (100 g dry matter)$^{-1}$)	314	12.5	9.8 – 17.8	0.44	0.55
9	Protein content of the dough or uncooked pasta (g (100 g dry matter)$^{-1}$)	328	15.5	4.9 – 33.3	0.34	0.47
10	Total dietary fiber content of the dough or uncooked pasta (g (100 g dry matter)$^{-1}$)	27	6.9	2.5 – 14.2	0.01	0.02
11	Farinograph dough development time (min)	115	3.9	1.0 – 13.8	0.04	0.17
12	Farinograph stability (min)	103	6.3	0.9 – 18.0	0.43	0.59
13	Farinograph water absorption (g (100 g dough)$^{-1}$)	129	60.2	40.9 – 104.4	0.01	0.20
14	Farinograph mixing tolerance index (FU)	82	42.0	2 – 130	0.20	0.35
15	Gelatinization temperature (°C)	61	64.5	59.8 – 80.9	0.39	0.40
16	Wet gluten (g (100 g dough)$^{-1}$)	58	40.8	31.0 – 50.2	0.29	0.24
17	Gluten index (%)	101	68.9	1 - 99	0.31	0.41
18	Thickness/diameter of the pasta after extrusion (mm)	41	2.1	1.6 – 2.6	0.64	0.84
19	Fresh pasta water content (g (100 g dry matter)$^{-1}$)	43	42.1	30.1 – 59.0	0.31	0.25
20	Equilibrium water content after drying (g (100 g dry matter)$^{-1}$)	84	9.3	2.6 – 14.8	0.47	0.48
21	Water effective diffusion coefficient (x 10^{-11} m^2 s^{-1})	32	6.4	3.3 - 12.1	0.38	0.63
22	Cooking time (min)	370	9.1	3 – 17.7	0.20	0.30
23	Cooking loss (g	456	6.3	1.6 – 21.6	0.22	0.24

	(100 g uncooked pasta)$^{-1}$)					
24	Weight increase during cooking (g (100 g uncooked pasta)$^{-1}$)	324	163.0	69.2 – 242.4	0.33	0.38
25	Volume increase during cooking (%)	81	156.0	89.0 – 240.8	0.72	0.79
26	*L* of uncooked pasta	264	57.0	16.8 – 87.6	0.35	0.34
27	*a* of uncooked pasta	232	3.8	-11.1 – 21.5	0.44	0.55
28	*b* of uncooked pasta	237	25.9	2.0 – 52.9	0.33	0.47
29	*L* of cooked pasta	94	61.1	30 – 84.6	0.52	0.59
30	*a* of cooked pasta	67	0.8	-10.9 – 10.5	0.62	0.78
31	*b* of cooked pasta	67	20.6	2.2 – 32.6	0.56	0.71

8.2.2 Matrix completion algorithms

The missing values in the database were estimated by the completion of matrix *M* using IPCA and VBPCA.

8.2.2.1 Iterative principal component analysis (IPCA)

To perform IPCA, matrix *M* was separated into matrices of calibration (M_{cal}), validation (M_{val}) and test (M_{test}), with each of the last two containing 10% of the measured values of *M* selected randomly. The calibration matrix was used to train the algorithm, the validation matrix was used for early stopping, and the test matrix was used to estimate the accuracy of the algorithm. Centred and scaled matrices M^*_{cal}, M^*_{val} and M^*_{test} were obtained by subtracting from the known values of each matrix the row-wise mean of M^*_{cal} and dividing by its row-wise standard deviation. Matrix M^*_{cal} was initialized by replacing its missing values with the null value. Matrix *B* was initialized as a $p \times n$ matrix of null values. The algorithm was applied as follows:

(1) Perform the PCA on matrix M^*_{cal} by the eigen-decomposition of the $C \in \mathbb{R}^{p\,x\,p}$ covariance matrix [4]:

$$C = \frac{1}{n} M^*_{cal} {M^*_{cal}}^T = UDU^T, \quad (8.3)$$

where $D \in \mathbb{R}^{p \times p}$ is a diagonal matrix containing the eigenvalues of C, and the columns of $U \in \mathbb{R}^{p \times p}$ are the unit-length eigenvectors of C. The principal component loading matrix W corresponds to the c columns of U associated with the largest eigenvalues, and the principal component score matrix X corresponds to $W^T M^*_{cal}$.

(2) Estimate the missing values of M^*_{cal} from the PCA:

$$M^*_{cal,ij} \leftarrow \begin{cases} M^*_{cal,ij} \text{ for } ij \in \Omega_{cal} \\ [WX + B]_{ij} \text{ otherwise'} \end{cases} \quad (8.4)$$

where Ω_{cal} is the set of measured elements ij of M^*_{cal}.

(3) Update the p x n bias matrix B by stacking the p x 1 vectors of row-wise means of M^*_{cal}.

(4) Center M^*_{cal} by subtracting the updated bias matrix B:

$$M^*_{cal} \leftarrow M^*_{cal} - B \quad (8.5)$$

(5) Calculate the *RMSE* of the validation matrix:

$$RMSE_{val} = \sqrt{\frac{1}{|\Omega_{val}|} \sum_{ij \in \Omega_{val}} \left([WX + B]_{ij} - M^*_{val,ij}\right)^2}, \quad (8.6)$$

where $|\Omega_{val}|$ is the cardinality of Ω_{val}, that is, the number of measured values of M^*_{val}.

(6) Repeat steps (1)-(5) until $RMSE_{val}$ begins to increase.

The performance of the algorithm was assessed from the *RMSE* of the test matrix, as follows:

$$RMSE_{test} = \sqrt{\frac{1}{|\Omega_{test}|} \sum_{ij \in \Omega_{test}} \left([WX + B]_{ij} - M^*_{test,ij}\right)^2}, \quad (8.7)$$

where $|\Omega_{test}|$ is the cardinality of the test matrix. The algorithm was repeated 200 times, each with different calibration, validation and test matrices selected randomly. The $RMSE_{test}$ presented in this paper is the average of these 200 trials. The algorithm was implemented using Matlab 7.12.

8.2.2.2 Variational Bayesian principal component analysis

To perform VBPCA, M was separated into matrices of calibration (M_{cal}) and test (M_{test}), with the latter containing 10% of the measured values of M selected randomly. Given that training in VBPCA is stopped when convergence is reached (no early stopping is applied), no validation matrix is required. Centred and scaled matrices M^*_{cal} and M^*_{test} were obtained as described in section 8.2.2.1. Matrices X, W and B were assumed to be composed of random variables described by joint probability density functions (pdf) (Nounou et al. 2002). Independent normal prior pdf were assigned to X, W and B:

$$p(X) = \prod_{i=1}^{c} \prod_{j=1}^{n} N(X_{ij}; 0,1) \tag{8.8}$$

$$p\left(W|\nu_{W_{:j}}\right) = \prod_{i=1}^{p} \prod_{j=1}^{c} N\left(W_{ij}; 0, \nu_{W_{:j}}\right) \tag{8.9}$$

$$p(B|\nu_B) = \prod_{i=1}^{p} N(B_{i1}; 0, \nu_B), \tag{8.10}$$

where $N(Z_{ij}; \mu, \tau)$ denotes the normal pdf over the element ij of a matrix Z with mean μ and variance τ. The hyperparameters $\nu_{W_{:j}} \in \mathbb{R}^p$ and $\nu_B \in \mathbb{R}$ describe the prior variance of the elements of W and B. Individual priors $\nu_{W_{:j}}$ were used for each column vector of W for an automatic selection of the right number of principal components (see section 8.3.1). Measurement noise of the known values of M^*_{cal} was assumed to be Gaussian and the likelihood function was as follows (Luttinen and Ilin, 2010):

$$p(M^*_{cal}|X, W, B, \nu_M) = \prod_{ij \in \Omega_{cal}} N(M^*_{cal,ij}; [WX + B]_{ij}, \nu_M), \tag{8.11}$$

where $\nu_M \in \mathbb{R}$ is an hyperparameter describing the variance of the noise. The posterior pdf of X, W, B was related to the prior pdf and the likelihood using Bayes' law (Nounou et al. 2002):

$$p(\theta|M^*_{cal}, \xi) \propto p(M^*_{cal}|\theta, \xi)p(\theta|\xi), \tag{8.12}$$

where $\theta = [X, W, B]$ represents the random matrices, and $\xi = \left[\nu_{W_{:1}}, \ldots, \nu_{W_{:p}}, \nu_B, \nu_M\right]$ represents the hyperparameters. The joint posterior pdf $p(\theta|M^*_{cal}, \xi)$ is generally a complex

pdf with no analytical formulation. Following the variational Bayesian approach, $p(\theta|M^*_{cal},\xi)$ was approximated by a pdf of a predetermined form $q(\theta)$:

$$p(\theta|M^*_{cal},\xi) \approx q(\theta), \tag{8.13}$$

where $q(\theta)$ is a pdf of a simpler form than $p(\theta|M^*_{cal},\xi)$. Independent Gaussian pdf were used for $q(\theta)$:

$$q(\theta) = \prod_{j=1}^{n} N\left(X_{:j}; \bar{X}_{:j}, \Sigma_{X_{:j}}\right) \prod_{i=1}^{p} N\left(W_{i:}; \bar{W}_{i:}, \Sigma_{W_{i:}}\right) \prod_{i=1}^{p} N\left(B_{i1}; \bar{B}_{i1}, \sigma_{B_{i1}}\right), \tag{8.14}$$

where $X_{:j} \in \mathbb{R}^c$ is the vector representing the j column of matrix X, $\bar{X}_{:j} \in \mathbb{R}^c$ is the vector of posterior means of $X_{:j}$, $\Sigma_{X_{:j}} \in \mathbb{R}^{c \times c}$ is the posterior covariance matrix of $X_{:j}$, $W_{i:} \in \mathbb{R}^c$ is the vector representing the i row of W, $\bar{W}_{i:} \in \mathbb{R}^c$ is the vector of posterior means of $W_{i:}$, $\Sigma_{W_{i:}} \in \mathbb{R}^{c \times c}$ is the posterior covariance matrix of $W_{i:}$, $B_{i1} \in \mathbb{R}$ is the $i1$ element of B, $\bar{B}_{i1} \in \mathbb{R}$ is the posterior mean of B_{i1}, and $\sigma_{B_{i1}} \in \mathbb{R}$ is the posterior variance of B_{i1}. The estimation of $\bar{X}_{:j}$, $\Sigma_{X_{:j}}$, $\bar{W}_{i:}$, $\Sigma_{W_{:i:}}$, $\bar{B}_{i1}$, $\sigma_{B_{i1}}$, $\nu_{W_{:j}}$, ν_B and ν_M was performed by the minimization of the cost function (Ilin and Raiko 2010; Liu et al. 2014):

$$C(q(\theta),\xi) = \int_{-\infty}^{\infty} q(\theta) \ln \frac{q(\theta)}{p(\theta|M^*_{cal},\xi)} d\theta - \ln p(M^*_{cal}|\xi) \tag{8.15}$$

The first term of the right hand side of Eq. (8.15) is the Kullback–Leibler divergence between the true posterior pdf $p(\theta|M^*_{cal},\xi)$ and its approximation $q(\theta)$, and the second term is the marginal log-likelihood. Minimization of the cost function $C(q(\theta),\xi)$ was performed using the expectation-maximization algorithm by minimizing $C(q(\theta),\xi)$ alternately with respect to $q(\theta)$ and ξ following the analytical formulations developed by Ilin and Raiko (2010). The *RMSE* of the test matrix was calculated from the matrices of posterior means $\bar{X}$, $\bar{W}$ and $\bar{B}$:

$$RMSE_{test} = \sqrt{\frac{1}{|\Omega_{test}|} \sum_{ij \in \Omega_{test}} \left([\bar{W}\bar{X} + \bar{B}]_{ij} - M^*_{test,ij}\right)^2}, \tag{8.16}$$

In accordance with the IPCA (section 8.2.2.1), the algorithm was repeated 200 times, each with different calibration and test matrices selected randomly, and the average $RMSE_{test}$ of these 200 trials was calculated to assess the performance of the algorithm. The algorithm was implemented using Matlab 7.12.

8.3 Results and discussion

8.3.1 Selection of the number of principal components

Fig. 8.2 presents the $RMSE_{test}$ for the two matrix completion algorithms as a function of the number of principal components c retained. For IPCA, considering nine principal components provided the most accurate estimation of the missing values of M. Increasing the number of principal components to nine decreased the $RMSE_{test}$, indicating that the first nine principal components are closely related to the underlying phenomena affecting the properties of the product and provide valuable information for the estimation of the missing values. Considering additional principal components increased the $RMSE_{test}$ and caused overfitting, indicating that these principal components were highly sensitive to measurement noise. For VBPCA, increasing the number of principal components to nine decreased the $RMSE_{test}$, in accordance with IPCA, but considering additional principal components did not increase the $RMSE_{test}$ and cause overfitting. The absence of overfitting when a large number of principal components were considered in VBPCA is attributed to the zero-mean prior attributed to the columns of W (Eq. 8.9). During training, if the relevance of the k^{th} principal component for the estimation of M_{cal}^{*} is weak, its prior variance $v_{W_{kj}}$ decreases. Consequently, the vector of posterior means of $\overline{W}_{:k}$ for this principal component shrinks towards the null value, providing an automatic determination of the right number of principal components for the PCA (Bishop 1999; Ilin and Raiko 2010).

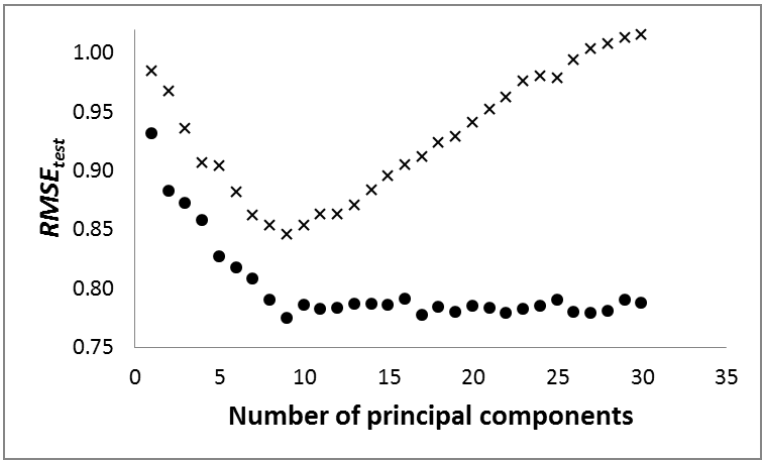

Figure 8.2. Root mean square error of the test matrix ($RMSE_{test}$) according to the number of principal components retained for matrix completion by IPCA (x) and VBPCA (●).

8.3.2 Accuracy of the missing value estimates

Table 8.1 presents the coefficient of determination R^2 between the measured values in the test matrix and the values estimated by matrix completion for each property in the database. Nine principal components were retained in the matrix completion algorithms. The coefficients of determination were higher for VBPCA than IPCA and indicated that VBPCA is a better algorithm for the estimation of missing values in a food property database. Similar results were obtained by Ilin and Raiko (2010). Ilin and Raiko (2010) generated 100 × 100 matrices of rank 10, corrupted the matrix with Gaussian noise with a standard deviation of 0.5, and removed some of the values randomly to obtain a sparse matrix. Their simulations indicated that missing values estimated using VBPCA were at least two times more accurate than those estimated using IPCA for a sparse matrix with more than 70% of the values missing. The authors attributed the better performance of VBPCA to the overfitting caused by IPCA.

The coefficients of determination between the measured values in the test matrix and the values estimated by VBPCA varied from 0.02 to 0.84 depending on the property considered (Table 8.1). For 10 of the 31 properties, the coefficient of determination was higher than 0.5, indicating that the majority of their variance was explained from the measured values in the database. However, no coefficient of determination was above 0.9, indicating that matrix completion may not be sufficient for a robust estimation of the missing values. For instance, Fig. 8.3 presents a parity plot between the measured values of the yellowness (*b* colour attribute) of pasta after cooking in the test matrix and the values estimated by VBPCA. The estimated values increase linearly with the measured values, and the coefficient of determination ($R^2 = 0.71$) is significant, but the difference between the estimated and measured values is higher than 25% for approximately 20% of the estimated values; those differences are probably too large for a direct application of the missing values estimates. The insufficient accuracy of matrix completion for a robust estimation of the missing values could be attributed to the absence of strong correlations between the properties, to measurement

errors masking these correlations, to an insufficient number of measured values in the database, or to nonlinear associations between the properties.

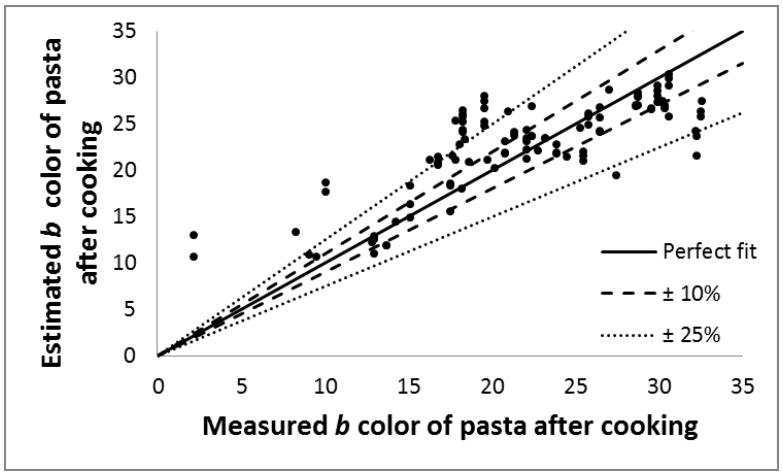

Figure 8.3. Parity plot between the measured values of the *b* colour attribute of pasta after cooking in the test matrix and estimated by VBPCA.

8.3.3 Removal of properties with a high proportion of missing values

The database has a high proportion of missing values, 68.7%. The impact of removing properties with a high proportion of missing values from the database on the accuracy of matrix completion was investigated. Properties known for fewer than 100 observations were removed from the original 31×663 database to obtain a reduced, 19×663 database. Removing 12 properties from the database decreased its proportion of missing values to 54.7%. For the completion of the reduced database by VBPCA and IPCA, retaining eight principal components, one fewer than for the completion of the original database, minimized the $RMSE_{test}$ (Fig. 8.2). Fig. 8.4 compares the accuracy of the missing values between estimation by the completion of the original database (with nine principal components retained) and estimation by the completion of the reduced database (with eight principal components retained). For VBPCA, removing the 12 properties known for fewer than 100 observations decreased the accuracy of the matrix completion for 18 of the remaining 19 properties. Similarly, for IPCA, removing the 12 properties known for fewer than 100 observations decreased the accuracy of the matrix completion for 17 of the remaining

19 properties. Removing the 12 properties known for fewer than 100 observations decreased the coefficient of determination of the 19 remaining properties by an average of 0.04 for VBPCA and 0.05 for IPCA. A comparison of the coefficients of determination indicates that it is better to include correlated properties in the database even if they are known only for few observations. Although including such properties increases the proportion of missing values in the database, the matrix completion algorithms successfully use the additional information that those properties provide to improve the accuracy of the other properties in the database.

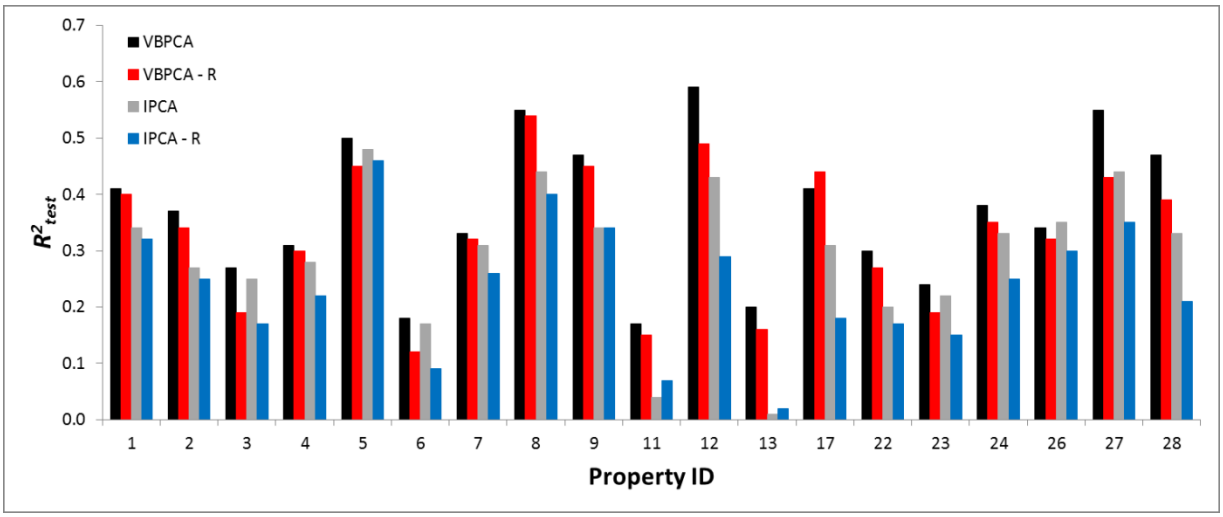

Figure 8.4. Accuracy (R^2_{test}) of the missing values estimated for each property from the completion of the original, 31 × 663 database (VBPCA and IPCA) and the reduced, 19 × 663 database (VBPCA - R and IPCA - R).

8.3.4 Confidence level of the missing value estimates

When a centred and scaled matrix M^* is being used, a positive element ij indicates that the property i for observation j is above the average value of this property, and a negative element ij indicates that the property i for observation j is below the average value of this property. Fig. 8.5 presents the proportion of missing values of M^*_{cal} estimated by matrix completion whose sign was in agreement with M^*_{test} as a function of the absolute value of the missing value estimate. This proportion indicates the confidence level at which we can conclude from matrix completion that the property for an observation is significantly above or below the average. The proportion of missing values estimated by matrix completion of the

sign in agreement with the test matrix was similar for IPCA and VBPCA. This proportion increased with the difference between the missing value estimates and the null value and was above 0.9 for missing value estimates above 1 or below −1. For matrix completion by VBPCA, 2382 of the 14,112 missing value estimates were below −1 or above 1. Consequently, for 17% of the missing values in the database, matrix completion indicates, with a confidence level of approximately 90%, whether their value is significantly above or below the average, providing valuable additional information for product characterization. For instance, Wu et al. (2001) studied the properties of traditional durum wheat pasta and durum wheat pasta enriched with corn gluten meal. The 12 properties measured by Wu et al. (2001) were included in the database of Mercier et al. (2016). Fig. 8.6 (left side) gives the value of these 12 properties for the traditional durum wheat pasta in Wu et al. (2001). After matrix completion by VBPCA, it can be concluded with a confidence level above 90% that the protein content of the wheat flour and the *L* colour attribute after cooking of this pasta were higher than the values for an average pasta, and the Farinograph mixing tolerance index, gelatinization temperature and water effective diffusion coefficient were lower than the values for an average pasta (Fig. 8.6, right side). Combining the measurements reported by Wu et al. (2001) with matrix completion made it possible to obtain valuable information on 17 of the 31 properties, improving the characterization of the product and providing a better assessment of the impact of the process specifications on the product properties at no additional experimental cost.

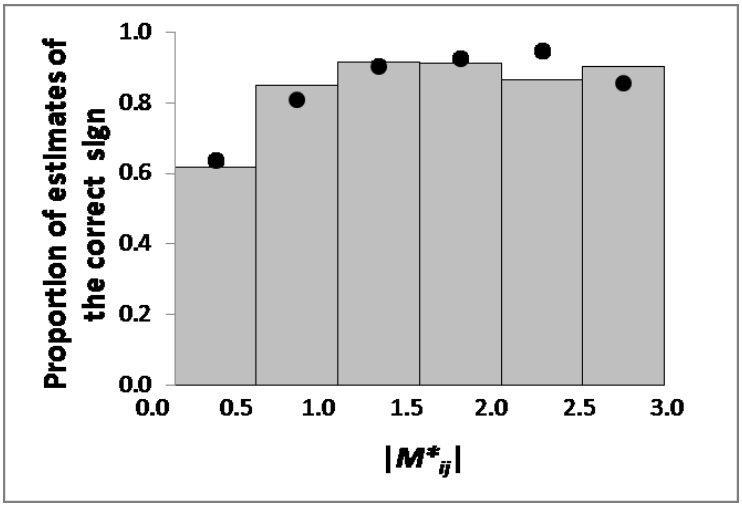

Figure 8.5. Proportion of missing values estimated by IPCA (●) or VBPCA (bars) correctly identified as above or below the average.

Figure 8.6. Properties of durum wheat pasta measured by Wu et al. [21] (highlighted in green) and identified from completion of the database by VBPCA as above or below the average (highlighted in yellow).

8.3.5 Improvements of the matrix completion algorithms

The analysis of the pasta database indicated that matrix completion explained a significant proportion of the missing value variance and, for a significant proportion of the missing values, correctly identified whether they were above or below the average. However, matrix completion was not sufficiently accurate to provide a robust estimation of the missing values for most properties. Two potential improvements, kernel and multilevel PCA, should be considered in future work to increase the accuracy of the algorithms.

Principal component analysis performs a linear dimensionality reduction and is inefficient for the description of nonlinear associations between the properties. Nonlinearity can be described using kernel PCA, a generalization of PCA for nonlinear dimensionality reduction. Kernel PCA assumes that nonlinear structures in a p-dimensional data space become linear using an appropriate mapping to a Q-dimensional feature space of dimension $Q > p$. To avoid explicit computations in the feature space, which can be computationally prohibitive, because its dimension may be significantly higher than the data space, the PCA is generally performed implicitly by solving the eigenvector equation considering a predetermined kernel function (Berar et al. 2005; Wang 2012). Kernel PCA can be implemented iteratively or in a Bayesian framework. Kernel PCA has been applied successfully for the completion of DNA microarrays (Ying and Guang 2009), traffic flow data (Li et al. 2013) and oil flow data (Nguyen and De La Torre 2009) and could improve the accuracy for the estimation of missing values in a food property database with respect to IPCA and VBPCA.

Regarding multilevel PCA, food property databases constructed from meta-analyses have a hierarchical structure, given that the n observations are generally distributed among $q < n$ studies (Fig. 8.7). Correlations or bias may occur at the study level and affect the values in the database. For instance, the same property can be measured in two studies using two

different measurement methods, one of which may inherently give slightly higher or lower values than the other. Correlations or bias at the study level are not explicitly considered in the IPCA or VBPCA algorithms described in section 8.2, because both algorithms are performed at the observation level. The VBPCA algorithm can be modified using a multilevel approach to consider the hierarchical structure of the database. In multilevel VBPCA, individual priors would be assigned to W and B for each of the q studies and linked by joint pdf, instead of a single prior for the database (Eqs. 8.9 and 8.10). Multilevel VBPCA would increase the computational complexity of the matrix completion but could improve the accuracy of the estimation of missing values in a food property database by considering the structure of the database.

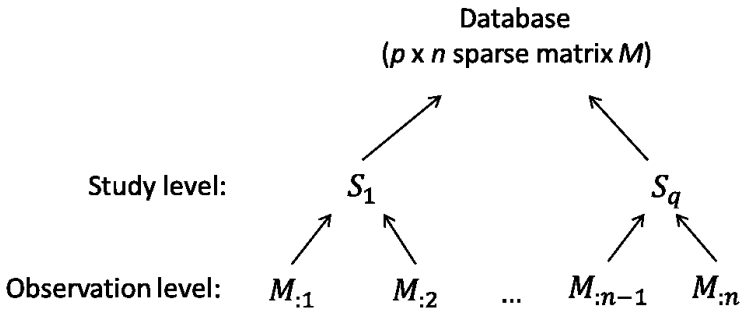

Figure 8.7. Schematization of the hierarchal structure of a food property database constructed from a meta-analysis: the properties are measured on n observations distributed among q studies.

8.4. Conclusion

In this study, an innovative approach based on matrix completion was considered to estimate missing values in a food property database and generate additional knowledge on the food product at no experimental cost. Two matrix completion algorithms, IPCA and VBPCA, were used to complete a database describing the properties of pasta products and containing 68.7% missing values. The following conclusions were drawn from this study:

(1) VBPCA performed better than IPCA did for the estimation of missing values in the food property database;

(2) Including in the database properties known only for a few observations, even though those properties increased the proportion of missing values, improved the accuracy of matrix completion by VBPCA and IPCA;

(3) Matrix completion by IPCA or VBPCA was not sufficiently accurate for a robust estimation of the missing values in the food property database; and

(4) For 17% of the missing values in the food property database, matrix completion by IPCA or VBPCA successfully determined, with a 90% confidence level, whether the property was above or below the average, providing valuable information for product characterization and a better assessment of the impact of the process specifications on the properties of the product.

Two proposed improvements to increase the accuracy of the matrix completion algorithms and the additional knowledge for product characterization that they provide are the consideration of nonlinear associations between properties by kernel PCA and the consideration of the hierarchical structure of the database by multilevel PCA. Future studies will aim to assess the improvements obtained by kernel and multilevel PCA and apply the matrix completion algorithms to other food property databases.

8.5 Acknowledgements

The authors thank the Vanier Canada Graduate Scholarships program (scholarship held by Samuel Mercier) and the Natural Sciences and Engineering Research Council of Canada (NSERC) for their financial support.

CHAPITRE 9. Conclusion et perspectives

9.1 Conclusion générale

Le projet de doctorat décrit dans cette thèse portait sur la modélisation de la production de pâtes alimentaires traditionnelles et enrichies pour l'accélération du développement de nouvelles pâtes enrichies. Le projet comportait deux objectifs généraux. Le premier objectif consistait à identifier et à quantifier les mécanismes de transfert influençant la qualité des pâtes lors du séchage. Cet objectif a été réalisé par des analyses de sensibilité, d'incertitude et d'identifiabilité appliquées aux modèles de séchage développés précédemment et le développement d'un nouveau modèle de séchage mécanistique couplant la description du transfert de masse de l'eau liquide par capillarité et convection, le transfert de masse de l'eau vapeur par diffusion et convection, le transfert d'énergie par conduction, convection et évaporation et la déformation mécanique. Le modèle mécanistique a été validé pour la description des profils internes de teneur en eau pour des températures de séchage basses (40 °C), moyennes (60 °C) et élevées (80 °C). Le deuxième objectif consistait à quantifier l'impact des variables de procédé sur les propriétés des pâtes traditionnelles et enrichies. Cet objectif a été atteint par la construction et la méta-analyse d'une base de données regroupant les propriétés des pâtes selon les variables de procédé et l'application d'algorithmes de complétion de matrice à la base de données. Les travaux ont favorisé la compréhension des relations entre les variables de procédé et les propriétés des pâtes traditionnelles et enrichies et l'amélioration de la caractérisation des pâtes sans coût expérimental additionnel. La méthodologie par complétion de matrice développée dans cette thèse est novatrice et originale et applicable au développement de nombreux produits.

La problématique considérée dans cette thèse était la durée et le coût significatif associé au développement de nouvelles pâtes enrichies. Cette thèse a conduit à la création de deux outils principaux que l'industrie pourra utiliser pour accélérer le développement de nouvelles pâtes enrichies. Le premier outil est le modèle mécanistique décrivant le séchage des pâtes (chapitre 6). L'utilisation du modèle nécessite la connaissance des propriétés thermodynamiques associées au transfert de masse et d'énergie (coefficient de diffusion, conductivité thermique, densité, etc.) de la pâte. Plusieurs de ces propriétés peuvent être

estimées à partir de la littérature. Les propriétés ne pouvant pas être estimées à partir de la littérature ou mesurées directement peuvent être estimées par moindres carrés à partir de mesures obtenues lors du séchage selon les contraintes d'identifiabilité développées aux chapitres 4 et 5. Une fois les propriétés thermodynamiques connues, le modèle mécanistique peut être utilisé pour prédire l'évolution de la teneur en eau, la température, la porosité, la densité et le rétrécissement des pâtes selon les conditions de séchage. Ces simulations permettent d'identifier efficacement des conditions de séchage appropriées selon les contraintes sur la qualité désirée des pâtes. Par exemple, les conditions de séchage ne générant pas d'important gradient de teneur en eau à l'intérieur des pâtes (afin de diminuer la probabilité de formation de craques) et maintenant la température sous une valeur respectant la sensibilité thermique de l'ingrédient d'enrichissement seraient considérées comme appropriées lors du développement de plusieurs pâtes enrichies. Ces conditions de séchage peuvent ensuite être validées par la vérification expérimentale que les pâtes obtenues respectent la qualité désirée. Le deuxième outil est la méthode par complétion de matrice développée pour l'amélioration de la caractérisation des pâtes. Lors du développement de nouvelles pâtes enrichies, une compagnie peut mesurer les propriétés de la pâte pour lesquelles elle possède l'équipement et l'expertise technique. Ces mesures peuvent être combinées à celles compilées dans la base de données (Mercier et al. 2016). L'application de la méthode par complétion de matrice permet alors d'estimer les propriétés manquantes des pâtes et de déterminer, avec un niveau de confiance élevé, si certaines propriétés sont supérieures ou inférieures à la moyenne. La méthode par complétion de matrice permet d'améliorer la caractérisation de la pâte sans coût expérimental additionnel, accélérant l'identification de conditions de production appropriées.

D'un point de vue général, le projet a également illustré la pertinence de combiner des approches mécanistiques et empiriques pour la modélisation d'un procédé. Ces deux approches de modélisation sont fondamentalement différentes. L'approche mécanistique est principalement *knowledge-driven*, c'est-à-dire que son point de départ est l'identification des phénomènes physiques impliqués dans un procédé. Dans cette thèse, le point de départ de la modélisation mécanistique du séchage était l'identification des mécanismes de transfert de masse et d'énergie affectant le séchage des pâtes (chapitre 6). Suite à l'identification de ces phénomènes physiques, leur description à partir des premiers principes permet de prédire

l'évolution de plusieurs propriétés à partir d'un faible nombre de mesures expérimentales. Dans cette thèse, des profils internes de teneur en eau obtenues à trois températures de séchage ont été utilisées pour valider le modèle de séchage mécanistique. Une fois validé, le modèle permet de prédire l'évolution de la teneur en eau, la température, la porosité, la densité et le rétrécissement des pâtes selon les conditions de séchage, propriétés fondamentales associées directement à la qualité des pâtes. À l'opposé, l'approche empirique est principalement *data-driven*. Son point de départ est généralement un ensemble de données expérimentales, dans cette thèse la base de données développée par méta-analyse (Mercier et al. 2016). Des méthodes statistiques et de régression sont ensuite appliquées pour dégager des tendances à partir des données. L'approche empirique est donc souvent utilisée comme méthode exploratoire, afin d'identifier des relations entre les variables *a priori* inconnues. Dans cette thèse, l'approche empirique a permis d'identifier les propriétés des pâtes étant de bons prédicteurs de leur qualité (chapitre 7). N'étant pas limitée aux formulations mathématiques définies par les premiers principes, l'approche empirique offre également une plus grande flexibilité, facilitant la modélisation de procédés complexes et dont les phénomènes physiques impliqués ne sont pas clairement définis. Cette flexibilité a permis le développement d'une méthode, basée sur la complétion de matrice, reliant toutes les variables de procédé et les propriétés pertinentes à la production des pâtes et utilisant leurs dépendances pour améliorer la caractérisation des pâtes sans coût expérimental additionnel (chapitre 8). En utilisant à la fois des approches de modélisation mécanistiques et empiriques, cette thèse a permis de combiner le développement d'un modèle détaillé décrivant l'étape de transformation la plus critique des pâtes traditionnelles et enrichies, le séchage, et d'un modèle général considérant les conditions de production à chacune des étapes de transformation.

9.2 Poursuite des travaux

Au fil de la réalisation du projet et à l'intérieur de chacun des chapitres, des recommandations ont été soulevées à l'égard de la poursuite des travaux. Cette thèse se termine par la proposition de deux avenues de recherche à considérer pour la poursuite de la recherche dans les secteurs du développement des pâtes et de la modélisation appliquée à la transformation alimentaire.

9.2.1 Description de l'impact de la déformation viscoélastique sur le transfert de masse lors du séchage des pâtes

Le volume des pâtes diminue d'environ 20 à 30% lors du séchage (Mercier et al. 2011b). Le rétrécissement influence le transfert de masse de l'eau de trois manières. En premier lieu, le rétrécissement diminue la distance que l'eau doit parcourir pour atteindre la surface des pâtes et être échangée avec l'air environnant. La diminution de la distance à parcourir accélère le séchage des pâtes et cet impact du rétrécissement est considéré dans le modèle mécanistique développé dans cette thèse par l'ajustement du volume de la pâte selon la réduction de sa teneur en eau (Eq. 6.20). En deuxième lieu, le rétrécissement cause une augmentation de la concentration d'eau (en masse par unité de volume). Le rétrécissement des pâtes étant plus important en surface qu'au centre lors du séchage, l'augmentation de la concentration d'eau par le rétrécissement est plus grande près de la surface des pâtes, ce qui a pour effet de diminuer le gradient de concentration d'eau $\frac{\partial C_w}{\partial l}$ et de réduire la vitesse de séchage. Cet impact du rétrécissement sur le transfert de masse est considéré dans le modèle mécanistique par l'ajustement de la concentration en eau selon le rétrécissement local (Eq. 6.30). En troisième lieu, le rétrécissement engendre, par le déplacement de la matrice solide vers le centre des pâtes, une force opposée au mouvement de l'eau et réduisant la vitesse de séchage. Lorsque la pâte est en transition de l'état vitreux à l'état visqueux, elle se comporte comme un matériau viscoélastique et la vitesse du déplacement de la matrice solide est d'un même ordre de grandeur que la vitesse du transfert de masse par capillarité de l'eau liquide (Takhar 2008). Le déplacement de la matrice solide engendre alors un transfert de masse non-Fickian et favorise l'établissement d'un profil interne de teneur en eau de forme sigmoïdale (Edwards 2005; Petropoulos et al. 2011). Des profils internes de teneur en eau de cette forme ont été observés pour des pâtes traditionnelles et enrichies en lin séchées à 80 °C (Annexe E). Ce troisième impact du rétrécissement sur le séchage des pâtes n'a pas été considéré dans le modèle mécanistique développé dans cette thèse. Sa considération nécessite la modification de l'équation décrivant le flux de l'eau liquide (Eq. 6.4), par exemple en y ajoutant un terme proportionnel à la force engendrée par le déplacement de la matrice solide (Vinjamur and Cairncross 2002; Edwards 2005; Vorotnikov 2013) :

$$n_w = D_w \frac{\partial c_w}{\partial l} + \rho_w \frac{k_w}{\mu_w} \frac{\partial P}{\partial l} + E \frac{\partial \sigma}{\partial l}, \quad (9.1)$$

où σ est la composante parallèle au transfert de masse de la force engendrée par le déplacement de la matrice solide et E est un coefficient de proportionnalité. Le coefficient E dépend de l'état de la pâte (visqueux, vitreux ou en transition) et est donc dépendant de la teneur en eau de la pâte. La force σ peut également être reliée à la teneur en eau de la pâte à partir d'un modèle déplacement-contrainte tels que les modèles de Maxwell, Maxwell généralisés, Kelvin-Voigt et Jeffreys (Bird et al. 1960; Cohen et White 1991; Petropoulos et al. 2011). Les essais de traction et de compression nécessaires à l'estimation des paramètres des modèles déplacement-contrainte ont été réalisés pour des pâtes traditionnelles par Takhar et al. (2006). La considération de la déformation viscoélastique dans le modèle de transfert de masse pourrait permettre une prédiction plus précise des profils internes de teneur en eau lorsque les pâtes sont en transition de l'état visqueux à l'état vitreux.

9.2.2 L'incorporation d'algorithmes de complétion de matrice dans une stratégie de gestion des résultats de recherche

Les études publiées en transformation alimentaire sont nombreuses. Une recherche par mots clefs sur *Scopus* permet d'estimer à près d'un million le nombre d'articles révisés par les pairs portant sur la transformation alimentaire, la plupart comportant des dizaines de mesures effectuées sur un aliment. Nous avons montré la pertinence d'analyser simultanément les résultats de plusieurs études par méta-analyse pour améliorer la compréhension de l'impact des variables de procédé sur un produit (chapitre 7) et le développement de modèles prédictifs (chapitre 8). L'étape la plus laborieuse dans la réalisation d'une méta-analyse est la construction de la base de données, en raison de la grande quantité de résultats et de la nécessité, dans la plupart des cas, de les compiler à la main. Pour faciliter la construction de la base de données, il serait pertinent de développer une stratégie de gestion des résultats de recherche, basée sur le développement d'une plateforme Web regroupant les propriétés classiques des aliments (propriétés mécaniques, structurelles et sensorielles, coefficients de transfert de masse et d'énergie, etc). Les chercheurs seraient invités à y inscrire les mesures réalisées dans leur laboratoire, accompagnées d'une description de la méthodologie utilisée,

permettant une construction et une mise à jour collective des bases de données. La publication des résultats non statistiquement significatifs serait encouragée au même titre que les résultats statistiquement significatifs, résuisant l'impact du biais de publication lors de reves de la littérature[2]. La disponibilité de ces bases de données valoriserait les mesures effectuées par les équipes de recherche et diminuerait le dédoublement de mesure d'une même propriété par plusieurs équipes de recherche. Les bases de données pourraient être annexées à des algorithmes d'analyse statistique (chapitre 7) et d'estimation des valeurs manquantes par complétion de matrice (chapitre 8) pour maximiser l'information tirée des mesures expérimentales. Les bases de données représenteraient un outil majeur pour l'avancement de la recherche en transformation alimentaire.

[2] Le biais de publication et son impact sur les méta-analyses et autres revues de la littérature sont discutés à la section B.8.1 (Annexe B).

RÉFÉRENCES

Abdel-Aal, E. -S. M. et Hucl, P. (2002). Amino Acid Composition and In Vitro Protein Digestibility of Selected Ancient Wheats and their End Products. *Journal of Food Composition and Analysis,* 15, p. 737-747.

AbuHammad, WA, Elias, EM, Manthey, FA, Alamri, MS, et Mergoum, M. (2012). A comparison of methods for assessing dough and gluten strength of durum wheat and their relationship to pasta cooking quality. *International Journal of Food Science and Technology*, 47, p. 2561–2573.

Agama-Acevedo, E, Islas-Hernandez, JJ, Osorio-Díaz, P, Rendón-Villalobos, R, Utrilla-Coello, RG, Angulo, O et Bello-Pérez, LA. (2009). Pasta with unripe banana flour: Physical, texture, and preference study. *Journal of Food Science,* 74, p. S263–267.

Aggarwal, P et Dollimore D. (1998). A thermal analysis investigation of partially hydrolyzed starch. *Thermochimica Acta,* 319, p. 17–25.

Agriculture et Agroalimentaire Canada. (2009). *Tendances de la consommation aliments fonctionnels*. En ligne: http://www.agrireseau.qc.ca/Marketing-Agroalimentaire/documents/Market%20Analysis%20%20Report_Functional%20Foods%20(FR%20Dec%201%202009).pdf (consulté le 11 novembre 2015).

Agriculture et Agroalimentaire Canada. (2014). *Opportunities and Challenges Facing the Canadian Functional Foods and Natural Health Products Sector.* En ligne: http://www.agr.gc.ca/eng/industry-markets-and-trade/statistics-and-market-information/by-product-sector/functional-foods-and-natural-health-products/reports-and-resources-functional-foods-and-natural-health-products/opportunities-and-challenges-facing-the-canadian-functional-foods-and-natural-health-products-sector/?id=1410206902299 (consulté le 14 décembre 2015).

Aguilera, J.M. et Stanley, D.W. (1999). Microstructural principles of food processing and engineering. (2nd ed.). New York (USA): Aspen Publishers.

Alasino, M.C., Osella, C.A., De La Torre, M.A. et Sanchez, H.D. (2011). Use of sodium stearoyl lactylate and azodicarbonamide in wheat flour breads with added pea flour. *International Journal of Food Sciences and Nutrition*, 62, p. 385-391.

Alireza Sadeghi, M. et Bhagya, S. (2008). Quality Characterization of Pasta Enriched with Mustard Protein Isolate. *Journal of Food Science,* 73, p. S229-S237.

Andrieu, J., Gonnet, E. et Laurent, M. (1989). Thermal conductivity and diffusivity of extruded durum wheat pasta. *LWT – Food Science and Technology,* 22, p. 6-10.

Andrieu, J. et Stamatopoulos, A.A. (1986). Durum wheat pasta drying kinetics. *LWT - Food Science and Technology,* 19, p. 448-456.

Ansari, S. A., Sattar, S. A., Springthorpe, V. S., Wells, G. A. et Tostowaryk, W. (1989). In vivo protocol for testing efficacy of hand-washing agents against viruses and bacteria: experiments with rotavirus and Escherichia coli. *Applied and Environmental Microbiology*, 55, p. 3113–3118.

Aravind, N, Sissons, M, Egan, N et Fellows, C. (2012a). Effect of insoluble dietary fibre addition on technological, sensory, and structural properties of durum wheat spaghetti. *Food chemistry,* 130, p. 299–309.

Aravind, N, Sissons, M, Egan, N, Fellows, CM Blazek, J et Gilbert EP. (2012b). Effect of β-glucan on technological, sensory, and structural properties of durum wheat pasta. *Cereal Chemisty,* 89, p. 84–93.

Aravind, N, Sissons, M et Fellows, CM. (2012c). Effect of soluble fibre (guar gum and carboxymethylcellulose) addition on technological, sensory and structural properties of durum wheat spaghetti. *Food Chemistry,* 131, p. 893–900.

Aravind, N, Sissons, MJ, Fellows, CM, Blazek, J et Gilbert, EP. (2012d). Effect of inulin soluble dietary fibre addition on technological, sensory, and structural properties of durum wheat spaghetti. *Food Chemistry,* 132, p. 993–1002.

Aravind, N, Sissons, M, Fellows, CM, Blazek, J et Gilbert, EP. (2013). Optimisation of resistant starch II and III levels in durum wheat pasta to reduce in vitro digestibility while maintaining processing and sensory characteristics. *Food Chemistry,* 136, p. 1100–1109.

Ashyraliyev, M., Fomekong-Nanfack, Y., Kaandorp, J.A. et Blom, J.G. (2009). Systems biology: Parameter estimation for biochemical models. *FEBS Journal,* 276, p. 886-902.

Ayliffe, G. A., Babb, J. R. et Quoraishi, A. H. (1978). A test for 'hygienic' hand disinfection. *Journal of Clinical Pathology*, 31, p. 923–928.

Ayliffe, G. A. J., Babb, J. R., Davies, J. G. et Lilly, H. A. (1988). Hand disinfection: a comparison of various agents in laboratory and ward studies. *Journal of Hospital Infection*, 11, p. 226–243.

Bahnassey, Y., Khan, K. et Harrold, R. (1986). Fortification of spaghetti with edible legumes. I. Physicochemical, antinutritional, amino acid, and mineral composition. *Cereal chemistry,* 63, p. 210-215.

Baiano, A, Fares, C, Peri, G, Romaniello, R, Taurino, AM, Siciliano, P, Gambacorta, G, Lamacchia, C, Pati, S et La Notte, E. (2008). Use of a toasted durum whole meal in the production of a traditional Italian pasta: Chemical, mechanical, sensory and image analyses. *International Journal of Food Science and Technology,* 43, p. 1610–1618.

Baiano, A, Lamacchia, C, Fares, C, Terracone, C et La Notte, E. (2011a). Cooking behaviour and acceptability of composite pasta made of semolina and toasted or partially defatted soy flour. *LWT - Food Science and Technology* 44, p. 1226–1232.

Baiano, A, Lamacchia, C et Terracone, C. (2011b). Effects of the addition of a meal deriving from toasted durum wheat kernels on dough properties and spaghetti cooking behavior. *CyTA - J of Food,* 9, p. 200–209.

Bartzokas, C. A., Corkill, J. E. et Makin, T. (1987). Evaluation of the Skin Disinfecting Activity and Cumulative Effect of Chlorhexidine and Triclosan Handwash Preparations on Hands Artificially Contaminated with *Serratia marcescens*. *Infection Control,* 8, p. 163–167.

Bérard, A. et Bravo, G. (1998). Combining Studies Using Effect Sizes and Quality Scores: Application to Bone Loss in Postmenopausal Women. *Journal of Clinical Epidemiology*, 51, p. 801–807.

Bettin, K., Clabots, C., Mathie, P., Willard, K. et Gerding, D. N. (1994). Effectiveness of Liquid Soap vs. Chlorhexidine Gluconate for the Removal of Clostridium Difficile from Bare Hands and Gloved Hands. *Infection Control & Hospital Epidemiology*, 15, p. 697–702.

Bird, R.B., Stewart, W.E. et Lightfoot, E.N. (1960). *Transport Phenomena*. London (UK): John Wiley and sons.

Bellman, R. et Åström, K.J. (1970). On structural identifiability. *Mathematical Biosciences*, 7, p. 329-339.

Berkey, C. S., Anderson, J. J. et Hoaglin, D. C. (1996). Multiple-Outcome Meta-Analysis of Clinical Trials. *Statistics in Medicine,* 15, p. 537–557.

Berar, M, Desvignes, M, Bailly, G, Payan, Y et Romaniuk, B. (2005). Missing data estimation using polynomial kernels. *Lecture Notes in Computer Science,* 3686, p. 390-399.

Berthoumieux, S., Brilli, M., Kahn, D., de Jong, H. et Cinquemani, E. (2013). On the identifiability of metabolic network models. *Journal of Mathematical Biology,* 67, p. 1795-1832.

Bhatnagar, S. et Hanna, M.A. (1997). Modification of Microstructure of Starch Extruded with Selected Lipids. *Starch,* 49, p. 12-20.

Bishop, CM. (1999). Variational principal components. In *Proceedings of the 9th International Conference on Artificial Neural Networks (ICANN99),* p. 509-514.

Borneo, R et Aguirre, A. (2008). Chemical composition, cooking quality, and consumer acceptance of pasta made with dried amaranth leaves flour. *LWT - Food Science and Technology,* 41, p. 1748–51.

Boroski, M, de Aguiar, AC, Boeing, JS, Rotta, EM, Wibby, CL, Bonafé, EG, de Souza, NE et Visentainer, JV. (2011). Enhancement of pasta antioxidant activity with oregano and carrot leaf. *Food Chemistry,* 125, p. 696–700.

Boumenir, A. et Tuan, V.K. (2009). Inverse Problems for Multidimensional Heat Equations by Measurements at a Single Point on the Boundary. *Numerical Functionnal Analysis and Optimization*, 30, p. 1215-1230.

Brennan, CS, Kuri, V et Tudorica, CM. (2004). Inulin-enriched pasta: Effects on textural properties and starch degradation. *Food Chemistry,* 86, p. 189–193.

Brennan, CS et Tudorica, CM. (2007). Fresh pasta quality as affected by enrichment of nonstarch polysaccharides. *Journal of Food,* 72, p. S659–S665.

Brereton, R.G. et Lloyd, G.R. (2010). Support Vector Machines for classification and regression. *Analyst,* 135, p. 230-267.

Brockwell, S.E. et Gordon, I. R. (2001). A comparison of statistical methods for meta-analysis. *Statistics in Medicine*, 20, p. 825–840.

Bustos, MC, Perez, GT et León, AE. (2011). Sensory and nutritional attributes of fibre-enriched pasta. *LWT - Food Science and Technology,* 44, p. 1429–1434.

Callcut, R. et Branson, R. (2009). How to read a review paper. *Respiratory Care*, 54, p. 1379–1385.

Candes, EJ et Plan, Y. (2010). *Matrix completion with noise*. *Proceedings of the IEEE*, 98, p. 925-936.

Candes, EJ et Recht, B. (2009). Exact matrix completion via convex optimization. Found. *Computational Mathematics,* 9, p. 717-772.

Candes, E.J. J., Romberg, K. et Tao, T. (2006). Stable signal recovery from incomplete and inaccurate measurements. *Communications on Pure and Applied Mathematics*, 59, p. 1207-1223.

Capraro, J, Magni, C, Scarafoni, A, Caramanico, R, Rossi, F, Morlacchini, M et Duranti, M. (2014). Pasta supplemented with isolated lupin protein fractions reduces body weight gain and food intake of rats and decreases plasma glucose concentration upon glucose overload trial. *Food & Function,* 5, p. 375–380.

Card, N.A. (2012). *Applied meta-analysis for social science research*. New York: Guilford Press.

Carini, E., Curti, E., Minucciani, M., Antoniazzi, F., and Vittadini, E. (2014). Pasta. Dans: Guiné, R.P.F., Reis Correira, P.M.D., editors. Engineering aspects of cereal and cereal-based products. Boca Raton: CRC Press. p. 211-238.

Carini, E, Curti, E, Spotti, E et Vittadini, E. (2012). Effect of formulation on physicochemical properties and water status of nutritionally enriched fresh pasta. *Food and Bioprocess Technology,* 5, p. 1642–1652.

Carini, E, Vittadini, E, Curti, E et Antoniazzi, F. (2009). Effects of different shaping modes on physico-chemical properties and water status of fresh pasta. *Journal of Food Engineering,* 93, p. 400–406.

Carini, E, Vittadini, E, Curti, E, Antoniazzi, F et Viazzani, P. (2010). Effect of different mixers on physicochemical properties and water status of extruded and laminated fresh pasta. *Food Chemistry,* 122, p. 462–469.

Cermak, P. et Trcala, M. (2012). Influence of uncertainty in diffusion coefficients on moisture field during wood drying. *International Journal of Heat and Mass Transfer,* 55, p. 7709-7717.

Chakrabortty, A. (2011). Optimal sensor placement for parametric identification of electrical networks using mixed phasor measurements. In *Proceedings of the American Control Conference*, p. 4540-4545.

Chaunier, L., Chrusciel, L., Delisée, C., Della Valle, G. et Malvestio, J. (2008). Permeability and expanded structure of baked products crumbs. *Food Biophysics,* 3, p. 344-351.

Chen, Y, Bhojanapalli, S, Sanghavi, S et Ward, R. (2014). Coherent matrix completion. In *Proceedings of the 31st International Conference on Machine Learning (IMCL 2014),* 2, p. 1017-1036.

Chillo, S., Laverse, J., Falcone, P.M., Protopapa, A. et Del Nobile, M.A. (2008). Influence of the addition of buckwheat flour and durum wheat bran on spaghetti quality. *Journal of Cereal Science,* 47, p. 144-152.

Chokmani, K., Viau, A. A. et Bourgeois, G. (2001). Analyse de l'incertitude de quatre modèles de phytoprotection relative à l'erreur de mesures des variables agrométéorologiques d'entrée. *Agronomie,* 21, p. 147–167.

Cnossen, A.G., Siebenmorgen, T.J., Yang, W. et Bautista, R.C. (2001). An application of glass transition temperature to explain rice kernel fissure occurrence during the drying process. *Drying Technology,* 19, p. 1661-1682.

Cohen, M.A., Eliashberg, J. et Ho, T.-H. (1996). New product development: The performance and time-to-market tradeoff. *Management Science,* 42, p.173-186.

Cohen, D. S., et White Jr., A. B. (1991). Sharp fronts due to diffusion and viscoelastic relaxation in polymers. *SIAM Journal on Applied Mathematics,* 51, p. 472-483.

Cohn, LD et Becker, BJ. (2003). How meta-analysis increases statistical power. *Psychological Methods,* 8, p. 243–253.

Coumans, W.J. (2000). Models for drying kinetics based on drying curves of slabs. *Chemical Engineering and Processing: Process Intensification*, 36, p. 53–68.

Crank, J. (1975). The Mathematics of Diffusion. (2nd ed.). Oxford (UK): Clarendon Press.

Cuq, B., Gonçalves, F., Mas, J.F., Vareille, L. et Abecassis, J. (2003). Effects of moisture content and temperature of spaghetti on their mechanical properties. *Journal of Food Engineering*, 59, p. 51-60.

Cuq, B. et Icard-Verniere, C. (2001). Characterisation of glass transition of durum wheat semolina using modulated differential scanning calorimetry. *Journal of Cereal Science*, 33, p. 213-221.

Da Silva, W.P., e Silva, C.M.D.P.S., Precker, J.W. et Duarte, M.E.M. (2012). Determination of the uncertainty for the thermal conductivity obtained as a function of the moisture content for several foodstuffs. *International Journal of Food Science and Technology,* 47, p. 2452-2459.

Datta, A.K. (2006). Hydraulic permeability of food tissues. *International Journal of Food Properties,* 9, p. 767-780.

Datta, A.K. (2007). Porous media approaches to studying simultaneous heat and mass transfer in food processes. I: Problem formulations. *Journal of Food Engineering,* 80, p. 80-95.

Daud, W.R.W., Ibrahim, M.H., et Talib, M.Z.M. (1997). Parameter estimation of fick's law drying equation. *Drying Technology,* 15, p. 1673-1686.

Davidescu, F.P. et Jorgensen, S.B. (2008). Structural parameter identifiability analysis for dynamic reaction networks. *Chemical Engineering Science,* 63, p. 4754-4762.

Day, R.A. et Gastel, B. (2012). How to Write and Publish a Scientific Paper, 5th ed. Phoenix, Az: Cambridge University Press.

Debbouz, A, Pitz, WJ, Moore, WR et D'Appolonia, BL. (1995). Effect of bleaching on durum wheat and spaghetti quality. *Cereal Chemistry,* 72, p. 128–131.

Deistler, M. (1978). The structural identifiability of linear models with autocorrelated errors in the case of cross-equation restrictions, *Journal of Econometrics,* 8, p. 23–31.

de la Peña, E et Manthey, FA. (2014). Ingredient composition and pasta:water cooking ratio affect cooking properties of nontraditional spaghetti. *International Journal of Food Science and Technology,* 49, p. 2323–2330.

De Noni, I. et Pagani, M.A. (2010). Cooking properties and heat damage of dried pasta as influenced by raw material characteristics and processing conditions. *Critical Reviews in Food Science and Nutrition,* 50, p. 465-472.

De Oliveira, MKS, Martinez-Flores, HE, De Andrade, JS, Garnica-Romo, MG et Chang YK. (2006). Use of pejibaye flour (*Bactris gasipaes Kunth*) in the production of food pastas. *International Journal of Food Science and Technology,* 41, p. 933–937.

DerSimonian R. et Laird, N. (1986). Meta-analysis in clinical trials. *Controlled Clinical Trials*, 7, p. 177–188.

De Temmerman, J., Verboven, P., Nicolaï, B. et Ramon, H. (2007). Modelling of transient moisture concentration of semolina pasta during air drying. *Journal of Food Engineering,* 80, p. 892-903.

De Temmerman, J., Verboven, P., Delcour, J.A., Nicolaï, B. et Ramon, H. (2008). Drying model for cylindrical pasta shapes using desorption isotherms. *Journal of Food Engineering,* 86, p. 414-421.

De Zorzi, M., Curioni, A., Simonato, B., Giannattasio, M. et Pasini, G. (2007). Effect of pasta drying temperature on gastrointestinal digestibility and allergenicity of durum wheat proteins. *Food Chemistry,* 104, p. 353-363.

Dobre, S. (2010). Analyses de sensibilité et d'identifiabilité globales - application à l'estimation de paramètres photophysiques en thérapie photodynamique, Thèse de doctorat, Université Henri Poincaré, Nancy, France.

Doi, S.A.R. et Thalib, L. (2008). A Quality-Effects Model for Meta-Analysis. *Epidemiology,* 19, p. 94–100.

DuChateau, P. (2013). An adjoint method for proving identifiability of coefficients in parabolic equations, *Journal of Inverse and Ill-Posed Problems,* 21, p. 639–663.

Duval, S. et Tweedie, R. (2000). Trim and Fill: A Simple Funnel-Plot–Based Method of Testing and Adjusting for Publication Bias in Meta-Analysis, *Biometrics*, 56, p. 455–463.

Duval, S. et Tweedie, R. (2000). A Nonparametric 'Trim and Fill' Method of Accounting for Publication Bias in Meta-Analysis. *Journal of the American Statistical Association*, 95, p. 89–98.

Dwan, K., Gamble, C., Williamson, P. R. et Kirkham, J. J. (2013). Systematic Review of the Empirical Evidence of Study Publication Bias and Outcome Reporting Bias — An Updated Review. *Plos One*, 8, p. 1–37.

Edwards, N.M., Dexter, J.E. et Scanlon, M.G. (2002). Starch participation in durum dough linear viscoelastic properties. *Cereal Chemistry*, 79, p. 850-856.

Edwards, D.A. (2005). A spatially nonlocal model for polymer desorption. *Journal of Engineering Mathematics,* 53, p. 221-238.

Escobedo-Avellaneda, Z., Pérez-Pérez, M.C., Bárcenas-Pozos, M.E. et Welti-Chanes, J. (2011). Moisture adsorption isotherms of freeze-dried and air-dried mexican red sauce. *Journal of Food Process Engineering,* 34, p. 1931-1945.

Feillet, P., Autran, J.-C. et Icard-Vernière, C. (2000). Pasta brownness: An assessment. *Journal of Cereal Science,* 32, p. 215-233.

Feng, H., Tang, J., Plumb, O.A. et Cavalieri, R.P. (2004). Intrinsic and relative permeability for flow of humid air in unsaturated apple tissues. *Journal of Food Engineering,* 62, p. 185-192.

Fey, Y.C. et Boles, M.A. (1987). An analytical study of the effect of convection heat transfer on the sublimation of a frozen semi-infinite porous medium. *International Journal of Heat and Mass Transfer,* 30, p. 771-779.

Fischler, G. E., Fuls, J. L., Dail, E. W., Duran, M. H., Rodgers, N. D. et Waggoner, A. L. (2007). Effect of hand wash agents on controlling the transmission of pathogenic bacteria from hands to food, *Journal of Food Protection*, 70, p. 2873–2877.

Fogliano, V. et Vitaglione, P. (2005). Functional foods: Planning and development. *Molecular Nutrition & Food Research,* 49, p. 256-262.

Fradique, M, Batista, AP, Nunes, MC, Gouveia, L, Bandarra, NM et Raymundo, A. (2010). Incorporation of Chlorella vulgaris and Spirulina maxima biomass in pasta products. Part 1: Preparation and evaluation. *Journal of Food Science and Agriculture,* 90, p. 1656–1664.

Fradique, M, Batista, AP, Nunes, MC, Gouveia, L, Bandarra, NM et Raymundo, A. (2013). Isochrysis galbana and Diacronema vlkianum biomass incorporation in pasta products as PUFA's source. *LWT - Food Science and Technology,* 50, p. 312–319.

Fuad, T. et Prabhasankar, P. (2010). Role of ingredients in pasta product quality: A review on recent developments. *Critical Reviews in Food Science and Nutrition,* 50, p. 787-798.

Fuller, E.N, Schettler, P.D. et Giddings., J.C. (1966). A new method for prediction of binary gas-phase diffusion coefficients. *Industrial and Engineering Research,* 58, p. 19-27.

Fuls, J. L., Rodgers, N. D., Fischler, G. E., Howard, J. M., Patel, M., Weidner, P. L. et Duran, M. H. (2008). Alternative Hand Contamination Technique To Compare the Activities of Antimicrobial and Nonantimicrobial Soaps under Different Test Conditions. *Applied and Environmental Microbiology*, 74, p. 3739–3744.

Gallegos-Infante, J.A., Rocha-Guzman, N.E., Gonzalez-Laredo, R.F., Ochoa-Martinez, L.A., Corzo, N., Bello-Perez, L.A., Medina-Torres, L. et Peralta-Alvarez, L.E. (2009). Quality of spaghetti pasta containing Mexican common bean flour (*Phaseolus vulgaris* L.). *Food Chemistry,* 119, p. 1544-1549.

Garcia, D.F., García, B., Burgos, J.C. et García-Hernando, N. (2012). Determination of moisture diffusion coefficient in transformer paper using thermogravimetric analysis. *International Journal of Heat and Mass Transfer,* 55, p. 1066-1075.

Garg, A.X., Hackam, D. et Tonelli, M. (2008). Systematic Review and Meta-analysis: When One Study Is Just not Enough. *Clinical Journal of the American Society of Nephrology*, 3, p. 253–260.

Gates, S. (2002). Review of methodology of quantitative reviews using meta-analysis in ecology. *Journal of Animal Ecology*, 71, p. 547–557.

Gauthier, J, Gélinas, P et Beauchemin, R. (2006). Effect of stone-milled semolina granulation on the quality of bran-rich pasta made from khorasan (Kamut®) and durum wheat. *International Journal of Food Science and Technology,* 41, p. 596–599.

Geankoplis, C.J. (2003). Transport Processes and Separation Process Principles. (4th ed.). New Jersey (USA): Prentice Hall.

Gelencsér, T, Gál, V, Hódsági, M et Salgó, A. (2008). Evaluation of quality and digestibility characteristics of resistant starch-enriched pasta. *Food and Bioprocess Technology,* 1, p. 171–179.

Giménez, MA, Drago, SR, De Greef, D, Gonzalez, RJ, Lobo, MO et Samman, NC. (2012). Rheological, functional and nutritional properties of wheat/broad bean (*Vicia faba*) flour blends for pasta formulation. *Food Chemistry,* 134, p. 200–206.

Godfrey, K.R. et DiStefano, J.J. (1987). Identifiability of Model Parameters. Oxford (UK): Pergamon Press.

Gogna, A et Majumdar, A. (2015). Matrix completion incorporating auxiliary information for recommender system design. *Expert Systems with Applications,* 49, p. 5789-5799.

Graciano, J.E., Mendoza, D.F. et Le Roux, G.A.C. (2014). Performance comparison of parameter estimation techniques for unidentifiable models. *Computers and Chemical Engineering,* 64, p. 24-40.

Green, B. N., Johnson, C. D., et Adams, A. (2006). Writing narrative literature reviews for peer-reviewed journals: secrets of the trade. *Journal of Chiropractic Medicine*, 5, p. 101–117.

Guilhermetti, M., Hernandes, S. E. D., Fukushigue, Y., Garcia, L. B. et Cardoso, C. L. (2001). Effectiveness of Hand-Cleansing Agents for Removing Methicillin-Resistant Staphylococcus aureus From Contaminated Hands. *Infection Control & Hospital Epidemiology*, 22, p. 105–108.

Güler, S., Köksel, H. et Ng, P.K.W. (2002). Effects of industrial pasta drying temperatures on starch properties and pasta quality. *Food Research International,* 35, p. 421-427.

Gutman, S. et Ha. J. (2009). Parameter identifiability for heat conduction with a boundary input. *Mathematics and Computers in Simulation,* 79, p. 2192-2210.

Hajidavalloo, E. et Hamdullahpur, F. (2000). Thermal analysis of a fluidized bed drying process for crops. Part I: Mathematical modelling. *International Journal of Energy Research*, 24, p. 791-807.

Halder, A., Dhall, A. et Datta, A.K. (2007). An improved, easily implementable, porous media based model for deep-fat frying. Part II: results, validation and sensitivity analysis. *Food and Bioproducts Processing,* 85, p. 220–230.

Hardy, R.J. et Thompson, S.G. (1998). Detecting and describing heterogeneity in meta-analysis. *Statistics in Medicine,* 17, p. 841–856.

Health Canada. 2014. Summary of Health Canada's Assessment of a Health Claim about Ground Whole Flaxseed and Blood Cholesterol Lowering. En ligne: http://www.hc-sc.gc.ca/fn-an/label-etiquet/claims-reclam/assess-evalu/flaxseed-graines-de-lin-eng.php. (consulté le 25 novembre 2015)

Henningsen, A. et Hamann, J. D. (2007). Systemfit: A Package for Estimating Systems of Simultaneous Equations in R. *Journal of Statistical Software,* 23, p. 1-40.

Higgins, J.P.T. et Thompson, S.G. (2002). Quantifying heterogeneity in a meta-analysis. *Statistics in Medicine*, 21, p. 1539–1558.

Hills, B.P., Godward, J. et Wright, K.M. (1997). Fast radial NMR microimaging studies of pasta drying. *Journal of Food Engineering,* 33, p. 321-335.

Hines, K.E., Middendorf, T.R. et Aldrich, R.W. (2014). Determination of parameter identifiability in nonlinear biophysical models: A bayesian approach. *Journal of General Physiology,* 143, p. 401-416.

Ho, Q.T., Carmeliet, J., Datta, A.K., Defraeye, T., Delele, M.A., Herremans, E., Opara, L., Ramon, H., Tijskens, E., Van Der Sman, R., Van Liedekerke, P., Verboven, P. et Nicolaï, B.M. (2013). Multiscale modeling in food engineering. *Journal of Food Engineering,* 114, p. 279-291.

Hong, H. P. (2013). Selection of regressand for fitting the extreme value distributions using the ordinary, weighted and generalized least squares methods. *Reliability Engineering & System Safet.*, 118, p. 71–80.

Howard, BM, Hung, Y-C et McWatters, K. (2011). Analysis of ingredient functionality and formulation optimization of pasta supplemented with peanut flour. *Journal of Food Science,* 76, p. E40–E47.

Hundal, J. et Takhar, P.S. (2010). Experimental study on the effect of glass transition on moisture profiles and stress-crack formation during continuous and time-varying drying of maize kernels. *Biosystems Engineering*, 106, p. 156-165.

Hunter, JE et Schmidt, FL. (2000). Fixed effects vs. random effects meta-analysis models: Implications for cumulative research knowledge. *International Journal of Selection and Assessment,* 8, p. 275–292.

Ilin, A et Raiko, T. (2010). Practical approaches to principal component analysis in the presence of missing values. *Journal of Machine Learning Research,* 11, p. 1957-2000.

Inazu, T., Iwasaki, K.I. et Furuta, T. (2003). Effect of air velocity on fresh Japanese noodle (Udon) drying. *LWT - Food Science and Technology,* 36, p. 277–280.

Inazu, T., Iwasaki, K.I. et Furuta, T. (2005). Stress and crack prediction during drying of Japanese noodle (udon). *International Journal of Food Science and Technology,* 40, p. 621-630.

Islas-Rubio, AR, Calderón de la Barca, AM, Cabrera-Chávez, F, Cota-Gastélum, AG et Beta, T. (2014). Effect of semolina replacement with a raw:popped amaranth flour blend on cooking quality and texture of pasta. *LWT - Food Science and Technology,* 57, p. 217–222.

Jang, S.S., Gopaluni R.B. (2011). Parameter estimation in nonlinear chemical and biological processes with unmeasured variables from small data sets. *Chemical Engineering Sicence,* 66, p. 2774-2787.

Jayasena, V et Nasar-Abbas, SM. (2012). Development and quality evaluation of high-protein and high-dietary-fiber pasta using lupin flour. *Journal of Texture Studies,* 43, p. 153–163.

Jayasankar, B.R., Ben-Zvi, A. et Huang, B. (2009). Identifiability and estimability study for a dynamic solid oxide fuel cell model. *Computers and Chemical Engineering,* 33, p. 484-492.

Jyotsna, R, Milind, Sakhare, SD, Inamdar, AA et Rao, GV. (2014). Effect of green gram semolina (*Phaseolus aureus*) on the rheology, nutrition, microstructure and quality characteristics of high-protein pasta. *Journal of Food Processing and Preservation,* 38, p. 1965–1972.

Kadam, SU et Prabhasankar P. (2012). Evaluation of cooking, microstructure, texture and sensory quality characteristics of shrimp meat-based pasta. *Journal of Textural Studies,* 43, p. 268–274.

Kang, D. D., Sibille, E., Kaminski, N. et Tseng, G.C. MetaQC: objective quality control and inclusion/exclusion criteria for genomic meta-analysis. *Nucleic Acids Research*, 40, p. e15.

Kaur, G, Sharma, S, Nagi, HPS et Dar, BN. (2012). Functional properties of pasta enriched with variable cereal brans. *Journal of Food Science and Technology,* 49, p. 467–474.

Kaur, G, Sharma, S, Nagi, HPS et Ranote, PS. (2013). Enrichment of pasta with different plant proteins. *Journal of Food Science and Technology,* 50, p. 1000–1005.

Kepes, S., Banks, G. C. et Oh, I.-S. (2014). Avoiding Bias in Publication Bias Research: The Value of 'Null' Findings. *Journal of Business and Psychology*, 29, p. 1–21.

Khan, R.S., Grigor, J., Winger, R. et Win, A. (2013). Functional food product development - Opportunities and challenges for food manufacturers. *Trends in Food Science and Technology*, 30, p. 27-37.

Khan, I, Yousif, AM, Johnson, SK et Gamlath, S. (2015). Acute effect of sorghum flour-containing pasta on plasma total polyphenols, antioxidant capacity and oxidative stress markers in healthy subjects: A randomised controlled trial. *Clinical Nutrition,* 34, p. 415–421.

Kies, C. et Fox, H. M. (1970). Determination of the first-limiting amino acid of wheat and triticale grain for humans. *Cereal Chemistry,* 47, p. 615–622.

Kim, YD et Choi, S. (2013). Variational bayesian view of weighted trace norm regularization for matrix factorization. *IEEE Signal Processing Letters,* 20, p. 261-264.

Kim, JH, Sim, JY et Kim, CS. (2015). Video deraining and desnowing using temporal correlation and low-rank matrix completion. *IEEE Transactions on Image Processing*, 24, p. 2658-2670.

Koç, B., Eren, I. et Kaymak Ertekin, F. (2008). Modelling bulk density, porosity and shrinkage of quince during drying: The effect of drying method. *Journal of Food Engineering,* 85, p. 340-349.

Koca, AF et Anil, M. (2007). Effect of flaxseed and wheat flour blends on dough rheology and bread quality. *Journal of the Science of Food and Agriculture,* 87, p. 1172–1175.

Koretz, R. (2002). Methods of meta-analysis: an analysis. *Current Opinion in Clinical Nutrition & Metabolic Care,* 5, p. 467–474.

Koricheva, J., Gurevitch, J. et Mengersen, K. (2013). *Handbook of Meta-Analysis in Ecology and Evolution.* Princeton University Press.

Kravaris, C. (1988). Identifiability of the nonlinearity in a quasilinear parabolic system. In *Proceedings of the 27th IEEE Conference on Decision and Control* , p. 245-248.

Krishnan, M. et Prabhasankar, P. (2012). Health Based Pasta: Redefining the Concept of the Next generation Convenience Food. *Critical Reviews in Food Science and Nutrition,* 52, p. 9-20.

Krokida, M.K. et Maroulis, Z.B. (1997). Effect of drying method on shrinkage and porosity. *Drying technology*, 15, p. 2441-2458.

Kulkarni, M. (2005). Determination of viscoelastic properties, glass transition behavior and sorption profiles of pasta as a function of temperature and moisture content. Thèse de doctorat, University of Idaho, Moscow, ID, USA.

Kumar, R, Da Silva, C, Akalin, O, Aravkin, AY, Mansour, H, Recht, B et Herrmann, FJ. (2015). Efficient matrix completion for seismic data reconstruction. *Geophysics,* 80, p. V97-V114.

Lagrange, S., Delanoue, N. et Jaulin, L. (2008). Injectivity analysis using interval analysis: Application to structural identifiability, *Automatica,* 44, p. 2959–2962.

Lajeunessei, M. J. (2011). On the meta-analysis of response ratios for studies with correlated and multi-group designs. *Ecology*, 92, p. 2049–2055.

Lamacchia, C., Di Luccia, A., Baiano, A., Gambacorta, G., la Gatta, B., Pati, S. et La Notte, E. (2007). Changes in pasta proteins induced by drying cycles and their relationship to cooking behaviour. *Journal of Cereal Science,* 46, p. 58-63.

Lee, RE, Manthey, FA et Hall, III CA. (2003). Effects of boiling, refrigerating, and microwave heating on cooked quality and stability of lipids in macaroni containing ground flaxseed. *Cereal Chemistry,* 80, p. 570–574.

Li, L, Li, Y et Li, Z. (2013). Efficient missing data imputing for traffic flow by considering temporal and spatial dependence. *Transporation Research Part C: Emerging Technologies*, 34, p. 108-120.

Li, M., Zhu, K.X., Guo, X.N., Brijs, K. et Zhou, H.M. (2014). Natural additives in wheat-based pasta and noodle products: Opportunities for enhanced nutritional and functional properties. *Comprehensive Reviews in Food Science and Food Safety,* 13, p. 347-357.

Lilly, H. A. et Lowbury, E. J. (1971). Disinfection of the skin: an assessment of some new preparations. *British Medical Journal,* 3, p. 674–676.

Litchfield, J.B. et Okos, M.R. (1988). Prediction of corn kernel stress and breakage induced by drying, tempering and cooling. *Transactions of the American Society of Agricultural Engineers,* 31, p. 585-594.

Litchfield, J.B. et Okos, M.R. (1992). Moisture diffusivity in pasta during drying. *Journal of Food Engineering,* 17, p. 117-142.

Liu, H., Qi, J. et Hayakawa, K. (1997). Rheological properties including tensile fracture stress of semolina extrudates influenced by moisture content. *Journal of Food Science,* 62, p. 813-820.

Liu, Y., Bhandari, B. et Zhou, W. (2006). Glass transition and enthalpy relaxation of amorphous food saccharides: A review. *Journal of Agricultural and Food Chemistry,* 54, p. 5701-5717.

Liu, Y, Pan, Y, Sun, Z et Huang, D. (2014). Statistical monitoring of wastewater treatment plants using variational Bayesian PCA. *Industrial and Engineering Chemistry Research,* 53, p. 3272-3282.

Liu, M., Zang, S. et Zhou, D. (2005). Fast leak detection and location of gas pipelines based on an adaptive particle filter. *International Journal of Applied Mathematics and Computer Science,* 15, p. 541-550.

Ljung, L. et Glad, T. (1994). On global identifiability for arbitrary model parametrizations. *Automatica*, 30, p. 265–276.

Lord, C.R. (2000). *Guide to information sources in engineering*. Englewood, CO: Libraries Unlimited.

Loulou, T., Adhikari, B. et Lecomte, D. (2006). Estimation of concentration-dependent diffusion coefficient in drying process from the space-averaged concentration versus time with experimental data. *Chemical Engineering Science,* 61, p. 7185–7198.

Lowbury, E. J. L. et Lilly, H. A. (1973). Use Of 4% Chlorhexidine Detergent Solution (Hibiscrub) And Other Methods Of Skin Disinfection. *British Medical Journal*, 1, p. 510–515.

Lowbury, E. J. L., Lilly, H. A. et Ayliffe, G. A. J. (1974). Preoperative Disinfection Of Surgeons' Hands: Use Of Alcoholic Solutions And Effects Of Gloves On Skin Flora. *British Medical Journal,* 4, p. 369–372.

Lucisano, M, Pagani, MA, Mariotti, M et Locatelli, DP. (2008). Influence of die material on pasta characteristics. *Food Research International,* 41, p. 646–652.

Luo, S., Pang, H., Li, J., Zhang, Q., Chen, D., Pan, M. et Luo, F. (2013). Calibration strategy and generality test of three-axis magnetometers. *Journal of the International Measurement Confederation,* 46, p. 3918-3923.

Luttinen, J et Ilin, A. (2010). Transformations in variational Bayesian factor analysis to speed up learning. *Neurocomputing*, 73, p. 1092-1102.

Madhumitha, S et Prabhasankar, P. (2011). Influence of additives on functional and nutritional quality characteristics of black gram flour incorporated pasta. *Journal of Textural Studies,* 42, p. 441–450.

Manno, D, Filippo, E, Serra, A, Negro, C, De Bellis, L et Miceli, A. (2009). The influence of inulin addition on the morphological and structural properties of durum wheat pasta. *International Journal of Food Science and Technology,* 44, p. 2218–2124.

Manthey, FA et Dash, S. (2010). Improving the physical and cooking qualities of pasta containing flaxseed flour. In *Proceedings of the 63rd Flax Institute of the United States* p. 82-86.

Manthey, FA et Hall III, CA. (2007). Effect of processing and cooking on the content of minerals and protein in pasta containing buckwheat bran flour. *Journal of the Science of Food and Agriculture,* 87, p. 2026–2033.

Manthey, F.A. et Schorno, A.L. (2002). Physical and cooking quality of spaghetti made from whole wheat durum. *Cereal Chemistry,* 79, p. 504-510.

Marconi, E, Carcea, M, Schiavone, M et Cubadda, R. (2002). Spelt (*Triticum spelta* L.) pasta quality: Combined effect of flour properties and drying conditions. *Cereal Chemistry,* 79, p. 634–639.

Marti, A., et Pagani, M.A. (2013). What can play the role of gluten in gluten free pasta? *Trends in Food Science and Technology,* 31, p. 63-71.

Martinez-Lopez, B., Peyron, S., Gontard, N. et Mauricio-Iglesias, M. (2015). Practical identifiability analysis for the characterization of mass transport properties in migration tests. *Industrial & Engineering Chemistry Research,* 54, p. 4725–4736.

Martínez-Villaluenga, C., Torres, A., Frias, J. et Vidal-Valverde, C. Semolina supplementation with processed lupin and pigeon pea flours improve protein quality of pasta. *LWT - Food Science and Technology,* 43, p. 617-622.

McDonald, K. et Sun, D.-W. (2001). The formation of pores and their effects in a cooked beef product on the efficiency of vacuum cooling. *Journal of Food Engineering*, 47, p. 175–183.

McDougall, P. (2010). The Cost of New Agrochemical Product Discovery, Development and Registration in 1995, 2000 and 2005-8. European Crop Protection Association. En ligne: http://www.croplifeamerica.org/wp-content/uploads/2015/10/PM-RD-Study_2-25-10.pdf. (consulté le 25 novembre 2015).

Mengersen, K, Schmid, CH, Jennions, MD et Gurevitch, J. (2013). Statistical models and approaches to inference. In: Koricheva J, Gurevitch J, Mengersen K, editors. Handbook of meta-analysis in ecology and evolution. Princeton, N.J.: Princeton University Press. p. 89–107.

Mercier, S, Des Marchais, L-P, Villeneuve, S et Foisy M. (2011a). Effect of die material on engineering properties of dried pasta. *Procedia Food Sci,* 1, p. 557–562.

Mercier, S, Marcos, B, Moresoli, C, Mondor, M et Villeneuve S. (2014a). Modeling of internal moisture transport during durum wheat pasta drying. *Journal of Food Engineering,* 124, p. 19–27.

Mercier, S, Marcos, B, Moresoli, C, Mondor, M et Villeneuve S. (2015). Effect of the water content measurements on the estimation and identifiability of water diffusion and

convection mass transfer coefficients. *International Journal of Heat and Mass Transfer,* 90, p. 480–490.

Mercier, S., Mondor, M., Moresoli, C., Villeneuve, S. et Marcos, B. (2013b). Drying of durum wheat pasta and enriched pasta: a review of modeling approaches. *Critical Reviews in Food Science and Nutrition.* Accepté pour publication. doi: 10.1080/10408398.2012.757691.

Mercier, S, Mondor, M, Villeneuve, S, Marcos, B et Moresoli C. (2014b). Assessment of the oxidative stability of flaxseed-enriched lasagna using the Rancimat method. *Journal of Food Processing and Preservation*. Accepté pour publication. doi:10.1111/jfpp.12404.

Mercier, S., Moresoli, C., Villeneuve, S., Mondor, M. et Marcos, B. (2013a). Sensitivity analysis of parameters affecting the drying behaviour of durum wheat pasta. *Journal of Food Engineering*, 118, p. 108-116.

Mercier, S., Moresoli, C., Mondor, M., Villeneuve, S. et Marcos, B. (2016). A meta-analysis of enriched pasta: what are the effects of enrichment and process specifications on the quality attributes of pasta? *Comprehensive Reviews in Food Science and Food Safety. Accepted for publication. DOI: 10.1111/1541-4337.12207.*

Mercier, S., Villeneuve, S., Mondor, M. et Des Marchais, L.P. (2011b). Evolution of porosity, shrinkage and density of pasta fortified with pea protein concentrate during drying. *LWT - Food Science and Technology,* 44, p. 883-890.

Mercier, S., Villeneuve, S., Mondor, M., Drolet, H., Ippersiel, D., Lamarche, F. et Des Marchais, L.P. (2012). Mixing Properties and Gluten Yield of Dough Enriched with Pea Protein Isolates. *Journal of Food Research,* 1, p. 13-23.

Mert, B, Tekin, A, Demirkesen, I et Kocak, G. (2014). Production of microfluidized wheat bran fibers and evaluation as an ingredient in reduced flour bakery product. *Food and Bioprocess Technology,* 7, p. 2889–2901.

Migliori, M., Gabriele, D., De Cindio, B. et Pollini, C.M. (2005a). Modelling of high quality pasta drying: Mathematical model and validation. *Journal of Food Engineering,* 69, p. 387-397.

Migliori, M., Gabriele, D., De Cindio, B. et Pollini, C.M. (2005b). Modelling of high quality pasta drying: Quality indices and industrial application. *Journal of Food Engineering,* 71, p. 242-251.

Mitra, K. (2008). Genetic algorithms in polymeric material production, design, processing and other applications: A review. *International Materials Reviews*, 53, p. 275-297.

Montgomery, D.C. (2013). *Design and analysis of experiments*. Hoboken, NJ: John Wiley and Sons.

Montville, R. et Schaffner, D. W. (2011). A Meta-Analysis of the Published Literature on the Effectiveness of Antimicrobial Soaps. *Journal of Food Protection*, 74, p. 1875–82.

Musielak, G. (1996). Internal stresses caused by outflow of moisture and phase change inside dried material. *Drying Technology,* 14, p. 289-306.

Nam, I.-S., Mengersen, K. et Garthwaite, P. (2003). Multivariate meta-analysis. *Statistics in Medicine*, 22, p. 2309–2333.

Nasrallah, S.B. et Perre, P. (1988). Detailed study of a model of heat and mass transfer during convective drying of porous media. *International Journal of Heat and Mass Transfer,* 31, p. 957-967.

Navarro-Laboulais, J., Cardona, S.C., Torregrosa, J.I., Abad, A. et Lopez, F. (2006). Structural identifiability analysis of the dynamic gas-liquid film model. *AICHE Journal,* 52, p. 2851-2863.

Nguyen, MH et De La Torre, F. (2009). Robust kernel principal component analysis. In *Advances in Neural Information Processing Systems 21 - Proceedings of the 2008 Conference,* p. 1185-1192.

Nguyen, V.V. et Wood, E.F. (1982). Review and unification of linear identifiability concepts, *SIAM Review,* 24, p. 34–51.

Ni, H. (1997). Multiphase moisture transport in porous media under internal heating of microwaves. Thèse de doctorat, Cornell University, Ithaca, New York.

Niazi, A. et Leardi, R. (2012). Genetic algorithms in chemometrics. *Journal of Chemometrics,* 26, p. 345-351.

Nicoletti, G., Boghossian, V. et Borland, R. (1990). Hygienic hand disinfection: a comparative study with chlorhexidine detergents and soap. *Journal of Hospital Infection*, 15, p. 323–337.

Nielsen, M.A., Sumner, A.K. et Whalley, L.L. (1980). Fortification of pasta with pea flour and air-classified pea protein concentrate. *Cereal Chemistry,* 57, p. 203-207.

NineSigma (2015). Cross Sectional Moisture Distribution in Dry Spaghetti. En ligne: https://ninesights.ninesigma.com/rfps/-/rfp-portlet/rfpViewer/2773?utm_source=Email&utm_medium=email&utm_campaign=2277372. (consulté le 27 novembre 2015).

Noshad, M., Shahidi, F., Mohebbi, M. et Ali Mortazavi, S. (2012). Desorption isotherms and thermodynamic properties of fresh and osmotic-ultrasonic dehydrated quinces. *Journal of Food Processing and Preservation,* 37, p. 381-390.

Nounou, MN, Bakshi, BR, Goel, PK et Shen, X. (2002). Bayesian principal component analysis. *Journal of Chemometrics,* 16, p. 576-595.

Oba, S, Sato, MA, Takemasa, I, Monden, M, Matsubara, KI et Ishii, S. (2003). A Bayesian missing value estimation method for gene expression profile data. *Bioinformatics,* 19, p. 2088-2096.

Ogawa, T., Kobayashi, T. et Adachi, S. (2012). Prediction of pasta drying process based on a thermogravimetric analysis. *Journal of Food Engineering,* 111, p. 129-134.

Ojajarvi, J. (1980). Effectiveness of hand washing and disinfection methods in removing transient bacteria after patient nursing. *The Journal of Hygiene,* 85, p. 193–203.

Ousegui, A., Moresoli, C., Dostie, M. et Marcos, B. (2010). Porous multiphase approach for baking process - Explicit formulation of evaporation rate. *Journal of Food Engineering,* 100, p. 535-544.

Ovando-Martinez, M, Sáyago-Ayerdi, S, Agama-Acevedo, E, Goñi, I et Bello-Pérez, LA. (2009). Unripe banana flour as an ingredient to increase the undigestible carbohydrates of pasta. *Food Chemistry,* 113, p. 121–126.

Owens, G. (2001). Cereals Processing Technology. London (UK): Woodhead Publishing.

Park, K.J., Ardito, T.H., Ito, A.P., Park, K.J.B., de Oliveira, R.A. et Chiorato, M. (2007). Effective diffusivity determination considering shrinkage by means of explicit finite difference method. *Drying Technology,* 25, p. 1313-1319.

Paulson, D. S., Riccardi, C., Beausoleil, C. M., Fendler, E. J., Dolan, M. J., Dunkerton, L. V. et Williams, R. A. (1999). Efficacy evaluation of four hand cleansing regimens for food handlers. *Dairy, food, and environmental sanitation*, 19, p. 680–684.

Perry, R.H. et Green, D. (1984). *Perry's Chemical Engineers' Handbook* (6th ed.). New York (USA): McGraw-Hill.

Perussello, C.A., Mariani, V.C., Masson, M.L. et Castilhos, F.D. (2013). Determination of thermophysical properties of yacon (Smallanthus sonchifolius) to be used in a finite element simulation. *International Journal of Heat and Mass Transfer,* 67, p. 1163-1169.

Peters, J. L., Sutton, A. J., Jones, D. R., Abrams, K. R. et Rushton, L. (2007). Performance of the trim and fill method in the presence of publication bias and between-study heterogeneity. *Statistics in Medicine,* 26, p. 4544–4562.

Petitot, M., Boyer, L., Minier, C. et Micard, V. (2010). Fortification of pasta with split pea and faba bean flours: Pasta processing and quality evaluation. *Food Research International,* 116, p. 401-412.

Petropoulos, J.H., Sanopoulou, M., et Papadokostaki, K.G. (2011). Physically insightful modeling of non-Fickian kinetic regimes encountered in fundamental studies of isothermal sorption of swelling agents in polymeric media. *European Polymer Journal,* 47, p. 2053-2062.

Pigott, T. D. (2012). *Advances in Meta-Analysis*. Boston, MA: Springer US.

Pillai, DS, Prabhasankar, P, Jena, BS et Anandharamakrishnan, C. (2012). Microencapsulation of garcinia cowa fruit extract and effect of its use on pasta process and quality. *International Journal of Food Properties,* 15, p. 590–604.

Ponsart, G., Vasseur, J., Frias, J.M., Duquenoy, A. et Méot, J.M. (2003). Modelling of stress due to shrinkage during drying of spaghetti. *Journal of Food Engineering,* 57, p. 277-285.

Power, KA, Villeneuve, S, Mondor, M, Fustier, P, Arcand, Y, Lamarche, F, Britten, M, Cui, S, Cao, R, Fofana, B et Wanasundara PKJPD. (2012). Recent progress on the incorporation of flaxseed into cereal based matrices: Delivery of bioactives to target sites and a comprehensive assessment of their biological effects. In *Proceedings of the 64th Flax Institute of the United States*, p. 57–63.

Qing-guo, H., Min, Z., Mujumdar, A., Wei-hua, D. et Jin-cai, S. (2006). Effects of different drying methods on the quality changes of granular edamame. *Drying Technology,* 24, p. 1025-1032.

Quintana, S. M. et Minami, T. (2006). Guidelines for Meta-Analyses of Counseling Psychology Research. *Journal of Counseling Psychology*, 34, p. 839–877.

Rahman, M.S. (1995). *Handbook of Food Preservation*. New York (USA): CRC Press.

Rahman, M.S. (2001). Toward prediction of porosity in foods during drying: a brief review. *Drying Technology,* 19, p. 1-13.

Rahman, M.S. (2006). State diagram of foods: Its potential use in food processing and product stability. *Trends in Food Science and Technology*, 17, p. 129-141.

Raiko, T, Valpola, H, Harva, M et Karhunen, J. (2007). Building blocks for variational Bayesian learning of latent variable models. *Journal of Machine Learning Research,* 8, p. 155-201.

Rajeswari, G, Susanna, S, Prabhasankar, P et Venkateswara Rao, G. (2013). Influence of onion powder and its hydrocolloid blends on pasta dough, pasting, microstructure, cooking and sensory characteristics. *Food Bioscioscience,* 4, p. 13–20.

Rakesh, V. et Datta, A.K. (2011). Microwave puffing: Determination of optimal conditions using a coupled multiphase porous media - Large deformation model. *Journal of Food Engineering,* 107, p. 152-163.

Ramachandran, R. et Barton, P.I. (2010). Effective parameter estimation within a multi-dimensional population balance model framework, *Chemical Engineering Science,* 65, p. 4884-4893.

Raue, A., Kreutz, C., Maiwald, T., Bachmann, J., Schilling, M., Klingmüller, U. et Timmer, J. (2009). Structural and practical identifiability analysis of partially observed dynamical models by exploiting the profile likelihood. *Bioinformatics,* 25, p. 1923-1929.

Ribotta, P.D., Edel Leon, A., Pérez, G.T. et Anon, M.C. (2005). Electrophoresis studies for determining wheat-soy protein interactions in dough and bread. *European Food Research and Technology,* 222, p. 48-53.

Roberts, P. D., Stewart, G. B. et Pullin, A. S. (2006) Are review articles a reliable source of evidence to support conservation and environmental management? A comparison with medicine, *Biological Conservation*, 132, p. 409–423.

Roccia, P., Ribotta, P.D., Pérez, G.T. et Leon, A. E. (2009). Influence of soy protein on rheological properties and water retention capacity of wheat gluten. *LWT - Food Science and Technology,* 42, p. 358-362.

Rothstein, H., Sutton, A. J. et Borenstein, M. (2005). *Publication bias in meta-analysis: prevention, assessment and adjustments*. Hoboken, NJ: Wiley.

Sabanis, D., Makri, E. et Doxastakis, G. (2006). Effect of durum flour enrichment with chickpea flour on the characteristics of dough and lasagne. *Journal of the Science of Food and Agriculture,* 86, p. 1938-1944.

Sabanis, D et Tzia, C. (2010). Effect of hydrocolloids on selected properties of gluten-free dough and bread. *Food Science and Technology International,* 17, p. 279–291.

Sánchez-Meca, J. et Marín-Martínez, F. (2010). Meta-analysis in Psychological Research. *International Journal of Psychological Research*, 3, p. 150–162.

Sant'Anna, V, Christiano, FDP, Marczak, LDF, Tessaro, IC et Thys, RCS. (2014). The effect of the incorporation of grape marc powder in fettuccini pasta properties. *LWT - Food Science and Technology,* 58, p. 497–501.

Saravacos, G.D. et Maroulis, Z.B. (2001). Transport properties of food. New York (USA): Basel.

Scanlon, M.G., Day, A.J. et Povey, M.J.W. (1998). Shear Stiffness and Density in Potato Parenchyma. *International Journal of Food Science and Technology,* 33, p. 461-464.

Schaber, J. et Klipp, E. (2011). Model-based inference of biochemical parameters and dynamic properties of microbial signal transduction networks. *Current Opinion in Biotechnology,* 22, p. 109-116.

Scheidegger, A. E. (1960). The physics of flow through porous media. Toronto (Canada): University of Toronto Press.

Schulze, R. (2007). Current methods for meta-analysis: Approaches, issues, and developments. *Zeitschrift für Psychologie*, 215, p. 90–103.

Selih, J., Sousa, A.C.M. et Bremner, T.W. (1996).Moisture transport in initially fully saturated concrete during drying. *Transport in Porous Media,* 24, p. 81-106.

Shogren, R.L., Hareland, G.A. et Wu, Y.V. (2006). Sensory Evaluation and Composition of Spaghetti Fortified with Soy Flour. *Journal of Food Science,* 71, p. S428-S432.

Shreenithee, CR et Prabhasankar, P. (2013). Effect of different shapes on the quality, microstructure, sensory and nutritional characteristics of yellow pea flour incorporated pasta. *Journal of Food Measurement and Characterization,* 7, p. 166–176.

Sickbert-Bennett, E. E., Weber, D. J., Gergen-Teague, M. F., Sobsey, M. D., Samsa, G. P. et Rutala, W. A. (2005). Comparative efficacy of hand hygiene agents in the reduction of bacteria and viruses. *American Journal of Infection Control*, 33, p. 67–77.

Silva, W.P., Precker, J.W., Silva, C.M.D.P.S. et Gomes, J.P. (2010). Determination of effective diffusivity and convective mass transfer coefficient for cylindrical solids via analytical solution and inverse method: Application to the drying of rough rice. *Journal of Food Engineering,* 98, p. 302-308.

Sinesio, F, Paoletti, F, D'Egidio, MG, Moneta, E, Nardo, N, Peparaio, M et Comendador FJ. (2008). Flavor and texture as critical sensory parameters of consumer acceptance of barley pasta. *Cereal Foods World,* 53, p. 206–213.

Singh, P., Cushman, J. et Maier, D. (2003). Multiscale fluid transport theory for swelling biopolymers. *Chemical Engineering Science,* 58, p. 2409–2419.

Singh, P.P., Maier, D.E., Cushman, J.H., Haghighi, K. et Corvalan, C. (2004). Effect of viscoelastic relaxation on moisture transport in foods. Part I: Solution of general transport equation. *Journal of Mathematical Biology*, 49, p. 1-19.

Sinha, S et Manthey, FA. (2008). Semolina and hydration level during extrusion affect quality of fresh pasta containing flaxseed flour. *Journal of Food Processing and Preservation,* 32, p. 546–559.

Sissons, MJ, Egan, NE et Gianibelli, MC. (2005). New insights into the role of gluten on durum pasta quality using reconstitution method. *Cereal Chemistry,* 82, p. 601–608.

Sivam, AS, Sun-Waterhouse, D, Quek, S et Perera, CO. (2010). Properties of bread dough with added fiber polysaccharides and phenolic antioxidants: A review. *Journal of Food Science,* 75, p. R163–R174.

Smidl, V and Quinn, A. (2007). On Bayesian principal component analysis. *Computational Statistics and Data Ananalysis,* 51, p. 4101-4123.

Smulders, Y. M. (2013). A two-step manuscript submission process can reduce publication bias. *Journal of Clinical Epidemiology*, 66, p. 946–947.

Sozer, N, Dalgıç, AC et Kaya, A. (2007). Thermal, textural and cooking properties of spaghetti enriched with resistant starch. *Journal of Food Engineering,* 81, p. 476–484.

Srikiatden, J. et Roberts, J.S. (2007). Moisture transfer in solid food materials: A review of mechanisms, models, and measurements. *International Journal of Food Properties,* 10, p. 739-777.

Starling, S. (2014). *Functional foods resist recession but failure rate stays high: analyst.* http://www.nutraingredients.com/Markets-and-Trends/Functional-foods-resist-recession-but-failure-rate-stays-high-Analyst (consulté le 14 décembre 2015).

Steglich, T, Bernin, D, Röding, M, Nydén, M, Moldin, A, Topgaard, D et Langton, M. (2014). Microstructure and water distribution of commercial pasta studied by microscopy and 3D magnetic resonance imaging. *Food Research International,* 62, p. 644–652.

Stewart-Knox, B., et Mitchell, P. (2003). What separates the winners from the losers in new food product development? *Trends in Food Science and Technology*, 14, p. 58-64.

Stiles M. E. et Sheena, A. Z. (1985). Efficacy of Low-Concentration Iodophors for Germicidal Hand Washing. *The Journal of Hygyene,* 94, p. 269–277.

Stuknyte, M, Cattaneo, S, Pagani, MA, Marti, A, Micard, V, Hogenboom, J et De Noni, I. (2014). Spaghetti from durum wheat: Effect of drying conditions on heat damage, ultrastructure and in vitro digestibility. *Food Chemistry,* 149, p. 40–46.

Sutton, A. J., Abrams, K. R. et Jones, D. R. (2001). An illustrated guide to the methods of meta-analysis. *Journal of Evaluation in Clinical Practice,* 7, p. 135–148.

Takhar, P.S., Kulkarni, M.V., et Huber, K. (2006). Dynamic viscoelastic properties of pasta as a function of temperature and water content. *Journal of Texture Studies,* 37, p. 696-710.

Takhar, P.S. (2008). Role of glass-transition on fluid transport in porous food materials. *International Journal of Food Engineering,* 4, art. no. 5

Takhar, P.S., Kulkarni, M.V. et Huber, K. (2006). Dynamic viscoelastic properties of pasta as a function of temperature and water content. *Journal of Texture Studies*, 37, p. 696-710.

Tan, H, Wu, Y, Cheng, B, Wang, W et Ran, B. (2014). Robust missing traffic flow imputation considering nonnegativity and road capacity. *Mathematical Problems in Engineering,* 763469.

Tayakout-Fayolle, M., Jolimaitre, E. et Jallut, C. (2000). Consequence of structural identifiability properties on state-model formulation for linear inverse chromatography. *Chemical Engineering Science* ,55, p. 2945-2956.

Teergele, J. et Danai, K. (2015). Selection of outputs for distributed parameter systems by identifiability analysis in the time-scale domain. *International Journal of Systems Science,* 46, p. 2939–2954.

Tonelli, M, Hackam, D et Garg, AX. (2009). Primer on systematic review and meta-analysis. In: Parfrey P, Barrett P, editors. Clinical epidemiology: Practice and methods. Methods in molecular biology series, vol. 473. New York: Humana Press. p. 217–33.

Toshima, Y., Ojima, M., Yamada, H., Mori, H., Tonomura, M., Hioki, Y. et Koya, E. (2001). Observation of everyday hand-washing behavior of Japanese, and effects of antibacterial soap. *International Journal of Food Microbiology*, 68, p. 83–91.

Torres, A., Frias, J., Granito, M., Guerra, M. et Vidal-Valverde, C. (2007a). Chemical, biological and sensory evaluation of pasta products supplemented with α-galactoside free lupin flours. *Journal of the Science of Food and Agriculture,* 87, p. 74-81.

Torres, A, Frias, J, Granito, M et Vidal-Valverde, C. (2006). Fermented pigeon pea (*Cajanus cajan*) ingredients in pasta products. *Journal of Agricultural and Food Chemistry,* 54, p. 6685–6691.

Torres, A, Frias, J, Granito, M et Vidal-Valverde, C. (2007b). Germinated *Cajanus cajan* seeds as ingredients in pasta products: Chemical, biological and sensory evaluation. *Food Chemistry,* 101, p. 202–211.

Tricco, A. C., Tetzlaff, J. et Moher, D. (2011). The art and science of knowledge synthesis. *Journal of Clinical Epidemiology,* 64, p. 11–20.

Tudorică, CM, Kuri, V et Brennan, CS. (2002). Nutritional and physicochemical characteristics of dietary fiber enriched pasta. *Journal of Agricultural and Food Chemistry,* 50, p. 347–356.

Tuorila, H. et Cardello, A.V. (2002). Consumer responses to an off-flavor in juice in the presence of specific health claims. *Food Quality and Preference,* 13, p. 561-569.

Ugarcic-Hardi, Z, Hackenberger, D, Šubarić, D et Hardi J. (2003). Effect of soy, maize and extruded maize flour addition on physical and sensory characteristics of pasta. *Italian Journal of Food Science,* 15, p. 277–290.

Valentine, J. C., Pigott, T. D. et Rothstein, H. R. How Many Studies Do You Need? A Primer on Statistical Power for Meta-Analysis. *Journal of Educational and Behavioral Statistics*, 35, p. 215–247.

van den Hof, J.M. (1998). Structural identifiability of linear compartmental systems, *IEEE Transactions on Automatic Control,* 43, p. 800–818.

Vanlier, J., Tiemann, C.A., Hilbers, P.A.J. et van Riel, N.A.W. (2013). Parameter uncertainty in biochemical models described by ordinary differential equations. *Mathematical Biosciences,* 246, p. 305–314.

Veladat, R., Zokaee Ashtiani, F., Rahmani, M. et Miri, T. (2011). Review of numerical modeling of pasta drying, a closer look into model parameters. *Asia-Pacific journal of chemical engineering,* 7, p. 159-170.

Verbeke, W. (2006). Functional foods: Consumer willingness to compromise on taste for health? *Food Quality and Preference,* 17, p. 126-131.

Vernaza, MG, Biasutti, E, Schmiele, M, Jaekel, LZ, Bannwart, A et Chang, YK. (2012). Effect of supplementation of wheat flour with resistant starch and monoglycerides in pasta dried at high temperatures. *International Journal of Food Science and Technology,* 47, p. 1302–1312.

Viechtbauer, W. (2005). Bias and Efficiency of Meta-Analytic Variance Estimators in the Random-Effects Model. *Journal of Educational and Behavioral Statistics,* p. 261–293.

Villeneuve, S, Des Marchais, L-P, Gauvreau, V, Mercier, S, Do, CB et Arcand, Y. (2013). Effect of flaxseed processing on engineering properties and fatty acids profiles of pasta. *Food and Bioproducts Processing,* 91, p. 183–191.

Villeneuve, S. et Gélinas, P. (2007). Drying kinetics of whole durum wheat pasta according to temperature and relative humidity. *LWT - Food Science and Technology,* 40, p. 465-471.

Vinjamur, M., et Cairncross, R.A. (2002). Non-Fickian nonisothermal model for drying of polymer coatings. *AIChE Journal,* 48, p. 2444-2458.

Vincent, J.F.V. (1989). Relationship Between Density and Stiffness of Apple Flesh. *Journal of the Science of Food and Agriculture,* 47, p. 443-463.

Vorotnikov, D.A. (2013). Anomalous diffusion in polymers: Long-time behaviour. *Fields Institute Communications,* 64, p. 481-496.

Waananen, K.M. et Okos, M.R. (1996). Effect of porosity on moisture diffusion during drying of pasta. *Journal of Food Engineering,* 28, p. 121-137.

Wagner, M., Morel, M.-H., Bonicel, J. et Cuq, B. (2011). Mechanisms of Heat-Mediated Aggregation of Wheat Gluten Protein upon Pasta Processing. *Journal of Agricultural and Food Chemistry*, 59, p. 3146-3154.

Walter, E. et Lecourtier, Y. (1982). Global approaches to identifiability testing for linear and nonlinear state space models. *Mathematics and Computers in Simulation,* 24, p. 472–482.

Wan, T.H., Saccoccio, M., Chen, C. et Ciucci, F. (2015). Assessing the identifiability of *k* and *D* in electrical conductivity relaxation via analytical results and nonlinearity estimates. *Solid State Ionics,* 270, p. 18–32.

Wang, N. et Brennan, J.G. (1995). Changes in structure, density and porosity of potato during dehydration. *Journal of Food Engineering,* 24, p. 61-76.

Wang, Q. (2013). Kernel Principal Component Analysis and its Applications in Face Recognition and Active Shape Models. *arXiv preprint 2012*, p.1207.3538.

Wang, H, Zhao, R et Cen, Y. (2014). Rank adaptive atomic decomposition for low-rank matrix completion and its application on image recovery. *Neurocomputing*, 145, p. 374-380.

Ward, A. (2013). Spurious Correlations and Causal Inferences. *Erkenntnis*, 78, p. 699–712.

Whitaker, S. (1977). Simultaneous heat, mass and momentum transfer in porous media: A theory of drying. *Advance in Heat Transfer*, 12, p. 119–203.

Wieseler, B. (2010). Reporting a Systematic Review. *Chest Journal*, 137, p. 1240.

Wood, J. A. (2009). Texture, processing and organoleptic properties of chickpea-fortified spaghettie with insights to the underlying mechanisms of traditional durum pasta quality. *Journal of Cereal Science,* 49, p. 128-133.

Wu, YV, Hareland, GA et Warner, K. (2001). Protein-enriched spaghetti fortified with corn gluten meal. *Journal of Agricultural and Food Chemistry,* 49, p. 3906–3910.

Xing, H., Takhar, P.S., Helms, G. et He, B. (2007). NMR imaging of continuous and intermittent drying of pasta. *Journal of Food Engineering,* 78, p. 61-68.

Yalla, SR et Manthey, FA. (2006). Effect of semolina and absorption level on extrusion of spaghetti containing non-traditional ingredients. *Journal of the Science of Food and Agriculture,* 86, p. 841–848.

Yanez-Farias, G.A., Bernal-Aguilar, V., Ramirez-Rodriguez, L. et Barron-Hoyos, J.M. (1999). Note. Fortification of some cereal foods with a chickpea protein concentrate. *Food Science Technology International,* 5, p. 89-93.

Ying, S et Guang, D. (2009). Kernel PCA regression for missing data estimation in DNA microarray analysis. In *Proceedings - IEEE International Symposium on Circuits and Systems*, 5118046, p. 1477-1480.

Zhang, J. et Datta, A.K. (2006). Mathematical modeling of bread baking process. *Journal of Food Engineering,* 75, p. 78-89.

Zhao, Y.H., Manthey, F.A., Chang, S.K.C., Hou, H.J. et Yuan, S.H. (2005). Quality characteristics of Spaghetti as Affected by Green and yellow Pea, Lentil, and Chickpea Flours. *Journal of Food Science,* 70, p. S371-S376.

Zhou, M., Li, Y., Xiang, Z., Swoboda, G. et Cen, Z. (2007). A Modified Extended Bayesian Method for Parameter Estimation. *Tsinghua Science and Technology,* 12, p. 546-553.

Zhu, A. et Shen, X. (2014). The model and mass transfer characteristics of convection drying of peach slices. *International Journal of Heat and Mass Transfer,* 72, p. 345-351.

Zouari, N, Abid, M, Fakhfakh, N, Ayadi, MA, Zorgui, L, Ayadi, M et Attia, H. (2011). Blue-green algae (*Arthrospira platensis*) as an ingredient in pasta: Free radical scavenging activity, sensory and cooking characteristics evaluation. *International Journal of Food Sciences and Nutrition,* 62, p. 811–813.

Zweifel, C., Handschin, S., Escher, F. et Conde-Petit, B. (2003). Influence of High-Temperature Drying on Structural and Textural Properties of Durum Wheat Pasta. *Cereal Chemistry,* 80, p. 159-167.

ANNEXE A. Impact du transfert d'énergie sur la modélisation du séchage des pâtes

Rapport interne rédigé le 05/2015 par Samuel Mercier. Titre Original: Contribution of heat transfer on the prediction of pasta glass transition and required drying time

Résumé

La revue de la littérature (chapitre 2) a montré que la résistance au transfert d'énergie est considérée négligeable dans la plupart des modèles décrivant le séchage des pâtes en raison de leur nombre de Lewis élevé. Cependant, l'impact de cette hypothèse sur la modélisation de la transition vitreuse et la prédiction du temps de séchage requis n'a pas été vérifié pour des températures de séchage élevées. Dans cet article, la modélisation de la transition vitreuse et du transport de l'eau à l'intérieur des pâtes obtenue avec un modèle couplant le transfert de masse et d'énergie est comparée avec un modèle Fickian isotherme. La comparaison confirme que la résistance au transfert d'énergie a un impact négligeable sur la prédiction de la teneur en eau globale des pâtes lors du séchage à basse température (40 °C). Pour un séchage à 70 °C ou 95 °C, le modèle isotherme sous-estime le temps requis pour sécher les pâtes. Les simulations indiquent que 38%, pour un séchage à 70 °C, et 50%, pour un séchage à 95 °C, de la pâte n'aurait pas atteint l'état vitreux si elle était retirée du séchoir au temps de séchage requis estimé à partir d'un modèle isotherme. Ce rapport indique la nécessité, à partir d'une température de séchage d'environ 70 ºC, de considérer la résistance au transfert d'énergie pour prédire avec précision la transition vitreuse et le temps requis pour sécher les pâtes.

Nomenclature

a_w	water activity coefficient, -
C	concentration, kg m^{-3}
C_P	heat capacity of the pasta, J kg^{-1} °C $^{-1}$
D_{eff}	effective water diffusion coefficient, m^2 s^{-1}
h_h	convection heat transfer coefficient, W m^{-2} °C $^{-1}$
h_m	convection mass transfer coefficient, m s^{-1}
k	thermal conductivity of the pasta, W m^{-1} °C $^{-1}$
L	half thickness of the pasta, m
M	pasta water content on a dry basis
M_w	molecular weight of water, kg mol^{-1}
N_w^{ext}	flux of water at the surface of the pasta, kg m^{-2} s^{-1}
P_{sat}	saturation pressure, Pa
R_g	ideal gas constant, J mol^{-1} °C $^{-1}$
RDT	pasta required drying time
RH	relative humidity in the dryer, %
t	time, s
T	temperature, °C
T_g	glass transition temperature of the pasta, °C
x	coordinate for thickness, m
z_i	mass fraction of component *i* in the pasta, -
Greek symbol	
λ	water latent heat of vaporization, J kg^{-1}
ρ	density, kg m^{-3}
Subscripts	
0	initial condition
DS	dry solid
S	at the surface of the pasta
∞	drying conditions

A.1 Introduction

Drying represents a critical step in pasta production because of its impact on the pasta cooking properties, appearance and overall quality (Owens, 2001; Carini et al., 2014). During pasta drying, transient mass and heat transfer phenomena occur until a state of equilibrium between the pasta and the air is reached. The water content of the pasta at the beginning of drying is about 0.5 (d.b), but decreases during drying to reach an equilibrium water content strongly dependant on the drying temperature (Villeneuve and Gelinas, 2007). Simultaneously, the temperature of the pasta rises from the extrusion temperature to the drying temperature at a rate which depends on the pasta thermal conductivity, convection heat transfer coefficient and water isosteric heat of desorption (Migliori et al., 2005; De Temmerman et al., 2007).

Models describing water transport inside the pasta during drying have been developed to streamline the selection of appropriate time-temperature drying conditions (Andrieu and Stamatopoulos, 1988; Litchfield and Okos, 1992; Migliori et al., 2005; Villeneuve and Gelinas, 2007; De Temmerman et al., 2008; Mercier et al., 2011b; Ogawa et al., 2012; Veladat et al., 2013). As the pasta reaches thermal equilibrium during drying quickly compared with the duration of mass transfer because of pasta high Lewis number (*Le* = thermal diffusivity / effective water diffusion coefficient $\approx 1 \times 10^4$ for pasta), a common hypothesis of drying models is to neglect heat transfer and describe drying as an isothermal process (Litchfield and Okos, 1992; Villeneuve and Gelinas, 2007; De Temmerman, 2008; Mercier et al., 2011b). Neglecting heat transfer simplifies the description of pasta drying as it eliminates a partial differential equation to be solved with the mass transfer equation.

However, the contribution of heat transfer on the description of pasta glass transition has not been verified. During drying, pasta transitions from an initial rubbery state to a glassy state, with a transition state in between. Glass transition is a critical phenomenon to consider when selecting time-temperature conditions for pasta drying. Glass transition significantly impacts the mechanical properties of the pasta, a visco-plastic and soft product in the rubbery state and an elastic and rigid product in the glassy state (Cuq et al., 2003). The uniformity of glass transition inside the pasta during drying also needs to be considered, as the simultaneous presence of rubbery and glassy regions causes local variations of the viscoelastic properties in the pasta, which can generate mechanical stresses and promote crack formation (Cnossen et al., 2001; Takhar et al., 2006; Xing et al., 2007; Hundal and Takhar, 2010). An accurate description of pasta glass transition requires an accurate description of the temperature of the pasta because it significantly affects the water content at which glass transition occurs (Cuq and Icard-Verniere, 2001). Considering that glass transition at the surface of the pasta can occur during the early stages of drying because of pasta low external resistance to mass transfer (De Temmerman et al., 2007), heat transfer may have a significant impact on the

description of glass transition because the temperature of the pasta during the early stages of drying may be close to the extrusion temperature and lower than the drying temperature.

The aim of this work was to determine the impact of heat transfer on modeling pasta drying, more specifically regarding the contribution of heat transfer on the description of pasta required drying time and glass transition. To accomplish this work, the coupled mass and heat transfer drying model of Migliori et al. (2005) and De Temmerman et al. (2007) was combined with the model describing the water content of pasta at glass transition of Cuq and Icard-Verniere (2001). The time required to dry the pasta and the state of the pasta (rubbery, glassy or in transition) during drying were simulated with the model for low (40 °C), high (70 °C) and ultra-high (95 °C) drying temperatures and estimates were compared with an isothermal drying model.

A.2 Methods

A.2.1 Coupled mass and heat transfer drying model

The 1-D coupled mass and heat transfer drying model of Migliori et al. (2005) and De Temmerman et al. (2007) was used to simulate drying of rectangular pasta of a thickness of 1.3 mm. Migliori et al. (2005) and De Temmerman et al. (2007) validated the model for the description of pasta average water content during drying for drying temperatures between 40 and 95 °C. The impact of pasta shrinkage was neglected (Mercier et al., 2013a). Mass transfer was described using Fick second law:

$$\frac{\partial M}{\partial t} = D_{eff} \frac{\partial^2 M}{\partial x^2}, \qquad \text{(A.1)}$$

where M is the water content of the pasta on a dry basis, t the drying time, D_{eff} the effective water diffusion coefficient and x the coordinate in the thickness direction. The initial water content of the pasta (M_0) was assumed to be known. A symmetry boundary condition at the center of the pasta ($x = 0$) and a Robin boundary condition at the surface of the pasta ($x = L$) were used to solve Eq. (A.1):

$$\frac{\partial M}{\partial x} = 0 \qquad (\text{at } x = 0) \qquad \text{(A.2)}$$

$$-D_{eff} C_{DS} \frac{\partial M}{\partial x} = N_w^{ext} = h_m (C_S - C_\infty), \qquad (\text{at } x = L) \qquad \text{(A.3)}$$

where M_0 is the initial water content of the pasta, L the pasta half thickness C_{DS} the concentration of dry solid in the pasta, N_w^{ext} the flux of water at the surface of the pasta, h_m the convection mass transfer coefficient, C_S the concentration of water vapor at the air-pasta interface (air side) and C_∞ the concentration of water vapor in the dryer. The effective water

diffusion coefficient of pasta generally decreases during drying as the amount of free water is reduced. The effective water diffusion coefficient was related to the water content of the pasta using the correlation developed by De Temmerman et al. (2007):

$$D_{eff} = 1.2\ x\ 10^{-11} \exp\left[-3036.95\left(\frac{1}{T+273.15} - \frac{1}{293}\right)\right] \exp(6.46\ x\ 10^{-3} M) \qquad \text{(A.4)}$$

The water vapor concentrations at the air-pasta interface (C_S) and in the dryer (C_∞) were calculated using the ideal gas law, Raoult's law and the water activity coefficient at the surface of the pasta (for C_S) or the relative humidity in the dryer (for C_∞):

$$C_S = \frac{p_{sat} a_w M_w}{R_g(T+273.15)} \qquad \text{(A.5)}$$

$$C_\infty = \frac{p_{sat} RH M_w}{R_g(T_\infty+273.15)}, \qquad \text{(A.6)}$$

where p_{sat} is the saturation vapor pressure (calculated with the Clausius-Clapeyron equation), a_w the activity coefficient, M_w the molecular weight of water, R_g the ideal gas constant, RH the relative humidity in the dryer and T_∞ the drying temperature. The activity coefficient was calculated from the temperature of the pasta (T) with the following Oswin equation (De Temmerman et al., 2007):

$$a_w = \frac{\left[\frac{M}{A_1 - A_2 T}\right]^{\left[\frac{1}{B_1 + B_2 T}\right]}}{1+\left[\frac{M}{A_1 - A_2 T}\right]^{\left[\frac{1}{B_1 + B_2 T}\right]}}, \qquad \text{(A.7)}$$

where A_1, A_2, B_1 and B_2 are empirical constants with values A_1 = 0.138, A_2 = 10.4 x 10^{-4}, B_1 = 0.396 and B_2 = 11.6 x 10^{-4}. The convection mass transfer coefficient was calculated from the convection heat transfer coefficient using Lewis relation (De Temmerman et al., 2007):

$$h_m = \frac{h_h}{-208.09 \ln T + 1795.4}, \qquad \text{(A.8)}$$

where h_h is the convection heat transfer coefficient.

Heat transfer was described using an energy balance:

$$\rho C_p \frac{\partial T}{\partial t} = k \frac{\partial^2 T}{\partial x^2}, \qquad \text{(A.9)}$$

where ρ, C_p and k are the pasta apparent density, heat capacity and thermal conductivity, respectively. The initial temperature of the pasta (T_0) was assumed to be known. A symmetry boundary condition at the center of the pasta ($x = 0$) and a Robin boundary condition with water evaporation at the surface of the pasta ($x = L$) were used to solve Eq. (A.9):

$$\frac{\partial T}{\partial x} = 0 \qquad (\text{at } x = 0) \qquad \text{(A.10)}$$

$$-k\frac{\partial T}{\partial x} = h_h(T_s - T_\infty) - \lambda N_w^{ext}, \qquad (\text{at } x = L) \qquad \text{(A.11)}$$

where T_0 is the initial temperature of the pasta, T_s the temperature at the surface of the pasta, h_h the convection heat transfer coefficient and T_∞ the drying temperature. The heat capacity of the pasta was calculated from the heat capacity of its main constituents, water, starch and proteins, weighted by their mass fraction (Migliori et al., 2005; De Temmerman et al., 2007):

$$C_p = \sum z_i C_{p,i}, \qquad \text{(A.12)}$$

where $C_{p,water} = 4184$, $C_{p,starch} = 5.737T + 1328$, $C_{p,proteins} = 6.329T + 1465$ and z_i is the mass fraction of each constituent. The mass fraction of the proteins was taken as 16% of pasta dry solid (Mercier et al., 2011b) and the mass fraction of water was calculated from the pasta water content *M*.

A.2.2 Isothermal drying model

To assess the impact of heat transfer on pasta drying, simulations of pasta water content with the coupled mass and heat transfer drying model (Eqs. A.1-A.12) were compared to estimates obtained with an isothermal drying model. The same constitutive equations as the coupled mass and heat transfer drying model were used to describe mass transfer (Eqs. A.1-A.8). However, in the isothermal drying model, heat transfer (Eqs. A.9-A.12) was neglected and the temperature of the pasta was assumed to be equal to the drying temperature:

$$T = T_\infty \qquad \text{(A.13)}$$

A.2.3 Glass transition model

The Kwei model of Cuq and Icard-Verniere (2001) was used to determine the glass transition temperature (T_g) of the pasta according to its water content:

$$T_g = \frac{\frac{1}{1+M}T_{g,1} + k\frac{M}{1+M}T_{g,2}}{\frac{1}{1+M} + k\frac{M}{1+M}} + q\frac{M}{(1+M)^2}, \qquad \text{(A.14)}$$

where $T_{g,1}$ and $T_{g,2}$ are the glass transition temperatures of semolina and water and k and q are two empirical constants. For durum wheat pasta drying, these parameters have the following values: $T_{g,1}$ = 273 ºC, $T_{g,2}$ = -135 ºC, k = 9.5 and q = 346 (Cuq and Icard-Verniere, 2001). The pasta was considered in the rubbery state when its water content was 0.015 (d.b.) higher than the water content at glass transition and in the glassy state when it was 0.015 (d.b.) below it (Cuq et al., 2003). Between these two thresholds, the pasta was considered to be in the transition state between the rubbery and glassy states.

A.2.4 Numerical implementation of the drying and glass transition models and calculation of pasta required drying time

The evolution of pasta water content during drying was simulated with the coupled mass and heat transfer drying model (Eqs. A.1-A.12) and the isothermal drying model (Eqs. A.1-A.8 and A.13) using the input parameters of Table A.1. The drying models were solved using the finite difference method (central differencing scheme) with a 2.24 x 10^{-5} m discretization in space and 1 s discretization in time using Matlab 7.5 software. The state of the pasta (rubbery, glassy or in transition) during drying was determined from its water content using Eq. (A.14). Pasta required drying time (*RDT*) was determined from the simulation of the pasta water content and glass transition and was defined as the time required for the pasta: (1) to reach an average water content below 14% and (2) to have completed its transition to the glassy state. The aforementioned criterion (1) is required to meet regulations in many countries, including Italy, the leading world producer of pasta, regarding the maximum water content of dried pasta (Carini et al., 2014). Regulations on the maximum water content of dried pasta were established to reduce microbiological spoilage of the pasta and ensure its safety for long storage periods. Criterion (2) is required to obtain dried pasta with adequate mechanical properties for storage and transportation (Cuq et al., 2003).

Table A.1. Input parameters of the drying models

Parameter	Value	Justification/Reference
Density (ρ)	1310 kg m^{-3}	Mercier et al. (2011b)
Thermal conductivity (k)	0.41 W m^{-1} °C^{-1}	Migliori et al. (2005)
Convection heat transfer coefficient (h_h)	29.62 W m^{-2} °C^{-1}	De Temmerman et al. (2007)
Water latent heat of vaporization (λ)	2.26 x 10^6 J kg^{-1}	De Temmerman et al. (2008)
Initial water content (M_0)	0.48 (d.b.)	Mercier et al. (2013a)
Initial temperature (T_o)	25 °C	Room temperature

A.3 Results and discussion

A.3.1 Pasta average water content

The evolution of pasta average water content ($\frac{1}{L}\int_0^L Mdx$) simulated with the coupled mass and heat transfer drying model (Eqs. A.1-A.12) and the isothermal drying model (Eqs. A.1-A.8 and A.13) are presented in Fig. A.1. For a drying temperature of 40 °C, the drying

curve estimated using the coupled mass and heat transfer drying model corresponds well with the isothermal drying model (Fig. A.1A), indicating that heat transfer has a limited impact on pasta average water content for low drying temperature. The limited impact of heat transfer on pasta average water content for low drying temperature is attributed to the rapid increase of the pasta temperature with respect to the decrease of its water content. Indeed, the time required to reach 63.2% (one time constant) of the difference between the initial and the equilibrium temperatures of the pasta is 300 s for a drying temperature of 40 °C and corresponds to 5% of the time required to reach 63.2% of the difference between the initial and the equilibrium average water contents of the pasta. The difference between the drying curves estimated using the coupled mass and heat transfer drying model and the isothermal drying model is more important for drying temperatures of 70 °C (Fig. A.1B) and 95 °C (Fig. A.1C). For instance, for a drying temperature of 95 °C, when the average water content reaches 0.30 according to the isothermal model, it is 20% higher (0.36) according to the coupled mass and heat transfer drying model. Comparison of the drying curves (Fig. A.1) indicates that the contribution of heat transfer on pasta water content increases with the drying temperature.

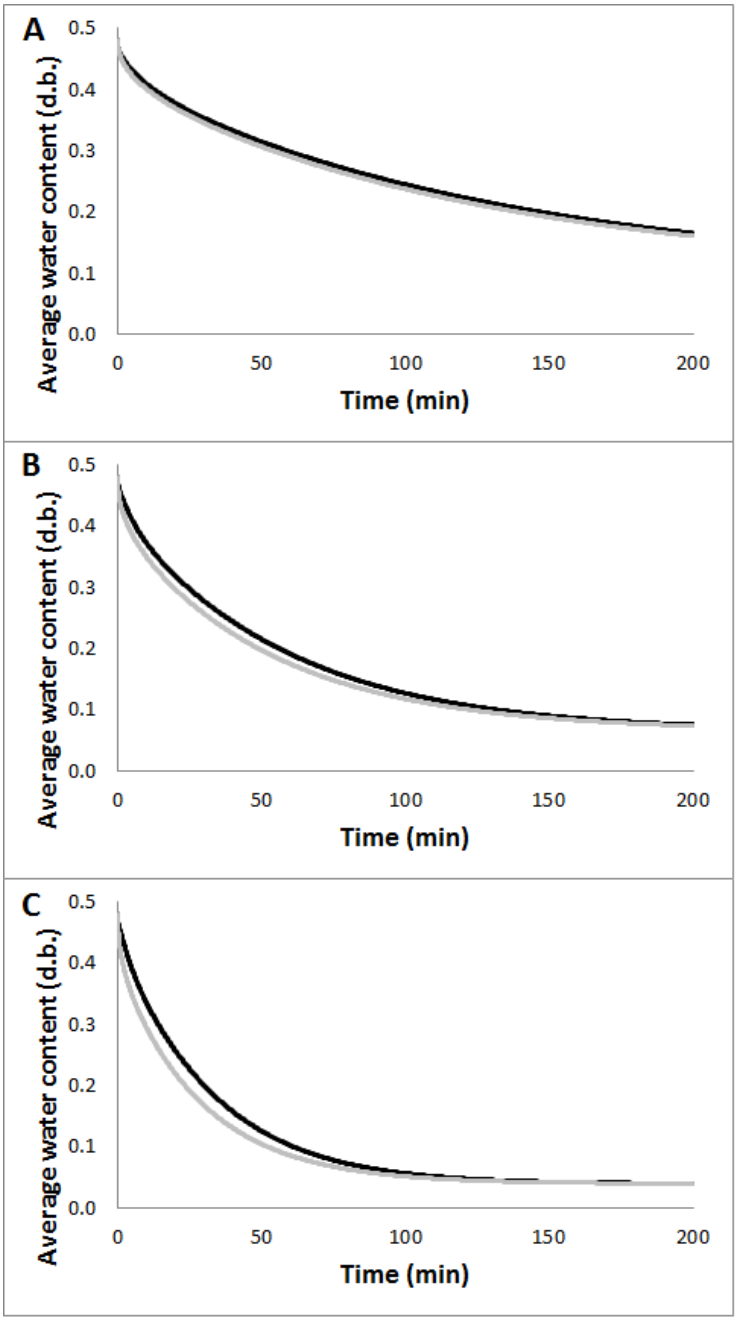

Figure A.1. Pasta average water content during drying estimated using the coupled mass and heat transfer drying model (black line) or the isothermal drying model (grey line) for a relative humidity (*RH*) of 50% and drying temperatures of 40 (A), 70 (B) and 95 °C (C).

A.3.2 Impact of heat transfer on pasta required drying time and glass transition

The glass transition temperature of pasta decreases with the water content because of the plasticization effect of water (Cuq et al., 2003). According to the glass transition model of

Cuq and Icard-Verniere (2001) (Eq. A.14), the water content of the pasta at which glass transition occurs is below 0.14 (d.b.) for pasta with a temperature above 66.2 °C (Fig. A.2). Consequently, when a drying temperature above 66.2 °C is used, pasta should be dried for a longer duration than the time required to reach a water content of 0.14 (d.b.), the maximum water content accepted for dried pasta in many countries, because the pasta will not have reached the glassy state.

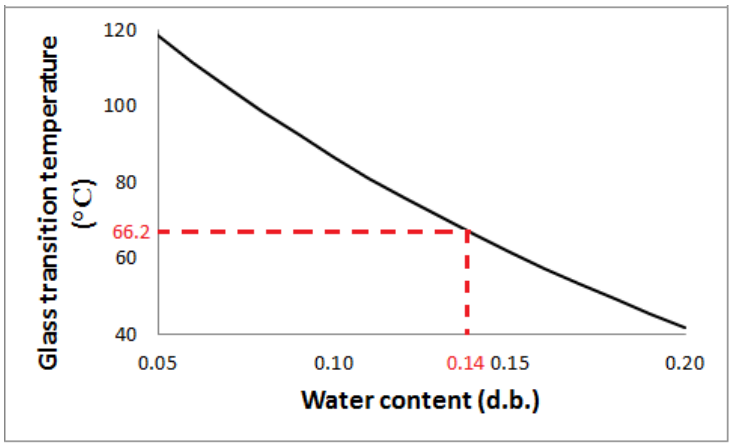

Figure A.2. Glass transition temperature of the pasta according to its water content estimated using the glass transition model of Cuq and Icard-Verniere (2001).

Fig. A.3 presents the state of the pasta (rubbery, glassy or in transition) during drying according to the drying time and temperature. The rate of water loss at the surface of the pasta is fast at the beginning of the drying process because of the low external resistance to mass transfer and a layer in the glassy state forms in the early stage of drying. After a given drying time, a glassy, a rubbery and a transition region coexist in the pasta. Depending on the drying temperature, a drying time between 1.5 and 2 h is required for the center of the pasta to reach the glassy state.

For a drying temperature of 40 °C, the pasta required drying time (*RDT*) is longer than the time required to reach the glassy state because glass transition occurs at a water content above 0.14 (d.b.). The pasta *RDT* is 3.5 h when estimated with the coupled mass and heat transfer drying model (Eqs. A.1-A.12) and 3.4 h when estimated with the isothermal drying model (Eqs. A.1-A.8 and A.13). The difference between the *RDT* estimated with the two drying models is below 5% indicating that, in accordance with the drying curves (Fig. A.1A), heat transfer has a negligible impact on pasta drying when a low (40 °C) drying temperature is used.

For high (70 °C) and ultra-high (95 °C) drying temperatures, the pasta *RDT* is longer than the time required to reach a water content of 0.14 (d.b.) because the glass transition of pasta occurs at a lower water content. For a drying temperature of 70 °C, the pasta *RDT* estimated with the isothermal drying model is 2.0 h. According to the coupled mass and heat

transfer drying model, 38% of the pasta would remain in the transition state if it were dried for this duration (Fig. A.3B). For a drying temperature of 95 °C, 50% of the pasta would be in the transition state according to the coupled mass and heat transfer drying model if the pasta were dried at the *RDT* estimated with the isothermal drying model (1.4 h). Pasta that have not reached the glassy state at the end of drying may have inappropriate mechanical properties for storage and transportation and may reach the glassy state during storage under uncontrolled temperature and relative humidity conditions, increasing the probability of crack formation in the pasta and the reduction of the pasta quality. Consequently, heat transfer should be considered for an accurate description of glass transition for high (70 °C) or ultra-high (95 °C) drying temperatures, because neglecting heat transfer underestimate the time required to dry the pasta and a significant portion of the pasta may remain in the transition state when it is removed from the dryer.

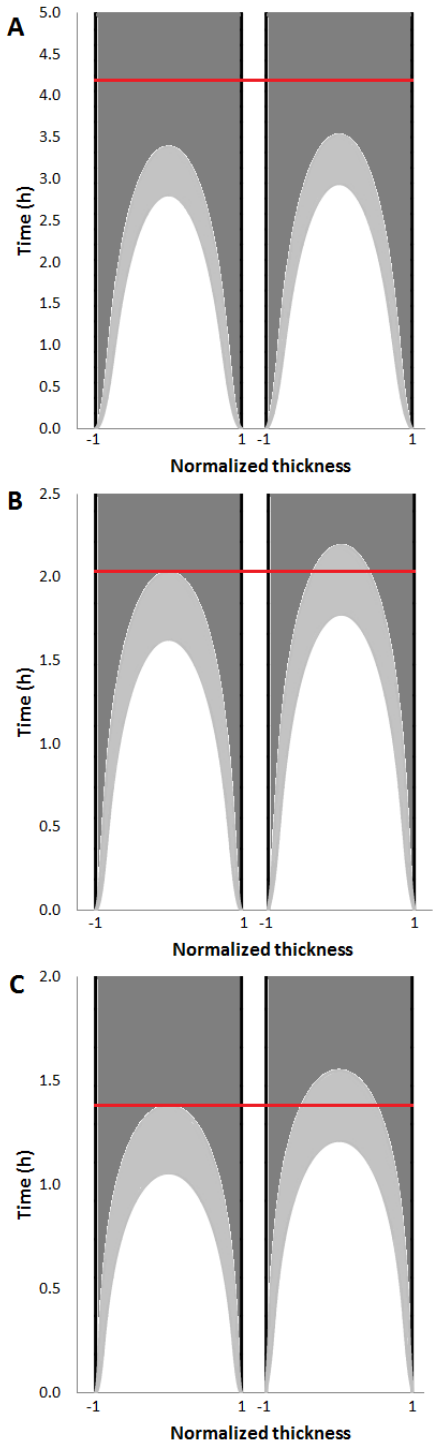

Figure A.3. Mapping of the rubbery (while), transition (light grey) and glassy (dark grey) regions in the pasta during drying for a relative humidity (*RH*) of 50% and drying temperatures of 40 (A), 70 (B) and 95 °C (C). The left panel represents the state of the pasta described using the isothermal drying model, the right panel using the coupled mass and heat transfer drying model and the red line the *RDT* estimated using the isothermal drying model.

A.4 Conclusion

The aim of this work was to assess the contribution of heat transfer on the description of pasta glass transition and required drying time. Analysis of drying curves and state of the pasta (rubbery, glassy or in transition) during drying indicated that heat transfer has a negligible impact on the description of pasta drying for a low drying temperature (40 °C). However, heat transfer should be considered when describing pasta required drying time and glass transition for high (70 °C) and ultra-high (90 °C) drying temperatures, because neglecting heat transfer can underestimate pasta required drying time and cause the presence of a region near the center of the pasta that has not reached the glassy state at the end of drying.

A.5 Acknowledgements

The authors thank the Vanier Ph. D. scholarship program (held by Samuel Mercier) and the Natural Sciences and Engineering Research Council (NSERC) of Canada for their financial support.

ANNEXE B. Révision des méthodes de revue de la littérature par méta-analyse

Rapport interne rédigé le 12/2013 par Samuel Mercier. Titre Original: Guidelines for knowledge synthesis using meta-analysis

Résumé

Les revues de la littérature scientifique quantitatives, méta-analyses, sont courantes dans les domaines des sciences de la santé et sciences humaines, mais sont encore rarement utilisées dans les domaines des sciences de la nature et de l'ingénierie. L'objectif de ce rapport est de réviser les 6 étapes traditionnelles d'une méta-analyse (établissement des objectifs de recherche, sélection des critères de qualité, recherche bibliographique, construction d'une base de données, analyse statistique de la base de données et analyse des résultats) et d'illustrer les avantages et limitations des méta-analyses par rapport aux revues de la littérature narratives traditionnelles. Les deux modèles couramment utilisés pour les méta-analyses, à effets fixes et effets aléatoires, sont considérés. Les développements récents par rapport à la compensation des biais de publication et au traitement des corrélations sont discutés. Tout au long du rapport, la méthodologie est illustrée à partir d'un exemple concret de recherche, l'efficacité de l'ajout d'agents antimicrobiens dans les savons sanitaires.

Nomenclature

C_1	concentration of microorganisms on the hand of the test subjects before hand washing
C_2	concentration of microorganisms on the hand of the test subjects after hand washing
df	number of degrees of freedom
eff	effectiveness of a soap
ES	effect size
$\boldsymbol{ES}$	vector of effect sizes
$\dot{ES}$	pooled effect sizes for effect sizes sharing a common control
$\overline{ES}$	pooled effect size
k	rank of the effect size determining the R estimator in the trim and fill method
K	number of effect sizes
LC	lower limit of the confidence interval
N	number of replicate measurements
Q	Q-statistic for the estimation of the between-study heterogeneity
$r_{a,b}$	Pearson correlation coefficient between group a and b
SD	standard deviation
SE	standard error
$\overline{SE}$	standard error of the pooled effect size
t	student's t-distribution
UC	upper limit of the confidence interval
R	number of effect sizes to add for publication bias according to the trim and fill method
VS	volume of soap
w	weight given to an effect size
$\boldsymbol{W}$	matrix of weights for the meta-regression
X	moderator variable
$\boldsymbol{X}$	matrix of moderator variables
y	result extracted from a study
Z	standard normal distribution

Greek symbols

α	significance level
β	regression coefficient of the moderator analysis
$\boldsymbol{\beta}$	vector of regression coefficients β
ε	sampling error
θ	true effect size (FEM)
$\boldsymbol{\Omega}$	variance-covariance matrix of effect sizes sharing a common control
μ	average value of the distribution of true effect sizes (REM)
ν	between-study heterogeneity
τ	weight given to an effect size related to the between-study heterogeneity

Subscripts
anti antimicrobial soap
between between-group variance for the moderator analysis
control nonantimicrobial soap
FEM fixed effects model
REM random effects model
res residual variance (after the moderator analysis)
total total group variance for the moderator analysis
within within-group variance for the moderator analysis

B.1 Introduction

The volume of scientific data available is in constant expansion. Indeed, as research teams are getting more numerous, analytical methods more efficient and results more easily available, the flux of information that we encounter is at an all-time high. In result, a researcher ability to apply efficient and systematic methods to process and synthetize all that information has become an extremely valuable skill.

The common method currently applied to synthetize research data in most fields of natural science and engineering is using narrative reviews. In a narrative review, the authors summarize the content of published articles on the considered topic and take a critical look at their methodology and findings (Green et al. 2006; Day and Gastel 2012). However, narrative reviews have several drawbacks inherent to the qualitative nature of their analysis. Because the analysis of the literature is qualitative, narrative reviews can be inconclusive in the presence of conflicting results in the literature and can lead to biased conclusions which are based more on opinion than data (Gates 2002; Koretz 2002; Roberts et al. 2006; Garg et al. 2008; Callcut and Branson 2009; Card 2012; Koricheva et al. 2013)

A more efficient and standardized method to combine and synthetize scientific data can be achieved using meta-analyses. A meta-analysis refers to the quantitative analysis of results from multiple studies (Nam et al. 2003; Green et al. 2006; Tricco et al. 2011). In a meta-analysis, the results of each studies meeting previously determined quality criteria are compiled in a database and appropriate statistical methods are applied to identify patterns from the combined analysis of these results. Meta-analyses differ from primary analyses because the statistical analysis is applied to effect sizes (such as the mean value of the considered parameter or a correlation coefficient between two variables) instead of individual level data (Card 2012). Since a meta-analysis involves the combined analysis of effect sizes from multiple studies, the sample size is much bigger, which generally improve the accuracy of the true effect size estimate and increase the statistical power of the analysis (Quintana and Minami 2006; Valentine et al. 2010). Because their conclusions are drawn from statistical analysis, meta-analyses are more objective than narrative reviews and suffer to a lesser extent of the possibility of a biased evaluation of the literature by the author (Koretz 2002; Card 2012).

While meta-analyses are common in health and human, the application of this method to research questions in natural sciences and engineering remains limited. Fig. B.1 shows the number of review articles containing “meta-analysis” in their title indexed since 1990 by the *Scopus* database that were published in journals specialized in subject area related to natural sciences or engineering along with the percentage that they represent with respect to the total number of review articles published in these journals. The application of meta-analyses was very scarce in the 1990’s and relatively stable in the 2000’s, but has become more popular in the last 2-3 years. It should be expected that this trend will continue in the next few years but,

as of now, meta-analysis still only represent under 10% of the total number of reviews conducted in natural sciences and engineering.

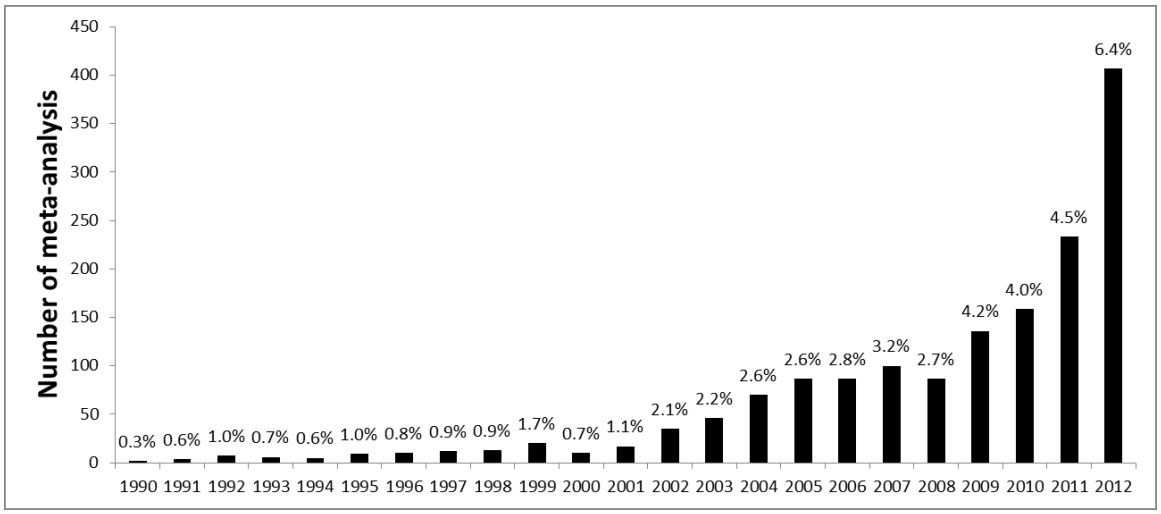

Figure B.1. Number of meta-analyses published in fields of natural sciences and engineering and their percentage of the total number of review articles indexed by the *Scopus* database since 1990.

In order to promote a more systematic application of meta-analyses for knowledge synthesis in natural sciences and engineering, this work aims to provide guidelines on the method of meta-analysis and to compare the results obtained from narrative and quantitative reviews. Each of the six main steps involved in a meta-analysis, which are the definition of the research objectives, the selection of the quality criteria, the literature search, the construction of the database, the pooling of the effect sizes and the moderator analysis, are detailed separately (Fig. B.2). This work concludes with a discussion on the challenges and limitations of knowledge synthesis using meta-analysis.

Throughout the paper, the methods and the issues discussed will be illustrated by reviewing and adapting a meta-analysis conducted by Montville and Schaffner (2011) on the effectiveness of soap on hand washing. Numerous studies have been conducted to assess soap effectiveness in providing proper hand washing to limit disease spreading in the community, health care institutions and food handling operations (Montville and Schaffner 2011). A common research objective of a large portion of these studies has been to determine if antimicrobial soaps are more effective than nonantimicrobial soaps. However, no consensus has been reached because conflicting results have been published on the effectiveness of these soaps. In this work, a meta-analysis is conducted to determine if conclusive evidence on the addition of antimicrobial agents in soaps can be achieved by combining the results from multiple studies.

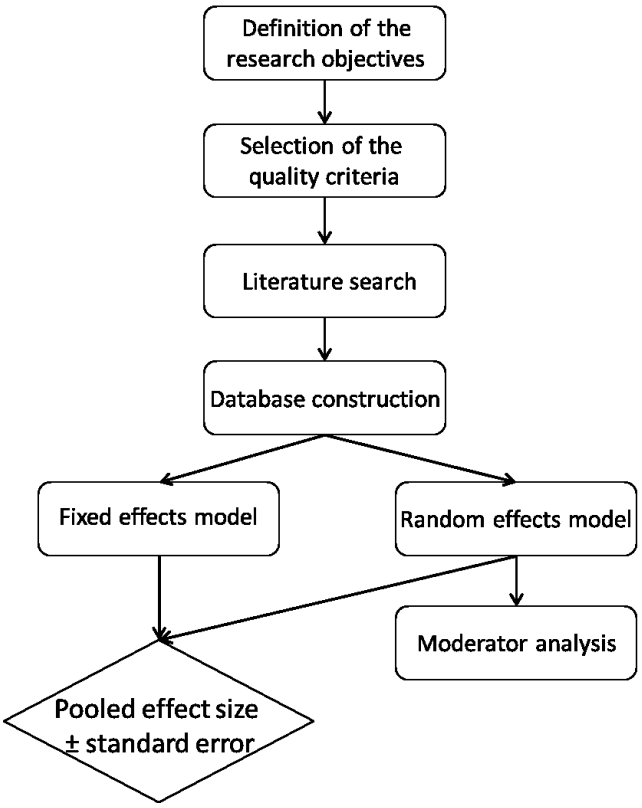

Figure B.2. Overview of the general meta-analysis process.

B.2 Definition of the research objectives

The first step in a meta-analysis is to define the research objectives that we wish to achieve from the quantitative analysis of the literature. Some typical research objectives involve the identification of a central tendency, the quantification of the level of association between two (or multiple) variables and the analysis of the level of agreement between studies (Pigott 2012). Although the formulation of the research objectives can be trivial in many cases, the research objectives need to be sufficiently detailed to guide the literature search and remove ambiguities during the selection of the studies considered for the meta-analysis. A good research objective should also indicate the variables that have to be extracted from the primary studies and how they should be coded in the database.

For the soap example, it was observed by Montville and Schaffner (2011) that conflicting results had been published on the effectiveness of antimicrobial soaps with respect to nonantimicrobial soaps regarding hand washing. The first research objective of their meta-analysis was to determine if antimicrobial soaps provide a greater reduction of the bacterial density on the hands than nonantimicrobial soaps after manual hand washing. Even though soap technically refers to a cleaning agent made from a mixture of salts of fatty acids, in order

to eliminate any ambiguity, the authors specified that soap was taken as any hand washing compound, excluding hand sanitizer.

Furthermore, the primary studies considered in the meta-analysis did not follow a unique methodology for the quantification of the soap effectiveness. Significant differences were observed between the studies, such as the volume of soap used and the method applied to quantify the bacterial density on the hands of the test subjects. Therefore, an additional research objective of the meta-analysis was to assess if these methodological parameters affected the soap effectiveness measured in the studies.

B.3 Selection of the quality criteria

In order to ensure consistency, transparency and reproducibility during the literature search and data extraction process, the selection of the primary studies for the meta-analysis should made following predetermined quality criteria. The quality criteria should prevent the incorporation of "low quality" results in the database for instance originating from studies with significant flaws in their methodology. These outliers dilute the results of the relevant studies, which can hinder the reliability of the meta-analysis (Berard and Bravo 1998; Sutton et al. 2001; Doi and Thalib 2008; Kag et al. 2012). However, over restrictive quality criteria should also be avoided, because the rejection of too many high quality studies can lead to a meta-analysis not representative of the entire body of work conducted on a research topic (Card 2012).

Typical quality criteria that should be specified in any meta-analysis include the types of publication (scientific articles, theses, dissertations, etc.), the language and the date of publication, the type of journals and the status of publication (Card 2012). Some additional criteria might also be included depending on the research objectives to specify the methodology applied in the primary studies, the type of results presented and the minimal sample size accepted.

In the Montville and Schaffner (2011) soap example, no restriction was applied regarding the date of publication, the status of publication or the type of journal, but only scientific articles written in English were considered. As specified in the research objectives, the meta-analysis focused on the ability of soaps to reduce the bacterial density on the hand after manual hand washing. Consequently, to be considered in the meta-analysis, primary studies had to measure the difference in bacterial (and not viral) density on the hands before and after hand washing, and studies using automatic washing machines or brushes were discarded. The meta-analysis was performed on quantitative results, meaning that studies reporting the effectiveness of the soaps qualitatively or semi-quantitatively (such as a scale from 1 to 5, where 1 means "really effective soap" and 5 "not effective soap") were excluded

from the meta-analysis. Since the first objective of the meta-analysis was to determine if antimicrobial soaps are more effective than nonantimicrobial soaps, only studies providing a direct comparison of antimicrobial and nonantimicrobial soaps were considered. Finally, as detailed in section B.6, pooling of the effect sizes (mean differences) using fixed or random effects models requires the knowledge of the standard error of the effect sizes. Consequently, an additional criterion used in the selection of the primary studies was that they provided the standard deviation of their results or a statistical measure (such as the *P*-value or least significant differences) from which this standard deviation could be estimated, along with the number of replicate measurements.

B.4 Literature search

The second step of a meta-analysis is to find the studies that respect the previously determined quality criteria. Most literature searches are conducted using well known electronic databases such as *Scopus*, *Compendex* and *Pubmed* using keywords search. A backward references search should also be performed, which consists to verify the relevance of the references cited in the articles yielded from the preliminary keywords search. It is important not to limit the literature search to a few journals or research groups, unless otherwise specified in the quality criteria, which could lead to conclusions not representative of all the studies conducted on a research topic. Additional grey literature resources such as conference proceedings, theses and dissertations, reference books, governmental reports and non-governmental reports can also be considered to retrieve the maximum of relevant information (Lord 2000; Wieseler 2010). Furthermore, if a study is relevant according to the research objectives, but includes missing data that renders it unusable for the meta-analysis, the corresponding author of this study can be contacted to inquire about the availability of these data.

In the Montville and Schaffner (2011) soap meta-analysis, the literature search revealed 25 relevant primary studies. In the present paper, 8 of these studies were discarded because they did not provide sufficient information to estimate standard error of the effect sizes. A research of the keyword “microbial soap” was also conducted on *Scopus*, *Compendex*, *Pubmed* and *Proquest dissertations and theses* databases to determine if additional relevant studies had been published since, but no studies respecting the quality criteria were identified.

B.5 Construction of the database

B.5.1 Compilation of the effect sizes

The relevant data from the primary studies retrieved during the literature search has to be extracted, coded and compiled in a database prior to its statistical analysis. Table B.1 presents the database compiled for the soap example. The most important variable in this database is the effect size (*ES*). The effect size represents the outcome of interest of the meta-analysis. Typical types of effect size relevant in natural sciences and engineering are measures of central tendency, such as the mean value of a parameter, or measures of association between two variables, such as raw mean differences, standardized mean differences and Pearson correlation coefficients. Table B.2 presents the general equation defining these effect sizes.

Table B.1. Database for the soaps meta-analysis

***ES* ID number**	**Reference**	***ES* (log CFU)**	***SE* (log CFU)**	**Volume of soap (mL)**	**Sampling method**	**Information from which the *SE* was calculated**	***ES* sharing a common control**
1	Ansari et al. (1989)	0.21	0.22	0.5	3	*SD* of 3 replicates	1 and 3
2	Ansari et al. (1989)	1.99	0.25	0.5	3	*SD* of 3 replicates	2 and 4
3	Ansari et al. (1989)	0.05	0.27	0.5	3	*SD* of 3 replicates	1 and 3
4	Ansari et al. (1989)	0.59	0.24	0.5	3	*SD* of 3 replicates	2 and 4
5	Ansari et al. (1989)	1.44	0.26	0.5	3	*SD* of 3 replicates	5 and 6
6	Ansari et al. (1989)	0.48	0.10	0.5	3	*SD* of 3 replicates	5 and 6
7	Ayliffe et al. (1978)	0.56	0.22	5	2	*SD* of 6 replicates	7 and 8
8	Ayliffe et al. (1978)	1.47	0.27	5	2	*SD* of 6 replicates	7 and 8
9	Ayliffe et al. (1978)	0.32	0.38	5	2	*SD* of 6 replicates	9 and 10
10	Ayliffe et al. (1978)	0.29	0.42	5	2	*SD* of 6 replicates	9 and 10
11	Ayliffe et al. (1978)	0.09	0.23	5	2	*SD* of 11 replicates	11 and 12
12	Ayliffe et al. (1978)	0.71	0.22	5	2	*SD* of 10 replicates	11 and 12
13	Ayliffe et al. (1978)	1.29	0.25	5	2	*SD* of 10 replicates	13-16
14	Ayliffe et al. (1978)	-0.50	0.17	5	2	*SD* of 10 replicates	13-16
15	Ayliffe et al. (1978)	1.22	0.22	5	2	*SD* of 11 replicates	13-16
16	Ayliffe et al. (1978)	-0.34	0.18	5	2	*SD* of 11 replicates	13-16
17	Ayliffe et al. (1978)	0.37	0.38	5	2	*SD* of 8 replicates	17-19
18	Ayliffe et al. (1978)	0.35	0.36	5	2	*SD* of 10 replicates	17-19
19	Ayliffe et al. (1978)	0.45	0.35	5	2	*SD* of 10 replicates	17-19
20	Ayliffe et al. (1988)	0.70	0.20	5	2	*P*-value of 20 replicates	
21	Ayliffe et al. (1988)	0.40	0.12	5	2	*P*-value of 45 replicates	
22	Ayliffe et al. (1988)	0.30	0.20	5	2	*P*-value of 20 replicates	
23	Ayliffe et al. (1988)	-0.10	0.14	5	2	*P*-value of 7 replicates	

24	Ayliffe et al. (1988)	0.10	0.14	5	2	*P*-value of 11 replicates	
25	Bartzokas et al. (1987)	0.05	0.11	3	1	*SD* of 12 replicates	
26	Bartzokas et al. (1987)	0.19	0.16	3	1	*SD* of 12 replicates	
27	Bettin et al. (1994)	-0.10	0.09	1	3	*SD* of 10 replicates	
28	Bettin et al. (1994)	-0.10	0.11	1	3	*SD* of 10 replicates	
29	Fischler et al. (2007)	1.85	0.20	3	1	*SD* of 7 replicates	
30	Fischler et al. (2007)	1.15	0.18	3	1	*SD* of 13 replicates	
31	Fischler et al. (2007)	1.70	0.16	3	1	*SD* of 10 replicates	
32	Fischler et al. (2007)	1.45	0.15	3	1	*SD* of 8 replicates	
33	Fuls et al. (2008)	1.18	0.09	3	1	*SD* of 8 replicates	
34	Fuls et al. (2008)	1.66	0.07	3	1	*SD* of 10 replicates	
35	Fuls et al. (2008)	2.27	0.06	1.5	1	*SD* of 12 replicates	
36	Fuls et al. (2008)	2.75	0.06	3	1	*SD* of 10 replicates	
37	Guilhermetti et al. (2001)	-0.05	1.09	5	2	*SD* of 5 replicates	37 and 38
38	Guilhermetti et al. (2001)	1.80	0.74	5	2	*SD* of 5 replicates	37 and 38
39	Guilhermetti et al. (2001)	-0.40	1.03	5	2	*SD* of 5 replicates	39 and 40
40	Guilhermetti et al. (2001)	2.62	2.07	5	2	*SD* of 5 replicates	39 and 40
41	Lilly and Lowbury (1971)	0.38	0.06	7	3	*SD* of 6 replicates	
42	Lowbury and Lilly (1973)	0.93	0.10	7	3	*SD* of 8 replicates	42-44
43	Lowbury and Lilly (1973)	0.35	0.06	7	3	*SD* of 8 replicates	42-44
44	Lowbury and Lilly (1973)	0.53	0.09	7	3	*SD* of 8 replicates	42-44
45	Lowbury et al. (1974)	0.40	0.05	5	3	*SD* of 6 replicates	45 and 46
46	Lowbury et al. (1974)	0.82	0.04	5	3	*SD* of 8 replicates	45 and 46
47	Nicoletti et al. (1990)	0.05	0.31	2	2	*SD* of 12 replicates	47 and 48
48	Nicoletti et al. (1990)	0.53	0.35	5	2	*SD* of 12 replicates	47 and 48
49	Nicoletti et al. (1990)	0.40	0.17	2	2	*SD* of 12 replicates	49 and 50
50	Nicoletti et al. (1990)	0.81	0.14	5	2	*SD* of 12 replicates	49 and 50
51	Ojajarvi (1980)	0.19	0.18	5	3	*SD* of 10 replicates	51-53

52	Ojajarvi (1980)	0.49	0.20	5	3	*SD* of 10 replicates	51-53
53	Ojajarvi (1980)	1.59	0.18	5	3	*SD* of 10 replicates	51-53
54	Ojajarvi (1980)	0.20	0.21	5	3	*SD* of 10 replicates	54-56
55	Ojajarvi (1980)	0.68	0.17	5	3	*SD* of 10 replicates	54-56
56	Ojajarvi (1980)	1.88	0.25	5	3	*SD* of 10 replicates	54-56
57	Ojajarvi (1980)	-0.20	0.17	5	3	*SD* of 10 replicates	57-59
58	Ojajarvi (1980)	0.60	0.22	5	3	*SD* of 10 replicates	57-59
59	Ojajarvi (1980)	0.68	0.20	5	3	*SD* of 10 replicates	57-59
60	Ojajarvi (1980)	0.17	0.19	5	3	*SD* of 10 replicates	60-62
61	Ojajarvi (1980)	1.04	0.25	5	3	*SD* of 10 replicates	60-62
62	Ojajarvi (1980)	0.87	0.88	5	3	*SD* of 10 replicates	60-62
63	Paulson et al. (1999)	-0.22	0.25	5	1	*SD* of 5 replicates	
64	Sickbert-Bennett et al. (2005)	0.11	0.08	3	1	*CI* of 5 replicates	64-69
65	Sickbert-Bennett et al. (2005)	0.14	0.06	3	1	*CI* of 5 replicates	64-69
66	Sickbert-Bennett et al. (2005)	0.02	0.07	3	1	*CI* of 5 replicates	64-69
67	Sickbert-Bennett et al. (2005)	0.03	0.09	3	1	*CI* of 5 replicates	64-69
68	Sickbert-Bennett et al. (2005)	-0.27	0.07	3	1	*CI* of 5 replicates	64-69
69	Sickbert-Bennett et al. (2005)	0.13	0.07	3	1	*CI* of 5 replicates	64-69
70	Stiles and Sheena (1985)	0.48	0.08	5	1	Duncan multiple range test of 9 replicates	70-76
71	Stiles and Sheena (1985)	0.08	0.04	5	1	Duncan multiple range test of 9 replicates	70-76
72	Stiles and Sheena (1985)	0.72	0.14	5	1	Duncan multiple range test of 9 replicates	70-76
73	Stiles and Sheena (1985)	0.31	0.06	5	1	Duncan multiple range test of 9 replicates	70-76
74	Stiles and Sheena (1985)	0.10	0.04	5	1	Duncan multiple range test of 9 replicates	70-76

75	Stiles and Sheena (1985)	0.39	0.07	5	1	Duncan multiple range test of 9 replicates	70-76
76	Stiles and Sheena (1985)	0.10	0.04	5	1	Duncan multiple range test of 9 replicates	70-76
77	Stiles and Sheena (1985)	0.52	0.12	5	1	Duncan multiple range test of 9 replicates	77-83
78	Stiles and Sheena (1985)	0.08	0.05	5	1	Duncan multiple range test of 9 replicates	77-83
79	Stiles and Sheena (1985)	0.75	0.20	5	1	Duncan multiple range test of 9 replicates	77-83
80	Stiles and Sheena (1985)	0.25	0.07	5	1	Duncan multiple range test of 9 replicates	77-83
81	Stiles and Sheena (1985)	0.07	0.05	5	1	Duncan multiple range test of 9 replicates	77-83
82	Stiles and Sheena (1985)	0.04	0.05	5	1	Duncan multiple range test of 9 replicates	77-83
83	Stiles and Sheena (1985)	0.29	0.07	5	1	Duncan multiple range test of 9 replicates	77-83
84	Toshima et al. (2001)	-0.05	0.07	1	3	*CI* of 10 replicates	

Table B.2. Definition of the effect sizes and their respective standard error (Card 2012; Sanchez-Meca and Marin-Martinez 2010)

Effect size	Definition	Standard error
Mean value	y	$\frac{SD}{\sqrt{N}}$
Raw mean difference	$y_a - y_b$	$\sqrt{\frac{SD_a^2}{N_a} + \frac{SD_b^2}{N_b}}$
Standardized mean difference	$\frac{y_a - y_b}{SD_{pooled}}$	$\sqrt{\frac{n_a + n_b}{n_a n_b} + \frac{(y_a - y_b)^2}{2\left(SD_{pooled}\right)^2 (n_a + n_b)}}$
Pearson correlation coefficient	$r_{a,b}$	$\frac{1 - r_{a,b}^2}{\sqrt{N-2}}$

Where y is the result extracted from a study, N is the number of replicate measurements of y, SD_{pooled} is the pooled standard deviation, the subscripts a and b refers to the two groups (raw or standardized mean difference) or continuous variables (Pearson correlation coefficient) compared and $r_{a,b}$ the Pearson correlation coefficient between a and b.

The type of effect size used in a meta-analysis is selected in accordance with its research objective. In the soap example, the results available in most studies were the effectiveness (*eff*) of different soaps, obtained from the difference between the concentration of the microorganisms measured on the hands of the test subjects before (C_1) and after (C_2) hand washing:

$$Eff = C_2 - C_1 \quad \text{(B.1)}$$

The effectiveness of the soap was generally expressed as the log of the amount of colony forming units (CFU). The first objective of the meta-analysis was to determine if antimicrobial soaps provide a greater reduction of the bacterial density on the hands than nonantimicrobial soaps. The simplest effect size (*ES*) that can be calculated from the results provided in the studies to achieve this research objective is a raw mean difference between the effectiveness of the soaps:

$$ES = Eff_{anti} - Eff_{control}, \quad \text{(B.2)}$$

where Eff_{anti} is the effectiveness of an antimicrobial soap tested in this study and $Eff_{control}$ is the effectiveness of the nonantimicrobial soap to which the antimicrobial soap was compared. A positive effect size indicates that the antimicrobial soap is more effective than the nonantimicrobial soap, and *vice versa* if it is negative. A total of 84 effect sizes were calculated from the 17 studies considered in the meta-analysis. These effect sizes are reported in the third column of Table B.1.

B.5.2 Compilation of the standard errors

When weighed methods are applied to conduct a meta-analysis, the weight given to each effect size is generally a function of their standard error (*SE*). The standard error is calculated from the standard deviation (*SD*) and the number of replicate measurements (*N*) of the results (Table B.2). However, multiple studies generally omit to report the standard deviation of their measurements. Under this circumstance, the standard error of the effect size might be estimated from the results of some statistical tests (*P*-value, *t*-tests, Tukey's least significant differences and so forth) providing they are available. The authors of the studies can also be contacted to acquire the missing data.

For the soap example, 163 effect sizes were rejected from Montville and Schaffner (2011) original meta-analysis because the studies did not provide sufficient information to estimate their standard error, highlighting the importance of systematically reporting the standard deviation of replicate measurements when publishing a scientific study. As noted in the seventh column of Table B.1, of the remaining 84 effect sizes, the *SE* of 58 of them was calculated from standard deviations, 7 from confidence intervals, 5 from *P*-values and 14 from least significance differences.

B.5.3 Compilation of the moderator variables

A typical research objective in a meta-analysis is to explain the differences between the effect sizes reported by the primary studies. Such research objective is usually met through a moderator analysis. A moderator analysis aims to determine how accurately the effect size can be predicted from moderator variables (Pigott 2012; Sanchez-Meca and Martin Martinez 2010). Moderator variables can be methodological parameters, such as the temperature of an experiment, the size of a reactor or the experiment duration, or uncontrolled variables, such as ambient environmental conditions.

In the soap example, the second research objective was to determine if the volume of soap and the method applied to quantify the bacterial density on the hands of the test subjects could have affected the effect sizes reported by the primary studies. The volume of soap used is a continuous variable that was compiled directly in the database without any transformation beside of a change in units when necessary. This variable was compiled in the fifth column of Table B.1. The method applied to quantify the bacterial density on the hands of the subjects is a categorical moderator. Montville and Schaffner (2011) identified seven methods used in the primary studies to measure the density of bacteria on the hands of the test subjects. The two most common methods were the glove juice sampling procedure, where the bacterial concentration in a sampling solution is measured after the hand has been submerged in this

solution, and fingertip bead sampling, where the bacterial concentration transferred to beads rubbed by the fingers of the test subjects is measured. In the database, the glove juice sampling procedure method was coded as 1, fingertip bead sampling as 2 and the other methods, because they were only considered in a few primary studies, were regrouped and coded as method 3. During the moderator analysis (section B.7), it will be determined whether there is a significant difference between the effect sizes reported by these three subgroups.

B.6 Pooling of the effect sizes

The research objectives of meta-analyses are achieved by pooling the effect sizes from multiples studies. Pooling can be accomplished using unweighted methods, in which the pooled effect size is the arithmetic average of the effect sizes retrieved from the primary studies, as was done in Montville and Schaffner (2011) original meta-analysis. However, primary studies can be significantly different with respect to, for instance, the number of replicate measurements they performed. Generally, studies performing a higher number of replicate measurements should be expected to yield more precise results, such that their contribution to the pooled effect size should be weighted accordingly (Card 2012).

Two main models have been developed to calculate pooled effect size: the fixed effects model (FEM) and random effects model (REM). Both models are illustrated in Fig. B.3. In the FEM, it is assumed that each study considered in the meta-analysis share a single true effect size (Schulze 2007). This unique true effect size is illustrated by the vertical line in Fig. B.3A. Some variation can be observed between the mean effect sizes reported by the studies, but these variations are assumed to be the result of the sampling errors only, which are variations that occur naturally because the samples of observations are not necessarily representative of the whole population of observations (Schulze 2007). When applying FEM, it is thus implicitly considered that, if primary studies had performed an infinite number of replicate measurements, they would have all produced the same average effect size.

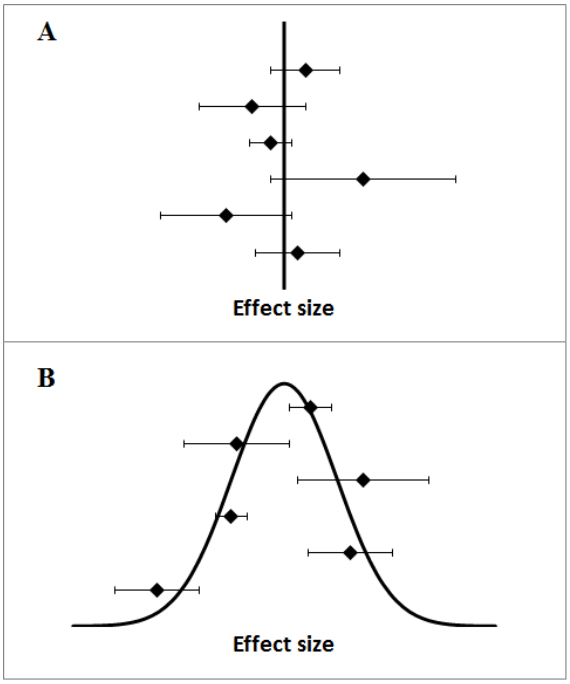

Figure B.3. Illustration of the fixed (A) and random (B) effects models.

In the REM, it is assumed that primary studies do not share a single true effect size, for instance because of methodological differences between the studies (Schulze 2007; Sanchez-Meca and Marin-Martinez 2010; Card 2012). Instead, it is assumed that each primary study has its own true effect size and that this population of effect sizes follows a predetermined distribution (Fig. B.3B). Consequently, there are two sources of variance in the REM, which are the variance resulting from the sampling errors (within-study variance) and the variance induced by the heterogeneity between the studies (between-study variance). The following sections detail how to conduct meta-analysis according to both models and criteria from the selection of the appropriate models.

B.6.1 Fixed effects model

In the FEM, the effect sizes ($ES_{FEM,i}$) are considered to be the sum of the population true effect size (θ) and the sampling error (ε_i):

$$ES_{FEM,i} = \theta + \varepsilon_i \quad \text{(B.3)}$$

The sampling errors of the studies are assumed to be normally distributed and independent of the effect sizes (Montgomery 2013). An unbiased estimator ($\overline{ES}_{FEM}$) of the population true effect size is the weighted average of $ES_{FEM,i}$:

$$\overline{ES}_{FEM} = \frac{\sum w_{FEM,i} ES_{FEM,i}}{\sum w_{FEM,i}}, \quad \text{(B.4)}$$

where $w_{FEM,i}$ is the weight given to each effect size, which are generally selected from the reciprocal of their squared standard error (Card 2012):

$$w_{FEM,i} = \frac{1}{SE_i^2} \quad \text{(B.5)}$$

The standard error of the pooled effect size ($\overline{SE}_{FEM}$) corresponds to the reciprocal of the sum of the weights (Sanchez-Meca and Marin-Martinez 2010):

$$SE_{FEM} = \sqrt{\frac{1}{\sum w_{FEM,i}}} \quad \text{(B.6)}$$

Assuming the effect sizes are normally distributed, the lower (LC_{FEM}) and upper (UC_{FEM}) limits of the confidence interval of $\overline{ES}_{FEM}$ can be computed by multiplying the standard error with *Z*-values obtained from the normal distribution:

$$LC_{FEM} = \overline{ES}_{FEM} - Z_{\alpha/2}\overline{SE}_{FEM} \quad \text{(B.7)}$$

$$UC_{FEM} = \overline{ES}_{FEM} + Z_{\alpha/2}\overline{SE}_{FEM}, \quad \text{(B.8)}$$

where α is the significance level. When the sample size is small, the *Z*-factor in Eqs. (B.7) and (B.8) can be replaced by Students *t*-factors using the adequate number of degrees of freedom. For a significance level of 0.05, the *Z*-factor takes the value of 1.96.

In the soap example, the pooled effect size and 95% confidence interval calculated with the FEM was of 0.45 ± 0.02 log CFU. The pooled effect size is significantly positive. The meta-analysis thus provides statistical evidence that antimicrobial soaps are more effective than nonantimicrobial soaps, assuming that the underlying hypothesis of the FEM are valid for this meta-analysis.

B.6.2 Random effects model

In the REM, the effect sizes ($ES_{REM,i}$) are considered to be the sum of the population average effect size (μ), the deviation due to the between-study heterogeneity (υ_i) and the sampling error (ε_i):

$$ES_{REM,i} = \mu + \upsilon_i + \varepsilon_i \quad \text{(B.9)}$$

The between-study heterogeneity υ_i is generally assumed to be normally distributed and independent of the effect sizes and sampling errors (Viechtbauer 2005). Multiple estimators have been proposed to estimate the between-study heterogeneity. The most

common is the DerSimonian and Laird (1986) estimator, which is based on the *Q*-statistic calculated from the weighted sum of square error of the FEM:

$$Q = \sum w_{FEM,i}(ES_{REM,i} - \overline{ES}_{FEM})^2, \quad \text{(B.10)}$$

where $w_{FEM,i}$ and $\overline{ES}_{FEM}$ are the weights and the pooled estimate calculated with the FEM (Eqs. B.5 and B.4, respectively). The between-study variance is then calculated from the number of degrees of freedom (*df*) of the meta-analysis:

$$\tau^2 = \begin{cases} \frac{Q-df}{c}, if\ Q > df \\ 0, \quad if\ Q < df \end{cases}, \quad \text{(B.11)}$$

where $c = \sum w_{FEM,i} - \frac{\sum({w_{FEM,i}}^2)}{\sum w_{FEM,i}}$

In Eq. (B.11), the number of degrees of freedom *df* is equal to the number of effect sizes $ES_{REM,i}$ minus 1. If *df* is superior to *Q*, τ^2 is commonly fixed to zero, because the between-study variance can not be negative. The weights of the REM ($w_{REM,i}$) are calculated from the reciprocal of the sum of both components of the variance (Viechtbauer 2005):

$$w_{REM,i} = \frac{1}{SE_i^2 + \tau^2} \quad \text{(B.12)}$$

The pooled mean effect size ($\overline{ES}_{REM}$) and the lower (LC_{REM}) and upper (UC_{REM}) limits of its confidence interval are calculated using equivalent forms of Eqs. (B.4); (B.6)-(B.8) (Brockwell and Gordon 2001):

$$\overline{ES}_{REM} = \frac{\sum w_{REM,i} ES_{REM,i}}{\sum w_{REM,i}} \quad \text{(B.13)}$$

$$\overline{SE}_{REM} = \sqrt{\frac{1}{\sum w_{REM,i}}} \quad \text{(B.14)}$$

$$LC_{REM} = \overline{ES}_{REM} - Z_{\alpha/2}\overline{SE}_{REM} \quad \text{(B.15)}$$

$$UC_{REM} = \overline{ES}_{REM} + Z_{\alpha/2}\overline{SE}_{REM} \quad \text{(B.16)}$$

For the soap example, the pooled effect size and confidence interval calculated with the REM was of 0.55 ± 0.15 log CFU. As always the case, the confidence interval of the REM is wider than the FEM because of the FEM more restrictive assumptions (Sutton et al. 2001). Nevertheless, the pooled effect size is significantly positive, which again provide quantitative evidence that antimicrobial soaps are, on average, more efficient than nonantimicrobial soaps.

B.6.3 Model selection

FEM is the preferred models for most meta-analysis because of its simplicity. However, the hypothesis of a single true population effect size is very restrictive and is valid only in selected cases depending on the extent of the heterogeneity between the primary studies. The underlying hypothesis of a single true effect size has to be validated prior to the use of the FEM.

The simplest method to validate the hypothesis of a single true effect size is based on the assessment of the effect sizes using a forest plot. In a forest plot, the mean effect size and the standard error of each primary studies are graphically displayed one above the others. If most effect sizes ± their standard error share a common value, the forest plot suggests that the FEM can be applied to conduct the meta-analysis. In contrast, if the spreading of the effect sizes is much wider, the forest plot suggests the presence of significant between-study heterogeneity, supporting that the REM would provide more reliable results (Higgins and Thompson 2002).

Quantitative methods have also been developed to assess the FEM validity. The most common method is based on the Q-statistic (Eq. B.10). Since the weight $w_{FEM,i}$ is the reciprocal of the squared standard error (Eq. B.5), the Q-statistic represents the ratio of between-study to within-study variances. Consequently, a high value of Q suggests the presence of significant heterogeneity. The Q-statistic follows a χ^2 distribution with *df* degrees of freedom (Higgins and Thompson 2002). When Q is superior to the value of the χ^2 distribution for a predetermined significance level, the heterogeneity is considered significant and a REM should be applied for the meta-analysis. However, studies have shown that the Q-statistic has low power to detect heterogeneity when the number of effect sizes in the meta-analysis is small, which leads to inaccurate estimates of the between-study variance (Eq. B.11) (Schulze 2007; Hardy and Thompson 1998). Given this inaccuracy, authors have proposed that for meta-analyses performed with a low number of effect sizes (under about 30), the FEM should be applied regardless of the between-study heterogeneity (Schulze 2007).

For the soap example, the forest plot of 20 effect sizes taken randomly from the database is shown in Fig. B.4. Most effect sizes are in the 0.3-0.6 range, but the effect sizes ± their standard error generally do not share a common value, suggesting the presence of significant between-study heterogeneity. Accordingly, the Q-statistic for this meta-analysis is of 4071, which is much higher than the threshold value of the χ^2 distribution for a 0.05 significance level and 83 degrees of freedom (105). Therefore, the REM should be considered more accurate than the pooled effect size calculated from the FEM.

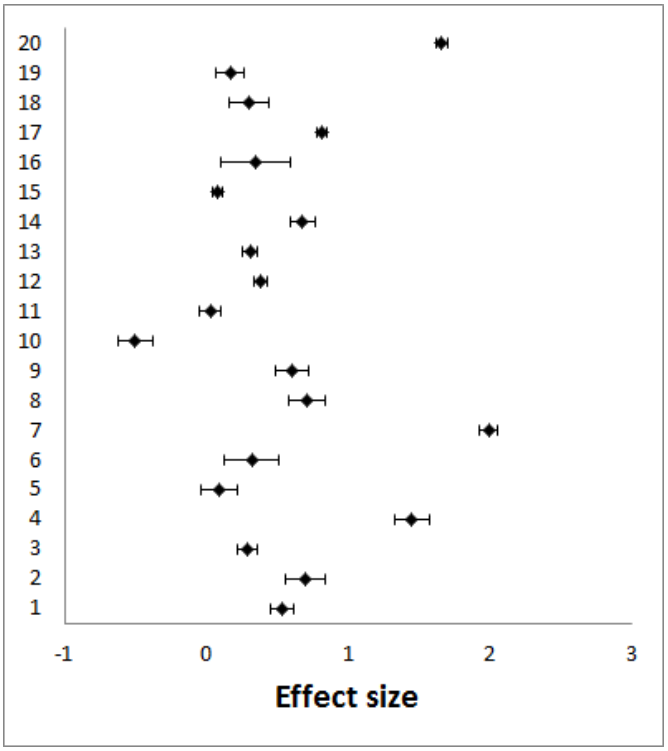

Figure B.4. Forest plot of 20 effect sizes taken randomly from the soap meta-analysis database (Table B.1).

B.7 Moderator analysis

When the primary studies have measured significantly different effect sizes, an additional objective of meta-analyses generally consists to investigate the causes of this heterogeneity. This objective is usually achieved from a moderator analysis. In a moderator analysis, the level of association between the moderator variables and effect sizes is quantified from subgroups analyses or meta-regressions.

When the moderator variables are continuous, the effect sizes are regressed on the moderator variables using weighted least squares. Although any model could be used for the analysis, because of its simplicity, a linear model is generally first assumed:

$$ES_i = \beta_0 + \beta_1 X_i + \upsilon_{res,i} + \varepsilon_i, \qquad \text{(B.17)}$$

where β_0 and β_1 are the model coefficients, X_i is the moderator variable related to the effect size " i " and $\upsilon_{res,i}$ the residual heterogeneity, that is the between-study heterogeneity unexplained by the moderator variable. The model coefficients are calculated from weighted least squares regression:

$$\boldsymbol{\beta} = (\boldsymbol{X^T W^{-1} X})^{-1} \boldsymbol{X^T W^{-1} ES}, \quad \text{(B.18)}$$

where $\boldsymbol{\beta} = \begin{bmatrix} \beta_0 \\ \beta_1 \end{bmatrix}$, $\boldsymbol{X} = \begin{bmatrix} 1 & X_1 \\ ... & ... \\ 1 & X_k \end{bmatrix}$, $\boldsymbol{W} = \begin{bmatrix} \frac{1}{w_{REM,1}} & 0 & 0 \\ 0 & ... & 0 \\ 0 & 0 & \frac{1}{w_{REM,k}} \end{bmatrix}$, $\boldsymbol{ES} = \begin{bmatrix} ES_1 \\ ... \\ ES_k \end{bmatrix}$, w_{REM} are the weights of the REM (Eq. B.12) and k is the number of effect sizes considered in the moderator analysis, which is equal to the total number of effect sizes in the database when every studies considered in the meta-analysis reported the value of the moderator variable. If a linear model is inaccurate, nonlinear models can also be used. The standard error of the regression coefficients is calculated from the variance of the error ε (Henningsen and Hamann 2007):

$$\boldsymbol{SE_\beta} = \sqrt{diag[(\boldsymbol{X^T W^{-1} X})^{-1}]}, \quad \text{(B.19)}$$

where $\boldsymbol{SE_\beta} = \begin{bmatrix} SE(\beta_0) \\ SE(\beta_1) \end{bmatrix}$. The interval of confidence is obtained by multiplying the standard error of the model coefficients with the appropriate Z-factor or t-factors at the desired significance level. When a statistically significant coefficient β_1 is obtained, the moderator analysis suggests that a portion of the between-study heterogeneity could be explained by the moderator variable.

When the moderator variable is categorical, the total heterogeneity (Q_{total}), calculated with Eq. (B.10), is separated in a between-group ($Q_{between}$) and within-group (Q_{within}) heterogeneity. A significant between-group heterogeneity suggests that the effect size of at least one group is significantly different from the others, indicating that the effect size could be affected by the moderator variable. The within-group heterogeneity is computed by applying Eq. (B.10) to each study within a group of the categorical moderator and summing the results obtained for each group. The between-group heterogeneity is then calculated by subtracting the within-group heterogeneity from the total heterogeneity. The statistical significance of the between-group heterogeneity is assessed from a χ^2 distribution with $G - 1$ degrees of freedom, where G is the number of groups.

For the soap example, the Q-statistic suggested the presence of significant heterogeneity between the effect sizes. This heterogeneity could be attributed to the methodological differences such as the volume of soap used in the experiments. To assess the impact of this parameter, a moderator analysis was conducted considering a linear model (Eq. B.17). The following model was obtained:

$$ES = 0.76(\pm 0.39) - 0.05(\pm 0.09)VS, \quad \text{(B.20)}$$

where VS is the volume of soap (mL) and the number in parenthesis denotes the 95% confidence interval of the coefficients. The coefficient β_1 is not statistically significant,

suggesting that the difference between the effectiveness of antimicrobial and nonantimicrobial soaps is not significantly affected by the volume of soap used.

It was also verified if the effect sizes measured by the studies were dependent on the sampling method used to quantify the bacterial content on the hand of the test subjects. Three groups of effect sizes (1, 2 and 3) were identified according to their sampling method, as shown in the sixth column of Table B.1. The total, within-group and between-group heterogeneity calculated for this moderator variable were Q_{total} = 4071, Q_{within} = 4039 and $Q_{between}$ = 31, respectively. The threshold value of the χ^2 distribution for a 0.05 significance level and 2 degrees of freedom is of 6.0, which is lower than the between-study heterogeneity. Therefore, there is significant between-group heterogeneity, which suggests that the effectiveness of soaps is dependent on the sampling method. The REM pooled effect size and 95% confidence interval calculated for groups 1, 2 and 3 were of 0.57 ± 0.26, 0.44 ± 0.21 and 0.58 ± 0.16, respectively. It can thus be concluded that antimicrobial soaps are on average more efficient than nonantimicrobial soaps regardless of the sampling method, but that the magnitude of the difference between their effectiveness depends on this methodological variable.

B.8 Meta-analyses limitations and further developments

B.8.1 Publication bias

A lot of research results remain unpublished. This would not represent a threat to the accuracy of meta-analyses if the publication of scientific results was a random process. However, researchers generally prefer to publish statistically significant results and these results generally have higher acceptance rates by journals (Kepes et al. 2014). The uneven publication of conclusive and inconclusive results, called the publication bias, generally increases the probability to calculate a statistically significant pooled effect size from a meta-analysis (Dwan et al. 2013; Smulders 2013).

Different techniques have been developed to investigate the extent of publication bias in a meta-analysis. The funnel plot is the most commonly used. A funnel plot is a scatter plot of the effect sizes (*X*-axis) against a measure of precision such as the inverse of the standard error (*Y*-axis). Generally, the funnel plot will have a triangular shape, because studies with large sample sizes tend to generate more accurate estimates of the population true effect size and are thus clustered at the top of the funnel plot, while the studies with smaller sample sizes are spread throughout the bottom of the funnel plot (Kepes et al. 2014). An asymmetric funnel plot suggests the presence of publication bias. For instance, funnel plot asymmetry arises if small studies with inconclusive effect sizes are suppressed while studies with large sample sizes are published (Kepes et al. 2014).

Quantitative methods have been developed to estimate the impact of publication bias on the pooled effect size. A method widely used is the trim and fill method of Duval and Tweedie (Rothstein et al. 2005; Duval and Tweedie 2000). The trim and fill method is based on the introduction of fictional effect sizes in the meta-analysis to correct for the funnel plot asymmetry. The procedure consists to delete ("trim") the most extreme effect sizes of the skewed side of the funnel plot until it becomes symmetric. Afterward, the deleted effect sizes are added back to the funnel plot in addition to fictional effect sizes ("fill") mirroring their value (Kepes et al. 2014). A new "adjusted" pooled effect size is then computed considering the fictional effect sizes as correction factors for the publication bias. To determine the number of effect sizes to trim, an iterative approach is applied as detailed in (Rothstein et al. 2005). The first step of this approach is to calculate the absolute difference between the effect sizes and the pooled effect size and noting if these effect sizes were lower or higher than the pooled effect size. The effect sizes are then ranked from 1 to *K,* where 1 is the effect size the most similar to the pooled effect size and *K* is the effect size of the greatest difference with the pooled effect. An estimator of the number of effect sizes to trim is then computed. Different estimators have been developed, the most common being the *R* estimator (Peters et al. 2007):

$$R = K - k - 1, \tag{B.21}$$

where k is the rank of the effect size with the greatest negative difference with the pooled effect size if the funnel plot is skewed to the right or the rank of the effect size with the greatest positive difference with the pooled effect size if the funnel plot is skewed to the left. The R most extreme effect sizes of the skewed side of the funnel plot are then deleted from the meta-analysis, a new pooled effect size is calculated on this trimmed set of data, the R estimator is recalculated on the whole set of data using this new central value and this process is repeated until it converges to a constant value of R. Once the iterations are completed, an equal number of effect sizes whose values are the mirror image of the previously trimmed effect sizes are added to the meta-analysis and a final estimate of the pooled effect size is calculated on this "filled" meta-analysis. If this adjusted estimate differs from the pooled effect size calculated without the fictional effect sizes, it suggests that publication bias might have affected the validity of the meta-analysis.

To investigate the impact of the publication bias, the trim and fill method was applied to the soap example considering a REM. The method indicated the need to add 16 fictional effect sizes mirroring the values of the 16 effect sizes with the greatest positive difference with the pooled effect size (Fig. B.5B). A pooled effect size of 0.29 ± 0.18 log CFU was obtained, compared to 0.55 ± 0.18 log CFU without the addition of these 16 fictional effect sizes. The pooled effect size after the trim and fill method is lower than the pooled effect size without the adjustment for publication bias, but remains significantly positive. Therefore, the trim and fill method suggests that publication bias caused an overestimation of the effectiveness of antimicrobial soaps compared to nonantimicrobial soaps, but did not alter the conclusion that antimicrobial soaps are on average more efficient than nonantimicrobial soaps.

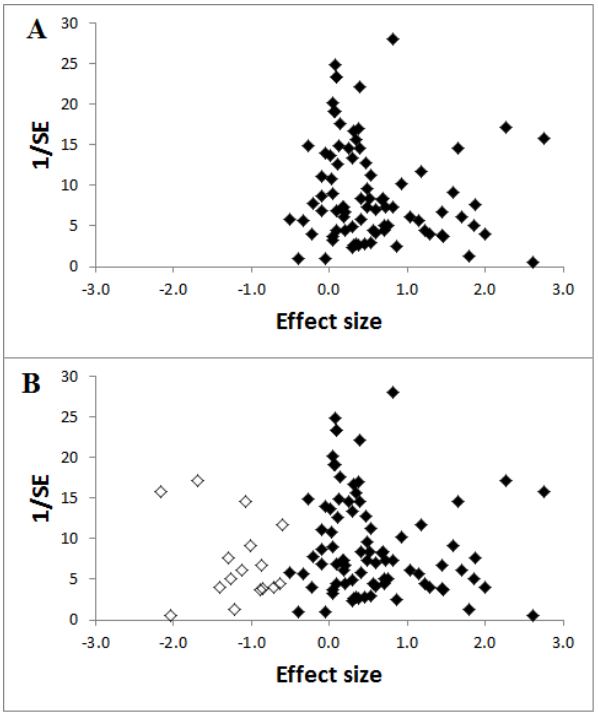

Figure B.5. Funnel plot of the soap meta-analysis before (A) and after (B) the addition of 16 fictional effect sizes (empty markers) to correct for the publication bias.

B.8.2 Correlated effect sizes

The raw mean difference, standardized mean difference and odds ratio are effect sizes describing the change of a variable between a control and a test group. Pooling these effect sizes represent a significant challenge when they are correlated, such as when multiple effect sizes share a common control. Under this circumstance, the hypothesis of independency between the effect sizes is violated, which should be taken into consideration to properly calculate the pooled effect size (Berkey et al. 1996).

The bias caused by shared controls in meta-analyses can be corrected by conducting a multilevel meta-analysis. In a multilevel meta-analysis, the effect sizes sharing a common control are first aggregated prior to being considered for the meta-analysis. The aggregation of the effect sizes sharing a common control is generally performed by generalized least squares regression (Lajeunessei 2011):

$$\dot{ES} = (\boldsymbol{X^T \Omega^{-1} X})^{-1} \boldsymbol{X^T \Omega^{-1} ES}, \quad \text{(B.22)}$$

where $\dot{ES}$ is the aggregated effect size of the p studies sharing a common control, $\boldsymbol{X}$ is a vector (p x 1) of ones, $\boldsymbol{ES}$ is the vector (p x 1) of the p effect sizes sharing the control and $\boldsymbol{\Omega}$ is the variance-covariance matrix (p x p) of the effect sizes. The diagonal elements of the

variance-covariance matrix are the squared standard error of the effect sizes. The off-diagonal elements represent the covariance between the effect sizes. When the effect size is a raw mean difference, the covariance corresponds to the squared standard error of the shared control. If an REM approach is used for the aggregation, the between-study heterogeneity of the effect sizes can be added to the elements of the matrix $\boldsymbol{\Omega}$. However, it is preferable to use an FEM approach to the aggregation in most cases, because the number of effect sizes sharing a common control is generally too low (under about 30) for the accuracy of the REM (Schulze 2007). The standard error of the aggregated effect size is calculated from Eq. (B.18), replacing $\boldsymbol{\beta}$ with $\dot{\boldsymbol{ES}}$ and $\boldsymbol{W}$ with $\boldsymbol{\Omega}$ (Hong 2013).

For the soap example, multiple antimicrobial soaps were compared to a single nonantimicrobial soap, as noted in the last column of Table B.1. For instance, the effect sizes 51, 52 and 53 share a common control having a standard error of 0.11 log CFU (Ojajarvi 1980). For these effect sizes, the matrices necessary for aggregation are:

$$\boldsymbol{\Omega} = \begin{bmatrix} 0.032 & 0.012 & 0.012 \\ 0.012 & 0.040 & 0.012 \\ 0.012 & 0.012 & 0.032 \end{bmatrix} \quad \text{(B.23)}$$

$$\boldsymbol{ES} = \begin{bmatrix} 0.19 \\ 0.49 \\ 1.59 \end{bmatrix}$$

Using Eq. (B.22), the aggregated effect size obtained for these matrices $\boldsymbol{\Omega}$ and $\boldsymbol{ES}$ was of 0.77 ± 0.14 log CFU. Applying this method to each group of antimicrobial soaps sharing a common control, 41 aggregated effect sizes were calculated. The pooled effect size and 95% confidence interval obtained with a REM considering these aggregated effect sizes is was of 0.63 ± 0.24 log CFU. This pooled effect size remains significantly positive and provides evidence that the bias related to shared controls does not affect the conclusion that antimicrobial soaps are on average more efficient than nonantimicrobial soaps.

B.9 Conclusion

In most cases, meta-analyses represent the best approach to perform scientific reviews. This was the case for the review on the effectiveness of antimicrobial and nonantimicrobial soaps. The meta-analysis provided reliable and quantitative evidences that antimicrobial are on average more effective regarding hand washing than nonantimicrobial soaps. The moderator analysis also provided additional insight on the impact of the study methodologies on the soap effectiveness which would not have been apparent from a narrative review. Finally, it was verified that publication bias and correlated effect sizes did not affect the validity of the review, which required the application of quantitative methods such as the trim and fill procedure and generalized least squares.

There are some instances where meta-analyses are not applicable and narrative reviews have to be conducted. These include the analysis of non-quantitative results such as the review of management procedures or of the fields of application of a new technology. However, when the review aims to draw conclusions from the combined analysis of effect sizes from multiple studies, quantitative methods as described in this manuscript should preferably be included in the review process, because they provide the best available evidence from which the research objectives can be achieved.

B.10 Acknowledgements

The authors thank Prof. D.W. Schaffner (Rutgers University) for providing its database on the effectiveness of soap (Montville and Schaffner 2011).

Annexe C. Résultats non publiés utilisés pour la méta-analyse (chapitre 7)

Note: Cette annexe a été publiée en tant qu'appendix à l'article sur la méta-analyse (chapitre 7). Son titre original est *Unpublished results included in the meta-analysis*

Unpublished results from our research team on the drying properties of pasta enriched with flaxseed ingredients were included in the meta-analysis (Table C.1). The results describe the water effective diffusion coefficient during drying and the equilibrium water content after drying of traditional pasta and pasta enriched with 15% ground flaxseed or 15% flaxseed reconstituted after oil extraction. Drying properties were measured for laminated pasta with a thickness of 1.4 or 2.8 mm and dried at 40 or 80 ° C. The pasta was produced as described in Mercier and others (2014b), and the drying properties were measured as described in Mercier and others (2011b).

Table C.1. Drying properties, plus or minus the standard deviation, of laminated pasta according to the type of flaxseed enrichment, the drying temperature, and the thickness of the pasta

Properties	Traditional pasta				Pasta enriched with 15% ground flaxseed				Pasta enriched with 15% flaxseed reconstituted after oil extraction			
	40 °C		80 °C		40 °C		80 °C		40 °C		80 °C	
	1.4 mm	2.8 mm	1.4 mm	2.8 mm	1.4 mm	2.8 mm	1.4 mm	2.8 mm	1.4 mm	2.8 mm	1.4 mm	2.8 mm
Water effective diffusion coefficient ($\times 10^{-11}$ m^2 s^{-1})	3.3 ± 0.1	5.0 ± 0.1	5.7 ± 0.4	9.8 ± 0.7	3.3 ± 0.1	5.1 ± 0.1	6.4 ± 0.4	12.1 ± 1.8	3.9 ± 0.1	4.8 ± 0.1	6.5 ± 0.1	9.7 ± 0.6
Equilibrium water content [g (100 g dry matter)$^{-1}$]	12.2 ± 1.2	11.3 ± 1.9	8.4 ± 0.7	8.3 ± 1.3	10.4 ± 0.2	10.6 ± 0.5	9.4 ± 0.4	9.6 ± 0.4	12.0 ± 0.5	13.1 ± 1.1	7.6 ± 1.1	8.0 ± 0.3

Annexe D. Comparaison de la combinaison des propriétés des pâtes par méta-analyse (chapitre 7) en utilisant un modèle non pondéré et un modèle à effets aléatoires

Note: Cette annexe a été publiée en tant qu'appendix à l'article sur la méta-analyse (chapitre 7). Son titre original est *Comparison of the pooled differences with the control pasta estimated with an unweighted model and a random effects model*

The appropriate model that should be used to pool differences with the control pasta (M_{ij}) is *a priori* the random effects model, because this model considers both the within-observation and between-observation variance (Hunter and Schmidt 2000; Schulze 2007). The within-observation variance is estimated from the standard error of M_{ij}, as follows (Montgomery 2013):

$$SE_{M_{ij}} = \sqrt{\frac{SD_{ic}^2}{n_{ic}} + \frac{SD_{ij}^2}{n_{ij}}}, \qquad \text{(D.1)}$$

where SD_{ic} and n_{ic} are the standard deviation and the number of replicate measurements of X_{ic} (the average measurement for the control pasta in study i), and SD_{ij} and n_{ij} are the standard deviation and the number of replicate measurements of X_{ij} (the average measurement [over n replicates] of the quality attribute or process specification X for observation j in study i). The between-observation variance is estimated from the Q-statistic as described in section 7.3.2. Pooling differences with the control pasta using a random effects model requires knowledge of the standard deviation of the measurements (Equation D.1). However, nearly half of the studies (47%) considered for the meta-analysis did not publish the standard deviation for some or all of their observations, reducing the sample size for the random effects model. A smaller sample size decreases the statistical power of the meta-analysis and increases the probability of type II (false negative) errors (Valentine and others 2010). It was relevant to verify if an unweighted model (Equation 7.2), which neglects the within-observation variance and does not require the standard deviation of the measurements, would provide more accurate results than a random effects model applied to a smaller sample size would.

To compare the results obtained using an unweighted model and a random effects model for a smaller sample size, random effects models were used to pool differences with the

control pasta for 4 quality attributes, namely, protein content, optimum cooking time, cooking losses, and uncooked pasta brightness. These quality attributes were selected because they were known for a large number of observations in the dataset (Table 7.3). The pooled differences with the control pasta and their standard error were calculated using a random effects model applied to the complete sample of differences with the control pasta. Results were compared with estimates obtained using an unweighted model applied to the complete sample of differences with the control pasta and using random effects models applied to samples of smaller size. The samples of smaller size were generated by removing the differences with the control pasta from half of the studies in the dataset, which were selected randomly. A total of 10 samples of smaller size were generated for each of the 4 quality attributes considered. Figure D.1 presents the pooled differences with the control pasta and their standard error obtained using these models. For the 4 quality attributes, the unweighted model provided similar results (less than 5% difference) compared to the random effects model applied to the complete sample of differences with the control pasta. The similarity between the random effects model and the unweighted model for the complete sample of differences with the control pasta is explained by the high accuracy of the quality attributes in the dataset, their relative errors being below 2.4% (Table 7.3). The high accuracy limits the contribution of the within-observation variance to the pooled difference with the control pasta with respect to the between-observation variance and decreases the difference between estimates obtained with a random effects model and an unweighted model. Although the majority (90%) of the pooled differences with the control pasta calculated with random effects models applied to samples of smaller size remained statistically significant, their difference with the random effects model applied to the complete sample of differences with the control pasta was generally over 5% and was highly dependent on the observations removed from the sample (Figure D.1). Consequently, an unweighted model was used in this work to pool differences with the control pasta, because a comparison of the models indicates that reducing the sample size is more significant than neglecting the within-observation variance is. A random effects model was used to pool Fisher transforms of the Pearson correlation coefficients, because knowledge of the standard deviation at the observation level is not required for their calculation (Equation 7.9).

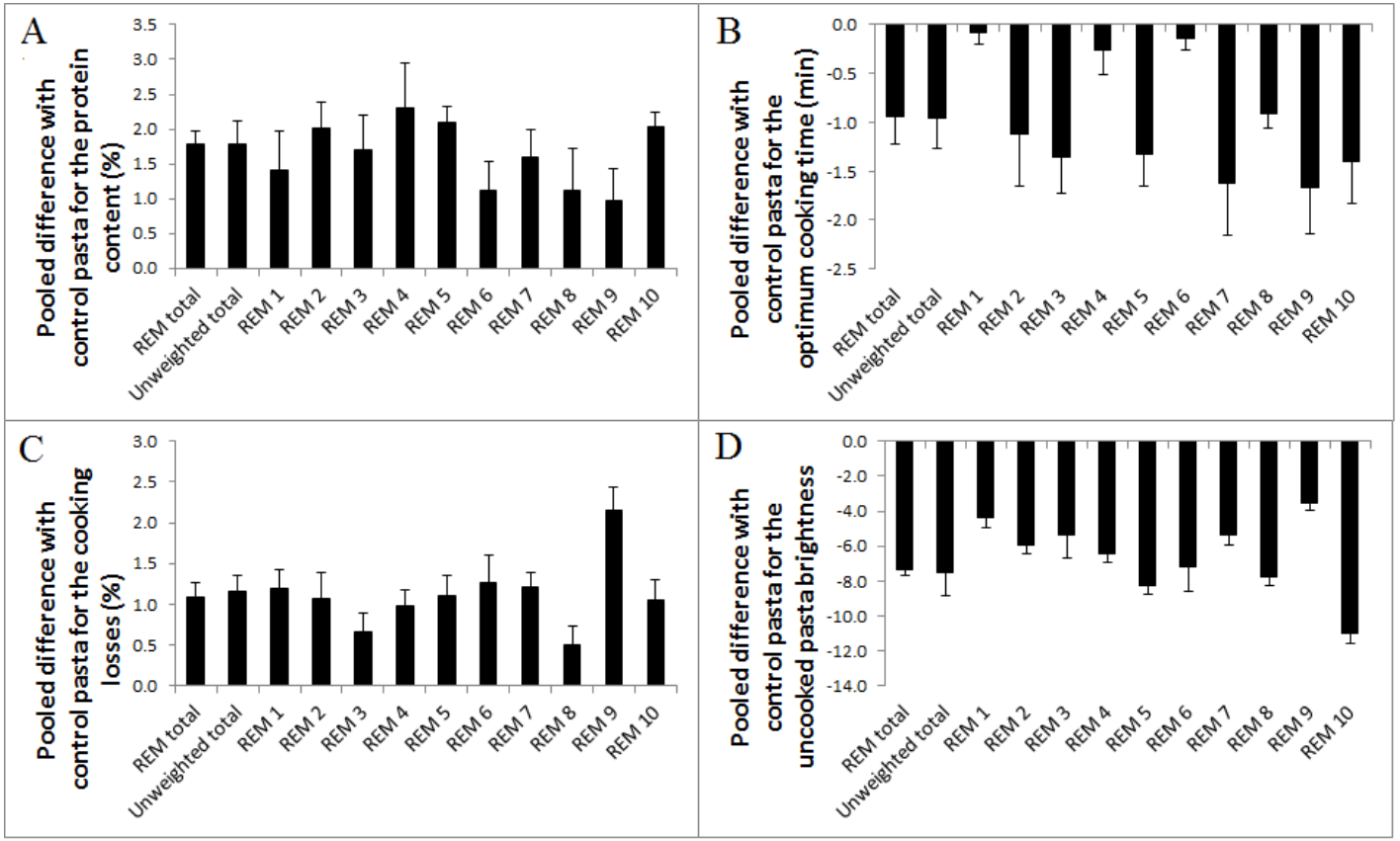

Figure D.1. Pooled differences with the control pasta ($\overline{\boldsymbol{M}}$) plus or minus the standard error ($\overline{\boldsymbol{SE}}_{\boldsymbol{M}}$) for pasta protein content (%) (A), optimum cooking time (min) (B), cooking losses (%) (C), and uncooked pasta brightness (*L* value) (D). The pooled difference with the control pasta was calculated using a random effects model applied to the complete sample of differences with the control pasta (REM total), an unweighted model applied to the complete sample of differences with the control pasta (unweighted total), and random effects models applied to samples of smaller size (REM 1–10).

Annexe E. Profils internes de teneur en eau non-Fickian

Il est extrêmement complexe de mesurer les profils internes de teneur en eau générés dans les pâtes lors du séchage. Les méthodes de mesure des profils internes de teneur en eau non destructives par résonnance magnétique nucléaire, microtomographie, sonication et spectroscopie infrarouge ne sont pas applicables au séchage des pâtes en raison de leur trop faible teneur en eau (Hills et al. 1997; NineSigma 2015). Les méthodes de mesure destructives, basées sur le sectionnement des pâtes et la mesure de la teneur en eau dans chaque section, peuvent être utilisées pour les pâtes, mais sont difficiles à appliquer en raison de la petite taille des pâtes et de la présence d'une couche vitreuse en surface (Litchfield et Okos 1992). Pour faciliter la mesure de profils internes de teneur en eau, une procédure a été développée pour modifier l'orientation du transfert de masse dans les pâtes de l'épaisseur vers la longueur. Cette procédure est illustrée à la Fig. E.1.

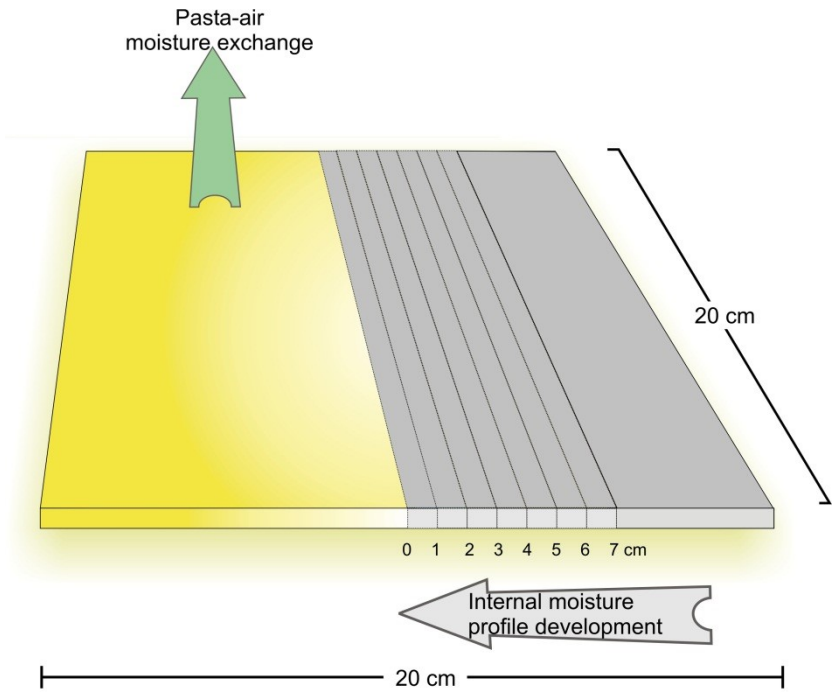

Figure E.1. Schématisation du système utilisé pour mesurer les profils internes de teneur en eau générés lors du séchage. (Merci à François Lamarche pour la préparation de la figure).

Dans cette procédure, la moitié d'une pâte rectangulaire (de style lasagne) de 20 cm x 20 cm x 2.8 mm est isolée à l'aide d'une pellicule de polyéthylène. La pâte semi-enveloppée est séchée dans une chambre à environnement contrôlé. Un profil interne de teneur en eau se forme alors dans la portion isolée de la pâte, qui est étudié en sectionnant des lanières de 1-cm à partir du centre de la pâte et en mesurant la teneur en eau dans chacune de celles-ci. La Fig.

E.2 montre les profils internes de teneur en eau mesurés selon cette procédure pour des pâtes traditionnelles et enrichies en lin après 0, 1, 5, 24 et 48 h de séchage à 80 ºC.

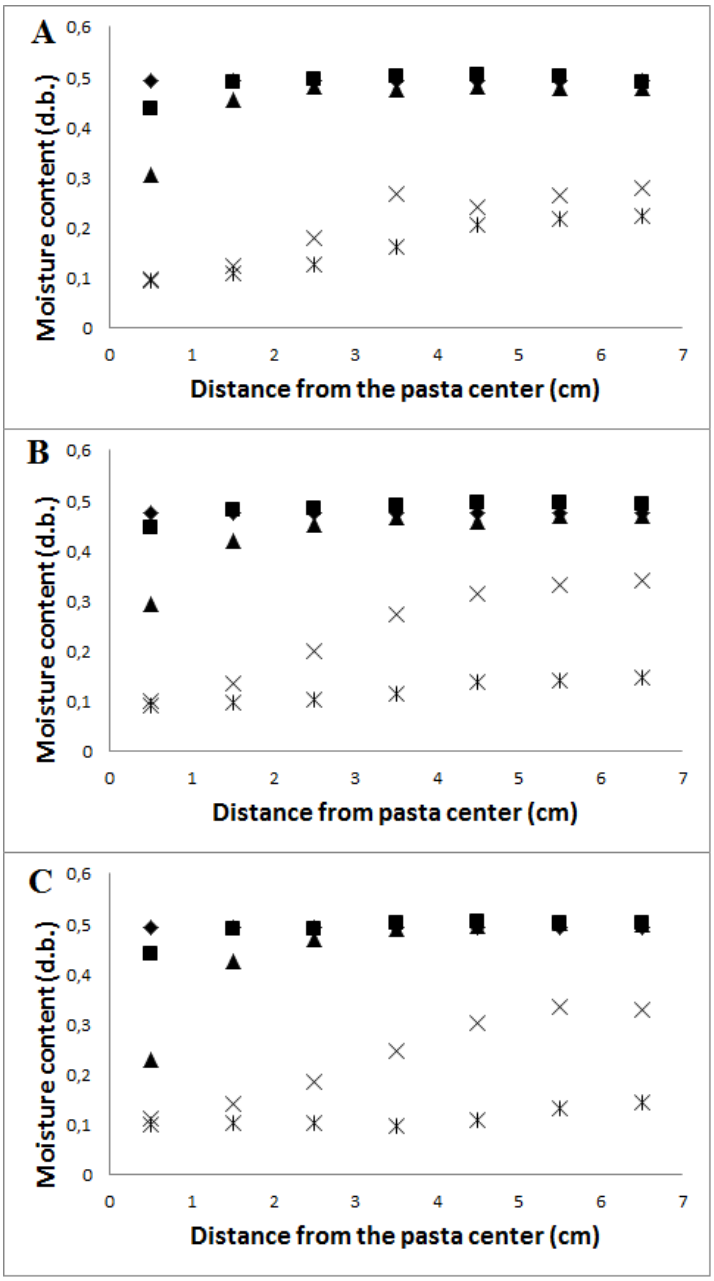

Figure E.2. Profils internes de teneur en eau mesurés pour des pâtes traditionnelles (A), enrichies avec 15% de lin moulu (B) et 15% d'un mélange d'huile de lin et de tourteau moulu (C) après 0 (♦), 1 (■), 5 (▲), 24 (×) et 48h (∗) de séchage à 80ºC.

Les résultats de la Fig. E.2 montrent qu'après 1 et 5 h de séchage, un profil de teneur en eau de forme ronde se développe, le gradient de teneur en eau étant le plus élevé près du centre de la pâte et de plus en plus faible vers l'extrémité. Ces profils de teneur en eau peuvent

être décrits adéquatement par un modèle de transfert de masse Fickian. Par contre, après 24 et 48 h de séchage, les profils de teneur en eau sont de forme sigmoïde. L'augmentation de la teneur en eau est faible près du centre de la pâte, mais est suivie d'une augmentation abrupte du gradient, puis d'un second plateau. Ces profils suggèrent un transfert de masse non-Fickian. La forme sigmoïde est possiblement causée par le déplacement à l'intérieur de la pâte d'une zone en transition de l'état visqueux à l'état vitreux causant l'établissement d'une force opposée au mouvement de l'eau dans la pâte.